



THE HONG KONG
POLYTECHNIC UNIVERSITY

香港理工大學

Pao Yue-kong Library

包玉剛圖書館

Copyright Undertaking

This thesis is protected by copyright, with all rights reserved.

By reading and using the thesis, the reader understands and agrees to the following terms:

1. The reader will abide by the rules and legal ordinances governing copyright regarding the use of the thesis.
2. The reader will use the thesis for the purpose of research or private study only and not for distribution or further reproduction or any other purpose.
3. The reader agrees to indemnify and hold the University harmless from and against any loss, damage, cost, liability or expenses arising from copyright infringement or unauthorized usage.

IMPORTANT

If you have reasons to believe that any materials in this thesis are deemed not suitable to be distributed in this form, or a copyright owner having difficulty with the material being included in our database, please contact lbsys@polyu.edu.hk providing details. The Library will look into your claim and consider taking remedial action upon receipt of the written requests.

The Hong Kong Polytechnic University

Department of Health Technology and Informatics

Protective Effects of Desacyl Ghrelin on
Doxorubicin-induced and Diabetic Cardiomyopathy

XIAO MENG PEI

A thesis submitted in partial fulfilment of the
requirements for the degree of Doctor of Philosophy

February 2013

CERTIFICATE OF ORIGINALITY

I hereby declare that this thesis is my own work and that, to the best of my knowledge and belief, it reproduces no materials previously published or written, nor material that has been accepted for the award of any other degree or diploma, except where due acknowledge has been made in the text.

Signed

PEI XIAO MENG

Abstract

Cardiomyopathy is a well-known clinical problem in the heart that occurs during doxorubicin chemotherapy and in type 2 diabetic mellitus. Cardiac cell culture studies have showed that desacyl ghrelin, a preproghrelin gene-derived peptide, exerts favorable effects on cardiomyocytes such as inhibition of apoptosis. Nonetheless, the in vivo protective effects of desacyl ghrelin on cardiomyopathy have not been investigated. In this dissertation, we examined the protective effects of desacyl ghrelin on doxorubicin-induced cardiomyopathy and type 2 diabetic cardiomyopathy by using corresponding mouse experimental models. The number of diabetic cancer patients is rapidly increasing but the cardiac damaging effects of the anti-cancer drug doxorubicin on a diabetic heart have not been examined. As the signaling mechanisms of the doxorubicin-induced cardiomyopathy in a type 2 diabetic heart are mostly unknown, we further investigated the molecular signaling that is responsible for doxorubicin-induced cardiotoxicity in type 2 diabetic heart.

The first part of this dissertation demonstrated that desacyl ghrelin improved the cardiac dysfunction induced by doxorubicin based on the functional results of ventricular fractional shortening and ejection fraction. Cardiac apoptosis and fibrosis induced by doxorubicin were prevented by desacyl ghrelin. Apoptotic DNA fragmentation, caspase-3 activity, apoptotic markers (Bcl-2, Bax and XIAP), fibrosis area and fibrotic regulatory factors (CTGF, BNP and TGF- β) were examined in cardiomyocytes. Desacyl ghrelin was found to exert

protective effects on doxorubicin -induced cardiotoxicity via the attenuation of apoptosis and fibrosis through the activation of pro-survival ERK1/2/Akt signaling pathway. The second part of this dissertation showed that desacyl ghrelin alleviated cardiac dysfunction in type 2 diabetic cardiomyopathy indicated by the improvement of functional fractional shortening of ventricle. Collagen deposition, fibrotic regulatory factors, autophagic markers and AMPK/Akt/ERK1/2/GSK3 α / β signaling pathway were examined. The results demonstrated that desacyl ghrelin reduced collagen deposition, up-regulated adiponectin expression, increased autophagic Beclin1 and Atg5-Atg12 conjugation, and enhanced phosphorylation of AMPK, Akt, ERK1/2 and GSK3 α / β signaling in type 2 diabetic heart. The third part of this dissertation focused on examining the molecular mechanisms of the doxorubicin-induced cardiotoxicity in type 2 diabetic hearts by using the technique of microarray analysis. The results identified a panel of regulatory genes associated with cardiac remodeling, inflammatory response, oxidative stress, and DNA/RNA stability/repair in the doxorubicin-induced cardiac injury in diabetic heart. The results of this microarray experiment were confirmed by the analysis of transcript expression of selected genes by using real time PCR. Notably, the analysis suggested two important genes, namely S100A8 and S100A9, might play a unique role in the pathogenesis of the doxorubicin-induced cardiomyopathy specifically in diabetic heart.

In conclusion, the results of this dissertation evidently demonstrated the

cardioprotective effects and the corresponding signaling mechanisms of desacyl ghrelin on the doxorubicin-induced cardiomyopathy and type 2 diabetic cardiomyopathy. These findings provide important pre-clinical information for future research to develop effective treatment or intervention in solving the clinical problem of the doxorubicin-induced cardiac toxicity in both non-diabetic and diabetic cancer patients.

Publications

Journal paper

Pei XM, Yung BY, Yip SP, Ying M, Benzie IF, and Siu PM. Desacyl ghrelin prevents doxorubicin-induced myocardial fibrosis and apoptosis via GHSR-independent pathway. *Am J Physiol Endocrinol Metab* (in revision)

Conference abstract

Siu PM, **Pei XM**, Ying M, and Benzie IF. Ghrelin ameliorates doxorubicin-induced cardiomyopathy and cardiac fibrosis. *FASEB Journal* 26: 1139.4, 2012.

Pei XM, Ying M, Benzie IF, and Siu PM. Protective effects of ghrelin on doxorubicin-induced cardiomyopathy and cardiac apoptosis. *Medicine and Science in Sports and Exercise* 42(5): S379, 2010.

Acknowledgements

During my PhD study, there are many people whom I need to acknowledge for their encouragement, support and guidance.

Firstly, I have the fortunate and unique opportunity to be supervised by Dr. Parco SIU. I cannot thank Dr. Parco SIU enough for his professional guidance, unfailing encouragement, patience, inspiration and care over the past years. I would like to express my deepest gratitude to him for the help and advice on presentation skill, all the precious comments and suggestions on experimental design, data collection and analysis in my PhD study. I am also profoundly impressed by his passion towards his research interests.

Secondly, I am most grateful to Prof. YUNG for his support, encouragement, and the best suggestions. Prof. YUNG has kindly offered help for me to get through some challenging time. I would also like to thank Prof. Iris BENZIE for providing numerous invaluable comments and suggestions for my PhD project. Special thanks to Dr. Lawrence CHAN and his team for providing the technical support on microarray analysis.

Grateful thanks to the technical and administrative colleagues in the Department of Health Technology and Informatics, The Hong Kong Polytechnic University. Many thanks to the past and present members of the lab, especially Thomas SIN, Bjorn TAM, Angus YU, Riva CHUANG, Blanka LEE,

Koh Su PIN, Xiaoxin HE, Caroline ZHANG, and Miaomiao ZHU. All your friendships are appreciated and I will never forget your help and encouragement.

Finally, I would like to thank my parents, younger sister and my best friends in Beijing. They were always there supporting me and cheering me up throughout the entire period of my study.

Table of Contents

Declaration of Originality	i
Abstract	ii
Publications	v
Acknowledgements	vi
Table of Contents	viii
List of Figures	xiii
List of Tables	xvii
Abbreviations	xviii
CHAPTER 1 Introduction.....	1
1.1 Cardiomyopathy: Definition and Classification.....	2
1.2 DOX-induced Cardiomyopathy	3
1.2.1 Epidemiologic Features.....	5
1.2.2 Pathologic Features	6
1.2.3 Current Treatment	8
1.2.4 Molecular Mechanisms	9
1.2.4.1 Cardiac Apoptosis	9
1.2.4.2 Cardiac Fibrosis	12
1.2.4.3 Cardiac Metabolism	13
1.2.4.4 Cardiac Calcium Signaling	17
1.3 Diabetic Cardiomyopathy	22
1.3.1 Epidemiologic Features.....	23
1.3.2 Pathologic Features	24
1.3.2.1 Cardiac Fibrosis	24
1.3.2.2 Lipid Accumulation	25
1.3.3 Current Treatment.....	28
1.3.4 Molecular Mechanisms	30
1.3.4.1 Cardiac Apoptosis	30
1.3.4.2 Cardiac Autophagy	34
1.3.4.3 Cardiac Metabolism	35
1.3.4.4 Cardiac Inflammation	39

1.3.4.5 Signaling Pathway.....	39
1.4 DOX-induced Cardiotoxicity in Diabetic Patients.....	41
1.4.1 Connection Between Cancer and Type 2 Diabetes	41
1.4.2 Potential Mechanism for the Link Between Type 2 Diabetes and Cancer.....	45
1.4.3 Clinical Challenge: DOX-induced Cardiotoxicity in Diabetic Heart.....	46
1.5 Ghrelin	48
1.5.1 Structure of Ghrelin and the Related Substances	48
1.5.2 Acylated and Desacylated Forms.....	52
1.5.3 Physiological Functions of Ghrelin.....	53
1.5.3.1 Central Actions of Acylated Ghrelin.....	54
1.5.3.2 Peripheral Effects of Acylated Ghrelin and Desacyl Ghrelin	56
CHAPTER 2 General Methods.....	69
2.1 Measurement of Cardiac Function by Echocardiography.....	70
2.2 Masson's Trichrome Staining	71
2.3 Protein Fraction Preparation	71
2.4 Apoptotic Cell Death Enzyme-Linked Immunosorbent Assay (ELISA).....	72
2.5 Fluorometric Caspase-3 Activity Assay	73
2.6 RNA Extraction and Real Time Quantitative PCR Analysis.....	73
2.7 Western Blot Analysis	77
CHAPTER 3 Desacyl Ghrelin Prevents DOX-induced Myocardial Fibrosis and Apoptosis via GHSR-independent Pathway	79
3.1 Introduction.....	80
3.2 Methods.....	82
3.2.1 Animals	82
3.2.2 Experimental Protocol.....	82
3.2.3 Echocardiographic Assessment.....	84
3.2.4 Measurement of Growth Hormone and Insulin Growth Factor-1 Levels in Plasma	84
3.2.5 TUNEL Assay.....	84
3.2.6 Masson's Trichome Staining	85
3.2.7 Protein Fraction Preparation	85
3.2.8 Apoptotic Cell Death Enzyme-Linked Immunosorbent Assay (ELISA).....	86

3.2.9 Fluorometric Caspase-3 Activity Assay	86
3.2.10 RNA Extraction and Real Time Quantitative PCR Analysis	86
3.2.11 Western Blot Analysis	86
3.2.12 Statistical Analysis.....	87
3.3 Results.....	87
3.3.1 Echocardiographic Parameters.....	87
3.3.2 Myocardial Fibrosis and Fibrotic Regulatory Factors	91
3.3.3 Myocardial Apoptosis and Apoptotic Regulatory Factors.....	95
3.3.4 Myocardial ERK/Akt Signaling.....	100
3.3.5 Plasma GH and IGF-1 Levels	102
3.3.6 Myocardial Metabolic Regulators.....	104
3.3.7 Myocardial Calcium Handling Factors	108
3.4 Discussion.....	110
3.4.1 Desacyl Ghrelin Prevents DOX-induced Impairment of Cardiac Function...	110
3.4.2 Anti-fibrotic Effect of Desacyl Ghrelin on DOX Cardiotoxicity.....	111
3.4.3 Anti-apoptotic Effect of Desacyl Ghrelin on DOX Cardiotoxicity.....	113
CHAPTER 4 Protective Effect of Desacyl Ghrelin on Type 2 Diabetic Cardiomyopathy.....	117
4.1 Introduction.....	118
4.2 Methods.....	120
4.2.1 Animals	120
4.2.2 Experimental Protocol.....	120
4.2.3 Measurement of Cardiac Function by Echocardiography.....	121
4.2.4 Masson's Trichome Staining	121
4.2.5 Protein Fraction Preparation	121
4.2.6 RNA Extraction and Real Time Quantitative PCR Analysis.....	122
4.2.7 Western Blot Analysis	122
4.2.8 Statistical Analysis.....	122
4.3 Results.....	123
4.3.1 Cardiac Function by Echocardiography.....	123
4.3.2 Cardiac Fibrosis and Fibrotic Regulatory Factors	124
4.3.3 Cardiac Inflammatory Markers.....	127

4.3.4 Cardiac Autophagic Markers: Beclin1 and Atg5-Atg12 Conjugation.....	129
4.3.5 Other Factors: Endothelial Dysfunction (Edn3), Cardiomyocyte Differentiation (p21 and GATA6), and FK506 Binding Protein (FKBP5 and FKBP10)	131
4.3.6 AMPK, Akt, ERK1/2 and GSK3 α/β Signaling.....	133
4.4 Discussion.....	137
4.4.1 Desacyl Ghrelin Improves Cardiac Dysfunction in Diabetic Cardiomyopathy	137
4.4.2 Desacyl Ghrelin Alleviates Cardiac Fibrosis in Diabetic Cardiomyopathy...	138
4.4.3 Genes Involved in Diabetic Cardiomyopathy But Not Affected by Desacyl Ghrelin	140
4.4.4 Enhanced Cardiac Autophagy by Desacyl Ghrelin in Diabetic Cardiomyopathy	142
4.4.5 Activation of AMPK, ERK1/2, Akt and GSK3 α/β Signaling by Desacyl Ghrelin in Diabetic Cardiomyopathy	143
CHAPTER 5	145
DOX-induced Cardiotoxicity in Type 2 Diabetic Heart	145
5.1 Introduction.....	146
5.2 Methods.....	147
5.2.1 Animals	147
5.2.2 Experimental Protocol.....	148
5.2.3 Measurement of Cardiac Function by Echocardiography.....	149
5.2.4 Protein Fraction Preparation	149
5.2.5 Apoptotic Cell Death Enzyme-linked Immunosorbent Assay (ELISA)	149
5.2.6 RNA Extraction and Microarray Analysis.....	149
5.2.7 Real Time Quantitative PCR Analysis.....	151
5.2.8 Western Blot Analysis	151
5.2.9 Statistical Analysis.....	151
5.3 Results.....	152
5.3.1 Survival Analysis	152
5.3.2 Fractional Shortening of Left Ventricle	154
5.3.3 Cardiac Apoptosis and Apoptotic Regulatory Factor	157
5.3.4 Cardiac Autophagic Factor: Beclin1	160
5.3.5 Microarray Analysis of the Effect of DOX on Diabetic Heart	162

5.3.5.1 Gene Expression Profile by Microarray Analysis.....	162
5.3.5.2 Pathway Analysis by MetacoreTM.....	167
5.3.6 Confirmation of Selected Gene Expressions by Real Time RT-PCR.....	183
5.3.7 Pathway Network: Inflammation Amphoterin Signaling	186
5.4 Discussion.....	191
5.4.1 Further Decrease in Cardiac Contractile Function at 7-day After DOX Administratio in Diabetic Heart.....	191
5.4.2 Underlying Mechanism of DOX-induced Cardiotoxicity in Diabetic Heart .	192
CHAPTER 6 Overall Discussion and Future Direction.....	198
6.1 Main Findings	199
6.1.1 Aims of the Dissertation	199
6.1.2 Summary of Main Findings	199
6.2 Cardiac Dysfunction of Cardiomyopathy Induced by Anti-cancer Drug DOX and Type 2 Diabetes Mellitus	201
6.3 Potential Mechanisms of Cardiomyopathy Induced by DOX and Type 2 Diabetes	203
6.3.1 Cardiac Cell Death.....	203
6.3.1.1 Cardiac Apoptosis	204
6.3.1.2 Cardiac Autophagy	205
6.3.2 Cardiac Fibrosis	207
6.4 Protective Effects of Desacyl Ghrelin on Cardiomyopathy	209
6.5 Limitations and Future Direction.....	212
6.6 Clinical Applications	213
Reference List	216

List of Figures

- Fig. 1.1 Structure of DOX
- Fig. 1.2 Cumulative probability of developing DOX-induced congestive heart failure versus total cumulative dose of DOX in 3,941 patients
- Fig 1.3 Development of histopathological changes in the myocardium of rabbit model response to DOX
- Fig 1.4 Two main apoptotic pathways in cardiac apoptosis
- Fig 1.5 Substrates of myocardial metabolism
- Fig 1.6 Calcium signaling in heart
- Fig 1.7 Representative photomicrographs of intramyocardial lipid accumulation in heart of type 2 diabetic patients (a) and Zucker diabetic fatty rat (b)
- Fig 1.8 Possible mechanisms by which diabetes mellitus induces myocardial cell death
- Fig 1.9 The role of altered myocardial metabolism in the development of diabetic cardiomyopathy
- Fig 1.10 Potential mechanism for the link between type 2 diabetes and cancer
- Fig 1.11 The post-translational modification
- Fig 1.12 Amino acid sequences of ghrelin precursors in human, rat, and mouse
- Fig 1.13 The modification process of octanoic acid by GOAT
- Fig 1.14 The biological roles of ghrelin
- Fig 1.15 Effect of acute bolus administration on insulin and glucose level
- Fig 1.16 Cardiovascular effects of ghrelin

- Fig 3.1 The Echocardiographic M-mode Image
- Fig 3.2 Collagen deposition in heart
- Fig 3.3 Fibrotic area was present by percent of collagen accumulation to total area of the microscopic field
- Fig 3.4 The transcript expression levels of myocardial fibrotic regulatory factors
- Fig 3.5 TUNEL index, apoptotic DNA fragmentation, and Caspase-3 protease activity in heart.
- Fig 3.6 Protein abundances of Bcl-2 and Bax, the ratio of the protein level of Bcl-2 to Bax
- Fig 3.7 Protein abundances of XIAP
- Fig 3.8 ERK and Akt signaling in heart
- Fig 3.9 Plasma concentration of GH and IGF-1
- Fig 3.10 The transcript expression levels of myocardial metabolic regulators
- Fig 3.11 Cytoplasmic and nuclear protein content of PGC-1 α
- Fig 3.12 AMPK signaling in heart
- Fig 3.13 The transcript expression levels of myocardial calcium handling factors
- Fig 4.1 Effect of des-acyl ghrelin on fractional shortening
- Fig 4.2 Collagen deposition after des-acyl ghrelin treatment in db/db mice heart
- Fig 4.3 The transcript expression levels of adiponectin, MMP-8, and MMP-13

- Fig 4.4 The transcript expression levels of Apelin, Wnt5a, and TLR4
- Fig 4.5 The protein abundance of Beclin1 and the conjugation of Atg5 and Atg12
- Fig 4.6 The transcript expression levels of Edn3, GATA6, FKBP10, p21, and FKBP5
- Fig 4.7 AMPK signaling in heart
- Fig 4.8 Akt and ERK1/2 signaling in heart
- Fig 4.9 GSK3 α/β signaling in heart
- Fig 5.1 Decreased survival rate in db/+DOX and db/db-DOX
- Fig 5.2 Cardiac function in DOX treated non-diabetes and diabetes mice on day 5 after the administration of DOX
- Fig 5.3 Cardiac function in DOX treated non-diabetes and diabetes mice on day 7 after the administration of DOX
- Fig 5.4 Apoptotic DNA fragmentation in heart
- Fig 5.5 The protein abundance of Bcl-2 and bax, the ration of protein abundance of Bcl-2 to Bax
- Fig 5.6 The protein abundance of Beclin1
- Fig 5.7 Cell adhesion - ECM remodelling
- Fig 5.8 Transcription - Role of AP 1 in regulation of cellular metabolism
- Fig 5.9 Immune response - IL 13 signaling via JAK STAT
- Fig 5.10 Transcription - Androgen Receptor Nuclear Signaling
- Fig 5.11 The transcript expression levels of S100A8
- Fig 5.12 The transcript expression levels of S100A9

Fig 5.13 Pathway Network: Inflammation Amphoterin Signaling

Fig 6.1 The Summary of Main Findings in the Dissertation

List of Tables

Table 1.1	Morphologic grading system for DOX cardiotoxicity
Table 1.2	DOX induced changes in cardiac metabolism
Table 1.3	DOX induced changes in cardiac calcium signaling
Table 1.4	Main and recent echocardiographic, population-based studies on diabetic cardiomyopathy
Table 1.5	Major studies on treatment strategies of diabetic cardiomyopathy
Table 1.6	Diabetes and relative risk of cancer by site
Table 1.7	Diabetes and relative risk of cancer mortality by site
Table 1.8	Cardiovascular effects of ghrelin
Table 1.9	Studies of anti-apoptotic effect of ghrelin
Table 2.1	Sequence of Primer Used in Real Time PCR Analysis
Table 2.2	Primary antibody information summary
Table 3.1	Echocardiographic Parameters
Table 5.1	Significantly regulated genes in response to DOX in diabetic heart
Table 5.2	Results of GO mapping, GO terms, p values and count, Cellular Component Ontology
Table 5.3	Results of GO mapping, GO terms, p values and count, Biological Process Ontology
Table 5.4	Results of GO mapping, GO terms, p values and count, Molecular Function Ontology

Abbreviations

ACC, Acetyl-CoA carboxylase

ACE, Angiotensin converting enzyme

AFC, 7-amino-4-trifluoromethyl coumarin

AGEs, Advanced glycation end products

AgRP, Agouti-related protein

Akt, Protein kinase B

AMPK, AMP-activated protein kinase

AP-1, Activator protein 1

ARC, Arcuate nucleus

ASA, Acetylsalicylic acid

ATP, Adenosine triphosphate

AWT, Anterior wall thickness

Bcl-2, B-cell lymphoma 2

Bcl-XL, B-cell lymphoma-extra large

BNP, Brain natriuretic peptide

BSA, Bovine serum albumin

CAMK2D, Calcium/calmodulin-dependent protein kinase II delta

cAMP, Cyclic adenosine monophosphate

Caspase, cysteine-aspartic proteases

CD14, Lipopolysaccharide receptor

COL1A, Collagen type 1

CPT, Carnitine-palmitoyl transferase

CTGF, Connective tissue growth factor

CVD, Cardiovascular disease death

DAG, Desacyl ghrelin

DAPI, 4',6-diamidino-2-phenylindole

DAPK, Death-associated protein kinase

DCM, Diabetic cardiomyopathy

DGAT, Diglyceride acyltransferase

DNA, Deoxyribonucleic acid

DOX, Doxorubicin

ECM, Extracellular matrix

Edn3, Endothelin-3

EDTA, Ethylenediaminetetraacetic acid

EF, Ejection fraction

EGF, Epidermal growth factor

EGFR, Epidermal growth factor receptor

ELISA, Enzyme-linked immunosorbent assay

eNOS, Endothelial nitric oxide synthase

ERBB, Erythroblastic Leukemia Viral Oncogene Homolog

ERK, Extracellular-signal-regulated kinases

FA, Fatty acid

FABP, Fatty acid-binding protein

FADH₂, Flavin-adenine dinucleotide (reduced)

FAS, Fatty acid synthase

FasL, Fas ligand

FHS, Framingham Heart Study

FKBP, FK506 binding protein

FS, Fractional shortening

FXYD2, FXYD domain containing ion transport regulator 2

GATA6, GATA-binding factor 6

GH, Growth hormone

GHRH, Growth-hormone-releasing hormone

GHSR, Growth hormone secretagogue receptor

GLUT4, Glucose transporter type 4

GOAT, Ghrelin O-acyltransferase

GPAT, Glycerol-3-phosphate acyltransferase

GSK, Glycogen synthase kinase

HBB, β -globinprotein

HBE, Hemoglobin E

HB-EGF, Heparin-binding EGF-like growth factor

HDL-C, High density lipoprotein-cholesterol levels

HEPES, 4-(2-hydroxyethyl)-1-piperazineethanesulfonic acid

HF, Heart failure

HR, Heart rate

HRP, Horseradish peroxidase

HSD, Honestly significant difference

HSP70, Heat shock 70kDa protein

IBP4, Insulin-like growth factor binding protein 4

IGF, Insulin-like growth factor

IGFBP, Insulin-like growth factor binding protein

IGF-1R, Insulin-like growth factor -1 receptor

I- κ B, nuclear factor of kappa light polypeptide gene enhancer in B-cells inhibitor

IKK, I- κ B kinase

IL-6, Interleukin- 6

IR, Insulin receptor

ITGA2, integrin, alpha 2

ITGAM, Integrin alpha M

ITGB2, Integrin beta-2

ITGB4, Integrin beta 4

JAK, Janus kinase

JNK, c-Jun N-terminal kinase

LC3, Light chain 3

LV, Left ventricle

LVEDD, Left ventricular end-diastolic dimension

LVESD, Left ventricular end-systolic dimension

MAPK, Mitogen-activated protein kinase

MCP-1, Monocyte chemotactic protein-1

MI, Myocardial infarction

MMP, Matrix metalloproteinase

mRNA, messenger RNA

mTOR, Mammalian target of rapamycin

MyD88, myeloid differentiation primary response 88

NADH, Nicotinamide adenine dinucleotide (reduced)

NEFAs, Non-esterified fatty acid

NF- κ B, Nuclear factor-kappa B

NPY, Neuropeptide

NTS, Nucleus tractus solitarii

OD, Optical density

PAI-1, Plasminogen activator inhibitor-1

PBS, Phosphate buffered saline

PBST, Phosphate buffered saline Tween 20

PCR, Polymerase chain reaction

PGC1, Peroxisome proliferator-activated receptor gamma, coactivator 1 alpha

PI3K, Phosphatidylinositol 3-kinase

PKA, Protein kinase A

PKC, Protein kinase C

PLAU, Plasminogen activator, urokinase

PLB, Phospholamban

PPAR, Peroxisome proliferator activated receptor

PTP, Permeability transition pore

PVDF, Polyvinylidene difluoride

PWT, posterior wall thickness;

RAGE, Receptor for advanced glycation end products

RNA, Ribonucleic acid

RSNB, Resistin like gamma

RR, Relative risk;

RyR2, Ryanodine receptor

SDS-PAGE, Sodium dodecyl sulfate polyacrylamide gel electrophoresis

SERCA, Sarcoendoplasmic reticulum calcium transport ATPase

SHBG, Sex hormone-binding globulin

SHP-1, Src homology phosphatase-1

SPARC, Secreted protein acidic and rich in cysteine

STAT, Signal transducers and activators of transcription

TBS, Tris-buffered saline

TBST, Tris-Buffered Saline Tween 20

TCA, Tricarboxylic acid

TCL1A, T-cell leukemia/lymphoma 1A

TGF- β , Transforming growth factor, beta

TIMP, Tissue inhibitor of metalloproteinase

TLR-4, Toll-like receptor 4

TNF, Tumor necrosis factor

TNFR, Tumor necrosis factor receptor

TRAF6, Tumor necrosis factor receptor-associated factor 6

TSG-6, Tumor necrosis factor-stimulated gene 6

TUNEL, Terminal deoxynucleotidyl transferase-mediated dUTP nick end-labeling

UCP3, Uncoupling protein 3

Wnt5a, Wingless-type MMTV integration site family, member 5A

XIAP, X-linked inhibitor of apoptosis protein

CHAPTER 1

Introduction

1.1 Cardiomyopathy: Definition and Classification

Cardiomyopathy, a disease of the heart muscle, results in a change of myocardium structure and impairs pumping function of the heart. It is the most common cause of heart failure that leads to sudden cardiac death. Increasing numbers of people are suffering from cardiomyopathy worldwide and more than 10,000 people die of cardiomyopathy each year in the United States.

Cardiomyopathy has become a significant health problem in the world. Every year in the United States, cardiomyopathy is a contributing factor in almost a quarter million deaths. Currently, about 3 million people are living with cardiomyopathy and approximately 400,000 people are diagnosed each year in the United States. The majority of these people suffer from heart failure – the prevailing clinical manifestation of cardiomyopathy. People with cardiomyopathy are always subject to arrhythmia or sudden cardiac death or both. When cardiomyopathy develops, the heart muscle becomes enlarged or abnormally thick or rigid. The weakening of heart function leads to the reduction of pumping blood through the body and causes heart failure, arrhythmias, fluid buildup in the lungs or legs, and endocarditis (a bacterial infection of the lining of the heart).

According to World Health Organization, cardiomyopathy is classified into four types: dilated, hypertrophic, restrictive, and arrhythmogenic right ventricular dysplasia/cardiomyopathy (Richardson *et al.*, 1996). Additionally,

there is one type of cardiomyopathy named secondary/specific cardiomyopathy which has a clear disease-related cause such as DOX-induced cardiomyopathy and diabetic cardiomyopathy. Various medical outcomes are caused by different types of cardiomyopathy, but all types ultimately have a common outcome – heart failure. With the progress and development of cardiomyopathy, the work efficiency of the heart muscle is gradually reduced. When the heart is not able to pump enough blood to meet the needs of the body, heart failure ultimately occurs.

1.2 DOX-induced Cardiomyopathy

DOX (DOX, Fig. 1.1) was originally isolated from the red pigment-producing bacterium *Streptomyces peucetius* in the early 1950s and was found to have the anti-tumor activity in 1960s (Arcamone *et al.*, 1969). DOX treats effectively leukaemia, Hodgkin's lymphoma, and cancers of the bladder, breast, stomach, lung, and others. However, DOX results in irreversible myocardial damage, which leads to dilated cardiomyopathy with sequential fatal congestive heart failure (Swain *et al.*, 2003). Several underlying mechanisms of the action of DOX in cancer cells have been suggested by researchers including DNA damage and lipid peroxidation from reactive oxygen species generation, DNA breakdown from inhibition of topoisomerase II, DNA cross-linking and alkylation, inhibition of macromolecules synthesis via intercalation into DNA, blocking of DNA strand separation and helicase activity, and interference with DNA replication (Takemura & Fujiwara, 2007).

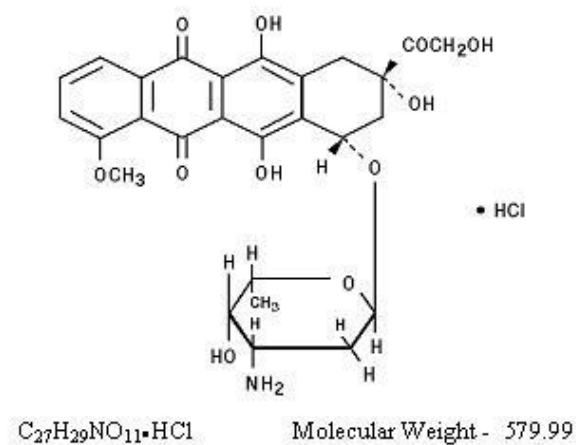


Fig. 1.1 Structure of DOX (Arcamone *et al.*, 1969)

Although the precise mechanisms of DOX-induced cardiotoxicity were not fully understood, the anti-tumor effect of DOX was differentiated from its mechanisms that induce toxicity in cardiomyocytes.

The mechanisms of DOX-induced cardiotoxicity have been the research focus since DOX-induced cardiomyopathy was first documented in the 1970s (Lefrak *et al.*, 1973). Several mechanisms have been suggested to explain the DOX-induced cardiomyopathy including cardiac muscle cell apoptosis (Nakamura *et al.*, 2000); adrenergic dysfunction (Tong *et al.*, 1991); changes in sarcolemmal calcium transport (Olson *et al.*, 2005); and altered cardiac metabolism (Carvalho *et al.*, 2010). DOX-induced cardiotoxicity involves mechanisms that are different from its anti-tumor activity. Difference of anti-tumor action from the cardiotoxic effects of DOX offers a hope that the therapeutic strategies can

be designed to prevent the adverse cardiotoxic effects of DOX but without sacrificing the beneficial anti-tumor ability of DOX.

1.2.1 Epidemiologic Features

DOX induces acute and chronic effects on the cardiovascular system. In response to DOX treatment, approximately 11% of patients showed arrhythmias, hypertension, and electrocardiographic changes (van Acker *et al.*, 1996). The chronic effects of DOX are the progression of the irreversible cardiomyopathy with 1.7% of the incidence and 50% of the mortality rate (Von Hoff *et al.*, 1979) and congestive heart failure in a dose-dependent manner (Fig 1.2). Retrospective analysis demonstrated that more than 4% of patients developed cardiotoxicity at a cumulative dose of 500 to 550 mg/m² of DOX in 339 patients. The incidence of cardiomyopathy induced by DOX rose to ~18% at a dose of 551 to 600 mg/m² and to ~36% at dose of 601 mg/m² or higher (Lefrak *et al.*, 1973). Nonetheless, the other study showed that 21% of patients presented DOX-related cardiotoxicity at a dose of even less than 300 mg/m² (Sawaya *et al.*, 2011). After the treatment of DOX, the congestive heart failure occurred and presented a peak incidence after 1 to 3 months (Von Hoff *et al.*, 1977).

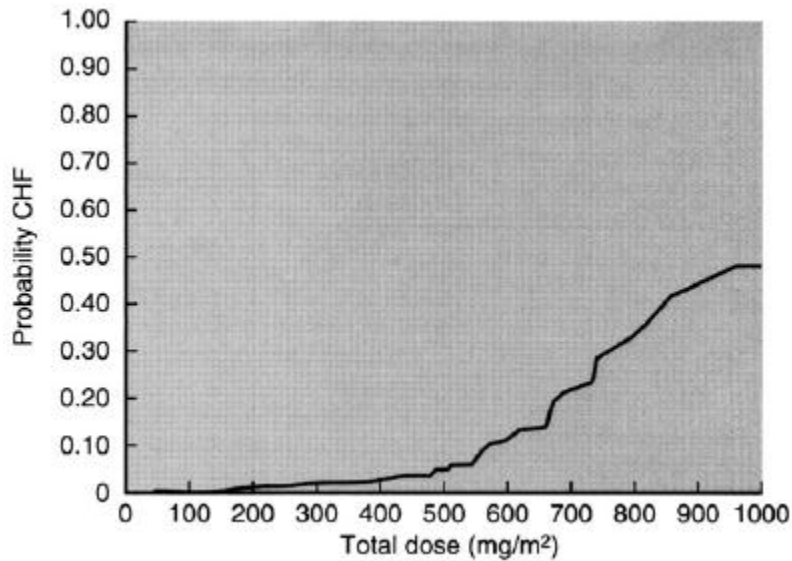


Fig 1.2 Cumulative probability of developing DOX-induced congestive heart failure vs total cumulative dose of DOX in 3,941 patients (Takemura & Fujiwara, 2007)

1.2.2 Pathologic Features

The development of histological changes of myocardium affected by DOX were shown in Fig 1.3 (Simunek *et al.*, 2004) and Table 1.1 (Rahman *et al.*, 2007). In the stage of grade 1, myocardium showed the normal appearance with the increased eosinophilia of cardiomyocyte cytoplasm (E) and scatter necrotic cells (N). DOX led to the dilatation of the sarcoplasmic reticulum, which further induced cytoplasmic vacuolization and myofibrillar loss of cardiomyocyte. Gradually, the connective tissue replaced the damaged cardiac muscle cells, which induced the development of interstitial myofibrosis and fibrotic scars (S) shown in histopathological changes of score 4 and 5. Such cellular changes eventually caused cardiac remodeling and heart failure

(Rahman *et al.*, 2007).

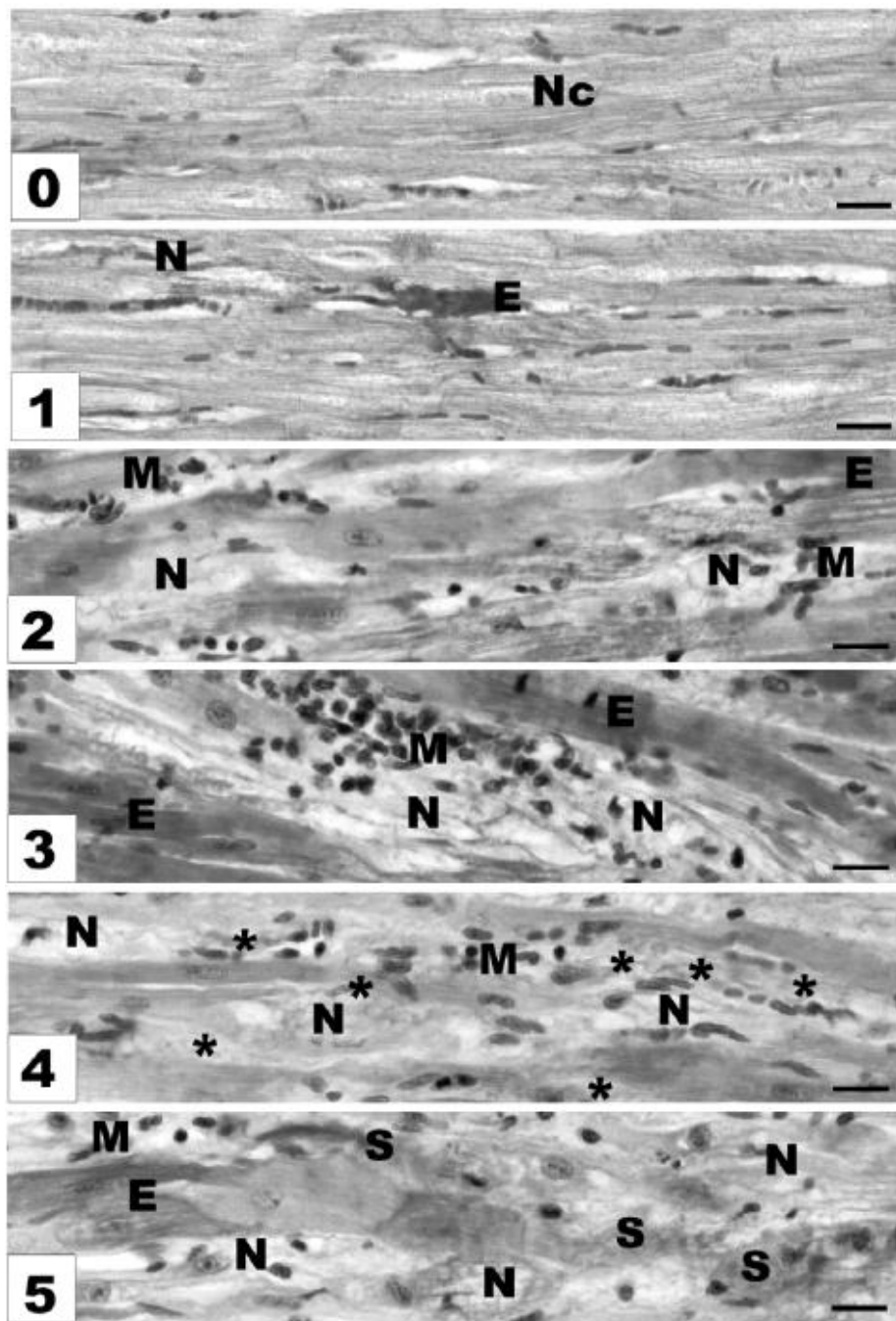


Fig 1.3 Development of histopathological changes in the myocardium of rabbit model response to DOX (Simunek *et al.*, 2004)

Table 1.1 Morphologic grading system for DOX cardiotoxicity (Rahman *et al.*, 2007)

Grade	Billingham scoring system (Billingham et al 1978) morphologic characteristics	Mackay scoring system (Mackay et al 1994; Ewer et al 1984)		
		Vacuoles	Myofibrillar dropout	Necrosis
0	Normal myocardial ultrastructural morphology			
0.5	Not completely normal but no evidence of anthracycline-specific damage	<4	0	1
1	Isolated myocytes affected and/or early myofibrillar loss; damage to <5% of all cells	4–10	<3	1
1.5	Changes similar to grade 1 except damage involves 6%–15% of all cells	>10	3–5	<2
2	Clusters of myocytes affected by myofibrillar loss and/or vacuolization, with damage to 16%–25% of all cells	any number	6–8	2–5
2.5	Many myocytes (26%–35% of all cells) affected by vacuolization and/or myofibrillar loss	(The grade of 2.5 is not included in the Mackay grading system)		
3	Severe, diffuse myocyte damage (>35% of all cells)	any number	>8	>5

1.2.3 Current Treatment

The treatment of cardiomyopathy mainly aims to reduce the symptoms and complications of cardiomyopathy and to optimize the efficiency of the weakening heart. The most common treatment remains medication including digitalis (to improve the contractile function of heart muscle), diuretics (to reduce the excess fluid retention), angiotensin converting enzyme (ACE) inhibitors (to decrease the work of the heart by dilating blood vessels in the body), and beta blockers (to block the effect of adrenaline in the body). In addition, some new medical interventions are being developed to treat cardiomyopathy, including cardiac transplantation, anti-arrhythmic therapy, cardiac resynchronization therapy and stem cell therapy. However, there are still many obstacles in curing cardiomyopathy. The reason for the lack of ideal treatment strategies is mainly due to the incomplete understanding of the

pathogenesis of cardiomyopathy. Recently, cardiomyocyte loss due to apoptosis has been reported to play a very important role in the development and progression of cardiomyopathy. Potential therapeutic strategies to inhibit and reduce cardiac apoptosis could have a clinical benefit on regressing cardiomyopathy progression beyond the alleviation of symptoms.

1.2.4 Molecular Mechanisms

1.2.4.1 Cardiac Apoptosis

Apoptosis, a form of cell death, is characterized by loss of cell volume, plasma membrane blebbing, nuclear condensation, chromatin aggregation, and endonucleolytic DNA degradation. The molecular mechanisms of apoptosis have been documented in cardiomyocytes. The balance between pro-survival and pro-death cell signals is tightly regulated in cardiomyocytes. The caspases, a family of intracellular proteases, play a key role in the terminal morphologic and biochemical changes during apoptosis. There are two main apoptotic pathways, the “extrinsic” and “intrinsic” cascades, in cardiac apoptosis. The extrinsic pathway involves the cell surface death receptors (e.g. tumor necrosis factor receptor superfamily of proteins, TNFR, and Fas receptor). The extracellular ligands (e.g., TNF and Fas Ligand, FasL) bind to their receptors and result in the activation of caspases via the signaling pathways such as MAP kinase, NF- κ B and Akt signaling to induce apoptosis. On the other hand, the intrinsic pathway is associated with the mitochondria to mediate the apoptotic signaling. Through the increase in the mitochondrial permeability transition

pore (PTP), pro-apoptotic factors (e.g., cytochrome c, Smac/DIABLO, endonuclease G, Omi/Htr A2 and apoptosis-inducing factor) are released to the cytosol. Once released, the binding of cytochrome c to cytosolic protein Apaf1 promotes the formation of the “apoptosome” complex that results in the activation of caspase-9 followed by the caspase-3 activation (Fig 1.4).

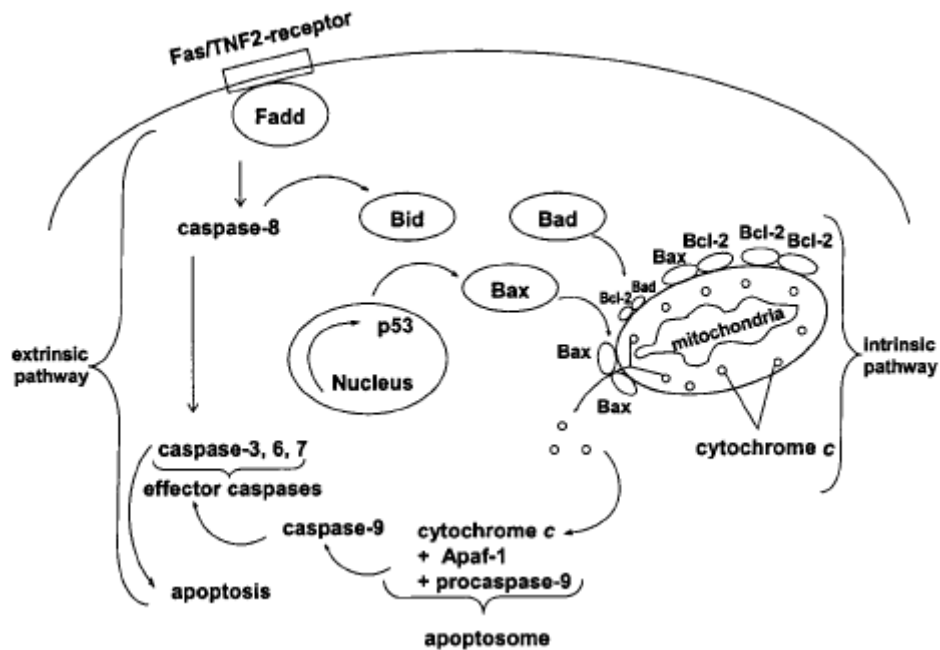


Fig 1.4 Two main apoptotic pathways in cardiac apoptosis (Kalyanaraman *et al.*, 2002)

Myocardial apoptosis is an essential determinant of cardiac pathogenesis because it results in a loss of contractile units, conduction disturbances, compensatory hypertrophy of myocardial cells, and fibrosis. Ample evidence shows that apoptosis plays a key role in the pathogenesis and progression of various etiological cardiomyopathies including those attributed to ischemia-reperfusion, toxic exposure such as DOX, and chronic diseases such as diabetes

mellitus and hypertension. In the recent years, there has been great breakthrough in understanding the molecular mechanisms that are involved in cardiomyopathy. Cardiac apoptosis has been shown as an important process in the development and progression of cardiomyopathy. Apoptosis is a systematically-regulated process and is a novel potential therapeutic target for alleviating cardiomyopathy. In the treatment of cardiomyopathy and heart failure, inhibiting cardiac apoptosis has become one of the potentially effective regimens. There is a variety of apoptotic stimuli in the animal models of cardiomyopathy and heart failure by using different species. That might explain why the results of cardiac apoptosis measured by terminal deoxynucleotidyl transferase-mediated dUTP nick end-labeling (TUNEL) assay are controversial in the literature. The apoptotic index varied from 0.42% as reported by Nakamura and colleagues in 2000 to 23.8% as reported by Liu and coworkers in 2008 (Nakamura *et al.*, 2000;Liu *et al.*, 2008). However, even though the percentage of cardiac apoptosis in the heart is not in the high range in some cases, it is already markedly elevated when compared to the normal heart. Most importantly, the cardiac function is evidently demonstrated to be considerably improved once the apoptosis of cardiomyocytes is inhibited by the experimental interventions (Chen *et al.*, 2007).

In cancer chemotherapy, DOX is one of the most effective drugs used frequently to treat many hematologic and solid tumor malignancies including breast cancer, leukemia, and sarcomas. However, DOX results in irreversible

myocardial damage, which leads to dilated cardiomyopathy with sequential fatal congestive heart failure (Swain *et al.*, 2003). It has been demonstrated that cardiomyocyte apoptosis is a key element in the development of DOX-induced cardiomyopathy (Nakamura *et al.*, 2000). Different from its anti-neoplastic activity via a cytostatic mechanism of tumor cell apoptosis, DOX induces a direct decrease in the reductase domain of the endothelial nitric oxide synthase (eNOS), which results in enhanced superoxide formation (Vasquez-Vivar *et al.*, 1997). Recently, Kalivendi and colleagues reported that DOX-induced apoptosis was associated with intracellular H₂O₂ formation and the increased transcription of eNOS expression (Kalivendi *et al.*, 2001).

1.2.4.2 Cardiac Fibrosis

Cardiac fibrosis is the proliferation of fibroblasts in the heart muscle. Fibrosis has been shown to cause cardiac stiffness and dysfunction in DOX-induced cardiotoxicity (Miyata *et al.*, 2010; Li *et al.*, 2007), ischemic, and hypertrophic cardiomyopathy (Khan & Sheppard, 2006). The increased collagen synthesized by the fibroblasts invades and replaces the necrosed or apoptotic myocytes (Khan & Sheppard, 2006; Diwan *et al.*, 2008). The excessive deposition of extracellular matrix (ECM) disturbs the mechano- electric coupling of cardiomyocytes and induces pathological signaling (de Bakker *et al.*, 1996).

Connective tissue growth factor (CTGF), a pro-fibrotic cytokine, acts as a downstream and cooperative mediator of TGF- β 1 in the fibrogenic process.

CTGF promoter activity was regulated by TGF- β 1/Smad (Smad2 and Smad3) cascade (Holmes *et al.*, 2001). Wang and colleagues reported that the interaction between TGF- β and CTGF is necessary for the development of multiorgan fibrosis, renal fibrosis, and pulmonary fibrosis (Wang *et al.*, 2011). Furthermore, the histologic signs and the pathologic severity of fibrosis were ameliorated by the treatment of human anti-CTGF antibody FG-3019 (Wang *et al.*, 2011).

1.2.4.3 Cardiac Metabolism

1.2.4.3.1 Metabolism in the Normal Heart

Cardiac metabolism is critical in maintaining the myocardial function. Energy is synthesized and transferred in the form of energy-rich adenosine triphosphate (ATP) to maintain excitation-contraction coupling in muscle cells. In the normal heart, almost all the ATP generation (>95%) are derived from mitochondrial oxidative phosphorylation. Furthermore, the adult healthy heart predominantly (~60-90%) metabolizes fatty acids to generate ATP under aerobic condition, while the fetal myocardial phenotype uses mainly glucose as its substrate for ATP production (Fig 1.5). Once transported across the myocardial cell membrane, fatty acids are esterified to fatty acyl-CoA by fatty acyl-CoA synthetase. Acyl-CoA moieties are transported across the outer mitochondrial membrane and converted to long chain fatty acylcarnitine by carnitine palmitoyltransferase I (CPT I), which is a rate-limiting enzyme in fatty acid oxidation. Once across the mitochondrial matrix, fatty acids subsequently undergo β -oxidation. The gene expression and activity of the β -

oxidation enzymes are highly regulated by some transcription factors such as PPAR α , PPAR β and PGC-1 α . Acetyl-CoA is released from fatty acyl-carnitine by reacting with coenzyme A. Acetyl-CoA then enters the tricarboxylic acid cycle (TCA cycle) to generate NADH and FADH₂, which are subsequently used in the electron transport chain to produce ATP.

The substrate of mitochondrial metabolism is affected by several conditions including changes in hormone state, workload, and oxygen supply to the heart. Cardiac metabolism is tightly regulated to produce accurate amounts of ATP because of the limited reservation of energy in the heart. The metabolic pathway in the heart is complicated and associated with cardiac diseases including DOX-induced cardiomyopathy, diabetic cardiac dysfunction, and ischemic heart failure.

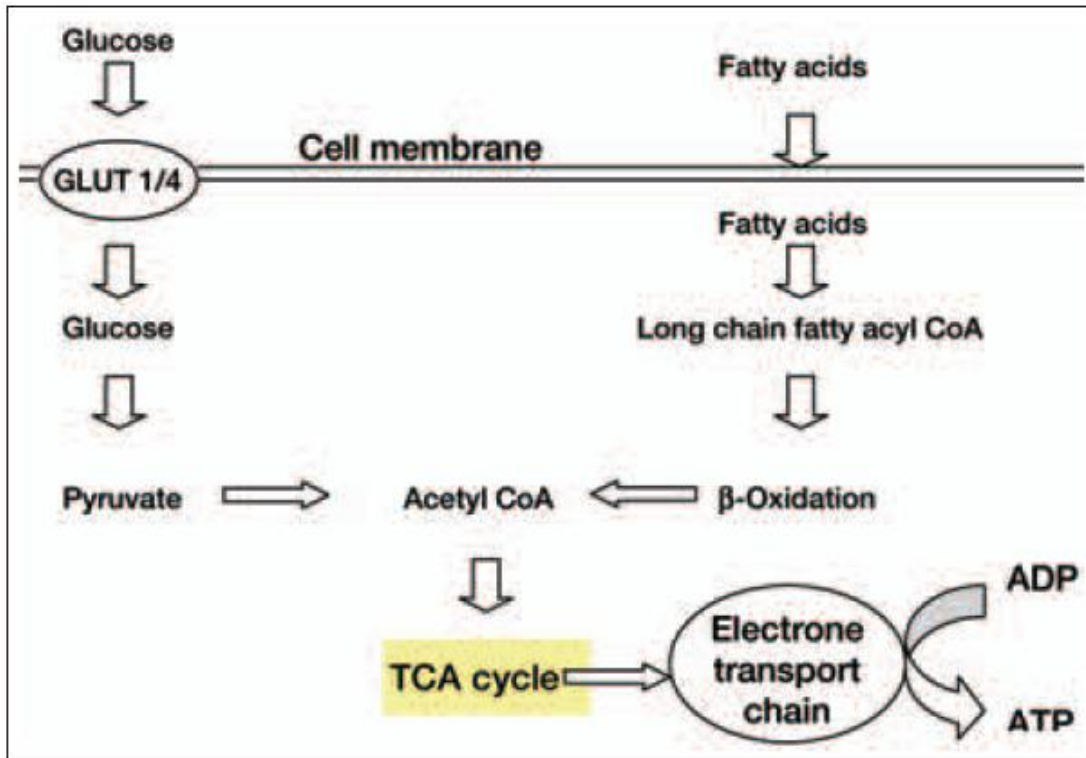


Fig 1.5 Substrates of myocardial metabolism (Ussher et al. 2006)

1.2.4.3.2 The Effect of DOX on Metabolic Signaling Pathway in Heart

The precise mechanisms for the development of the DOX-induced cardiomyopathy have not been fully elucidated. It has been proposed that fatty acid oxidation in the heart was inhibited by DOX (Carvalho *et al.*, 2010; Mitra *et al.*, 2008; Hong *et al.*, 2002; Bordonni *et al.*, 1999; Sayed-Ahmed *et al.*, 1999) and the utilization of substrates was decreased (Wakasugi *et al.*, 1993). A decrease in long chain fatty acid was observed in isolated cardiomyocytes treated with DOX (Tokarska-Schlattner *et al.*, 2006). The impairment of CPT-1 was suggested to be involved in the underlying mechanisms. CPT-1 is located

in the outer membrane of mitochondria and is a critical enzyme in regulating the fatty acid oxidation. It is not surprising that CPT-1 activity was inhibited by DOX exposure (Table 1.2). Choi and colleagues demonstrated that DOX down-regulated the gene expression of CPT-1 in H9c2 cardiomyocyte (Choi *et al.*, 2008). They further demonstrated that the elevated *CPT-1* gene expression increased the resistance to cardiac cell injury induced by DOX. Peroxisome proliferator-activated receptor- α (PPAR- α) is a key regulator of lipid and glucose metabolism in the heart. Gene expression of PPAR- α in the heart has been shown to be down-regulated by DOX treatment (Mitra *et al.*, 2008).

Mitochondrial oxidative metabolism is critical to the ATP generation in cardiac muscle cells. The mitochondrial function and biogenesis are the important and essential agents in maintaining cardiac function. The alteration of a key transcription factor PPAR γ co-activator (PGC-1 α) in control of mitochondrial function and biogenesis is thus investigated in DOX-induced cardiotoxicity. Miyagawa and co-workers observed that DOX significantly reduced the gene expression of PGC-1 α in the heart (Miyagawa *et al.*, 2010). They reported that the DOX-induced cardiomyopathy and mitochondrial damage were attenuated when the mitochondrial biogenesis was protected by upregulating the level of PGC-1 α .

Table 1.2 DOX-induced changes in cardiac metabolism

Author, date	Model	Species	Affected parameters
(Yoon <i>et al.</i> , 2003)	Animal model	Rat	Decreased CPT1 activity
(Choi <i>et al.</i> , 2008)	H9c2 cardiomyocyte	Rat	Down-regulation of CPT-1 mRNA level
(Mitra <i>et al.</i> , 2008)	Animal model	Rat	Down-regulation of PPAR α mRNA expression
(Miyagawa <i>et al.</i> , 2010)	Animal model	Mice	Decreased mRNA levels of PGC-1 α

1.2.4.4 Cardiac Calcium Signaling

1.2.4.4.1 Calcium Signaling Pathway in the Normal Heart

Calcium-dependent signaling is critical in the myocardial function (Fig 1.6). Intracellular calcium release from the sarcoplasmic reticulum (SR) stimulates heart muscle contraction. Indeed, the calcium concentration in the cytosol of cardiomyocyte is varied from a resting level of ~100 nM to 1 μ M during the cardiac systole (Bers, 2002). Therefore, the disturbance in calcium signaling has been proposed to be involved in different heart disorders. During each heart pumping cycle, cardiac contraction is triggered by the influx of calcium through L-type calcium channels located in the heart cell membrane. Calcium release from the sarcoplasmic reticulum through the ryanodine receptor (RyR) is

further induced by the elevation of intracellular calcium. Calcium then binds to troponin C in the contractile apparatus, which initiates cardiac muscle contraction; then sarcoplasmic reticulum Ca^{2+} -ATPase (SERCA) pumps calcium back into the sarcoplasmic reticulum and results in cardiac relaxation. The ability of SERCA depends on its interaction with phospholamban, which is an integral membrane protein. Under the non-phosphorylated condition, phospholamban inhibits the re-uptake of calcium into the sarcoplasmic reticulum by SERCA. Phosphorylation of phospholamban induced by Protein kinase A (PKA) diminishes its inhibitory ability, which can promote cardiac relaxation (Olson, 2004).

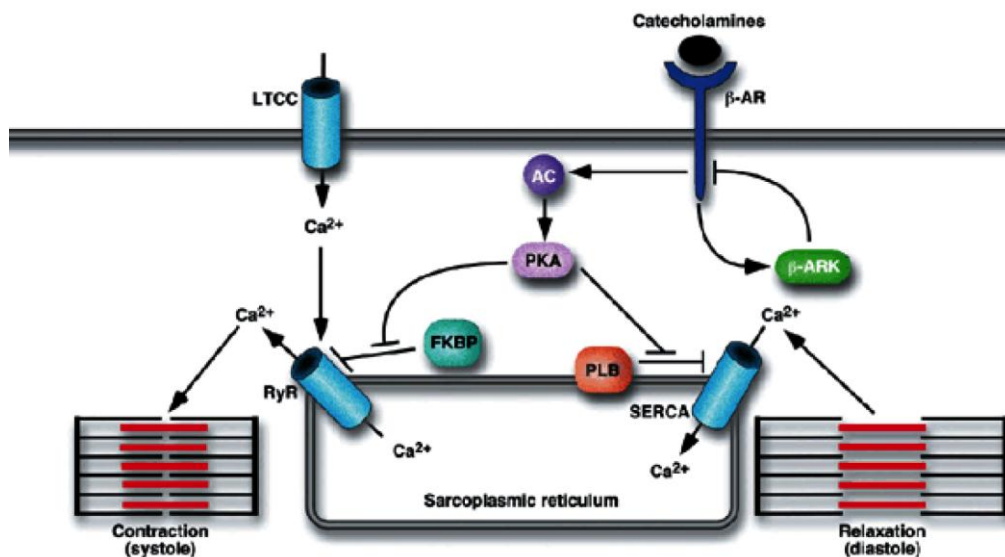


Fig 1.6 Calcium signaling in heart (Olson, 2004)

1.2.4.4.2 The Effect of DOX on Calcium Signaling Pathway in

Heart

Altered calcium handling is a key pathophysiological process in DOX-induced cardiomyopathy, leading to the decreased contractile ability and transcriptional activity (Ventura-Clapier *et al.*, 2004; Tian *et al.*, 1998). Extensive studies have demonstrated that DOX has a unique effect on cardiac-specific gene expression in calcium signaling pathway (Table 1.3). However, the reported changes of gene expression are not totally consistent. Arai and co-workers (Arai *et al.*, 1998) determined whether gene expression in calcium handling was altered in the heart chronically treated with DOX in a rabbit model. They observed that mRNA level of RyR2, SERCA2a, phospholamban were significantly diminished by the treatment of DOX. In contrast to their results, decreased gene expression of RyR2 has been shown in the other studies (Gambliel *et al.*, 2002; Olson *et al.*, 2005). Arai and colleagues administrated DOX to rabbits by intravenous injection at a dose of 2.5 mg/kg once a week for 8 weeks whereas Gambliel *et al.* and Olson *et al.* treated the rabbits with DOX by intravenous injection with a dose of 1 mg/kg twice weekly for 8 weeks. Taken together, these findings suggested that the chronic effects of DOX on the cardiac-specific gene expression in calcium signaling pathway is largely dependent on the dosage of DOX administered.

For the SERCA, Su and colleagues have demonstrated that the SERCA2a mRNA level was decreased and the *RyR2* gene expression is not affected

following six equal doses of DOX (cumulative dose, 12 mg/kg) over a period of 2 weeks in rat hearts (Su *et al.*, 2009). Intriguingly, they demonstrated that the impaired cardiac function and survive were significantly improved by attenuating the changes of SERCA2a expression in the injured hearts.

Table 1.3 DOX-induced changes in cardiac calcium signaling

Author, date	Model	Species	Affected parameters
(Berdichevski <i>et al.</i> , 2010)	Isolated cardiomyocyte	Rat	Down-regulation of gene expression of SERCA2a
(Su <i>et al.</i> , 2009)	Animal model	Rat	Decreased mRNA expression of SERCA2a
(Olson <i>et al.</i> , 2005)	Animal model	White rabbit	Regressed mRNA levels of RyR2
(Huang <i>et al.</i> , 2003)	Animal model	Rabbit	Decrease of SERCA2a mRNA level
(Gambliel <i>et al.</i> , 2002)	Animal model	Rabbit	Decreased gene expression of RyR2
(Arai <i>et al.</i> , 1998)	Animal model	White rabbit	Diminished mRNA level of RyR2, SERCA2a, phospholamban

1.3 Diabetic Cardiomyopathy

Diabetes mellitus has become a major chronic disease worldwide because of the growing prevalence of obesity and lack of physical activity. The International Diabetes Federation (IDF) reported that approximately 347 million people lived with diabetes in 2011 and the prevalence is expected to rise to 552 million in 2030 (Whiting *et al.*, 2011). The death rate from diabetes was 4.6 million in 2011, an increase of 13.3% from the estimates in 2010 (Roglic & Unwin, 2010). Cardiovascular disease accounts for 50-80% of deaths in diabetic patients. Patients with diabetes have a higher risk of atherosclerotic coronary artery disease than non-diabetic people (Voulgari *et al.*, 2010). Rubler and coworkers first proposed a new type of cardiomyopathy for diabetes according to four diabetic patients who developed congestive heart failure but no coronary arteries, hypertension, or other etiologies (Rubler *et al.*, 1972). Increasing amount of studies have demonstrated the presence of diabetic cardiomyopathy in patients with diabetes (Voulgari *et al.*, 2010). Clinically, diabetic cardiomyopathy is identified by the asymptomatic diastolic dysfunction with delayed opening of the mitral valve, followed by decreased ejection and systolic dysfunction in the late cardiac stage. Voulgari and colleagues defined diabetic cardiomyopathy as “the cardiovascular damage present in diabetes patients, which is characterized by myocardial dilatation and hypertrophy, as well as a decrease in the systolic and diastolic function of the left ventricle, and its presence is independent of the coexistence of ischemic heart disease or hypertension” (Voulgari *et al.*, 2010).

1.3.1 Epidemiologic Features

The prevalence of diabetic cardiomyopathy is alarmingly high; recent studies have demonstrated a prevalence of 40% to 60% in diabetic patients by using Doppler ultrasound (Bertoni *et al.*, 2003) and 48% in diabetic patients by echocardiography (Kiencke *et al.*, 2010). The Framingham Heart Study (FHS) showed that diabetes is a risk factor of cardiovascular disease; the incidence of heart failure is twice in men with diabetes and five times in diabetic women compared with the age-matched healthy controls (Kannel & McGee, 1979). The key echocardiographic findings and the incidence of diabetic cardiomyopathy were summarized by Voulgari and colleagues and shown in Table 1.4 (Voulgari *et al.*, 2010).

Table 1.4 Main and recent echocardiographic, population-based studies on diabetic cardiomyopathy (Voulgari *et al.*, 2010)

Population sample	Findings	Incidence of DCM
186 type 2 diabetes patients with normal ejection fraction	Systolic dysfunction: ↓ peak strain and ↓ strain rate ↑ calibrated IB (myocardial reflectivity)	15.8% in both sexes
41 diabetes patients with normal resting LV function and a normal dobutamine echo	↓ peak myocardial systolic velocity ↓ early diastolic velocity	16% subtle dysfunction in both sexes
35 type 2 diabetes patients	↓ longitudinal peak systolic velocity at rest and at peak stress, ↓ functional reserve, ↑ radial systolic velocity	20% in both sexes
134 type 2 diabetes patients	↓ mean peak systolic early + diastolic velocity, ↓ mean isovolumic relaxation time, ↑ systolic + diastolic synchronicity	20% in both sexes

Abbreviations: DCM, diabetic cardiomyopathy; IB, integrated backscatter.

1.3.2 Pathologic Features

The morphologic features of diabetic heart include matrix collagen deposition, interstitial fibrosis, and lipid accumulation (Maya & Villarreal, 2010).

1.3.2.1 Cardiac Fibrosis

Cardiac fibrosis is a major pathological feature of type 2 diabetic cardiomyopathy. The reduction of integrated backscatter (myocardial ultrasound reflectivity) from echocardiographic analysis indicates the fibrosis of heart tissue in diabetic patients (Asbun & Villarreal, 2006). Fibrosis has been reproducibly demonstrated in the experimental animal model of type 2 diabetes. Excess deposition of collagen has been found in the diabetic heart. Cardiac necrosis and fibrosis in diabetes are resulted from the activation of myocardial rennin-angiotensin and endothelin system (Chen *et al.*, 2000b). Collagen type I and III mainly accumulated in the epicardial and perivascular regions and collagen type IV predominated in the endocardium. In the diabetic heart, the interaction of collagen and glucose formed Schiff bases and further glycated collagen. Advanced glycation end products are eventually formed via the chemical modification of glycated collagen and contribute to myocardial stiffness. Advanced glycation end products also exert a role in cross-linking of collagen and low-density lipoprotein, as well as affect the nitric oxide signaling via interacting with advanced glycation end-product receptors. Therefore, decreased cardiac reflectivity and impaired left ventricle function in diabetic patients can be explained by increased fibrosis and abnormal collagen

deposition (Aronson, 2003).

The molecular mechanism underlying the myocardial fibrosis in diabetes is not fully understood. It is reported that the excessive collagen deposition and extracellular matrix synthesis resulted from overexpression of transforming growth factor- β 1 stimulated by hyperglycemia and hyperinsulinemia in diabetes (Mizushige *et al.*, 2000). CTGF expression might also contribute to cardiac fibrosis. Interestingly, transgenic PKC- β 2 mice showed increased CTGF expression in the myocardium, suggesting that CTGF may act directly or indirectly with other cytokines to induce cardiac fibrosis.

1.3.2.2 Lipid Accumulation

The presence of lipid accumulation in a heart depends on the uptake, transport and storage of fatty acids (FA). In diabetic status, the storage ability of adipose tissue is low and becomes hypertrophic, which leads to the release of pro-inflammatory cytokines. This in turn suppresses insulin signaling and increases the release of free fatty acids and lipid accumulation as shown in Fig 1.7 (Kankaanpaa *et al.*, 2006; Sharma *et al.*, 2004). The uptake of plasma free fatty acids is regulated by a flip-flop mechanism via passive diffusion and facilitated by a protein-mediated process (van de *et al.*, 2011). There are three critical groups of FA transporters in heart muscle: CD36 (human homologue of FA transporter protein), FABP-pm (plasma membrane fraction of FA-binding protein), and FATP1, 4 and 6 (FA translocase Protein 1, 4 and 6) (Glatz *et al.*,

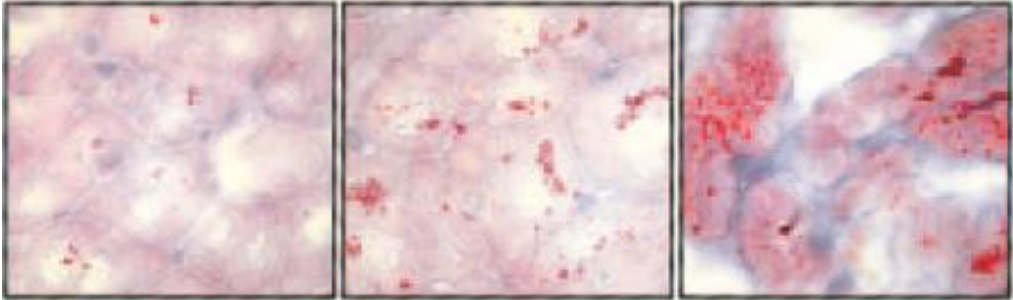
2010).

CD36 was shown to be responsible for up to 60% of the fatty acid uptake in the heart. Over-expression of CD36 in the cardiac muscle has been demonstrated to increase the fatty acid uptake and metabolism whereas knockdown of CD36 was shown to reduce the rate of fatty acid uptake and fatty acid metabolism (Bonen *et al.*, 2004). Cardiac-specific FATP-1 over-expression has been demonstrated to increase fatty acid uptake by 4-fold and cardiac lipid accumulation by 2-fold (Chiu *et al.*, 2005). It has been speculated from the studies in skeletal muscle that FATP-1-facilitated fatty acid uptake might mainly serve the fuel oxidation, though evidence in the heart is still lacking. Also, very little is known about the physiological stimuli that regulate the expression of FATP-1 (Nickerson *et al.*, 2007). FATP-4 is expressed in cardiac tissue but the contribution to lipid uptake in cardiac tissue is still undetermined (Nickerson *et al.*, 2009).

In addition to fatty acid uptake, triglyceride storage and lipolysis in cardiomyocytes also control the fate of fatty acids. Glycerol-3-phosphate acyltransferase (GPAT) is an important rate-limiting enzyme in triglyceride synthesis, which is suppressed by AMPK activation stimulated by Acetyl-CoA carboxylase (ACC). Knockout of GPAT1 was found to protect mice from a high fat diet-induced cardiac fat accumulation and cardiac dysfunction (Lewin *et al.*, 2008). Moreover, another enzyme, diglyceride acyltransferase (DGAT),

has also been shown to be associated with lipid accumulation (Glenn *et al.*, 2011).

a.



b.

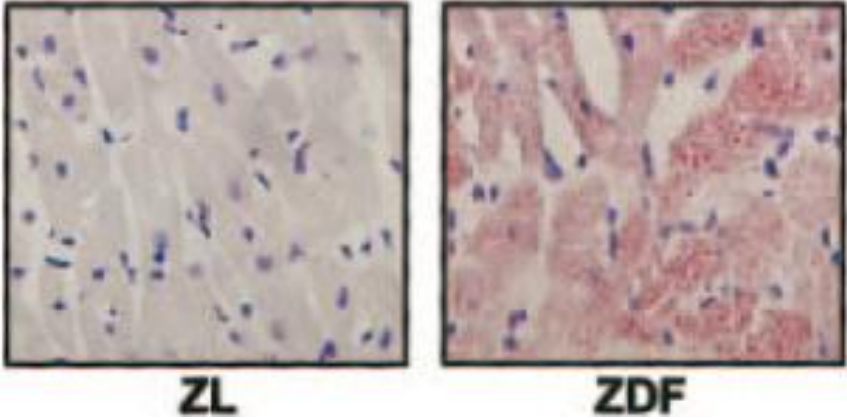


Fig 1.7 Representative photomicrographs of intramyocardial lipid accumulation in heart of type 2 diabetic patients (a) and Zucker diabetic fatty rat (b). lipid droplet was stained as the orange color by oil red O (Sharma *et al.*, 2004)

1.3.3 Current Treatment

The therapeutic strategies focus on the prevention of the development of diabetic cardiomyopathy in the early stages and the reduction of the incidence of diabetic cardiomyopathy or heart failure, as shown in Table 1.5 (Voulgari *et al.*, 2010; Kannel & McGee, 1979). Moreover, several potential treatments targeting the alleviation of the increased fibrosis or disturbed cardiac metabolism are under investigation in the experimental stages. These treatments include the manipulation of advanced glycation end product inhibitors or cross-link breakers, copper chelater and regulators of fatty acid metabolism (Aneja *et al.*, 2008).

Table 1.5 Major studies on treatment strategies of diabetic cardiomyopathy (Voulgari *et al.*, 2010)

Type of diabetes	Intervention	Purpose	Follow-up period	Treatment regimen	Results
2	Diet/ exercise	↓ incidence of DCM	6y	Control (n=195) vs exercise (n=211) vs diet + exercise (n=194)	33% ↓ in the diet group 47% ↓ in the exercise group 38% ↓ in the diet + exercise
2, newly diagnosed	Prolonged dietary management	↓ DCM incidence ↓ of cardiovascular mortality	10y	Diet alone (n = 219) vs diet + tolbutamide 500 mg/metformin twice a day (n = 140) vs insulin (n = 73)	1.04 RR for MI per ↑ 1 mmol/L in fasting plasma glucose, no difference between treatments for the risk of MI
2	Simvastatin	Prevention of	5.4y	Placebo vs simvastatin	55% ↓ in CVD risk

	20 to 40 mg	recurrent CVD in DCM		20 to 40 mg per day	
2	Gemfibrozil 1,200 mg/day	Changes in plasma lipids could reduce major CVD events	7y	Placebo (n = 1.267) vs gemfibrozil 1,200 mg/day (n = 1.264)	22% ↓ of CVD events for every 5 mg/dL ↑ in HDL-C, there was an 11% ↓ in CVD events
2	Diuretic or Ca-blocker or ACE	Differences in CVD risk between antihypertensive regimens	4.9y	Diuretic (chlorthalidone 12.5 to 25 md/d, n = 15.255) or Ca-blocker (amlodipine 2.5 to 10 mg/d, n = 9.048), or ACE inhibitor (lisinopril 10 to 40 mg/d, n = 9.054)	10.2% ↑ risk of HF with amlodipine 19% ↑ risk of HF with lisinopril 33.3% ↑ risk of DCM with lisinopril, better blood pressure control with chlorthalidone
2	Ramipril 10 mg/day	Prevention death from CVD, MI, allcause mortality, HF, DCM, development of diabetes	5y	Placebo (n = 4.652) vs ramipril (n = 4.645)	6.1% ↓ of CVD death 9.9% ↓ of MI 10.4% ↓ of all-cause death 9% ↓ of HF 6.4% ↓ of DCM 3.6% ↓ in new diabetes
2	Felodipine 5 mg/day	Achievement of blood pressure targets with the addition of ASA and association to DCM and CVD risk	3.8y	Felodipine 5 mg/d + ASA vs felodipine 5 mg/d + placebo	51% ↓ of CVD risk in target #135/80 mm Hg + 15% ↓ of CVD risk with ASA and 36% ↓ in MI
2	Losartan 50 to 100 mg/d	↓ of CVD risk with losartan vs atenolol	4.7y	Losartan 50–100 mg/d (n = 586) vs atenolol 50–100 mg/d (n = 609)	76% ↓ of relative CVD risk

				With irbesartan:
	↓ of blood pressure		Irbesartan (300 mg/d,	37% ↓ risk of doubling
2	76% ↓ of relative	provides protection	n = 579) vs amlodipine	serum creatinine
	CVD risk	against progression	(10 mg/d, n = 567)	23% ↓ risk of end-stage
		of nephropathy	vs placebo	renal disease
				23% ↓ risk of HF

Abbreviations: DCM, diabetic cardiomyopathy; RR, relative risk; MI, myocardial infarction; CVD, cardiovascular disease death; HF, heart failure; HDL-C, high density lipoprotein-cholesterol levels; Ca-blocker, calcium channel blocker; ACE, angiotensin-converting-enzyme; ASA, acetylsalicylic acid.

1.3.4 Molecular Mechanisms

1.3.4.1 Cardiac Apoptosis

Cardiac apoptosis is one of the most essential mechanisms in the development of diabetic cardiomyopathy and it occurs both at the early phase and the late stage of diabetic cardiomyopathy (Cai & Kang, 2003). In human research, an 85-fold increase in apoptosis and a 4-fold increase in necrosis present in the hearts of the patients with type 2 diabetes (Frustaci *et al.*, 2000). High glucose-induced cardiac apoptosis was mediated by the production of monocyte chemotactic protein-1 (MCP-1) and the induction of a novel zinc-finger protein in H9c2 cardiomyoblasts and isolated neonatal rat cardiomyocytes (Younce *et al.*, 2010). Ample evidence showed that cardiomyopathy presented in the animal model of type 1 diabetes (i.e., diabetic rats and mice induced by streptozotocin) (Cai *et al.*, 2006; Borges *et al.*, 2006) and type 2 diabetes (i.e.,

Zucker diabetic fatty rats and db/db mice) (Belke *et al.*, 2000;Young *et al.*, 2002). Furthermore, in the animal model of type 1 and type 2 diabetes, elevated cardiac apoptosis was observed in the hearts (Fiordaliso *et al.*, 2000;Barouch *et al.*, 2006). In the diabetic rats and mice induced by streptozotocin, cardiac apoptosis markedly increased on day 3-14 and decreased on day 28 after streptozotocin treatment (Cai *et al.*, 2002). Young db/db mice (2 to 3-month-old) showed obviously elevated cardiac apoptosis compared with wild type controls (Barouch *et al.*, 2006). Diabetic cardiomyopathy can occur in the absence of vascular diseases but the co-existence of hypertension accelerates the progress of diabetes. There is no difference in the cardiac apoptosis found in diabetic patients with hypertension versus diabetic patients without hypertension. This suggests that cardiac apoptosis in the diabetic patients is solely affected by diabetes (Frustaci *et al.*, 2000).

Currently, the precise mechanisms by which diabetes mellitus induces myocardial apoptosis are not clearly understood. There are several possible mechanisms for the increase in cardiac apoptosis depending on the metabolic disturbances in diabetes (Fig 1.8). The two most important metabolic changes in diabetes are hyperglycemia and hyperlipidemia (usually increase in triglycerides and non-esterified fatty acid, NEFAs) and these conditions are suspected to be involved in inducing cardiac apoptosis in cardiomyocytes.

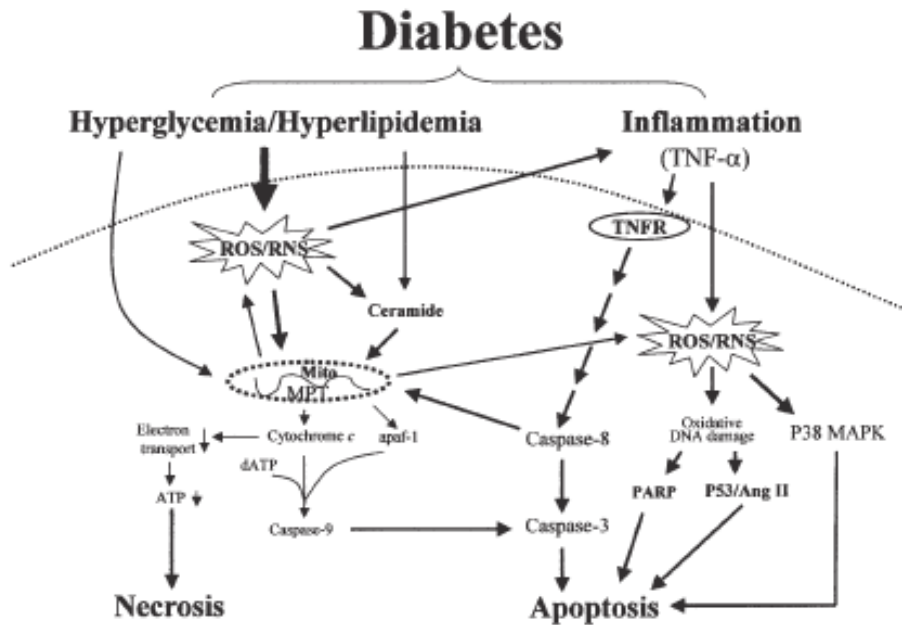


Fig 1.8 Possible mechanisms by which diabetes mellitus induces myocardial cell death

(Cai & Kang, 2003)

Hyperglycemia

Diabetes-induced cardiac apoptosis is supported by the *in vitro* findings. Exposure of rodent H9c2 myoblast cells and adult cardiomyocytes to high levels of glucose showed an increase in apoptotic cell death. However, elevation of apoptosis was not observed when exposed to the same concentration of mannitol (Cai *et al.*, 2002; Shizukuda *et al.*, 2002). Cai and colleagues reported that there was no significant increase in cardiac apoptosis in the mice treated with streptozotocin without hyperglycemia. Three days after

streptozotocin injection, administration of insulin in diabetic mice reduced the elevation of blood glucose levels and cardiomyocyte apoptosis (Cai *et al.*, 2002). These data suggest that hyperglycemia directly results in myocardial apoptosis in diabetes. Hyperglycemia was proposed to provoke the production of reactive oxygen and nitrogen species, which cause cytochrome c-mediated caspase 3 activation and myocardial apoptosis (Cai *et al.*, 2002).

Hyperlipidemia

In the diabetic heart, energy produced from fatty acid oxidation increases from 60-70% to 90-100%. This condition leads to lipid (triglyceride) accumulation in the hearts of diabetic animals (Chiu *et al.*, 2001) and patients with diabetes mellitus (Avogaro *et al.*, 1990). A significant elevation of cardiac apoptosis and fibrosis resulting from the increased lipid accumulation has been reported (Chiu *et al.*, 2001). The cause might be attributed to the fact that the elevation of fatty acid oxidation increases mitochondrial action potential, which leads to augmented reactive oxygen species production and sequential cardiomyocyte apoptosis. In addition, excessive fatty acid leads to the generation of ceramide, which is an intracellular messenger known to initiate apoptosis. Accumulation of ceramide has been observed in the diabetic condition both *in vivo* (Zhou *et al.*, 2000) and *in vitro* (Dyntar *et al.*, 2001). Ceramide directly induces cytochrome c release from the mitochondria. Moreover, inducible nitric oxide synthase is upregulated by ceramide via the activation of NF- κ B, which results in accumulation of nitric oxide and peroxynitrite. Peroxynitrite would then lead

to the release of cytochrome c and the activation of the apoptotic process by triggering the activation of caspases.

1.3.4.2 Cardiac Autophagy

It is becoming clear that autophagy mediates the response of cells to stress in the brain, liver, skeletal muscle and heart (Gottlieb & Mentzer, Jr., 2012). Cardiac autophagy controls homeostasis of cytoplasmic components under the physiological and pathological conditions (Xie *et al.*, 2011a). Numerous studies have demonstrated that abnormal cardiac autophagy is involved in various heart diseases such as cardiac hypertrophy (Wang *et al.*, 2012b), ischemia-reperfusion injury, cardiac remodeling and heart failure (Gottlieb & Mentzer, Jr., 2012). Inhibition of autophagy would lead to abnormal proteins and organelles to be accumulated, further resulting in cardiac dysfunction. However, up-regulation of autophagy might damage the cytosol and organelles such as mitochondria and this would cause the subsequent release of the pro-apoptotic factors to trigger the execution of cardiac apoptosis.

H9c2 cardiomyoblasts treated with a high concentration of glucose has showed the up-regulation of autophagy and further induction of apoptosis, which was also confirmed in isolated neonatal rat cardiomyocytes (Younce *et al.*, 2010). In a rat model of streptozotocin-induced type 1 diabetic cardiomyopathy, Lee and co-workers observed the activation of autophagy based on the elevated expression level of Beclin1 and microtubule-associated protein light chain 3

(LC3) in the heart (Lee *et al.*, 2012). Moreover, OVE26 diabetic mice (a type 1 diabetes mouse model) demonstrated the reduced cardiac autophagy and cardiac dysfunction and these reductions were associated with the decrease in the activity of AMP-activated protein kinase (AMPK) (Xie *et al.*, 2011b). Collectively, these findings suggest that autophagic homeostasis is critical for the maintenance of cardiac function.

There are few data about the role of autophagy in type 2 diabetic cardiomyopathy. Mellor and co-workers reported the association of myocardial autophagy activation and the systemic insulin resistance by using a mouse model of insulin resistance induced by high fructose intake (Mellor *et al.*, 2011). The induction of autophagy (as indicated by a 46% increase in LC3B-II-to-LC3B-I ratio) was accompanied with the inhibition of the survival factors rather than apoptotic signaling (unchanged Bax-to-Bcl-2 ratio). However, a recent study showed that cardiac autophagy was suppressed and this was accompanied with the activated apoptosis in diabetic heart through the inhibition of AMPK activity and the depression of MAPK8/JNK1-Bcl-2 signaling (Zou & Xie, 2013). Notably, the interaction of autophagy and diabetes in heart is not fully understood and still needs to be further investigated.

1.3.4.3 Cardiac Metabolism

Normal hearts use predominantly free fatty acids as the energy substrate and only a small amount of glucose. There is a decrease of fatty acid usage and an

elevation of glucose consumption during heart failure. However, the usage of fat is enhanced and that of glucose is reduced in a diabetic heart when compared to the normal heart (Carley & Severson, 2005). With diabetes, oxygen consumption and fatty acid oxidation are enhanced in the heart but cardiac energy efficiency is decreased. It is demonstrated that there is a two-fold increase in cardiac palmitate oxidation and around 30-40% decrease in glucose oxidation in type 2 diabetic patients (Rijzewijk *et al.*, 2009). The alteration of metabolic substrate in the heart accompanied with the decrease in cardiac contractility was shown in the db/db mice which is a mouse model of type 2 diabetes (Boudina *et al.*, 2007). The findings of working hearts isolated from diabetic animals also confirmed that the left ventricle dysfunction is related to the increased oxidation of fatty acid (Belke *et al.*, 2000).

This kind of metabolic switch in the diabetic heart is related to the reduced glucose usage because of insulin resistance and the elevated circulating fatty acids released by the adipocyte and liver. These factors contribute to the increased uptake and oxidation of fatty acids in the heart (Shen *et al.*, 2005). Cardiac glucose uptake is inhibited due to insulin resistance or increased fatty acid levels, and accompanies a chronic decrease in glycolytic capacity (Stanley *et al.*, 1997). In addition, the decrease in cardiac glucose usage has been shown to be directly induced by the deletion of glucose transporter-1 and -4 (Aneja *et al.*, 2008).

The gene expression of critical enzymes involved in fatty acid oxidation is induced by the activation of the transcriptional factors PPAR α and/or PPAR β and the interaction of PPAR factors and PGC-1 α (Finck *et al.*, 2002). As shown in Fig. 1.9, the activity of pyruvate dehydrogenase is inhibited by free fatty acid that further reduced the energy production and the elevation of the production of glycolytic intermediates and ceramide, which activates apoptosis (Eckel & Reinauer, 1990; Russo *et al.*, 2012). Furthermore, elevated fatty acid can impair the oxidative phosphorylation and cardiac calcium handling, which are critical factors that affect the myocardial mechanics and contribute to the development of diabetic cardiomyopathy.

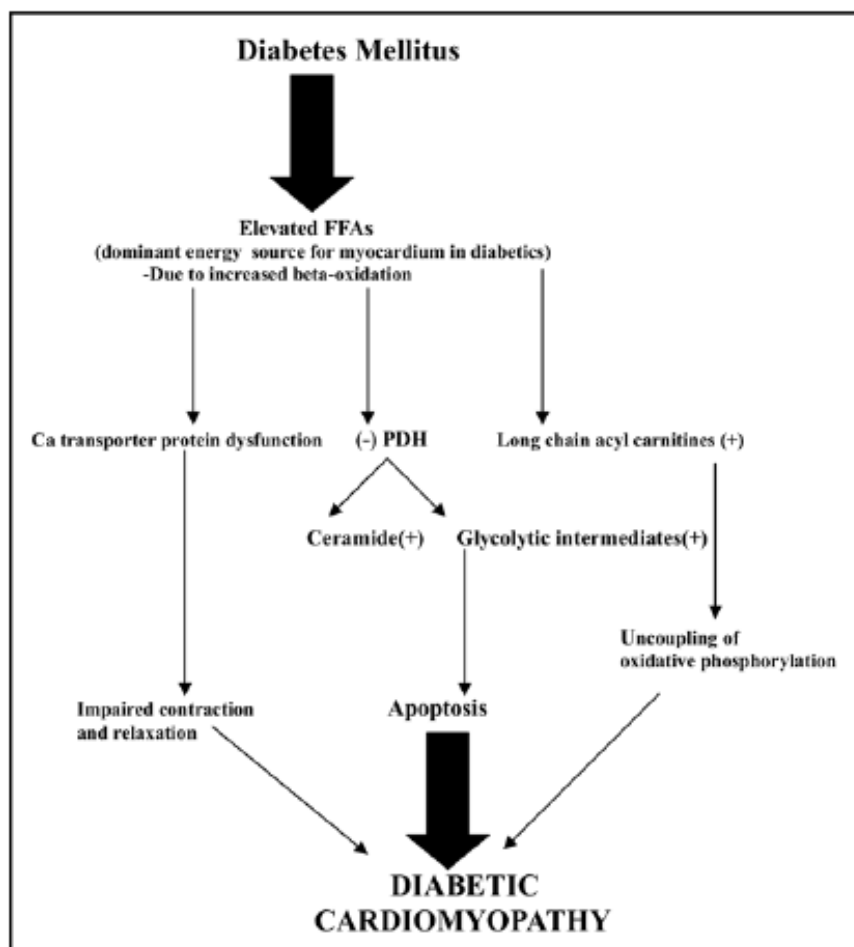


Fig 1.9 The role of altered myocardial metabolism in the development of diabetic cardiomyopathy. FFA, free fatty acid; PDH, pyruvate dehydrogenase (Aneja *et al.*, 2008)

1.3.4.4 Cardiac Inflammation

It is well studied that obesity and type 2 diabetes are marked by a status of low-grade inflammation (Bastard *et al.*, 2006). Adipose tissue has been suggested as an active system of secreting adipokines and cytokines including TNF- α , plasminogen activator inhibitor-1 (PAI-1), interleukin-1 β (IL-1 β), IL-6, IL-8, leptin, adiponectin and others (Berg & Scherer, 2005). Wilson and colleagues reported that the gene expression of IL-16 and adiponectin were down-regulated in the hearts of db/db mice (a type 2 diabetic mouse model) by using microarray analysis (Wilson *et al.*, 2008). Epicardial adipose tissue stores free fatty acid for the heart, and secretes pro- and anti-inflammatory cytokines to modulate the myocardium remodeling. Cellular processes of all tissues, including the heart, are affected by the systemic inflammation in diabetes, which may promote the progression of the cardiac fibrosis (van de *et al.*, 2011). In addition, impaired autophagy is associated with increased inflammation in a wide variety of disorders, and inflammation contributes to various forms of cardiac pathology. However, the underlying relationship of the inflammation and fibrosis or autophagy has not been well investigated.

1.3.4.5 Signaling Pathway

1.3.4.5.1 Protein Kinase C Activation

Protein kinase C (PKC), a family of the protein kinase enzyme, plays a key role in several signal transduction cascades by phosphorylating the hydroxyl groups

of serine and threonine amino acid residues of proteins. The conventional PKCs (isoforms α , β II, and γ) are activated by calcium ions and diacylglycerol (DAG) and phosphatidylserine, whereas the novel PKCs (δ , ϵ , η and θ) are activated by DAG and phosphatidylserine (Newton, 2003).

PKC signaling regulates multiple cellular functions including cell growth, differentiation, apoptosis, motility and secretion (Loegering & Lennartz, 2011). PKC signaling pathway has been suggested to be involved in several diseases such as cancer, stroke, and cardiovascular diseases (Poole *et al.*, 2004). In heart diseases, different isoforms of PKC are involved in different aspects of the disease including myocyte hypertrophy, cardiac function, fibrosis, and inflammation (Loegering & Lennartz, 2011).

The elevation of DAG levels in diabetes is the chronic response to the increase in the glycolytic intermediate dihydroxyacetone phosphate (Geraldés & King, 2010). DAG-PKC activation affected multiple tissues including heart (Inoguchi *et al.*, 1992), renal glomeruli (Craven *et al.*, 1990), liver and skeletal muscle (van Herpen & Schrauwen-Hinderling, 2008) in diabetic condition. Different isoforms of PKC activation have been shown to be involved in the development of diabetic cardiomyopathy through different ways.

1.4 DOX-induced Cardiotoxicity in Diabetic Patients

1.4.1 Connection Between Cancer and Type 2 Diabetes

Epidemiologic evidence has suggested a strong connection between type 2 diabetes and certain cancers such as kidney, pancreas, liver, colon, and other cancers. The risk and mortality of these cancers have been demonstrated to be increased by diabetes (Table 1.6 and 1.7) (Cannata *et al.*, 2010). The connection between diabetes and certain cancers might partly result from the common risk factors of these two diseases including aging, obesity, diet, and physical inactivity (Giovannucci *et al.*, 2010).

Table 1.6 Diabetes and Relative Risk of Cancer By Site (Cannata *et al.*, 2010)

Cancer	Meta-Analysis	Relative Risk (95% Confidence Interval)
Breast	Larsson <i>et al.</i> ⁴³ (2007) 5 case control studies	1.18 (1.05–1.32)
	15 cohort studies	1.20 (1.11–1.30)
Colon	Larsson <i>et al.</i> ⁶⁵ (2005) 6 case control studies	1.36 (1.23–1.50)
	9 cohort studies	1.29 (1.16–1.43)
Pancreas	Huxley <i>et al.</i> ⁸⁰ (2005) 17 case control studies	1.94 (1.53–2.46)
	19 cohort studies	1.73 (1.59–1.88)
Prostate	Kasper and Giovannucci ⁹¹ (2006) 9 case control studies	0.89 (0.72–1.11)
	10 cohort studies	0.81 (0.71–0.92)

Table 1.7 Diabetes and Relative Risk of Cancer Mortality by Site (Cannata *et al.*, 2010)

Cancer	Studies	Relative Risk (95% Confidence Interval)
Breast	Coughlin <i>et al.</i> ⁵⁴ (2004)	1.27 (1.11–1.45)
	Verlato <i>et al.</i> ⁵³ (2003)	1.40 (1.06–1.81)
	Yancik <i>et al.</i> ⁵² (2001)	1.76 (1.23–2.52)
Colon	Larsson <i>et al.</i> ⁶⁵ (2005)	1.26 (1.05–1.50)
	Coughlin <i>et al.</i> ⁵⁴ (2004)	Male: 1.20 (1.06–1.37); female: 1.24 (1.07–1.43)
Pancreas	Coughlin <i>et al.</i> ⁵⁴ (2004)	Male: 1.48 (1.27–1.73); female: 1.44 (1.21–1.72)
Prostate	Coughlin <i>et al.</i> ⁵⁴ (2004)	0.90 (0.80–1.02)
	Ma <i>et al.</i> ⁹⁸ (2008)*	2.38 (1.31–4.30) [†]

Diabetes and Breast Cancer

A meta-analysis of 43 studies performed by Hardefeldt and co-workers found that type 2 diabetic patients had a significant increase in the risk of breast cancer when compared to non-diabetic controls (Hardefeldt *et al.*, 2012). The link of type 2 diabetes and breast cancer has been extensively investigated. It was proposed that the link between these two disorders was attributed to activation of insulin/IGF pathway via hyperinsulinemia and dysregulation of sex hormones (Larsson *et al.*, 2007). *In vitro* studies have demonstrated that insulin induced cell cycle progression and DNA synthesis of breast cancer cells (Chappell *et al.*, 2001). The *in vivo* studies have also shown the mitogenic effect of insulin on breast tumor growth (Shafie & Hilf, 1981).

Diabetes and Colorectal Cancer

Human studies have demonstrated an association between type 2 diabetes and colorectal cancer. There was a relative risk of 1.43 for colorectal cancer and a relative risk of 2.39 for fatal colorectal cancer in type 2 diabetic patients (Hu *et al.*, 1999). The findings of a meta-analysis of 24 cohort studies suggested that patients with type 2 diabetes had a higher risk of colorectal cancer development (Luo *et al.*, 2012). Additionally, mortality of colorectal cancer is also affected by type 2 diabetes. Coughlin and colleagues reported the elevation of the mortality of colorectal cancer in diabetic patients who aged over 30 years (Coughlin *et al.*, 2004). The proposed potential mechanisms for the connection

between colorectal cancer and type 2 diabetes include a slower bowel transit time among type 2 diabetic patients with resultant increased exposure to toxins, increased production of carcinogenic bile acids, and hyperinsulinemia (Will *et al.*, 1998). Among these potential mechanisms, hyperinsulinemia is the most thoroughly explored issue and it appears to be a major player in the type 2 diabetes-mediated increase in colorectal cancer risk (Giovannucci, 1995).

Diabetes and Pancreatic Cancer

A high risk of pancreatic cancer in type 2 diabetes patients has been extensively documented (Ben *et al.*, 2011; Li *et al.*, 2011; Huxley *et al.*, 2005). A meta-analysis of 35 cohort studies found that the relative risk of pancreatic cancer was increased in type 2 diabetes for both males and females and was associated negatively with the duration of diabetes. The patients with the highest risk of pancreatic cancer were found among the diabetic patients diagnosed within one year (Ben *et al.*, 2011). Another study also showed that type 2 diabetes was more prevalent (47% vs. 7%) and predominantly of new onset (< 2-year duration) (74% vs. 53%) among cases compared with controls (Pannala *et al.*, 2008). In a cohort study using record-linkage health-care datasets, a 3-fold increased risk of pancreatic cancer in type 2 diabetes patients was reported (Ogunleye *et al.*, 2009). Hyperinsulinemia in type 2 diabetes may lead to pancreatic cancer. Pancreatic carcinogenesis was enhanced by insulin resistance via increased proliferation of islet cells. On the other hand, type 2 diabetes was thought to be a result of pancreatic cancer. However, it is not clear how

pancreatic cancer can lead to the development of insulin resistance.

Taken together, type 2 diabetes has been clearly linked to different types of cancer. Hyperinsulinemia is proposed to play a key role in explaining the connection.

1.4.2 Potential Mechanism for the Link Between Type 2 Diabetes and Cancer

The high level of insulin associated with type 2 diabetes leads to increased production of insulin-like growth factor 1 (IGF-1), which exerts an important role in cell growth, proliferation, and differentiation. The induction of bioavailable IGF-1 by insulin might result from the inhibition of the two transporters of IGF-1: insulin-like growth factor binding protein (IGFBP) 1 and 2. IGF-1 receptor (IGF-1R) and insulin receptor (IR) have been found to be up-regulated in cancer cells (Cannata *et al.*, 2010; Kuramoto *et al.*, 2008). The mutations of the tumor suppressor genes (such as p53 and p63) cause tumor growth and proliferation through a defect of inhibition of IGF-1R (Bruchim *et al.*, 2009). Aside from the direct effects of hyperinsulinemia on cancer cells via IR and IGF-1R, insulin might play an indirect role in growth and development of cancer cells. Insulin stimulates aromatase activity and inhibits the production of sex hormone-binding globulin (SHBG), which increases bioavailable estrogen level. Collectively, the increases in IGF-1 and estrogen levels are hypothesized to contribute to the development of cancer (Fig 1.10).

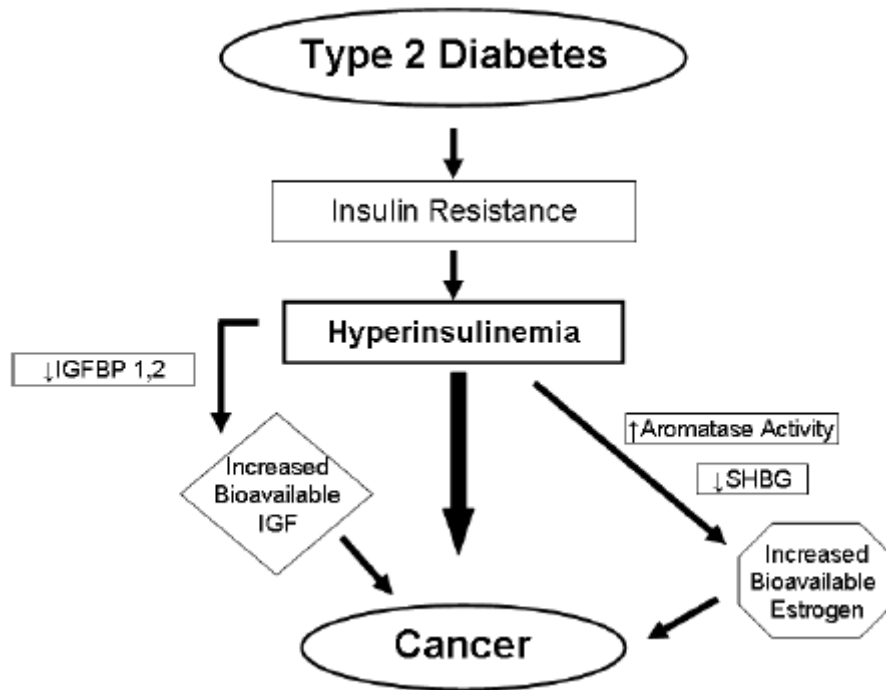


Fig 1.10 Potential mechanism for the link between type 2 diabetes and cancer (Cannata *et al.*, 2010)

1.4.3 Clinical Challenge: DOX-induced Cardiotoxicity in Diabetic Heart

It is well established that there is a strong connection between type 2 diabetes and certain cancers. Therefore, a specific clinical challenge is raised by the complicated features of diabetic patients with cancer, who have poorer prognosis, higher infection rates, and higher mortality rates in comparison with the non-diabetic cancer patients. For the cancer chemotherapy, around 85% of the chemotherapeutic drug needs to be given to the patient for successful cancer treatment. The clinical condition of diabetic patients with cancer must be

monitored during the chemotherapy. Patients with a long history of poorly controlled type 2 diabetes might present with the pre-existing cardiac, renal or neuropathic complications during the cancer treatment. These pre-existing complications could be further deteriorated by the side effects of the anti-cancer drug during chemotherapy. For example, DOX causes severe cardiotoxicity and cisplatin is known to be renal and neurotoxic. Therefore, the use of chemotherapeutic agents must be applied very carefully in diabetic cancer patients.

DOX is a well-known and effective chemotherapeutic agent for treating many types of cancer including leukemias, cancers of bladder, breast, stomach, lung, and others. But the clinic application of DOX has been largely limited by its cardiotoxicity. Therefore, extensive studies have focused on finding a novel and effective therapeutic strategy to prevent or alleviate the DOX-induced cardiotoxicity. However, there is no information available to delineate the toxic effects of DOX on the heart of type 2 diabetic individuals. It is not clear on how the diabetic heart is being affected by DOX. This makes it very difficult to determine the effective measures to protect the heart during DOX chemotherapeutic treatment in type 2 diabetic patients. It is urgent and worthy to investigate the underlying mechanisms for the DOX-induced cardiotoxicity in diabetic heart. This information is essential to lead to the development of novel effective measures to protect the heart and therefore to enhance the treatment opportunities of the diabetic cancer patients.

1.5 Ghrelin

1.5.1 Structure of Ghrelin and the Related Substances

Ghrelin, an endogenous ligand for the growth hormone secretagogue receptor (GHSR), is synthesized principally in the stomach and is released in response to fasting. Ghrelin secreted from the stomach accounts for two-thirds of circulating ghrelin. Ghrelin is also produced by other organs including heart, intestine, kidney and pancreas at lower levels. Ghrelin is composed of 28 amino acids and is uniquely modified by the addition of an octanoyl group (i.e., acylation) to the third amino acid serine residue from the N-terminus of the polypeptide (Fig 1.11). This acylation is necessary for ghrelin to bind to the GHSR1a (also called the ghrelin receptor) and to cross the blood-brain barrier (Kojima & Kangawa, 2005).

The gene of human ghrelin is localized on chromosome 3p25- 26 (Kanamoto *et al.*, 2004) and consists of five exons with four introns and two transcriptional initiation sites (Tanaka *et al.*, 2001). The 28 amino acids of ghrelin protein are encoded in exons 1 and 2. Ghrelin has been identified in many species including human, rat, mouse, monkey and others. The amino acid sequences of ghrelin in human, rat and mouse are shown in Fig 1.12.

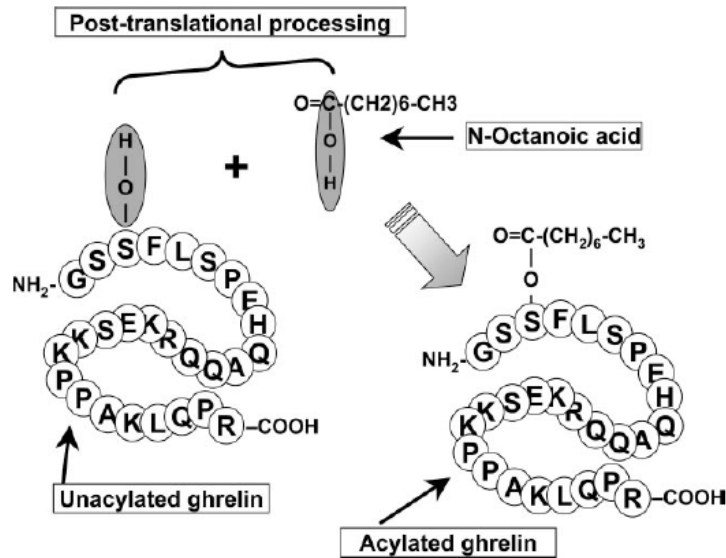


Fig 1.11 The post-translational modification of ghrelin (van der Lely *et al.*, 2004)

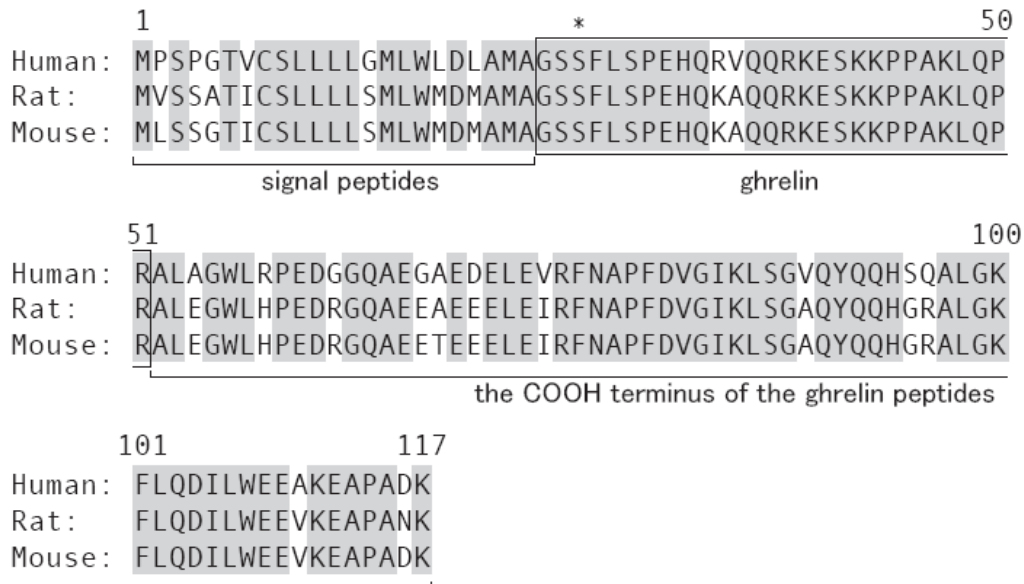


Fig 1.12 Amino acid sequences of ghrelin precursors in human, rat, and mouse. Identical amino acids are colored in gray. The asterisk shows the position of acyl-modified Ser3

(Sato *et al.*, 2012).

Ghrelin Receptor

The human gene of ghrelin receptor is also located on chromosome 3 at the position q26-27 (Smith *et al.*, 1997). Ghrelin receptor (GHSR) has two different mRNAs: GHSR type 1a and 1b. GHSR1a has the binding and functional ability of receptor for ghrelin while GHSR1b is physiologically inactive with a COOH-terminal truncated form of GHSR1a. It is known that the acylated ghrelin serves the essential biological function via its binding with the GHSR1a.

Ghrelin O-acyltransferase (GOAT)

Yang and colleagues discovered a specific enzyme named ghrelin O-acyltransferase (GOAT) which catalyzes the acyl-modification of ghrelin (Yang *et al.*, 2008) (Fig 1.13). GOAT is the only enzyme known to be responsible for the acylation of ghrelin in the body and is found to be distributed in various tissues including gastrointestinal tract, testis, heart, and other peripheral tissues that secrete ghrelin. GO-CoA-Tat, a peptide-based bi-substrate analog that antagonizes GOAT, has been exhibited to inhibit the activity of GOAT in cell experiments and rodent tissues. GO-CoA-Tat has been shown to offer the beneficial effects on glucose metabolism via the inhibition of GOAT (Taylor *et al.*, 2012).

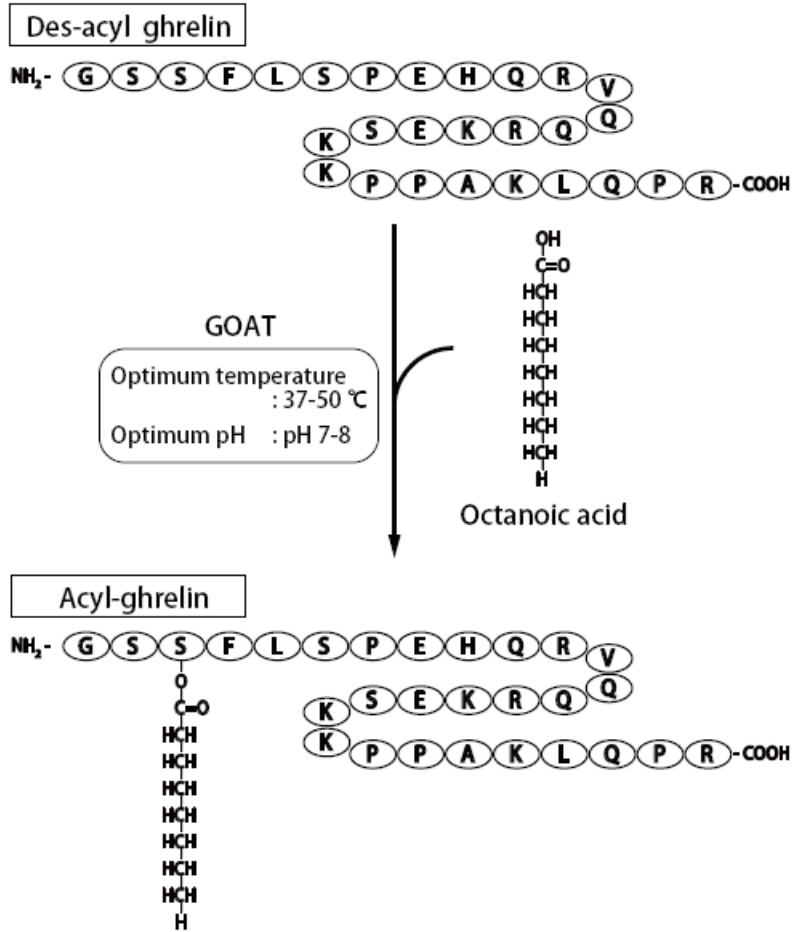


Fig 1.13 The modification of octanoic acid by GOAT (Sato *et al.*, 2012)

1.5.2 Acylated and Desacylated Forms

Ghrelin has two forms in circulation: acylated ghrelin and desacyl ghrelin (lacking of octanoic acid at Ser3). The normal concentration of ghrelin in human plasma is 10-20 fmol/ml for acylated ghrelin and 100-150 fmol/ml for total ghrelin (both acylated and desacyl ghrelin). Plasma level of ghrelin is elevated by fasting and is decreased by food consumption. The biological activity of acylated ghrelin is well known, such as stimulating growth hormone release, increasing food intake and body weight, protecting against cardiac injury and so on. On the other hand, although desacyl ghrelin is the predominant form of ghrelin in the circulation, the physiological functions of desacyl ghrelin are quite unclear. While desacyl ghrelin is known not to be able to bind to GHSR (Hosoda *et al.*, 2003), some studies suggested that desacyl ghrelin might have some non-endocrine-related physiological effects that are regulated by un-identified receptors other than GHSR1a. The effects that are mediated by desacyl ghrelin include the inhibition of glucose output by primary hepatocytes, inhibition of lipolysis, promotion of adipogenesis, inhibition of cell apoptosis, beneficial cardiotropic outcome, promotion of vasodilation, stimulation of food intake, and relaxation of iris muscles (Leite-Moreira & Soares, 2007).

Ghrelin receptor, GHSR1, has two variants, GHSR1a and GHSR1b. Acylated ghrelin binds only to GHSR1a but not GHSR1b (Camina, 2006). GHSR1a is a G-protein-coupled receptor, and the octanoyl group at Ser3 and the 4-5 amino

acids at the N-terminus are vital for the binding of acylated ghrelin, which is essential for the activation of multiple intracellular pathways and the endocrinological effects of acylated ghrelin (Bednarek *et al.*, 2000). In somatotrophic cell, activation of GHSR1a induces calcium mobilization that is regulated by the Gq11-phosphatidylinositol-phospholipase C system. In neurons, acylated ghrelin binds to GHSR1a and activates the Gs/cAMP/protein kinase A (PKA), leading to the release of calcium from intracellular stores. However, acylated ghrelin has been shown to be able to bind to and activate cellular effects in cells lines that are deficient of GHSR1a. According to the binding studies, GHSR1a is not the sole receptor for acylated ghrelin and the common receptors for acylated ghrelin and desacyl ghrelin might exist.

In hypothalamus and pituitary glands, desacyl ghrelin has no ability to bind to GHSR and thus could not induce the release of growth hormone (GH) and exert endocrine effects in rats and humans. It is proposed that desacyl ghrelin might have a specific receptor and have different functions distinct from acylated ghrelin (Kojima & Kangawa, 2005). It has been investigated that desacyl ghrelin might share some non-endocrinological functions with acylated ghrelin such as the regulation of cell proliferation and beneficial effects on the cardiovascular system.

1.5.3 Physiological Functions of Ghrelin

Ghrelin is predominantly produced by the X/A cells in stomach but its

expression is also found in many other tissues including pituitary gland, hypothalamus, heart, pancreas, and kidney (De & Delporte, 2008). The wide tissue diversity of the expression of ghrelin suggests that ghrelin might have multiple functions in various tissues in the body (Fig 1.14)

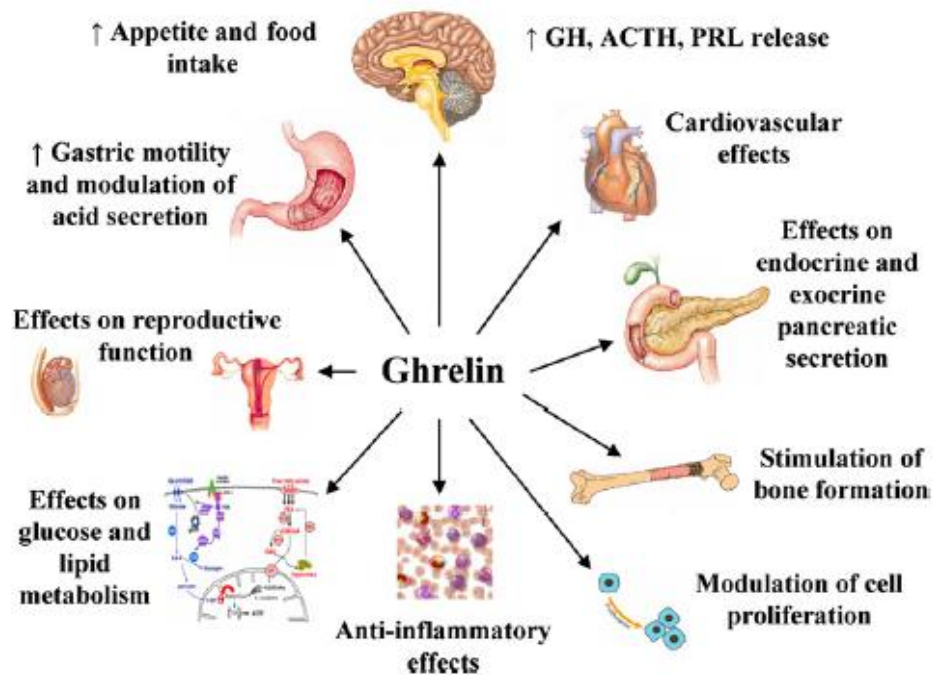


Fig 1.14 The biological roles of ghrelin (De & Delporte, 2008)

1.5.3.1 Central Actions of Acylated Ghrelin

Brain and Pituitary

Acylated ghrelin stimulates growth hormone secretion directly through pituitary somatotroph cells (Arvat *et al.*, 2001). Acylated ghrelin also has a direct effect

on hypothalamus and stimulates vagal afferents for further induction of growth hormone secretion (Popovic *et al.*, 2003). High dose of acylated ghrelin has been exhibited to induce the secretion of prolactin, corticotropin, and cortisol in humans (Takaya *et al.*, 2000). Growth hormone concentration peaks at around 5-15 minutes after the intravenous injection of acylated ghrelin. Plasma growth hormone level is observed to be increased after a single intracerebroventricular injection of acylated ghrelin in rats (Date *et al.*, 2000). Moreover, growth-hormone-releasing hormone (GHRH), an important inducer for growth hormone release, has been demonstrated to be stimulated by acylated ghrelin. A higher level of growth hormone has been shown to be induced by co-administration of acylated ghrelin and GHRH when compared to the administration of acylated ghrelin alone (Hataya *et al.*, 2001).

Appetite Regulation

The secretion of acylated ghrelin is taken as the “hunger signal” to stimulate food intake. Acylated ghrelin is produced predominantly from the stomach in response to hunger, and is then released to the circulation and across the blood-brain barrier to signal the central nervous system to induce feeding. Food intake has been observed after the intravenous or subcutaneous injection of acylated ghrelin and this observation is shown to be associated with the stimulation of hypothalamic neurons (Wang *et al.*, 2002; Wren *et al.*, 2001). As GHSR locates in vagal afferent neurons, it is suggested that ghrelin might signal from peripheral tissue to the brain through the vagus nerve (Zhang *et al.*, 2004).

Additionally, it has been demonstrated that the fasting-induced increase in the plasma acylated ghrelin concentration was completely inhibited by sub-diaphragmatic vagotomy or atropine treatment, suggested the intimate relationship between the acylated ghrelin and vagus nervous system (Williams *et al.*, 2003).

Ghrelin is expressed in the neurons of arcuate nucleus (ARC) of the hypothalamus (Kojima *et al.*, 1999). Intracerebroventricular injection of acylated ghrelin has been shown to increase food intake and reduce energy consumption, leads to body weight gain (Kamegai *et al.*, 2001). It is exhibited that ghrelin-containing neurons in the hypothalamus send efferent fibers to the neurons contained neuropeptide (NPY) and agouti-related protein (AgRP), and these further stimulate the release of orexigenic peptides and inhibit the secretion of anorexigenic peptides (Cowley *et al.*, 2003).

1.5.3.2 Peripheral Effects of Acylated Ghrelin and Desacyl

Ghrelin

As desacyl ghrelin does not bind to GHSR, desacyl ghrelin was originally thought to be an inactive form of ghrelin without any biological functions. However, a growing number of recent studies showed that desacyl ghrelin also carries a variety of physiological effects. It appears that desacyl ghrelin shares the common activities with acylated ghrelin but works independently of acylated ghrelin through different signaling pathways.

1.5.3.2.1 Metabolic Effects of Acylated Ghrelin and Desacyl Ghrelin

Recently, a growing number of studies focused on the metabolic effects of acylated ghrelin and desacyl ghrelin. These studies demonstrated that both acylated ghrelin and desacyl ghrelin have important effects on the metabolism of glucose and lipid.

Glucose Metabolism

Both acylated ghrelin and desacyl ghrelin involved in the regulation of insulin action and glucose homeostasis. GHSR1a and GHSR1b are present in animal and human endocrinological tissues such as pancreas (Gnanapavan *et al.*, 2002). Experimental data indicated that desacyl ghrelin inhibits insulin secretion in cell culture, animal and human settings (Broglia *et al.*, 2003;Egido *et al.*, 2002). These data suggested a negative association between the systemic ghrelin and insulin level. For desacyl ghrelin, it might have different effects from acylated ghrelin in glucose metabolism. A human study investigating the biological activities of desacyl ghrelin revealed the antagonizing properties of desacyl ghrelin on the hyperglycemic effects exerted by acylated ghrelin. More specifically, bolus intravenous injections of desacyl ghrelin were shown to cause a significant reversal of the acylated ghrelin-induced reduction of insulin level and the acylated ghrelin-induced increase in plasma glucose level (Fig 1.15) (Broglia *et al.*, 2003). Recently, the antagonistic activity of desacyl ghrelin is suggested to be mediated by an indirect mechanism that probably

involves a specific desacyl ghrelin receptor. These findings suggested that desacyl ghrelin might play an important role in the regulation of glucose and insulin level, although the exact mechanisms remain to be elucidated (Gauna *et al.*, 2007).

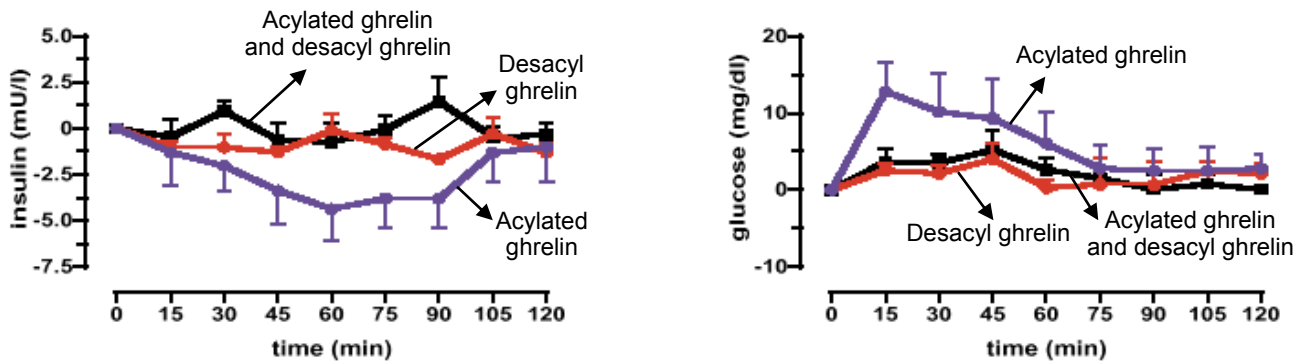


Fig 1.15 Effect of acute bolus administration (i.v.) of **acylated ghrelin (AG: 1.0 µg/kg)** or **des-acyl ghrelin (1.0 µg/kg)** or **acylated ghrelin (1.0 µg/kg) + des-acyl ghrelin (1.0 µg/kg)** on insulin and glucose level (Broglia *et al.*, 2003).

Lipid Metabolism

Ghrelin has been shown to affect lipid metabolism. Acylated ghrelin induces the elevation of liver lipogenic and triglyceride content. In the gastrocnemius muscle, acylated ghrelin leads to a decrease in triglyceride content, an increase in the activity of mitochondrial oxidative enzymes, and an up-regulation of gene expression of uncoupling protein 2. All these alterations were observed independent of the changes of the gene expression that were associated with fat metabolism and phosphorylation of 5'-AMP-activated protein kinase (AMPK). In addition, acylated ghrelin increases gene expression of peroxisome

proliferator-activated receptor gamma (PPAR γ) which reduces the fat content of muscle in mixed skeletal muscle (Barazzoni *et al.*, 2005). Collectively, acylated ghrelin induces triglyceride deposition in the liver rather than in skeletal muscle. Moreover, both *in vitro* and *in vivo* findings suggested that acylated ghrelin acted directly on differentiated adipocytes to stimulate lipogenesis via the up-regulation of the levels of PPAR γ and the insulin-induced glucose uptake (Patel *et al.*, 2006). Studies of the effect of desacyl ghrelin on lipid metabolism are very limited. Muccioli and co-workers have shown that both desacyl ghrelin and acylated ghrelin inhibited isoproterenol-induced lipolysis in rat adipocytes via an unknown receptor and might have a direct anti-lipolytic effect on the adipose tissue (Muccioli *et al.*, 2004). Taken together, although many aspects of the metabolic effects of acylated ghrelin and desacyl ghrelin remain to be clarified, existing evidences suggest that acylated ghrelin and desacyl ghrelin play an important role in the regulation of metabolism.

1.5.3.2.2 Cardiovascular Effects of Acylated Ghrelin and Desacyl Ghrelin

Acylated ghrelin and desacyl ghrelin have diverse effects on the cardiovascular system (Fig. 1.16). Extensive evidence demonstrated that ghrelin (mainly demonstrated in acylated ghrelin) had a strong therapeutic effect on different cardiovascular diseases (Table 1.8). The expression of ghrelin and its receptor have been studied in the heart and vasculature of murine and human at the mRNA level by RT-PCR (Gnanapavan *et al.*, 2002). Cardiomyocytes are

known to synthesize and secrete ghrelin. In endothelial cells of human arteries and veins, acylated ghrelin and desacyl ghrelin are detected to be localized to intracellular vesicles by standard immunocytochemical analysis. Both acylated ghrelin and desacyl ghrelin are demonstrated to regulate the vascular tone via the paracrine manner in humans (Kleinz *et al.*, 2006). Increasing amount of evidence support a role of ghrelin in the regulation of cardiovascular function. Moreover, by inhibiting the activation of NF- κ B in human endothelial cells and mononuclear cell adhesion, ghrelin is demonstrated to prevent inflammation of the cardiovascular system. Acylated ghrelin and desacyl ghrelin exert vasodilatory effects by an endothelium-independent mechanism. Administration of acylated ghrelin has been shown to decrease the mean arterial pressure without changing the heart rate. The effects of acylated ghrelin on blood pressure might be mediated through the direct vasodilatory effect and the inhibitory effect on sympathetic activity of the acylated ghrelin. Furthermore, acylated ghrelin has been demonstrated to improve cardiac contractility, left ventricular function, peak workload, and peak oxygen consumption in chronic heart failure patients (Isgaard & Johansson, 2005). In rats with heart failure, chronic treatment of acylated ghrelin has been shown to improve left ventricular dysfunction and to prevent the development of left ventricle remodeling and cardiac cachexia (Nagaya *et al.*, 2001). Consistently, microinjection of desacyl ghrelin into a rat nucleus tractus solitarii (NTS) was shown to reduce the mean arterial pressure and heart rate (Tsubota *et al.*, 2005).

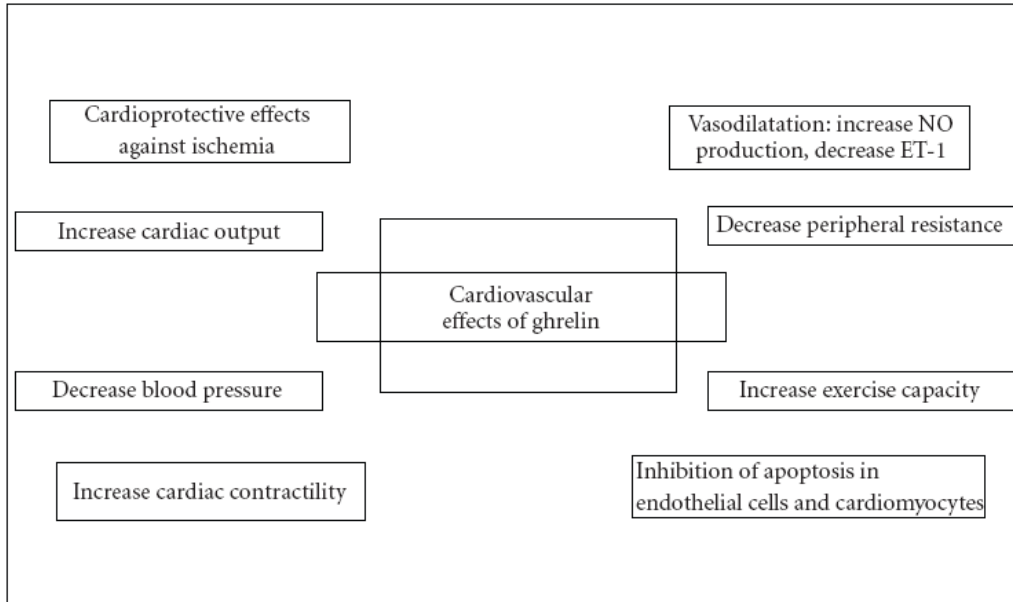


Fig 1.16 Cardiovascular effects of ghrelin (Tesauro *et al.*, 2010)

Table 1.8 Cardiovascular effects of ghrelin

Author, date	Treatment	Model	Main outcomes
(Nagaya <i>et al.</i> , 2001)	Acylated ghrelin	left coronary artery ligation in rats	Improved LV dysfunction and attenuated remodelling
(Frascarelli <i>et al.</i> , 2003)	Acylated ghrelin	Isolated working rat heart (ischemic injury)	Cardioprotective effect
(Li <i>et al.</i> , 2006)	Acylated ghrelin and des-acyl ghrelin	Isoproterenol-induced myocardial injury in rats	Improved cardiac function, attenuated myocardial lipid peroxidation injury and relieved cardiac fibrosis
(Chang <i>et al.</i> , 2004)	Acylated ghrelin	Isolated working rat heart (ischemic injury)	Cardioprotective effect
(Ma <i>et al.</i> , 2012b)	Acylated ghrelin	Isolated hearts from adult mice (ischemic injury)	Maintenance or recovery of normal cardiac contractility by recovery of phosphorylated phospholamban
(Zhang <i>et al.</i> , 2009)	Acylated ghrelin	Isolated working rat heart (ischemic injury)	Cardiac protection through inhibition of myocardial endoplasmic reticulum stress
(Xu <i>et al.</i> , 2008)	Acylated ghrelin	DOX induced toxicity in primary cultured cardiomyocyte	Cardiac protection by anti-oxidative and anti-apoptotic effects
(Aoki <i>et al.</i> , 2013)	Acylated ghrelin	Dahl salt-sensitive hypertensive rats	Decreased blood pressure and prevention of high salt induced increase in heart thickness
(Mao <i>et al.</i> , 2012)	Acylated ghrelin	Acute myocardial infarction in ghrelin-knockout mice	Inhibition of cardiac sympathetic nerve activity and reduction of malignant arrhythmia via the vagal afferent nerves
(Yang <i>et al.</i> , 2012)	Acylated ghrelin	Angiotensin II induced H9c2 cardiomyocyte apoptosis	Inhibition of apoptosis via decreasing Ang II type 1 receptor expression and inhibiting the activation of endoplasmic reticulum stress pathway

1.5.3.2.3 Anti-apoptotic Affect of Acylated Ghrelin and Desacyl Ghrelin

Both acylated ghrelin and desacyl ghrelin have been documented to have anti-apoptotic effects in diverse experimental settings (Table 1.9). Acylated ghrelin and desacyl ghrelin have been shown to inhibit apoptosis of cardiomyocytes and endothelial cells through extracellular signal-regulated kinase (ERK) 1/2 and phosphatidylinositol-3 (PI3)-kinase/AKT (Baldanzi *et al.*, 2002). Furthermore, ghrelin was demonstrated to decrease the toxic effects of cytotoxic agents such as DOX (Baldanzi *et al.*, 2002) and cytarabine (Iglesias *et al.*, 2004). When cell integrity is threatened, signaling pathways involving extracellular ERK1/2 and Akt are known to be activated aimed to lead the cell towards either survival or demise. In H9c2 cells (a rodent cardiac cell line that does not express the ghrelin receptor), acylated ghrelin and desacyl ghrelin have been shown to activate ERK1/2 and reduce cell death following the administration of DOX (Baldanzi *et al.*, 2002). Furthermore, inhibiting the pathway with an ERK1/2 inhibitor or a PI3 kinase inhibitor (wortmannin) was demonstrated to abolish the protective effect of ghrelin, suggesting that the cardioprotective effects of ghrelin are mediated through the ERK1/2 and PI3 kinase/Akt pathways. ERK1/2 and Akt are dynamically regulated in the cell, and reversible cysteine switches in upstream and downstream modulators regulate the fate of these proteins. The findings show that the protective effects of ghrelin are independent of its acylation suggest that ghrelin gene product might act as a survival factor in the cardiovascular system through the

mediation of an un-identified receptor distinct from GHSR-1a.

Table 1.9 Studies of anti-apoptotic effect of ghrelin

Author, date	species	Treatment	Model	Main outcomes
(Baldanzi <i>et al.</i> , 2002)	H9c2 cardiomyocyte	Acylated ghrelin and des-acyl ghrelin	DOX induced apoptosis	Inhibit apoptosis by PI3K/Akt pathway
(Kim <i>et al.</i> , 2005)	MC3T3-E1 cells	Acylated ghrelin	TNF-alpha induced apoptosis in osteoblastic MC3T3-E1 cells	Inhibit apoptosis by PI3K/Akt pathway
(Zhao <i>et al.</i> , 2007)	ECV-304 cells	Acylated ghrelin	High glucose induced apoptosis	Inhibit apoptosis by PI3K/Akt pathway
(Chung <i>et al.</i> , 2007)	Primary rat hypothalamic neuronal cultures	Acylated ghrelin	Ischemia induced apoptosis	Inhibit apoptosis by increasing Bcl-2/Bax ratio
(Yang <i>et al.</i> , 2007)	PC12 cells	Acylated ghrelin	SNP induced apoptosis	Inhibition of PC12 cells apoptosis by inducing HSP70 expression
(Park <i>et al.</i> , 2008)	Sprague Dawley rats	Acylated ghrelin	Intestinal mucosal apoptosis	Suppression of apoptosis by decreasing caspase-3 expression
(Xu <i>et al.</i> , 2008)	Primary rat cardiomyocyte culture	Acylated ghrelin	DOX induced apoptosis	Exert anti-apoptotic effect by TNF-alpha/NF-kappaB activation pathway
(Granado <i>et al.</i> , 2009)	Wistar rats	Acylated ghrelin	Lactotrophs apoptosis in the pituitary of diabetic rats	Prevent diabetes induced lactotrophs apoptosis by increasing pituitary Bcl-2 and Hsp70 expression
(Kui <i>et al.</i> , 2009)	Adult rat cardiomyocyte	Acylated ghrelin	High glucose induced apoptosis	Protect cardiomyocyte from apoptosis by PI3K/Akt pathway

1.5.3.2.4 The Difference Between Acylated Ghrelin and Desacyl Ghrelin

The concentration of desacyl ghrelin is decreased in obese mice and humans while the level of acylated ghrelin is relatively stable (Pacifico *et al.*, 2009). The ratio of acylated ghrelin-to-desacyl ghrelin is observed to be elevated in insulin-resistant individuals when compared to insulin-sensitive obese individuals (Barazzoni *et al.*, 2007). The acylated ghrelin level was shown to be increased in obesity-associated type 2 diabetic patients whereas desacyl ghrelin level was found to be reduced (Rodriguez *et al.*, 2009). Acute acylated ghrelin administration induced an increase in blood glucose level and a decrease in serum insulin level in humans (Broglia *et al.*, 2001). The *in vivo* study showed that peripheral acylated ghrelin treatment increased the triglyceride content in liver and white adipose tissue (Barazzoni *et al.*, 2005). Interestingly, co-administration of acylated ghrelin and desacyl ghrelin was demonstrated to reverse the hyperglycemic effect of acylated ghrelin (Gauna *et al.*, 2004).

Gauna and colleagues also reported the antagonistic role of desacyl ghrelin in primary hepatocytes (Gauna *et al.*, 2005). In addition, desacyl ghrelin was shown to inhibit the glucose release and to prevent the acylated ghrelin-induced increase in glucose output. In the murine HL-2 adult cardiomyocytes, desacyl ghrelin was shown to have distinct metabolic effects from acylated ghrelin (Lear *et al.*, 2010). Medium-chain fatty acid uptake was also demonstrated to be enhanced by desacyl ghrelin but not acylated ghrelin. In HL-1 cell line and

neonatal rat cardiomyocytes, desacyl ghrelin was observed to increase insulin-dependent translocation of GLUT4 from nucleus to cytoplasm but this effect was not observed in acylated ghrelin. The epididymal and perirenal fat masses were shown to be reduced in the transgenic mice that over-expressed desacyl ghrelin (Zhang *et al.*, 2008). Interestingly, these transgenic mice also showed the resistance to high-fat diet induced obesity and significant improvement of insulin sensitivity, suggesting the potential therapeutic role of desacyl ghrelin in diabetes mellitus and other metabolic diseases.

PROJECT SIGNIFICANCE

Ghrelin has diverse physiological effects including the stimulation of food intake, regulation of metabolism of glucose and lipid, and inhibition of apoptotic cell death. In particular, the anti-apoptotic effect of ghrelin on cardiomyocytes becomes a focus and provides the opportunity for exploring novel therapy for heart disease. Previous findings have consistently demonstrated the cardioprotective effects of ghrelin in ischemic cardiac injury and chronic heart failure. Although cardiac apoptosis has been shown to have an essential role in the DOX-induced cardiomyopathy and diabetic cardiomyopathy, the effects of ghrelin, particularly desacyl ghrelin, on these cardiomyopathies are largely unknown. This dissertation project mainly focused on the study of desacyl ghrelin because the therapeutic role of this form of ghrelin is far more unclear. Moreover, the desacyl ghrelin is possibly a good target for the development of the treatment for the DOX-induced

cardiomyopathy and diabetic cardiomyopathy.

OBJECTIVES OF THE PROJECT

The general objective of this project is to investigate the protective effects of desacyl ghrelin on two essential forms of cardiomyopathy namely dilated cardiomyopathy (DOX-induced cardiomyopathy) and diabetic cardiomyopathy.

This project proposed the following specific objectives:

1. To examine the protective effects of desacyl ghrelin on the DOX-induced cardiomyopathy.
2. To examine the protective effects of desacyl ghrelin on diabetic cardiomyopathy.
3. To examine the underlying mechanisms of the DOX-induced cardiotoxicity in type 2 diabetic heart.

HYPOTHESIS OF THE PROJECT

This project tested the general hypothesis that desacyl ghrelin prevented the progress of cardiomyopathy. Additionally, this project aimed to examine the cardiotoxic effects of DOX on diabetic heart. This project proposed the following specific hypotheses:

1. Desacyl ghrelin exerts a cardioprotective role in preventing the DOX-induced cardiomyopathy.
2. Desacyl ghrelin protects the heart against type 2 diabetic cardiomyopathy.
3. Distinct molecular mechanisms are responsible for the DOX-induced

cardiotoxicity in type 2 diabetic heart compared to non-diabetic heart.

CHAPTER 2
General Methods

2.1 Measurement of Cardiac Function by Echocardiography

Transthoracic echocardiography was used to assess the cardiac function at the pre- and post-intervention levels. Echocardiography was performed by following the published procedure (Siu *et al.*, 2007). Mice were anesthetized with an intraperitoneal injection of ketamine HCl (80 mg/kg) and xylazine (10 mg/kg). The ventral thorax was shaved and covered with ultrasonic transmission gel. Echocardiography was performed in prone decubitus position with an Esaote MyLab 70 X-Vision Ultrasound System in conjunction with a 10 MHz linear transducer (Esaote, Italy). Two-dimensional grey scale ultrasound scanning was performed to assess the cardiac structures in parasternal short-axis view at the mid-papillary level. The grey scale echocardiographic view was used to position the M-mode echocardiographic line. The M-mode echocardiographic image was examined while the heart rate of mice was at 450-550 beat/min. Left ventricle (LV) internal dimensions were then measured according to the leading-edge method of the American Society of Echocardiography (Lang *et al.*, 2006). LV end-diastolic and end-systolic dimensions including LV internal diameter at end diastole (LVIDd) and LV internal diameter at end systole (LVIDs) were assessed from the M-mode tracing. Quantitative measurements were performed by using the analytical software of the ultrasound scanner. Fractional shortening (FS), the percent change in LV cavity dimension, was calculated using the equation of $FS (\%) = [(LVIDd - LVIDs) / LVIDd] \times 100$ (Dittoe *et al.*, 2007). Ejection fraction (EF) represents stroke volume as a percentage of end diastolic LV volume and was

derived as $EF (\%) = Y + [(100 - Y) \times 0.15]$, where $Y = [(LVIDd^2 - LVIDs^2) / LVIDd^2] \times 100$ (Stein *et al.*, 2007). The heart rate was determined by counting the diastole and systole cycles in M-mode images within a defined time interval. All measurements were averaged over three consecutive cardiac cycles.

2.2 Masson's Trichrome Staining

Collagen deposition in the left ventricle was determined by Masson's trichrome staining kit (Sigma). Collagen was stained blue in the frozen tissue transverse sections (5 μ m thick) according to the manufacturer's instructions. Images were obtained in five random fields per section using the total magnification of 200x. Analysis was performed using NIH Image J analysis software. The area of fibrosis was then divided by the total area of the microscopic field.

2.3 Protein Fraction Preparation

The protein fraction of cardiac muscles was prepared by adopting the previously described protocol (Siu *et al.*, 2004; Siu *et al.*, 2005). Forty mg of ventricular tissue samples were minced and homogenized in an ice-cold lysis buffer (10 mM NaCl, 1.5 mM MgCl₂, 20 mM HEPES, pH 7.4, 20% glycerol, 0.1% Triton X-100, and 1 mM DTT). The homogenates were centrifuged at $122 \times g$ for 5 minutes at 4°C. The supernatant was collected and further centrifuged at $2,675 \times g$ for 5 minutes at 4°C; this procedure was repeated three times to collect the final supernatant as the cytoplasmic protein fraction. A protease inhibitor cocktail (P8340, Sigma-Aldrich) was added to a portion of the

extracted protein fraction. The protein concentration of the extracted protein fraction was then measured in duplicate by using the method of Bradford (Coomassie Protein Assay, Pierce) with bovine serum albumin used as standard. The protein fraction with the addition of a protease inhibitor was later used in the apoptotic cell death enzyme-linked immunosorbent assay (ELISA) and western blot analysis. Caspase enzymatic activity assay was performed in the protein fraction without the addition of protease inhibitor.

2.4 Apoptotic Cell Death Enzyme-Linked Immunosorbent Assay (ELISA)

Apoptotic DNA fragmentation in ventricle samples was determined by using the Cell Death Detection ELISA Kit (Roche Diagnostics). In brief, 100 μ l of protein fraction was added in a streptavidin-coated microplate that had been incubated with a mouse monoclonal anti-histone antibody for 1 hour at room temperature. After washing, the reaction mixtures were incubated with a peroxidase conjugated anti-DNA-POD mouse monoclonal antibody. The amount of histone-associated DNA fragments including mono- and oligo-nucleosomes, were then determined by measuring the absorbance at 405 nm using ABTS (2,2'-azino-di[3-ethylbenzthiazoline sulfonate-6-diammonium salt]) as a substrate using a microplate reader (Infinite F200, Tecan). All measurements were performed in duplicate. The absorbance was normalized to the amount of protein content used in the assay and was expressed as OD405 (optical density) normalized to mg protein used.

2.5 Fluorometric Caspase-3 Activity Assay

Caspase-3 activity in the ventricle muscle tissues was examined by a fluorometric assay as described previously (Siu *et al.*, 2004). Fifty μ l of the extracted protein fraction was incubated in 50 μ l of reaction buffer (50 mM PIPES, 0.1 mM EDTA, 10% glycerol, 10 mM DTT, pH 7.2), which contained 7-amino-4-trifluoromethyl coumarin (AFC)-conjugated substrate (Ac-DEVD-AFC; Biovision Research Products) at 37°C for 2 hours. A negative control experiment was performed by including caspase inhibitor, z-VAD-fmk (BD Pharmingen) or in the absence of the AFC-conjugated substrate. The fluorescence intensity was detected before and after the 2 hours incubation using a microplate reader (Infinite F200, Tecan) at an excitation wavelength of 405 ± 10 nm and an emission wavelength of 500 ± 25 nm. The enzymatic activity of caspase-3 was expressed as the change in the fluorescence intensity normalized to mg of protein used in the assay.

2.6 RNA Extraction and Real Time Quantitative PCR

Analysis

The transcriptional expression of interested genes was examined in cardiac tissues by quantitative RT-PCR analysis. Total RNA was extracted from the ventricle muscles by using TriReagent (Molecular Research Center, USA) based on the guanidine thiocyanate method. Forty micrograms of muscle tissues were mechanically minced and homogenized on ice in ice-cold TriReagent. The

homogenate was centrifuged following the addition of bromochloropropane to separate the aqueous and organic phases. The RNA in the aqueous phase was precipitated by adding isopropanol and was washed with 75% ethanol. The extracted RNA was then dissolved in DEPC-treated water and quantified in triplicate by measuring the optical density (OD) at 260 nm. The purity of RNA was assured by examining the OD₂₆₀/280 ratio. The trace amount of DNA was removed from the extracted RNA by treating with RNase-free DNase I (Fermentas, USA). One microgram of RNA was reverse transcribed with the RevertAid™ First Strand complementary DNA (cDNA) synthesis kit (Fermentas, USA) by using oligo-dT primers in a total volume of 20 µl according to the manufacturer's instruction. One µl of the diluted cDNAs was then used to perform quantitative polymerase chain reaction (PCR) in SYBR green/ROX qPCR master mix (Fermentas, USA) with forward and reverse primers (Table 2.1) and RNase/DNase-free water using ABI 7500 thermal cycler system. According to the manufacturer's instruction, PCR was performed using a two-step cycling protocol with pre-treatment at 50°C for 2 minutes followed by a step of initial denaturing at 95°C for 10 minutes and then 40 cycles of denaturation at 95°C for 15 seconds and annealing/extension at 60°C for 1 minute. β-tubulin was used as the internal control reference gene. The sequences of PCR products were confirmed by sequencing. All samples were run in duplicate on the same plate. A relative standard curve (concentration vs. threshold cycle) of target and reference genes for quantification of PCR products was generated by diluting of cDNA from the

calibrator. Complementary DNAs prepared from all samples were pooled and used as the calibrator to generate the standard curve. Results were expressed as the concentration ratio of the target gene normalized to the internal control β -tubulin gene.

Table 2.1 Sequence of Primer Used in Real Time PCR Analysis

Gene	Gene Full Name	GenBank Accession No.	Forward primer	Reverse primer
PPAR α	Peroxisome proliferator activated receptor alpha	NM_011144	5'GGGTACCACTACGGAGTTCACG3'	5'CAGACAGGCACCTTGTGAAAACG3'
mCPT1	Carnitine palmitoyltransfer-ase 1b, muscle	NM_009948	5'AAGTCATGGTGGGCAACTAACTAT3'	5'TGTAGTGTGAACATCCTCTCCAT3'
UCP3	Uncoupling protein 3	NM_009464	5'GGAGTCTCACCTGTTACTGACAAC3'	5'GCACAGAAGCCAGCTCCAA3'
FAS	Fatty acid synthase	NM_007988	5'TTGTCTGGCACTACAGAATGC3'	5'AACAGCCTCAGAGCGACAAT3'
TGF- β 1	Transforming growth factor, beta 1	NM_011577	5'CGATTCAGCGCTCACTGCTC3'	5'GCTGTACTGTGT GTCCAGGC3'
CTGF	Connective tissue growth factor	NM_010217	5'CAAAGCAGCTGCAAATACCA3'	5'GGCCAAATGTGTCTTCCAGT3'
BNP	Natriuretic peptide type B	NM_008726	5'CAGCTCTTGAAGGACCAAGG3'	5'AGACCCAGGCAGAGTCAGAA 3'
CAMK2D	Calcium/calmodulin-dependent protein kinase II, delta	NM_001025439	5'CTGCCTTTGAACCTGAAGCATTG3'	5'TGAACGTGTGGGTTGAGGATGAT3'
SERCA2a	ATPase, Ca ²⁺ transporting, cardiac muscle, slow twitch 2	NM_009722	5'GGAACAACCCGCAATACTGG3'	5'CTTTTCCCAACCTCAGTCATG3'
RyR2	Ryanodine receptor 2, cardiac	NM_023868	5'CATGGACAGCTTCCCCTGAA3'	5'GTGTGACTGCCGTGCTTGG3'
PLB	Phospholamban	NM_023129	5'CGATCACCGAAGCCAAGGTCTCC3'	5'CGGTGCGTTGCTTCCCCCAT3'
Adipo	Adiponectin	NM_009605	5'GATGGCAGAGATGGCACTCC3'	5'CTTGCCAGTGTGCCGTCAT3'
MMP-8	Matrix metalloproteinase 8	NM_008611	5'GGTAACTAACTCTGCAGCCCTCTT3'	5'CGAACCAGGGACGGAATATG3'
MMP-13	Matrix metalloproteinase 13	NM_008607	5'AATCTATGATGGCACTGCTGACAT3'	5'GTTTGGTCCAGGAGGAAAAGC3'
Apelin	Apelin	NM_013912	5'CGAGTTGCAGCATGAATCTGAG3'	5'TGTTCCATCTGGAGGCAACATC3'
Wnt5a	Wingless-related MMTV integration site 5A	NM_009524	5'TTCTGTCTTTGGCAGGGTGAT3'	5ACCCAGCTGCGCTCA3'
TLR-4	Toll-like receptor 4	NM_021297	5'GGAAGTTTCTCTGGACTAACAAGT TTAGA3'	5'AAATTGTGAGCCACATTGAGTTTC3'
Edn3	Endothelin 3	NM_007903	5'CTGTGTGCTTGAGACCTGGA3'	5'TCCCAAGGATCCACATTTA3'
GATA6	GATA binding protein 6	NM_010258	5'TTGTCTCCGTAACAGCAGTG3'	5'GTGGTTCGCTTGTGTAGAAGGA3'
FKBP10	FK506 binding protein 10	NM_010221	5'AGAGAGGAGGCAGCTCATTG3'	5'TCAAATAGCAGCACAGCACTG3'
p21	Cyclin-dependent kinase inhibitor 1A	NM_007669	5'GACAAGAGGCCAGTACTTCC T3'	5'CAATCTGCGCTTGGAGTGATA3'
FKBP5	FK506 binding protein 5	NM_010220	5'CTGTGGTGGGAAGGACATTTG3'	5'AAACCATAGCGTGGTCCA A3'
S100A8	S100 calcium binding protein A8	NM_013650	5'TGCCCTCTACAAGAATGACT3'	5'AAGCTCTGCTACTCCTTGTG3'
S100A9	S100 calcium binding protein A9	NM_009114	5'CGACACCTTCCATCAATACT3'	5'TCAGCATCATACTCCTCA3'
β -tubulin	Tubulin, beta	NM_011655	5'CCGACAGTGTGGCAACCAGATCGG3'	5'TGGCCAAAAGGACCTGAGCGAACGG3'

2.7 Western Blot Analysis

The protein expression of interested protein targets was evaluated in cardiac tissues by Western immunoblot. Fifty micrograms of protein was denatured at 95°C for 5 minutes in Laemmli buffer with 5% β -mercaptoethanol. Protein samples and pre-stained marker were fractionated in a 10% SDS-PAGE gel followed by transference to polyvinylidene difluoride (PVDF) membrane (Immobilon P, Millipore) using Bio-Rad Mini Protein II system. The appropriate condition was applied during protein separation and transferred based on the different molecular weight of target protein. The membrane was then blocked with 5% skimmed milk powder in PBS/0.1% Tween-20 (PBST) followed by primary antibody incubation overnight at 4°C. For the detection of protein phosphorylation, the 5% Albumin from bovine serum (BSA) in tris-buffered saline (TBS)/0.1% Tween-20 (TBST) was used for the membrane blocking. On the next day, the membrane was washed three times with PBST or TBST for 15 minutes per session. The primary antibodies used in the project summarized in Table 2.2. After washing, membranes were incubated with a secondary antibody [anti-mouse IgG or anti-rabbit IgG horseradish peroxidase (HRP)-conjugated antibodies (Cell Signaling, 1:3000)]. The whole procedure of western blotting was finished following the three further washings of the membrane. The resulting immunoreactivity was determined using the ECL chemiluminescence reaction kit (Perkin Elmer) and the image was captured by a Kodak 4000R Pro camera system. Detection of β -tubulin (Sigma, 1:2000) was

included as an internal control reference. The arbitrary units of the blot signal were presented as net intensity x band area, normalized to β -tubulin signal.

Table 2.2 Primary antibody information summary

Name	Company	Dilution
Bcl-2	Santa Cruz	1: 500
Bax	Abcam	1: 1000
XIAP	BD Biosciences	1: 500
phospho-(Ser473)-Akt	Cell Signaling	1: 1000
Akt	Cell Signaling	1: 1000
phospho-(Thr402-Tyr204)-ERK1/2	Cell Signaling	1: 1000
ERK1/2	Cell Signaling	1: 1000
PGC-1 α	Santa Cruz	1: 500
phospho-(Thr172)-AMPK α	Cell Signaling	1: 1000
AMPK α	Cell Signaling	1: 1000
Phosphor-(Ser108)-AMPK β 1	Cell Signaling	1: 1000
AMPK β 1	Cell Signaling	1: 1000
Beclin1	Cell Signaling	1: 1000
Atg5-12	Cell Signaling	1: 1000
GSK3 α/β	Cell Signaling	1: 1000
phospho-(Ser21/9)- GSK3 α/β	Cell Signaling	1: 1000
β -tubulin	Sigma	1: 2000

CHAPTER 3

Desacyl Ghrelin Prevents DOX-induced Myocardial Fibrosis and Apoptosis via GHSR-independent Pathway

3.1 Introduction

DOX is a commonly used chemotherapeutic agent for treating various malignancies including breast cancer, leukemia, and sarcomas. The mechanism of the anti-tumor action of DOX is probably mediated through the inhibition of gene transcription and replication by intercalation into the DNA structure. Although DOX is extensively used in chemotherapy, it is known to induce organ toxicities, including cardiotoxicity, which results in cardiomyopathy and congestive heart failure (Swain *et al.*, 2003). Cellular mechanisms including myocardial fibrosis (Zhu *et al.*, 2008;Miyata *et al.*, 2010), apoptosis (Nakamura *et al.*, 2000;Sharma *et al.*, 2010) and altered energy metabolism (Mitra *et al.*, 2008;Carvalho *et al.*, 2010) have been proposed to account for the cardiomyopathy caused by DOX.

Ghrelin, an endogenous ligand for GHSR1a, is mainly synthesized in the stomach. Ghrelin exists in two forms in the circulation, ghrelin (acylated) and desacyl ghrelin which lacks octanoic acid at the serine 3 residue. Desacyl ghrelin is the predominant form of ghrelin in the circulation, with ghrelin in its acylated form contributing only approximately 5% of the total amount of circulating ghrelin (van der Lely *et al.*, 2004). Acylated ghrelin has been shown to be capable of efficient binding to and activation of GHSR1a, and this mediates most of its endocrinological effects (Kojima & Kangawa, 2005;Kojima *et al.*, 1999). Desacyl ghrelin was initially considered to be the inactive form of ghrelin, devoid of any biological activity because of its

inability to bind to the classic GHSR1a receptor. However, increasing evidence indicates that desacyl ghrelin is bioactive, and exerts cellular effects such as stimulation of adipogenesis and modulation of lipogenic and insulin signaling (Delhanty *et al.*, 2010; Gauna *et al.*, 2007).

Accumulating evidence suggests that ghrelin, and possibly desacyl ghrelin, is protective to the cardiovascular system (Garcia & Korbonits, 2006). The beneficial cardiovascular effects such as protection against myocardial ischemia/reperfusion injury, improved prognosis of heart failure, and inhibition of atherosclerosis have been clearly demonstrated for ghrelin (acylated) (Garcia & Korbonits, 2006). The beneficial effect of ghrelin (acylated) on DOX cardiotoxicity in primary cultured cardiomyocytes has also been shown, with effects mediated by anti-apoptotic and anti-oxidative mechanisms (Xu *et al.*, 2008). Intriguingly, similar to ghrelin (acylated), desacyl ghrelin has been demonstrated to inhibit DOX-induced cardiac apoptosis by activating the pro-survival ERK1/2 and PI3K/Akt serine kinase signaling pathways through GHSR-independent manner in H9c2 cardiomyocytes (Baldanzi *et al.*, 2002). Cardioprotection by ghrelin (acylated) against DOX was later supported by *in vivo* evidence showing that endogenous ghrelin is increased during the progression of the heart failure, this was suggested to represent a compensatory protective response to maintain the cardiac function during DOX-induced cardiomyopathy (Xu *et al.*, 2007). However, to date the therapeutic role of desacyl ghrelin in DOX cardiotoxicity has not been demonstrated *in vivo*. Therefore, the present study aimed to examine the cellular effects of desacyl

ghrelin on DOX-induced cardiomyopathy using a mouse DOX cardiotoxicity model. We also tested the hypothesis that desacyl ghrelin protects against myocardial fibrosis and apoptosis induced by DOX. To further examine whether the effects of desacyl ghrelin are mediated through the GHSR pathway, the GHSR antagonist [D-Lys3]-GHRP-6 was used to block GHSR signaling in the desacyl ghrelin-treated animals after the administration of DOX.

3.2 Methods

3.2.1 Animals

Male 10- to 12-week-old C57BL/6 mice obtained from the Laboratory Animal Services Centre of The Chinese University of Hong Kong were used. Mice were housed in a temperature- and humidity-controlled environment and were exposed to a 12:12-hour light: dark cycle in the Centralised Animal Facilities of The Hong Kong Polytechnic University. Mice were allowed to have access to standard animal diet and water ad libitum. Animal ethics approval was obtained from the Animal Ethics Sub-committee of The Hong Kong Polytechnic University.

3.2.2 Experimental Protocol

Mice were assigned randomly to one of four groups as follows: Control (n = 10), DOX (DOX; n = 11), DOX+DAG (DOX treated with desacyl ghrelin; n = 10), DOX+DAG+[D-Lys3]-GHRP-6 (DOX treated with desacyl ghrelin in the presence of GHSR1a antagonist [D-Lys3]-GHRP-6; n = 6). Mice assigned to

DOX, DOX+DAG and DOX+DAG+[D-Lys3]-GHRP-6 groups were exposed to an intraperitoneal (i.p.) injection of DOX (Pharmacia & Upjohn SpA, Milan, Italy) at a dose of 15 mg/kg, which has been previously demonstrated to induce cardiomyopathy, cardiac fibrosis and apoptosis (Suliman *et al.*, 2007). Mice in the Control group were i.p. injected with the same volume of saline instead of DOX. Twelve hours after the injection of DOX, mice were administered with saline (for Control and DOX groups), desacyl ghrelin (for DOX+DAG group) (des-acyl ghrelin, Tocris Bioscience, USA) or co-administration of desacyl ghrelin and [D-Lys3]-GHRP-6 ([D-Lys3]-GHRP-6, Tocris Bioscience, USA) by i.p. injection for four consecutive days. In this study, the previously reported dosage of 100 µg/kg bodyweight of desacyl ghrelin injected twice daily was adopted (Li *et al.*, 2006; Nagaya *et al.*, 2001). We adopted a dosage of 3.75 mg/kg of [D-Lys3]-GHRP-6 (37.5-fold dose of desacyl ghrelin), which was shown to effectively abolish the ghrelin-GHSR signaling (Kobashi *et al.*, 2009). Mice in DOX+DAG+[D-Lys3]-GHRP-6 group were administered with [D-Lys3]-GHRP-6 immediately before desacyl ghrelin injection. After the four-day experimental period, mice were euthanized by overdose of ketamine and xylazine. Hearts were immediately removed and washed with cold phosphate buffered saline (PBS). The left ventricle was quickly dissected and frozen in liquid nitrogen and stored at -80°C for later analysis.

3.2.3 Echocardiographic Assessment

Transthoracic echocardiography was conducted before the DOX injection and after the 4-day experimental period to assess the cardiac structure and function. Echocardiography was performed according to a previously described protocol in CHAPTER 2.

3.2.4 Measurement of Growth Hormone and Insulin Growth Factor-1 Levels in Plasma

Blood samples were collected in EDTA-coated tubes from mice at sacrifice. Plasma was separated within 1 hour and stored at -80°C until analysis. Growth hormone and insulin growth factor (IGF-1) were measured using commercial immunoassay kits from Millipore (GH) and R&D System (IGF-1).

3.2.5 TUNEL Assay

Myocardial apoptosis was determined by terminal deoxynucleotide transferase-mediated dUTP nick end labeling (TUNEL) in ventricle muscle sections using the *in situ* cell death detection kit (Roche). Briefly, 5 µm thick transverse sections were prepared by cutting the frozen tissues at the apex of the left ventricle. Tissue sections were air-dried at room temperature, fixed in 4% paraformaldehyde in PBS, pH 7.4 at room temperature for 20 minutes, and permeabilized with 0.2% Triton X-100 in sodium citrate at 4°C for 2 minutes. Slides were incubated with terminal deoxynucleotidyl transferase (TdT) enzyme with buffer and biotin tagged nucleotides in a humidified chamber at

37°C for 1 hour in the dark. Tagged nucleotides were detected by using anti-fluorescein-HRP conjugates. The section incubated with 5 µg/ml of DNase for 10 minutes was used as positive control. A negative control experiment was performed by omitting the TdT enzyme from the labeling solution. Troponin T was co-stained in sections for the identification of cardiomyocytes. Sections were treated with 5% horse serum in PBS for 30 minutes and incubated for 1 hour with monoclonal mouse Troponin T antibody (Thermo Science) diluted at 1:200 with 2% horse serum in PBS. Sections were incubated with anti-mouse IgG Cy3-conjugated antibody (1:200; Sigma). Sections were then mounted with DAPI Vectashield mounting medium to label all nuclei. Sections were examined under a Nikon 80i microscope. Images were captured with a Nikon DXM 1200C camera using Nikon ACT-1C software. The number of TUNEL positive nuclei and total nuclei originating from cardiomyocytes was counted and expressed as the TUNEL index.

3.2.6 Masson's Trichome Staining

Collagen deposition in the left ventricle was determined by Masson's trichome staining kit (Sigma). The details of the staining protocol were described in CHAPTER 2.

3.2.7 Protein Fraction Preparation

The protein fraction of cardiac muscles was prepared by adopting the previously described protocol in CHAPTER 2.

3.2.8 Apoptotic Cell Death Enzyme-Linked Immunosorbent Assay (ELISA)

Apoptotic DNA fragmentation in ventricle samples was determined by using the Cell Death Detection ELISA Kit (Roche Diagnostics). The details of the procedure were described in CHAPTER 2.

3.2.9 Fluorometric Caspase-3 Activity Assay

Caspase-3 activity of ventricle muscle tissues was examined by a fluorometric assay. The details of the procedure were described in CHAPTER 2.

3.2.10 RNA Extraction and Real Time Quantitative PCR Analysis

Myocardial metabolic regulators (PPAR α , mCPT1, UCP3, and FAS), fibrosis signaling factors (TGF- β 1, CTGF, and BNP), and calcium handling signaling factors (CAMK2D, PLB, SERCA2a, and RyR2) were examined in cardiac tissues by quantitative RT-PCR analysis. The details of the procedure used for total RNA extraction and real time PCR analysis were described in CHAPTER 2.

3.2.11 Western Blot Analysis

The protein expression of apoptotic factors (Bcl-2, Bax and XIAP), metabolic regulators (PGC-1 α , phospho-AMPK α , total AMPK α , phospho-AMPK β 1, and

total AMPK β 1), and prosurvival ERK-Akt signaling markers (phospho-ERK1/2, total ERK1/2, phospho-Akt and total Akt) were evaluated in cardiac tissues by Western immunoblot. The details of the procedure were described in CHAPTER 2.

3.2.12 Statistical Analysis

Data were expressed as mean \pm standard error of mean. Statistical analysis was performed by using Statistics Package for Social Science (SPSS) version 11.0. Differences among groups were evaluated by ANOVA followed by Tukey's Honestly Significant Difference (HSD) post hoc test. Statistical significance was set at $P < 0.05$.

3.3 Results

3.3.1 Echocardiographic Parameters

The representative echocardiographic M-mode images obtained in animals of control, DOX and DOX with desacyl ghrelin treatment groups are shown in Figure 3.1. DOX-induced cardiac dysfunction was illustrated by a significant decrease from 60.3% to 37.7% in the left ventricle fractional shortening (Table 3.1). However, this DOX-induced decrease was not found in the animals treated with desacyl ghrelin and desacyl ghrelin plus [D-Lys3]-GHRP-6 (Table 3.1). Similarly, the ejection fraction was significantly decreased from 86.2% to 65.8% after exposure to DOX, but this decrease was not seen in animals treated with desacyl ghrelin or a combination of desacyl ghrelin and [D-Lys3]-GHRP-6

(Table 3.1). Heart rate, left ventricular anterior wall thickness, posterior wall thickness, end-diastolic dimension were observed to be significantly decreased following DOX administration, but all these changes were not found in the animals treated with desacyl ghrelin (Table 3.1).

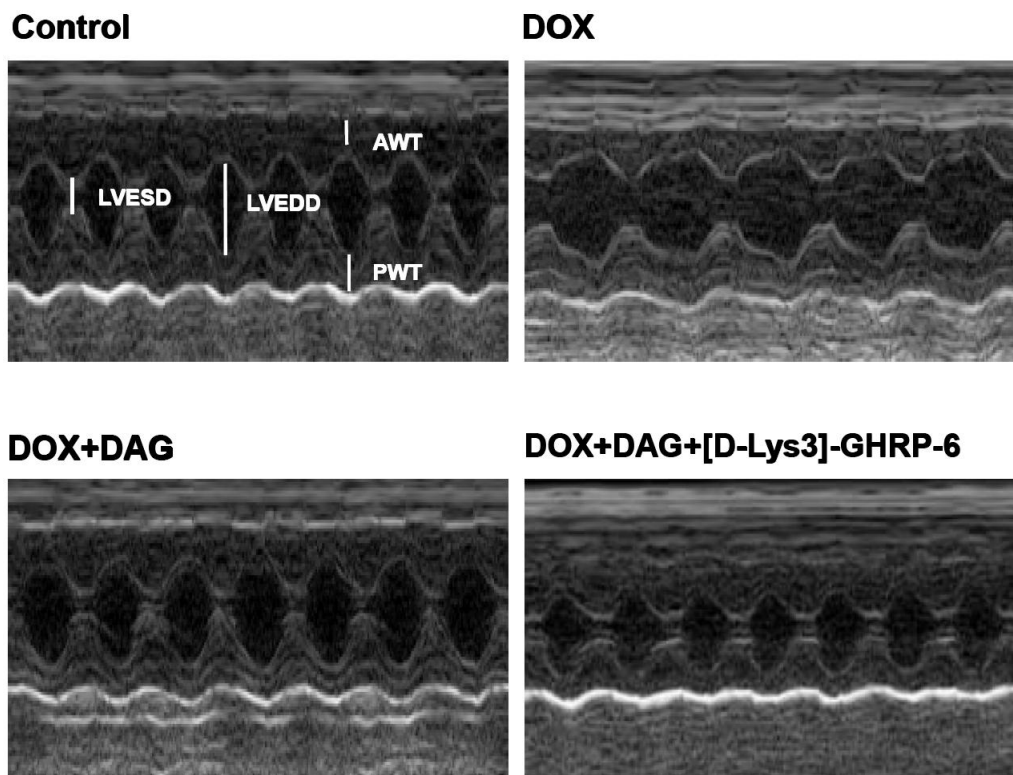


Figure 3.1 The Echocardiographic M-mode Image.

Transthoracic echocardiography was conducted before (Pre) and after (Post) the 4-day experimental period to examine the functional and structural parameters of left ventricle. The pictures show representative M-mode images obtained in animals of Control, DOX, DOX+DAG and DOX+DAG+[D-Lys3]-GHRP-6 groups during the Post echocardiographic measurements. DOX, DOX; DOX+DAG, DOX with treatment of desacyl ghrelin; DOX+DAG+[D-Lys3]-GHRP-6, DOX with treatment of desacyl ghrelin plus [D-Lys3]-GHRP-6; LVEDS, left ventricular end-systolic dimension; LVEDD, left ventricular end-diastolic dimension; AWT, anterior wall thickness; PWT, posterior wall thickness.

Table 3.1 Echocardiographic Parameters

	Control		DOX		DOX+DAG		DOX+DAG+[D-Lys3]-GHRP-6	
N	9		11		10		6	
	Pre	Post	Pre	Post	Pre	Post	Pre	Post
HR (bpm)	474±10	483±11	506±10	304±25*	509±8	428±28	471±18	415±33
AWT (cm)	0.11±0.01	0.10±0.002	0.10±0.003	0.08±0.01*	0.09±0.002	0.08±0.006	0.10±0.003	0.09±0.005
PWT (cm)	0.10±0.01	0.10±0.004	0.11±0.01	0.09±0.01*	0.10±0.01	0.09±0.005	0.11±0.01	0.10±0.006
LVEDD (cm)	0.30±0.01	0.31±0.01	0.32±0.01	0.26±0.01*	0.33±0.01	0.30±0.01	0.32±0.01	0.30±0.01
LVESD (cm)	0.12±0.01	0.10±0.01	0.13±0.01	0.16±0.01	0.12±0.01	0.10±0.01	0.11±0.01	0.10±0.01
FS (%)	61.3±1.8	65.4±2.7	60.3±2.1	37.7±1.6*	62.4±2.5	64.2±4.0	68.2±1.8	62.7±2.6
EF (%)	87.0±1.3	89.3±1.6	86.2±1.3	65.8±4.3*	87.6±1.8	88.1±2.9	90.4±1.7	87.6±1.8

Transthoracic echocardiography was conducted before the DOX injection (Pre) and after the 4-day experimental period (Post) to examine the ventricular parameters. DOX, DOX; DOX+DAG, DOX with treatment of desacyl ghrelin; DOX+DAG+[D-Lys3]-GHRP-6, DOX with treatment of desacyl ghrelin plus [D-Lys3]-GHRP-6; HR, heart rate; AWT, anterior wall thickness; PWT, posterior wall thickness; LVEDD, left ventricular end-diastolic dimension; LVESD, left ventricular end-systolic dimension; FS, fractional shortening; EF, ejection fraction.

*P < 0.05 compared to the corresponding Pre.

3.3.2 Myocardial Fibrosis and Fibrotic Regulatory Factors

As shown in Figure 3.2 and 3.3, the fibrotic area in left ventricles of the DOX group was markedly increased (by 15 fold) compared to the control group ($P < 0.05$), and this DOX-induced collagen accumulation was reduced by desacyl ghrelin and desacyl ghrelin plus [D-Lys3]-GHRP-6 ($P < 0.05$). Doxorubicin, desacyl ghrelin and [D-Lys3]-GHRP-6 had no effect on gene expression of TGF- β 1 ($P > 0.05$) (Figure 3.4A). However, DOX significantly increased (by 8-fold) CTGF expression compared to that in the control group. This DOX-induced increase was significantly modulated by desacyl ghrelin (Figure 3.4B). The modulation of desacyl ghrelin on CTGF expression was not blocked by [D-Lys3]-GHRP-6 (Figure 3.4B). The BNP expression was significantly up-regulated by DOX, but this change was not affected by desacyl ghrelin ($P > 0.05$) and significantly reversed to basal level by [D-Lys3]-GHRP-6 (Figure 3.4C). The ratio of CTGF to BNP, which serves as a critical determinant in the progress of cardiac fibrosis, was increased (by 150%) in the DOX group compared to the control group ($P < 0.05$), but this DOX-induced increase was significantly lowered in the desacyl ghrelin group (Figure 3.4D).

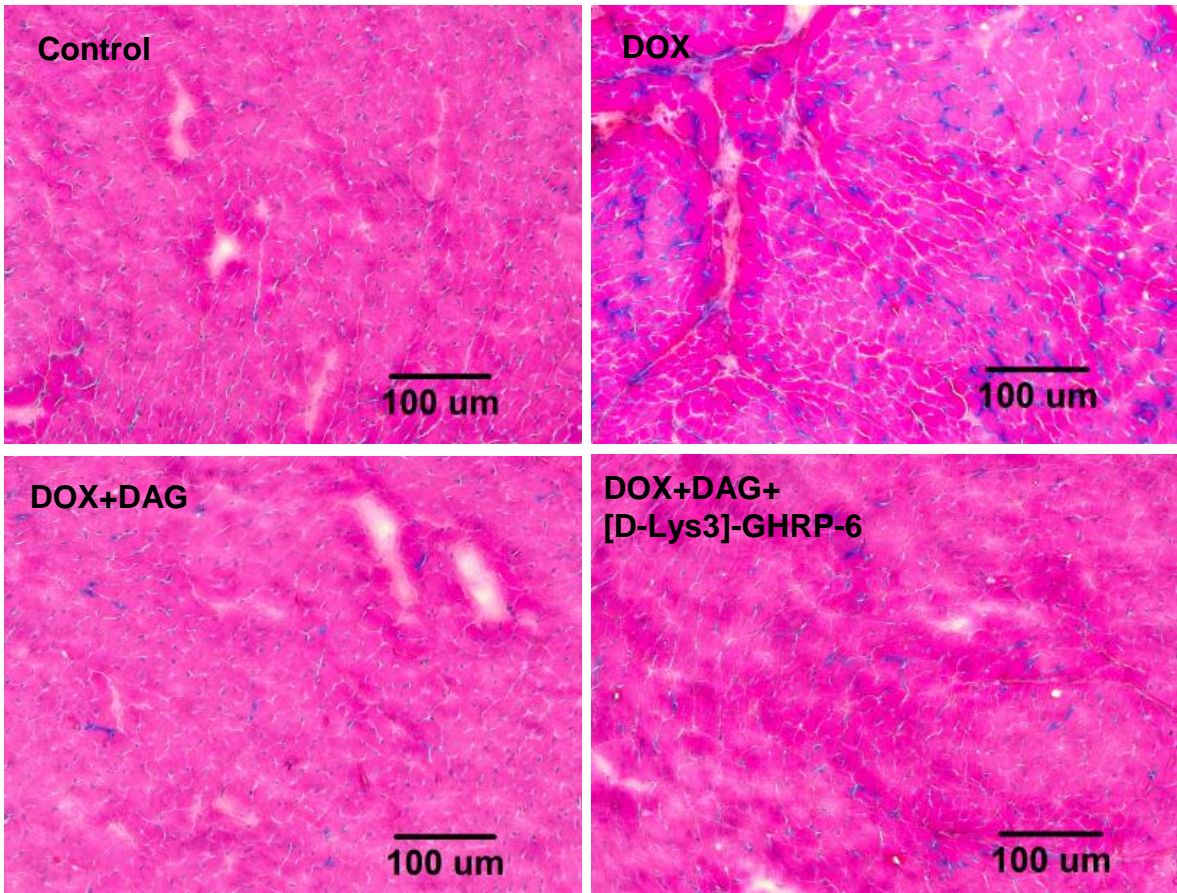


Fig 3.2 Collagen deposition in heart. Representative stained sections of hearts from control, DOX, DOX+DAG and DOX+DAG+ [D-Lys3]-GHRP-6 mice. DOX, doxorubicin; DOX+DAG, doxorubicin with treatment of desacyl ghrelin; DOX+DAG+[D-Lys3]-GHRP-6, doxorubicin with treatment of desacyl ghrelin plus [D-Lys3]-GHRP-6; Original magnification, $\times 200$.

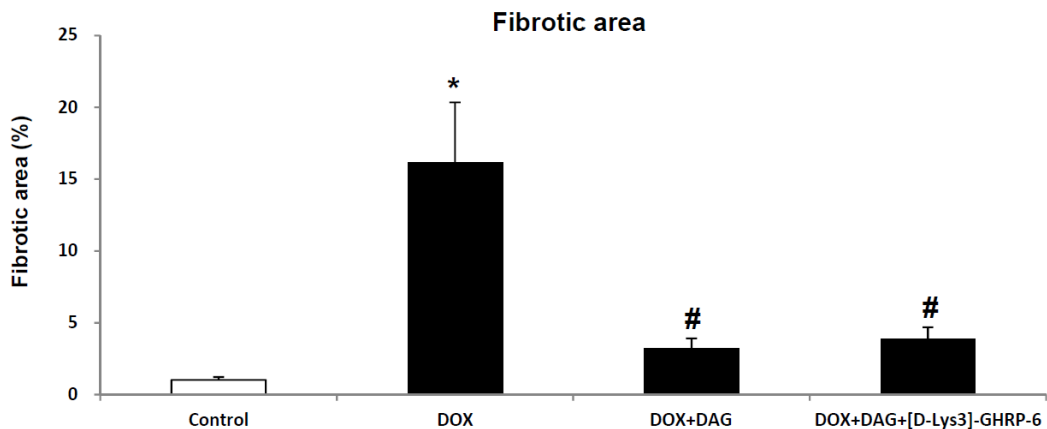


Fig 3.3 Fibrotic area was present by percent of collagen accumulation to total area of the microscopic field. DOX, doxorubicin; DOX+DAG, doxorubicin with treatment of desacyl ghrelin; DOX+DAG+[D-Lys3]-GHRP-6, doxorubicin with treatment of desacyl ghrelin plus [D-Lys3]-GHRP-6; Data are expressed as mean \pm SEM (n = 6 per group).

*P < 0.05 compared to Control. #P < 0.05 compared to DOX.

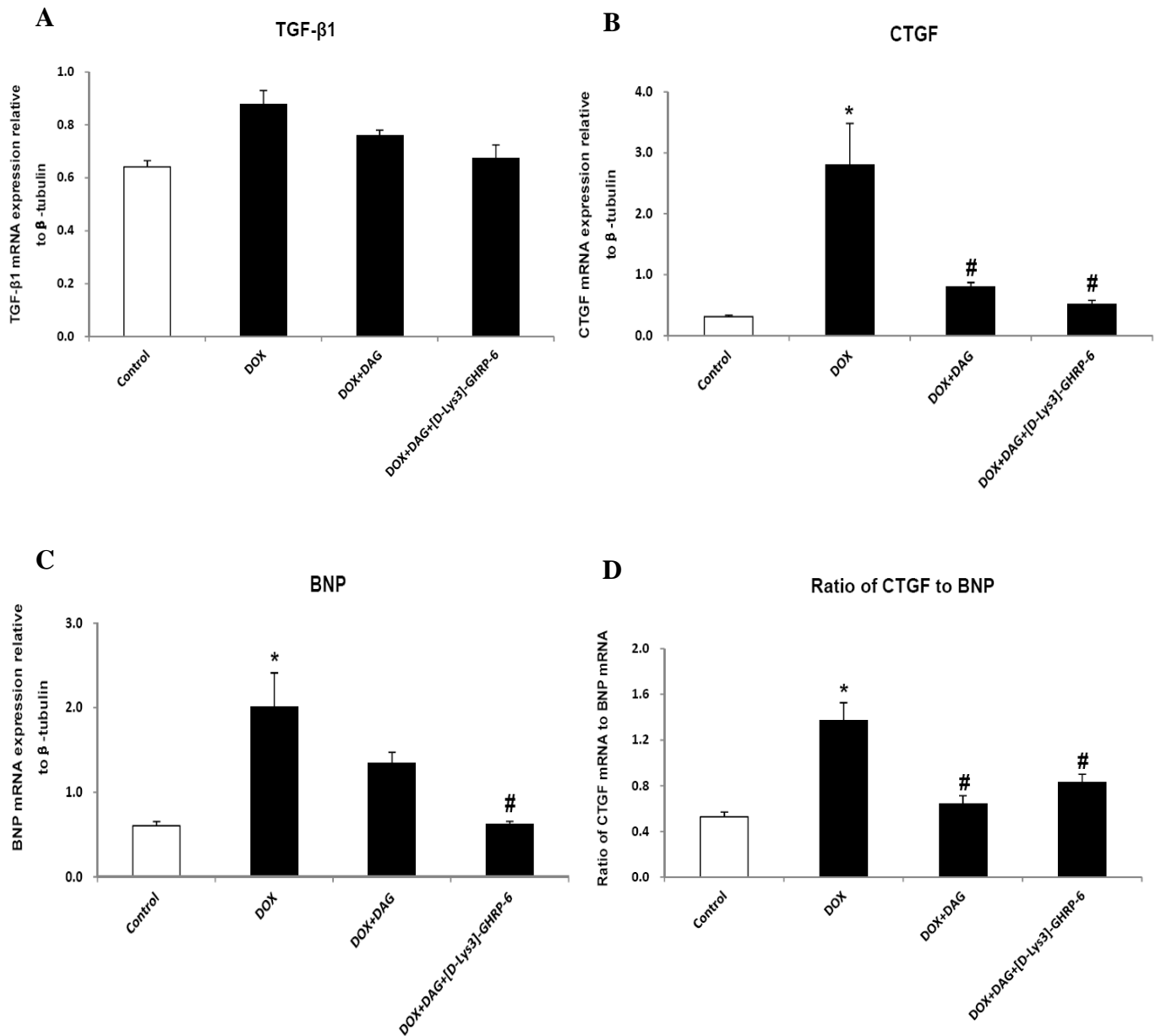


Fig 3.4 The transcript expression levels of myocardial fibrotic regulatory factors: TGF-β1 (A), CTGF (B) and BNP (C) were analyzed by real time quantitative PCR. Data were expressed as expression ratio normalized to β-tubulin gene. The balance between CTGF and BNP was presented by the ratio of mRNA level of CTGF to BNP (D). Data are expressed as mean ± SEM (n = 6 per group). *P < 0.05 compared to Control. #P < 0.05 compared to DOX.

3.3.3 Myocardial Apoptosis and Apoptotic Regulatory Factors

The number of myocardial apoptotic nuclei as indicated by the TUNEL index was increased (by 467%; $P < 0.05$) in ventricles of the DOX group when compared to those of the control group (Figure 3.5A). The TUNEL index was lowered in the desacyl ghrelin and desacyl ghrelin plus [D-Lys3]-GHRP-6 groups relative to the DOX group ($P < 0.05$) (Figure 3.5A). Similarly, the level of apoptotic DNA fragmentation was elevated (by 298%; $P < 0.05$) in the DOX group relative to the control group, and this DOX-induced increase was inhibited significantly by desacyl ghrelin (Figure 3.5B). Caspase-3 protease activity was increased (by 32%; $P < 0.05$) in ventricles of the DOX group when compared to those of the control group, and this DOX-induced increase was prevented by desacyl ghrelin (Figure 3.5C). No significant change was found in the protein content of anti-apoptotic Bcl-2 in ventricles of the DOX group compared to the control group (Figure 3.6A). However, Bcl-2 protein content was significantly higher (by 138%) in the desacyl ghrelin group when compared to the DOX group (Figure 3.6A). The protein content of pro-apoptotic Bax was elevated by DOX ($P < 0.05$), but this change was not affected by desacyl ghrelin ($P > 0.05$) (Figure 3.6B). The protein expression ratio of Bcl-2-to-Bax was further analyzed and was found to be lowered (by 46%; $P < 0.05$) in the DOX group compared to the control group (Figure 3.6C). This DOX-induced decrease in the Bcl-2-to-Bax ratio was not seen in the desacyl ghrelin group (Figure 3.6C). The inhibitory roles of desacyl ghrelin in apoptotic markers were not blocked by desacyl ghrelin plus [D-Lys3]-GHRP-6

treatment (Figure 3.6C). No significant difference was found in the protein level of antiapoptotic XIAP among all groups (Figure 3.7).

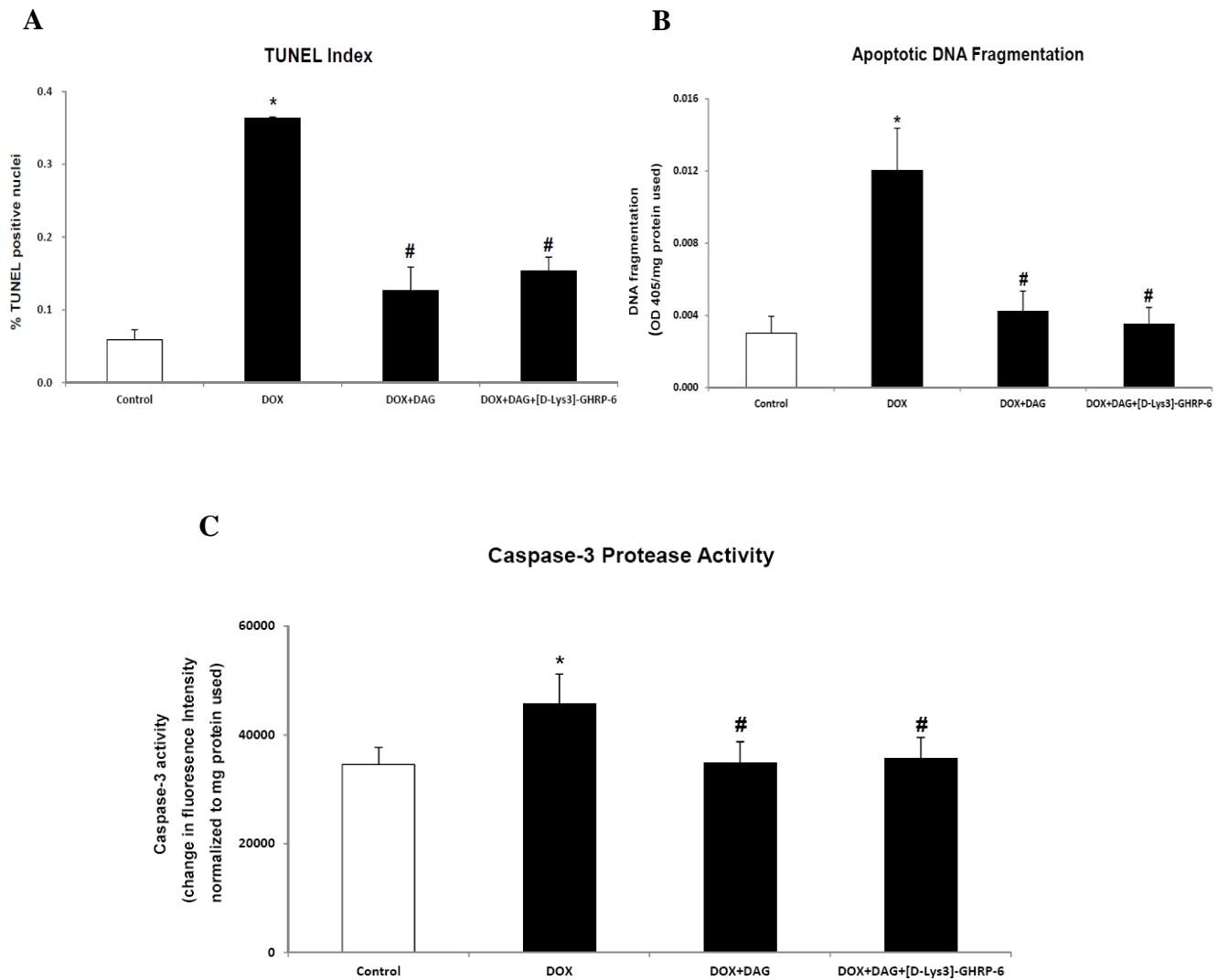


Fig 3.5 TUNEL index, apoptotic DNA fragmentation, and Caspase-3 protease activity in heart. The number of TUNEL-positive cardiomyocyte nuclei relative to the total number of nuclei was quantified as TUNEL index (A). The extent of apoptotic DNA fragmentation was estimated by measuring the cytosolic mono- and oligo-nucleosomes. The optical density at 405 nm (OD405) was normalized to the amount of protein used in the assay (B).

Caspase-3 protease activity was presented as the change of fluorescence intensity normalized to the total mg protein used in the assay (C). Data are expressed as mean \pm SEM (n = 6 per group). *P < 0.05 compared to Control, #P < 0.05 compared to DOX.

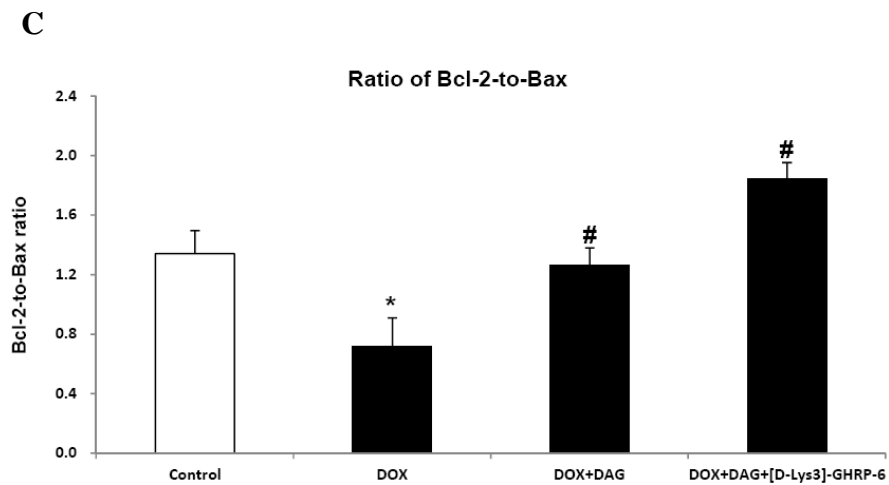
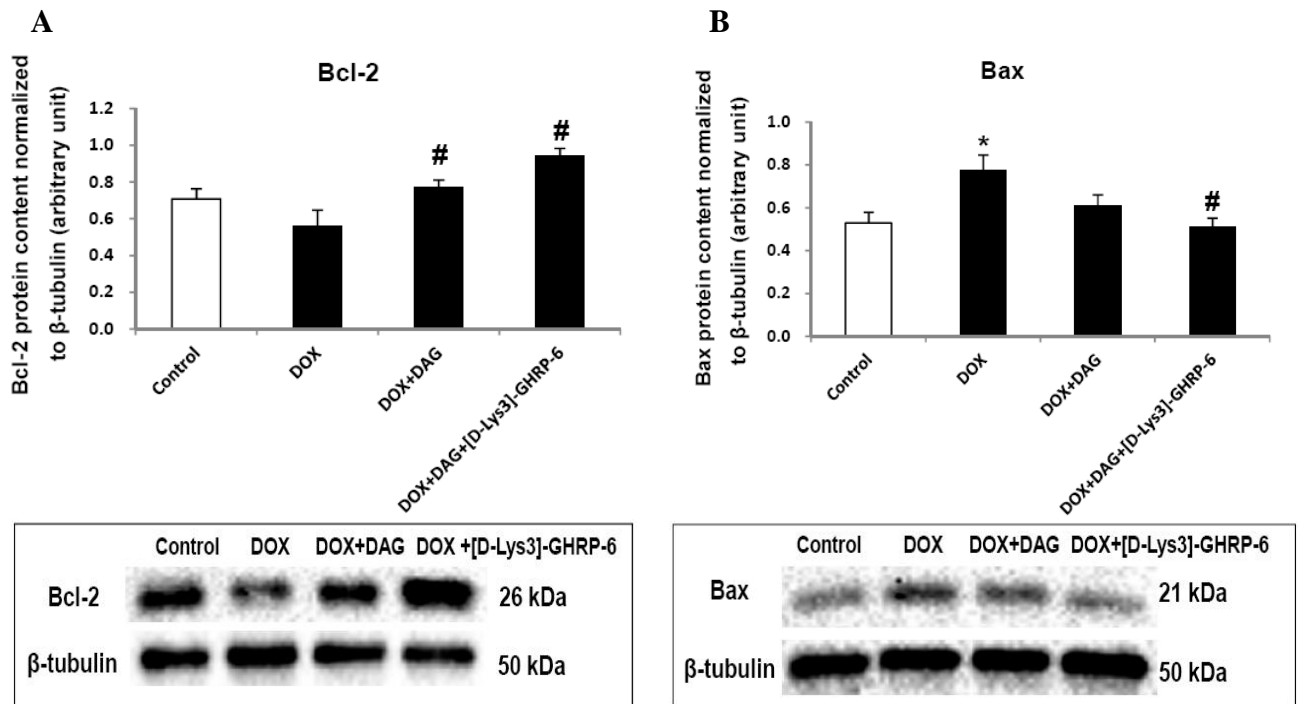


Fig 3.6 Protein abundances of Bcl-2 (A) and Bax (B) were determined by Western blot. Desitometric quantification was performed and data were presented as net intensity x resulting band area and expressed in arbitrary units. Results were normalized to corresponding β -tubulin signal. The ratio of the protein level of Bcl-2-to-Bax was shown (C). Data are expressed as mean \pm SEM (n = 6 per group). *P < 0.05 compared to Control, #P < 0.05 compared to DOX.

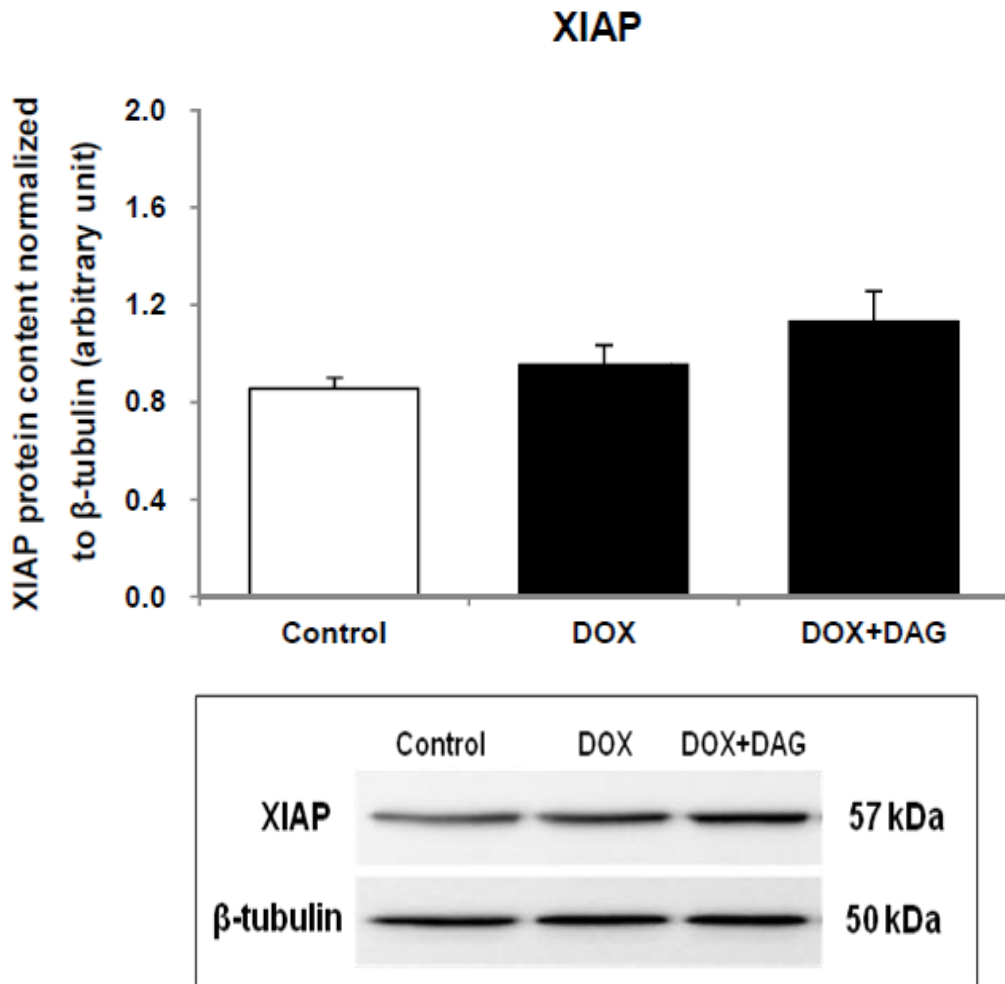


Fig 3.7 Protein abundances of XIAP were determined by Western blot. Desitometric quantification was performed and data were presented as net intensity x resulting band area and expressed in arbitrary units. Results were normalized to corresponding β -tubulin signal.

Data are expressed as mean \pm SEM (n = 6 per group).

3.3.4 Myocardial ERK/Akt Signaling

The ratio of phospho-ERK1/2-to-total ERK1/2 was significantly decreased (by 52%) in the DOX group relative to the control group (Figure 3.8A). This DOX-induced decrease was not seen in the desacyl ghrelin group (Figure 3.8A). However, the activation of ERK1/2 was blocked by [D-Lys3]-GHRP-6. The ratio of phospho-Akt-to-total Akt was reduced (by 28%; $P < 0.05$) in the DOX group relative to the control group but this decrease was not seen in the desacyl ghrelin desacyl ghrelin plus [D-Lys3]-GHRP-6 groups (Figure 3.8B).

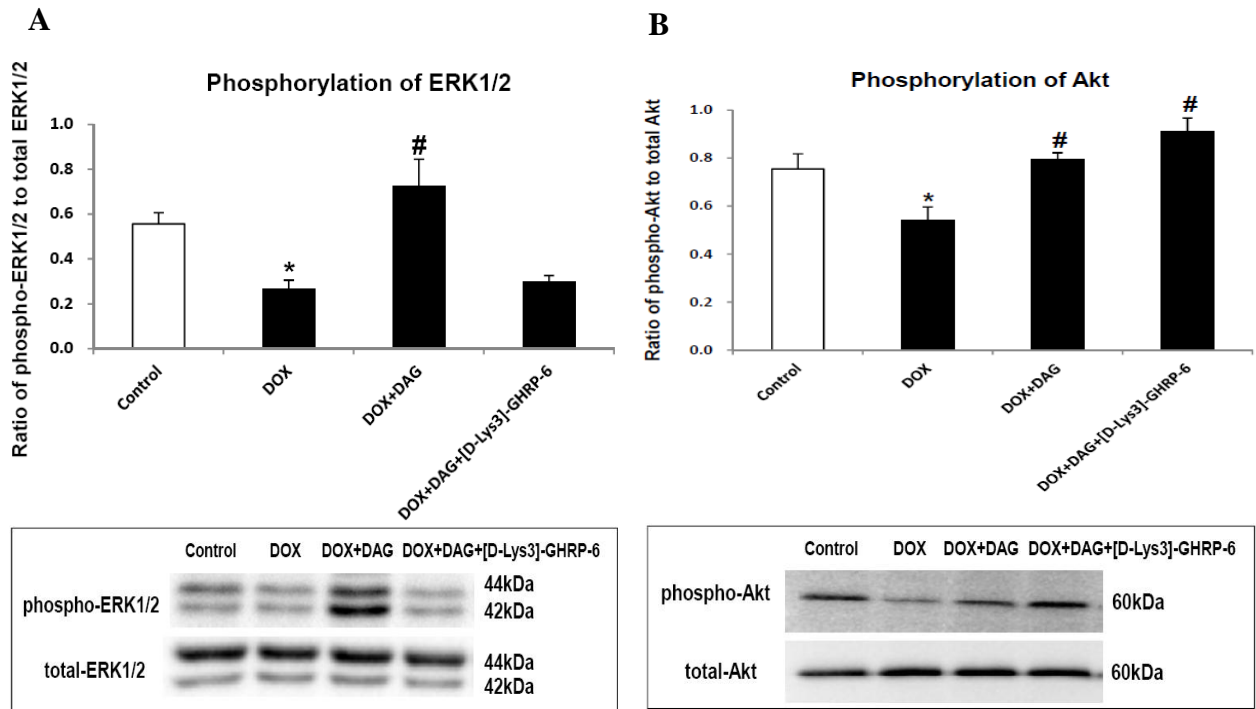
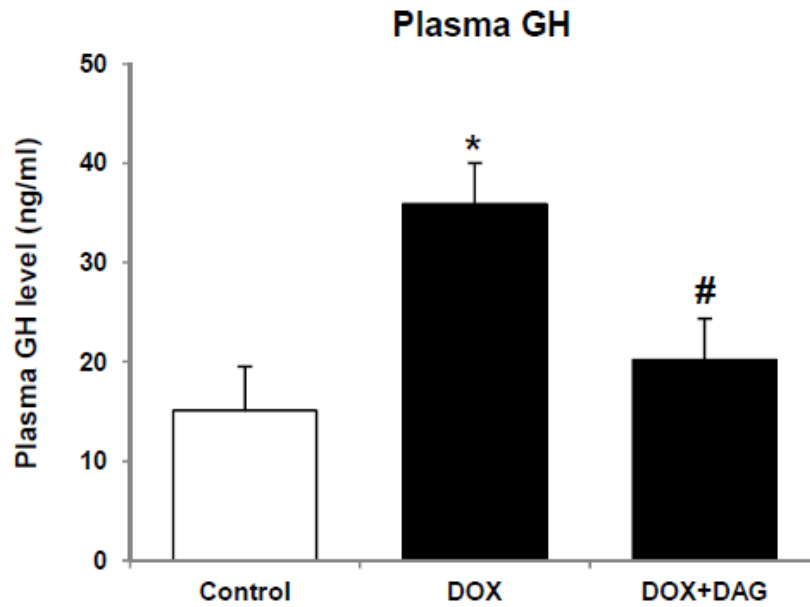


Fig 3.8 ERK and Akt signaling pathways were examined by detecting the phosphorylation statuses of ERK1/2 and Akt. Protein abundances of phospho(Thr402-Tyr204)-ERK1/2 and total ERK1/2 were examined by Western blot analysis and the ratio of phospho-ERK1/2-to-total ERK1/2 was presented (A). Protein abundances of phospho(Ser473)-Akt and total Akt were examined by Western blot analysis and the ratio of phospho-Akt-to-total Akt was shown (B). Data are expressed as mean \pm SEM (n = 6 per group). *P < 0.05 compared to Control. #P < 0.05 compared to DOX.

3.3.5 Plasma GH and IGF-1 Levels

A single intraperitoneal (i.p.) injection of DOX resulted in an elevation of growth hormone level in the circulation ($P < 0.05$) (Figure 3.9A). The DOX-induced growth hormone increase was not seen in the desacyl ghrelin group (Figure 3.9A). There was a significant (by 58%) reduction in the plasma IGF-1 level after DOX exposure (Figure 3.9B). This decrease was significantly lowered by the treatment with desacyl ghrelin (Figure 3.9B).

A



B

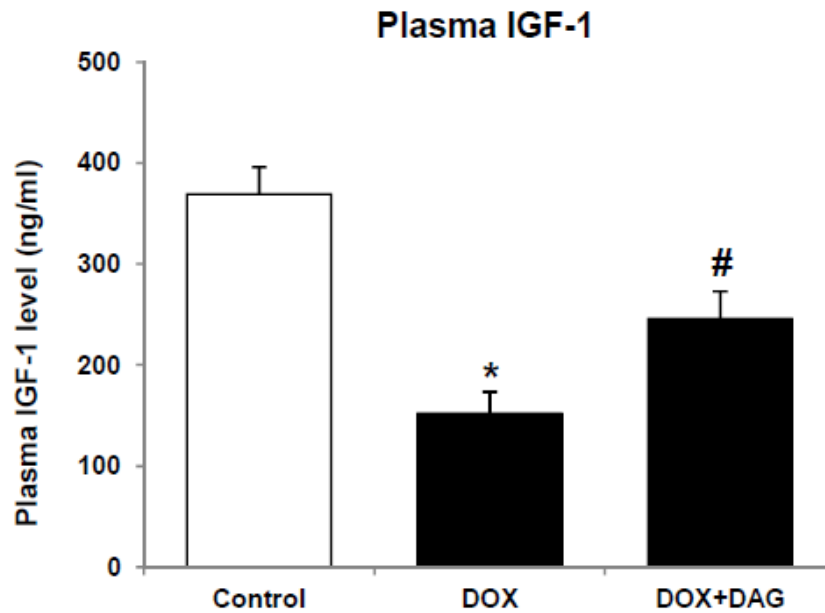


Fig 3.9 Plasma concentration of GH (A) and IGF-1 (B) was measured by ELISA. DOX, doxorubicin; DOX+DAG, doxorubicin with treatment of desacyl ghrelin. Data are expressed as mean \pm SEM (n = 6 per group). *P < 0.05 compared to Control. #P < 0.05 compared to DOX.

3.3.6 Myocardial Metabolic Regulators

The transcript expression of PPAR α was increased (by 82%; P<0.05) in the DOX group when compared to the control group. This DOX-induced increase was not observed in the desacyl ghrelin group (Figure 3.10A). Similar to the pattern of PPAR α , the transcript content of mCPT1 was significantly elevated (by 45%) in the DOX group relative to the control group. This increase was lower in the desacyl ghrelin group when compared to the DOX group (P < 0.05) (Figure 3.10B). The transcript content of UCP3 was reduced (by 54%; P<0.05) in the DOX group relative to the control group. This DOX-induced decrease was significantly less in the desacyl ghrelin group (Figure 3.10C). The transcript level of FAS was not significantly affected by DOX, and was not significantly different among all groups (Figure 3.10D). These changes of metabolic regulators induced by the treatment of desacyl ghrelin were not affected by the GHSR antagonist [D-Lys3]-GHRP-6. The protein levels of PGC-1 α in the cytosol and nucleus of the cardiomyocytes were not significantly affected by DOX and desacyl ghrelin (Figure 3.11A and 3.11B). No significant changes were seen in the ratio of phospho-AMPK α to total AMPK α or in phosphorylation of AMPK β 1 after DOX and desacyl ghrelin treatment (Figure 3.12A and 3.12B).

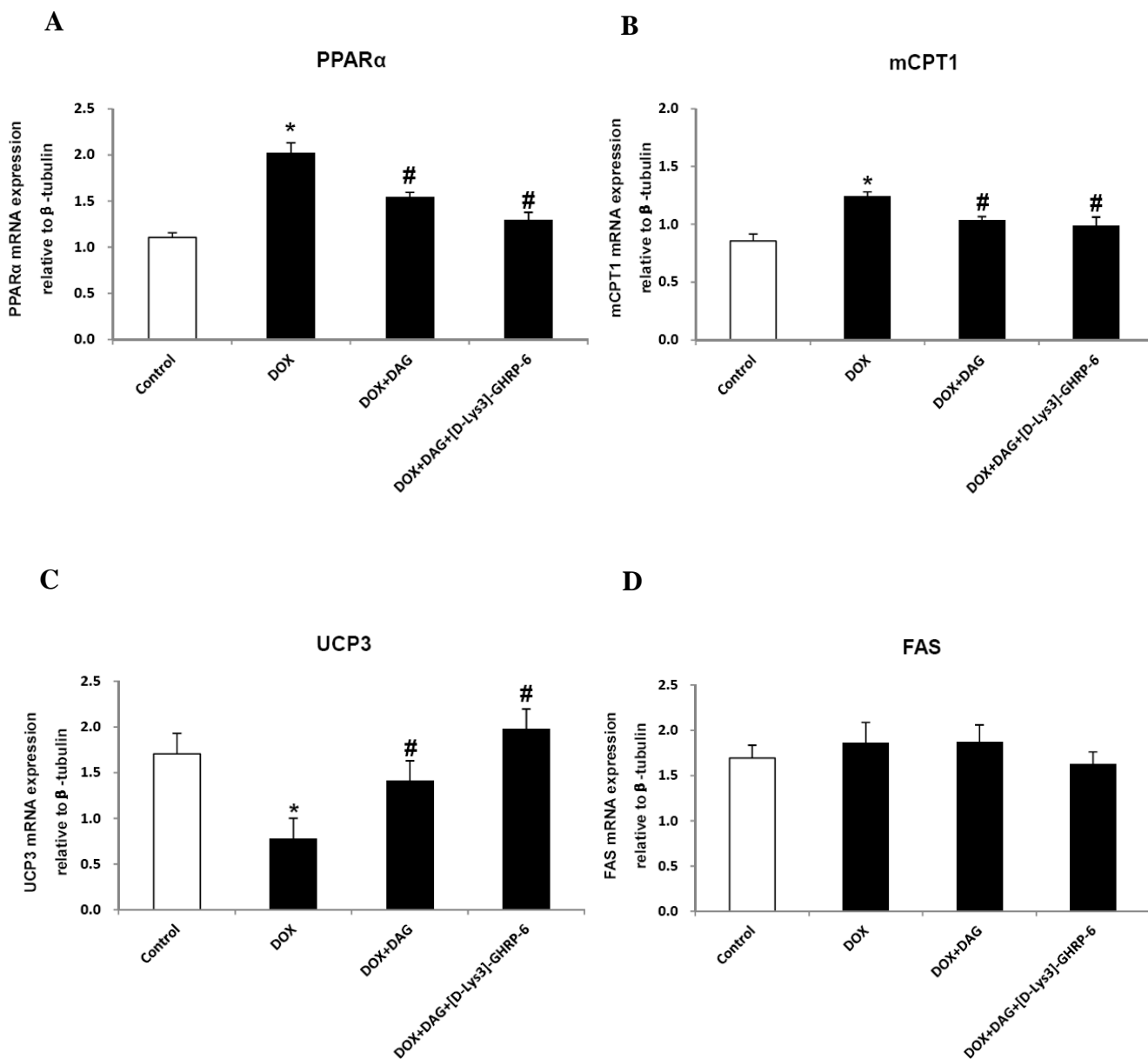
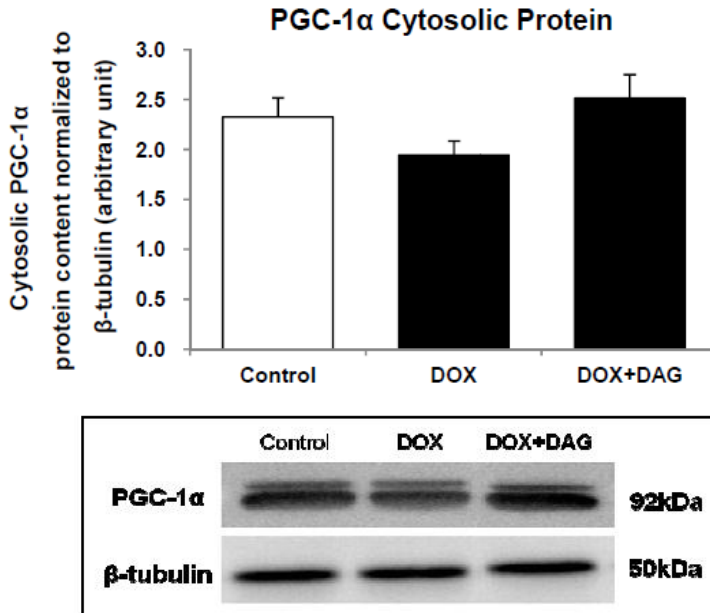


Fig 3.10 The transcript expression levels of myocardial metabolic regulators: PPAR α (A), mCPT1 (B), UCP3 (C), and FAS (D) were examined by real time quantitative PCR analysis. Data were presented as expression ratio normalized to β -tubulin gene. Data are expressed as mean \pm SEM (n = 6 per group). *P < 0.05 compared to Control. #P < 0.05 compared to DOX.

A



B

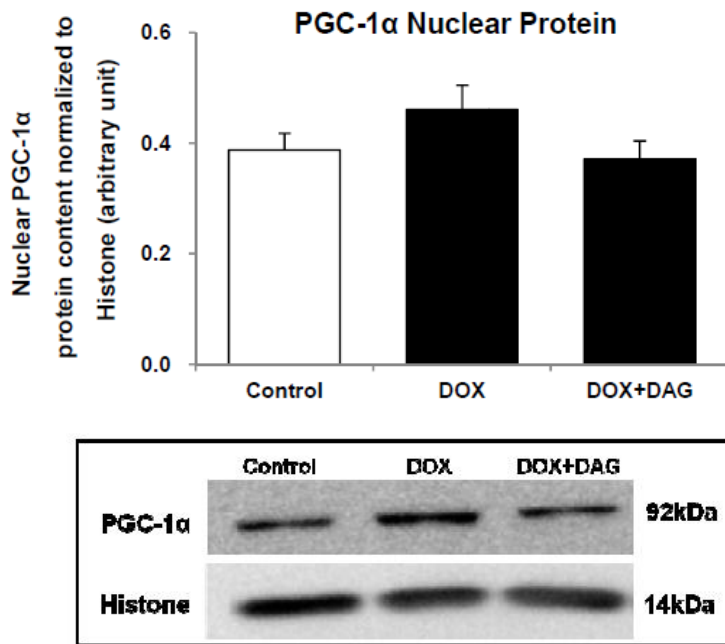


Fig 3.11 Cytoplasmic protein content (A) and nuclear protein content of PGC-1 α (B) in mice heart were measured by Western blot analysis. Data are expressed as mean \pm SEM (n = 6 per group).

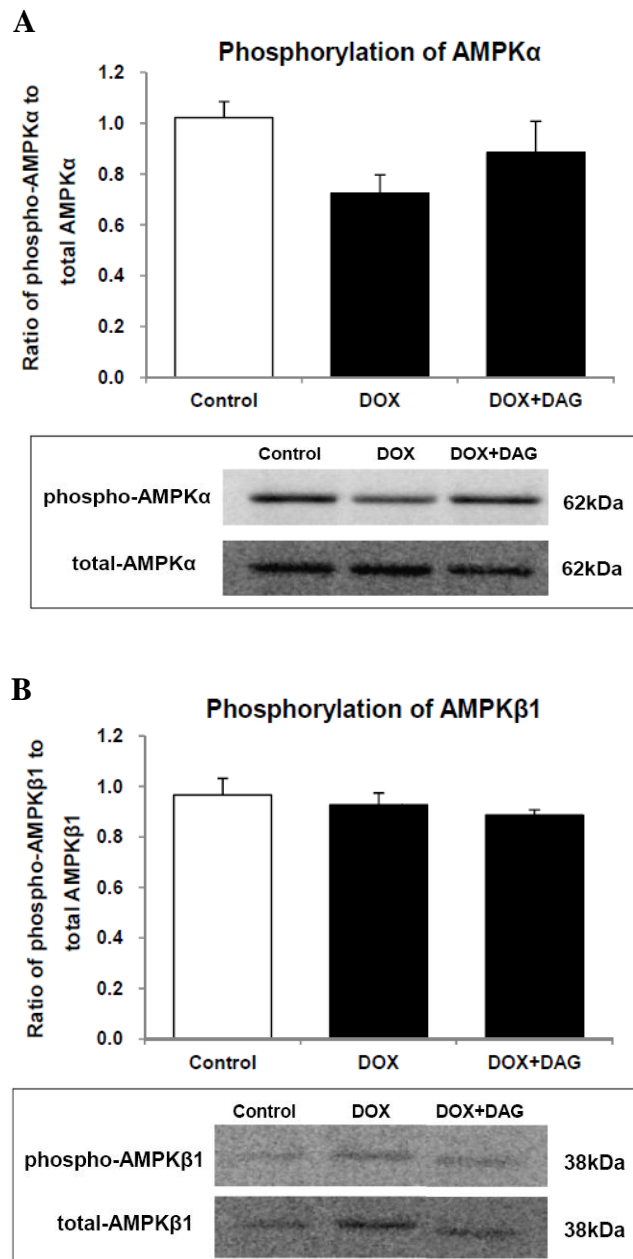


Fig 3.12 AMPK signaling in heart. Protein abundances of phospho(Thr172)-AMPK α , total AMPK α , phospho(Ser108)-AMPK β 1 and total AMPK β 1 were assessed by Western blot analysis. The activity of AMPK α and AMPK β 1 was indicated by the ratio of phospho-AMPK α -to-total AMPK α (A) and phospho-AMPK β 1-to-total AMPK β 1 (B). DOX, doxorubicin; DOX+DAG, doxorubicin with treatment of desacyl ghrelin. Data are expressed as mean \pm SEM (n = 6 per group).

3.3.7 Myocardial Calcium Handling Factors

The transcript levels of CAMK2D and PLB were significantly increased, by 37% and 81%, respectively, in the DOX group relative to the control group (Figure 3.13A and 3.13B). No significant differences were observed in the transcript levels of SERCA2a and RyR2 among all groups (Figure 3.13C and 3.13D).

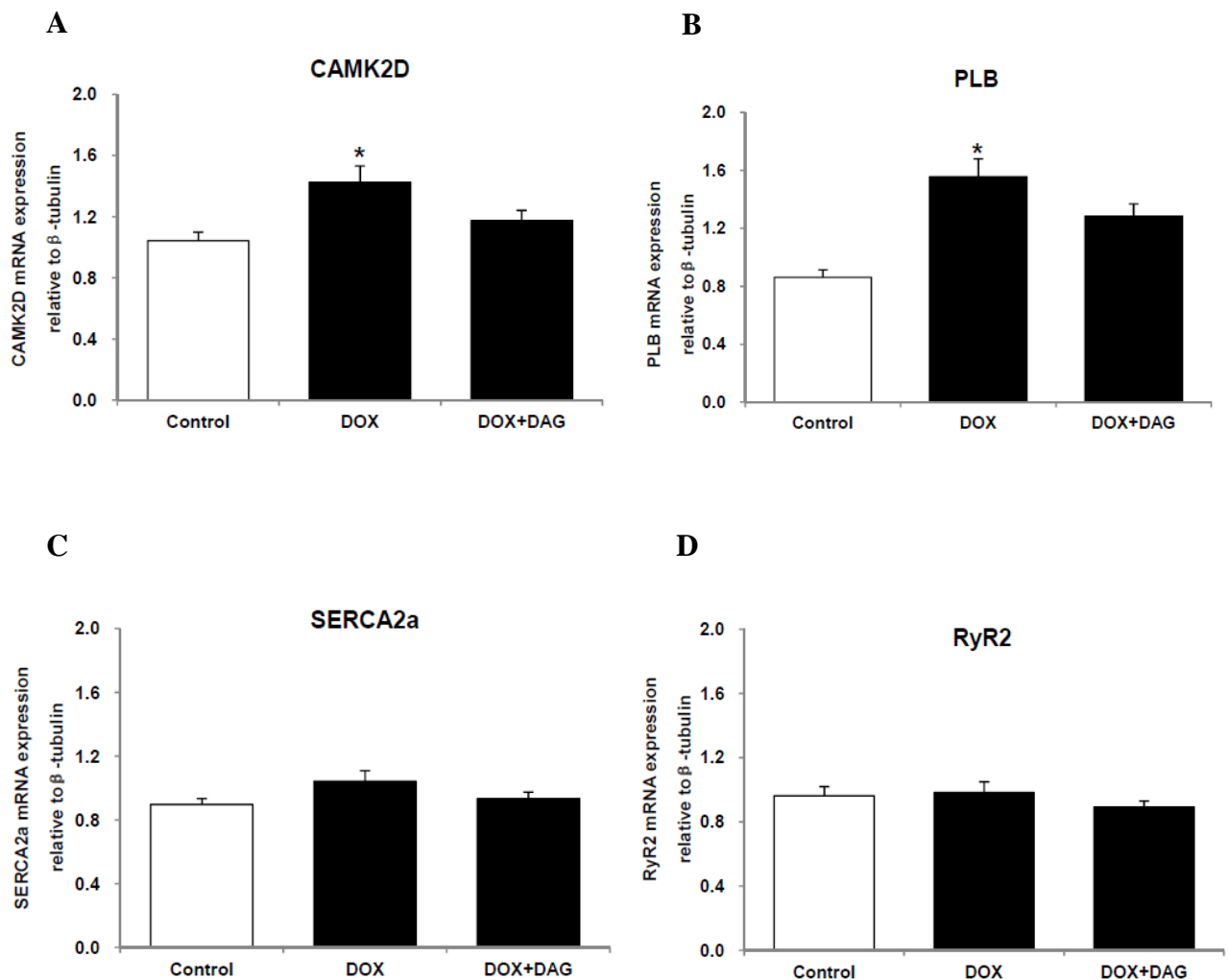


Fig 3.13 The transcript expression levels of myocardial calcium handling factors: CAMK2D (A), PLB (B), SERCA2a (C), and RyR2 (D) were examined by real time quantitative PCR analysis. Data were expressed as expression ratio normalized to β -tubulin gene. DOX, doxorubicin; DOX+DAG, doxorubicin with treatment of desacyl ghrelin. Data are expressed as mean \pm SEM (n = 6 per group). *P < 0.05 compared to Control.

3.4 Discussion

3.4.1 Desacyl Ghrelin Prevents DOX-induced Impairment of Cardiac Function

DOX induces cardiomyopathy, which presents a major clinical challenge to its wide therapeutic application in oncology (Floyd *et al.*, 2005). Our data indicate that treatment with desacyl ghrelin is effective to prevent the cardiac contractile dysfunction induced by DOX. These echocardiographic functional data are important to confirm the physiological and cardioprotective role of desacyl ghrelin. Previously, the *in vivo* data of ghrelin showing cardiac improvement were limited to ghrelin (acylated). Ghrelin (acylated) has been shown to improve infarction-induced ventricular dysfunction and ventricular remodeling by inhibiting inflammatory response and expression of matrix metalloproteinases in rats (Huang *et al.*, 2009). Ghrelin (acylated) has also been demonstrated to protect against ischemia-reperfusion myocardial injury in a rat isolated heart model (Frascarelli *et al.*, 2003; Chang *et al.*, 2004). In a later study, ghrelin (acylated) was demonstrated to protect the isolated rat heart against ischemia-reperfusion injury by attenuating myocardial apoptosis and inhibiting myocardial endoplasmic reticulum stress as indicated by the decreased glucose-regulated protein-78, C/EBP homologous protein and caspase-12 (Zhang *et al.*, 2009). In regard to heart failure, ghrelin (acylated) has been shown to improve ventricular dysfunction and ameliorate ventricular remodeling and cardiac cachexia in rats with chronic heart failure induced by experimental ligation of the left coronary artery (Nagaya *et al.*, 2001).

Specifically for DOX cardiotoxicity, there is *in vivo* evidence that endogenous ghrelin (acylated) level is increased during the progression of heart failure induced by DOX (Xu *et al.*, 2007), leading to the suggestion that ghrelin (acylated) might contribute to a compensatory self-protective mechanism, linked to anti-apoptosis and anti-oxidative mechanisms, that maintains cardiac function (Xu *et al.*, 2007). Notably, the functional effects of desacyl ghrelin on cardiac disorders are relatively unidentified, although there are some *in vitro* data suggestive of beneficial effects of desacyl ghrelin on DOX cardiotoxicity by inhibiting cardiomyocyte cell death (Baldanzi *et al.*, 2002). Here, our study provides novel functional evidence and molecular insights that substantiate physiological protection by desacyl ghrelin in DOX cardiotoxicity.

3.4.2 Anti-fibrotic Effect of Desacyl Ghrelin on DOX Cardiotoxicity

Fibrosis has been suggested to be involved in cardiac stiffness and dysfunction in DOX cardiotoxicity (Miyata *et al.*, 2010; Li *et al.*, 2007). The increased collagen synthesized by the fibroblasts invades and replaces the necrosed or apoptotic myocytes (Khan & Sheppard, 2006; Diwan *et al.*, 2008). In the present study, we observed that DOX-induced fibrosis was prevented by desacyl ghrelin as demonstrated by the attenuation of collagen deposition. Previously, ghrelin (acylated) treatment has been shown to ameliorate bleomycin-induced acute lung fibrosis (Imazu *et al.*, 2011) and liver fibrogenesis (Iseri *et al.*, 2008; Moreno *et al.*, 2010). Ghrelin-deficient mice have also been shown to be

more susceptible to develop liver fibrosis and hepatocellular damage after CCL4-induced chronic liver injury (Moreno *et al.*, 2010). Our present findings that desacyl ghrelin protects the heart from DOX by preventing myocardial fibrosis extend the previous demonstration of the effects of ghrelin (acylated) on preventing early left ventricle collagen volume increase in rats with myocardial infarction (Soeki *et al.*, 2008). Additionally, our data exhibit that the inhibitory effect of desacyl ghrelin on the DOX-induced myocardial collagen deposition is mediated through mechanisms that are not associated with the GHSR pathway. Consistent with our observations, Li and coworkers have reported that isoproterenol-induced cardiac fibrosis is relieved by both acylated and desacyl ghrelins in rats (Li *et al.*, 2006). Our present data further demonstrate the anti-fibrotic role of desacyl ghrelin particularly in DOX myocardial toxicity.

CTGF, a pro-fibrotic cytokine, has been shown to be upregulated by TGF- β in heart with myocardial infarction (Ohnishi *et al.*, 1998;Chen *et al.*, 2000a), carotid artery balloon injury (Hwang *et al.*, 2012), and type 1 diabetic cardiomyopathy (Rajesh *et al.*, 2009;Rajesh *et al.*, 2010). Wang and colleagues found that the interaction between TGF- β and CTGF is necessary for the development of multiorgan fibrosis, renal fibrosis, and pulmonary fibrosis (Wang *et al.*, 2011). In the present study, DOX-induced increase in CTGF expression in the heart is seen in the absence of the increase in TGF- β 1 expression. This is consistent with the notion that fibrosis in renal and heart may not be fully regulated by TGF- β , but essentially dependent on CTGF

(Zhou *et al.*, 2004;Way *et al.*, 2002). Our findings suggest that CTGF might play an important role in DOX-induced fibrotic injury through a TGF- β -independent pathway. Brain natriuretic peptide (BNP) serves as an anti-fibrotic factor by activating guanylyl cyclase-A (Tamura *et al.*, 2000) or interacting directly with CTGF (Koitabashi *et al.*, 2007). The balance between CTGF and BNP in cardiomyocyte has been suggested to be a central determinant of cardiac fibrosis (Koitabashi *et al.*, 2007). Our data show that desacyl ghrelin decreases the relative abundance of CTGF to BNP, which partly explains the effect of desacyl ghrelin on preventing fibrosis induced by DOX. Taken together, our data clearly demonstrate that desacyl ghrelin prevents the activation of fibrosis in DOX cardiotoxicity through a CTGF/BNP-associated regulatory pathway.

3.4.3 Anti-apoptotic Effect of Desacyl Ghrelin on DOX

Cardiotoxicity

DOX exposure causes activation of mitochondrial apoptosis in cardiomyocytes (Childs *et al.*, 2002;Shan *et al.*, 2003). DOX-induced cardiac dysfunction has been shown to be improved by interventions that inhibit apoptosis in cardiomyocytes, such as administration of erythropoietin (Chen *et al.*, 2007) and transgenic overexpression of Nd1 Kelch family protein in the heart (Matsudo *et al.*, 2006). Previously, the anti-apoptotic effect of ghrelin has been reported in an in vitro study showing that both acylated and desacyl ghrelins inhibit DOX-induced apoptosis in H9c2 cardiomyocytes (Baldanzi *et al.*, 2002).

Consistent with these *in vitro* findings, the presently observed improvement of the DOX-induced cardiac dysfunction with desacyl ghrelin was accompanied by suppression of the TUNEL index, apoptotic DNA fragmentation, and protease activity of caspase-3. This is in line with the observed ratio of Bcl-2/Bax which is significantly decreased by DOX, a change that is prevented by desacyl ghrelin. It is noted that our findings also agree with the previous *in vitro* findings demonstrating that desacyl ghrelin is protective against apoptosis in isolated cardiomyocytes (Lear *et al.*, 2010). Experimental expression of constitutively active PI3K has been demonstrated to inhibit the activation of caspase-3 and apoptosis in cardiomyocytes (Wu *et al.*, 2000). There are *in vitro* data showing that acylated and desacyl ghrelins inhibit DOX-induced apoptosis by activating the intracellular prosurvival signaling pathways conveyed by ERK1/2 and PI3K/Akt in cultured cardiomyocytes (Baldanzi *et al.*, 2002). Consistent with these suggestions, our data show that the phosphorylation statuses of ERK1/2 and Akt are suppressed in the heart tissues in response to DOX exposure and these suppressions are opposed by desacyl ghrelin. The observation that the reverse of Akt activation induced by the treatment of desacyl ghrelin is not affected by the GHSR antagonist [D-Lys3]-GHRP-6 suggests that desacyl ghrelin activates Akt signaling through a GHSR-independent pathway. Surprisingly, the increased level of ERK1/2 phosphorylation following desacyl ghrelin treatment was blocked by the GHSR antagonist [D-Lys3]-GHRP-6 (Figure 4A), [D-Lys3]-GHRP-6 showed the inhibitory effect on ERK1/2 activation induced by acylated ghrelin in in

primary oligodendrocyte cultures (Lee et al., 2011). However, the ERK1/2 expression was increased in porcine ovarian granulosa cell after addition of [D-Lys3]-GHRP-6 alone (Sirotkin et al., 2011). The effect of [D-Lys3]-GHRP-6 on basal ERK1/2 activity in cardiomyocyte is uncertain. In the present study, The inhibition of ERK1/2 phosphorylation by [D-Lys3]-GHRP-6 suggest that desacyl ghrelin effect on impaired ERK1/2 phosphorylation may result from GHSR-dependent pathway. Although the exact mechanisms remain to be elucidated, these prosurvival signaling results are in support of the changes of Bcl-2/Bax ratio, suppression of caspase-3 activity and inhibition of myocardial apoptosis in the heart treated with desacyl ghrelin following DOX exposure. Collectively, our data suggest that desacyl ghrelin prevents the activation of myocardial apoptosis induced by DOX and the anti-apoptotic effect of desacyl ghrelin is probably mediated through the cellular signaling of ERK1/2 and PI3K/Akt pathways.

In conclusion, the present investigation demonstrated that desacyl ghrelin significantly modulated several cardiotoxic effects of DOX, including contractile dysfunction, myocardial fibrosis and apoptosis, suppression of cellular prosurvival signaling, and disruption of myocardial metabolic regulators, and this was via a GHSR-independent pathway. These results are consistent with the hypothesis that desacyl ghrelin protects the heart against DOX-induced cardiomyopathy. It is worth noting that our data were collected in a mouse model of acute DOX cardiotoxicity (i.e., 4-days after a single

administration of DOX). Further research might be warranted to further investigate the cardioprotective effects of desacyl ghrelin in response to chronic prolonged exposure to DOX. Furthermore, the potential clinical application of desacyl ghrelin in resolving or preventing the cardiotoxic effect of DOX during chemotherapy is worth further exploration.

CHAPTER 4

Protective Effect of Desacyl Ghrelin on Type 2

Diabetic Cardiomyopathy

4.1 Introduction

Cardiovascular disease, a common complication of diabetes, accounts for around 80% of the mortality in diabetic patients (Voulgari *et al.*, 2010). Although coronary artery disease is found to be the main cause of the increased cardiovascular mortality in diabetes, clinical and experimental studies demonstrated that heart structure and function are yet to be affected by diabetes even in the patients that coronary artery atheroma and hypertension are absent (Voulgari *et al.*, 2010;Rubler *et al.*, 1972). This refers to a specific type of cardiac disorder called diabetic cardiomyopathy, which is independent of coronary artery disease and featured by the asymptomatic diastolic dysfunction, fibrosis, and metabolic disturbance in the heart of diabetic patients.

Ghrelin is a recently identified peptide hormone mainly secreted in stomach. Acylated ghrelin has a post-translational modification with O n-octanoyl acid at serine 3 position. This acylation for ghrelin is necessary for its binding with GHSR to mediate the endocrinological effects of ghrelin such as the stimulation of growth hormone release. Desacyl ghrelin, another form of ghrelin, accounts for around 80%- 90% of circulating ghrelin (van der Lely *et al.*, 2004). This desacylated form of ghrelin lacks the ability to stimulate the release of growth hormone due to the lacking of the post-translational modification of acylation. However, desacyl ghrelin has been demonstrated to have an important role in the cardiovascular system and the metabolisms of glucose and lipid (Tesauro *et al.*, 2010;van der Lely *et al.*, 2004). Ghrelin, including acylated ghrelin and

desacyl ghrelin, have been illustrated to inhibit cardiac apoptosis through the activation of PI3K/Akt pro-survival signaling in H9c2 cardiomyocytes (Baldanzi *et al.*, 2002). There are ample of studies that reported the protective effects of acylated ghrelin on cardiac ischemic injury, heart failure, hypertension and myocardial infarction by improving the cardiac contractility and remodeling. However, there is a scarcity of investigation that examined the cardioprotective effects of desacyl ghrelin on cardiac disorders including diabetic cardiomyopathy.

Therefore, this study was designed to examine the effects of peripheral administration of desacyl ghrelin on diabetic cardiomyopathy in a type 2 diabetic mouse experimental model. There are several reasons to propose the desacyl, but not acylated, form of ghrelin as the therapeutic agent for diabetic cardiomyopathy in type 2 diabetic patients in the present study. Firstly, acylated form of ghrelin has been shown to increase blood glucose level (Broglio *et al.*, 2001) and triglyceride contents in liver and white adipose tissue (Barazzoni *et al.*, 2005), which might not be favorable to diabetic individuals. In contrast, desacyl ghrelin has been shown to decrease the glucose release and to improve the insulin sensitivity, which are beneficial to diabetic patients. Secondly, desacyl ghrelin has been demonstrated to protect the pancreatic β -cells and prevent the development of diabetes induced by streptozotocin in rats (Granata *et al.*, 2012). Indeed, an analog of desacyl ghrelin is currently under development by pharmacological company to treat type 2 diabetes mellitus.

4.2 Methods

4.2.1 Animals

Male 14- to 18-week-old db/db mice obtained from the Laboratory Animal Services Centre of The Chinese University of Hong Kong were used in this project. The db/db mouse is a well-established leptin receptor-deficient animal model (homozygous allelic deficient of leptin receptor gene) that mimics the disease phenotype of type 2 diabetes mellitus in human. Non-diabetic db/+ mice (heterozygous allelic deficient of leptin receptor gene) were used as the non-diabetic control because they share similar genetic background with db/db diabetic mice but they exhibit normal blood glucose level in the absence of any type 2 diabetic phenotype. Mice were housed in a temperature- and humidity-controlled environment and were exposed to a 12:12-hour light: dark cycle in the Centralised Animal Facilities of The Hong Kong Polytechnic University. Mice were allowed to have access to standard animal diet and water ad libitum. Animal ethics approval was obtained from the Animal Ethics Sub-committee of The Hong Kong Polytechnic University.

4.2.2 Experimental Protocol

Mice in non-diabetic group (db/+) and diabetic group (db/db) were randomly assigned to the following sub-groups: db/+Saline (n = 7), db/+DAG (DAG, desacyl ghrelin; n = 7), db/db-Saline (n = 7), and db/db-DAG (n = 7). Mice assigned to DAG treatment groups were exposed to an intraperitoneal injection

of desacyl ghrelin (Tocris Bioscience, USA) for ten consecutive days. Mice in sham (Saline) groups were intraperitoneally injected with the same volume of saline instead of desacyl ghrelin. The previously reported administered dosage of 100 µg/kg bodyweight of ghrelin injected twice daily was adopted (Li *et al.*, 2006; Nagaya *et al.*, 2001). After the ten days of experimental period, mice were euthanized by overdose of ketamine and xylazine. Heart was immediately removed and washed with cold phosphate buffered saline (PBS). Left ventricle was quickly dissected and frozen in liquid nitrogen and stored at -80°C for later analysis.

4.2.3 Measurement of Cardiac Function by Echocardiography

The detailed procedure of the measurement of the cardiac function using echocardiography was described in CHAPTER 2.

4.2.4 Masson's Trichome Staining

Fibrosis was determined by measuring the collagen deposition in the left ventricle of mice by Masson's trichome staining. The procedure is described in CHAPTER 2.

4.2.5 Protein Fraction Preparation

The protein fraction of cardiac muscle samples was prepared by adopting the protocol described in CHAPTER 2.

4.2.6 RNA Extraction and Real Time Quantitative PCR

Analysis

Myocardial fibrosis regulatory factors (adiponectin, MMP-8, and MMP-13), inflammatory markers (apelin, Wnt5a, and TLR4), and other factors (Edn3, GATA6, p21, FKBP10, and FKBP5) were examined in cardiac tissues by quantitative RT-PCR analysis. Total RNA extraction and real time PCR analysis were performed by following the procedure described in CHAPTER 2.

4.2.7 Western Blot Analysis

The protein expression of autophagic factors (Beclin1 and Atg5-Atg12 conjugation) and pro-survival ERK-Akt signaling, AMPK and GSK3 α/β signaling markers (phospho-ERK1/2, total ERK1/2, phospho-Akt, total Akt, phospho-AMPK, total AMPK, phospho-GSK3 α/β , and total GSK3 α/β) were evaluated in cardiac tissues by Western immunoblot. The detailed procedure is described in CHAPTER 2.

4.2.8 Statistical Analysis

Data were expressed as mean \pm standard error of mean. Statistical analysis was performed by using Statistics Package for Social Science (SPSS) version 11.0. Differences among groups were evaluated by ANOVA followed by Tukey's HSD post hoc test. Statistical significance was set at $P < 0.05$.

4.3 Results

4.3.1 Cardiac Function by Echocardiography

The cardiac dysfunction in diabetic cardiomyopathy was indicated by the decreased fractional shortening (by 25%, $P < 0.05$) in diabetic mice compared to non-diabetic mice at the pre-interventional level. This decrease in the left ventricle fractional shortening was found to be alleviated by desacyl ghrelin treatment (Fig 4.1).

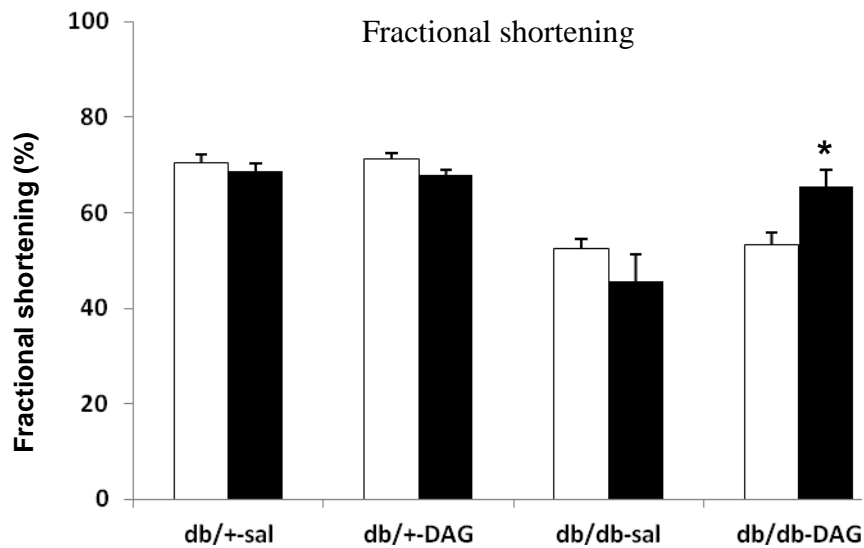


Fig 4.1 Effect of desacyl ghrelin on fractional shortening. Data are expressed as mean \pm SEM (n = 6 per group). * $P < 0.05$ compared to Pre intervention level in db/db mice.

4.3.2 Cardiac Fibrosis and Fibrotic Regulatory Factors

The collagen deposition in left ventricle was shown in Fig 4.2. Elevated accumulation of collagen (shown in blue color) was observed in the heart of diabetic db/db mice when compared to non-diabetic db/+ mice heart, and this induction of cardiac fibrosis was apparently alleviated by desacyl ghrelin treatment. The anti-inflammatory adiponectin expression was decreased in diabetic heart (by 30%, $P < 0.05$) but this decrease was not found in the animals that have received the treatment of desacyl ghrelin (Fig 4.3A). The transcript expression of collagenase-2 (MMP-8) was significantly up-regulated in the heart of db/db diabetic mice (by 15 fold, $P < 0.001$) relative to db/+ non-diabetic mice. But this up-regulation of MMP-8 expression was not observed to be affected by desacyl ghrelin treatment (Fig 4.3B). The transcript expression of MMP-13 was suppressed in the heart of diabetic mice (by 80%, $P < 0.001$) when compared to non-diabetic control heart. This suppression of MMP-13 was not found to be reversed by desacyl ghrelin treatment (Fig 4.3C).

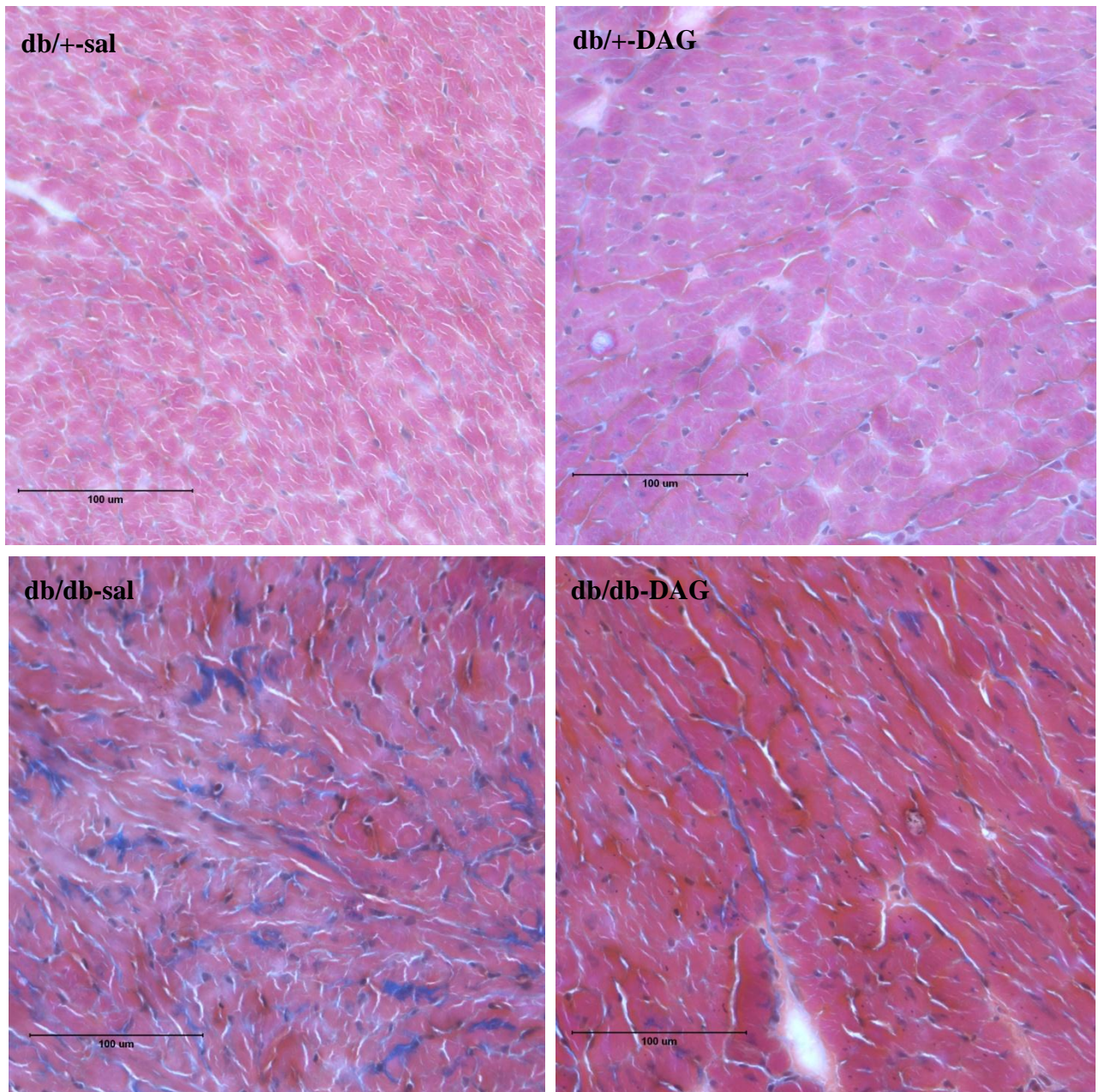


Fig 4.2 Collagen deposition after desacyl ghrelin treatment in the heart of db/db diabetic mice. Representative stained sections of hearts from db/+-Sal, db/+-DAG, db/db-Sal and db/db-DAG mice. Original magnification, $\times 400$.

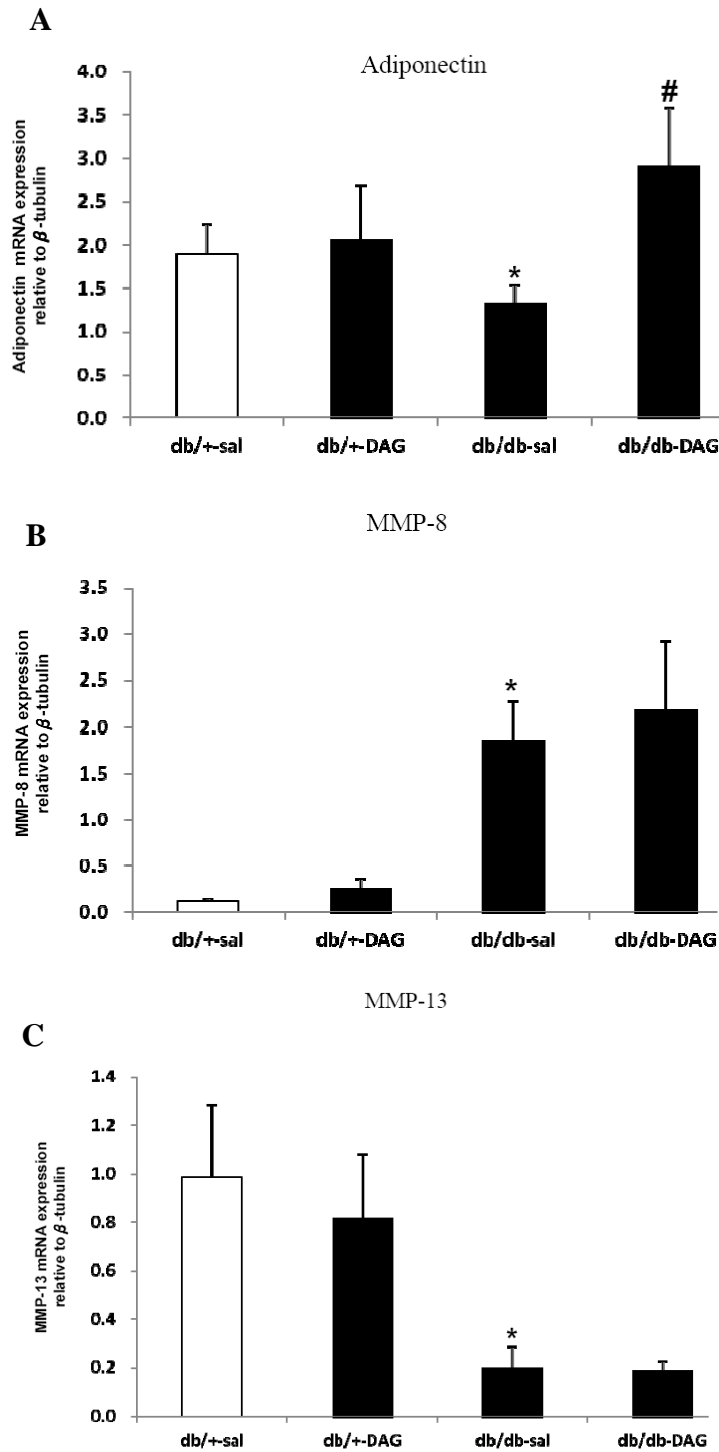


Fig 4.3 The transcript expression of adiponectin (A), MMP-8 (B), and MMP-13 (C). Data were presented as expression ratio normalized to β -tubulin gene. Data are expressed as mean \pm SEM (n = 6 per group). *P < 0.05 compared to non-diabetic control group (db/+Sal), #P < 0.01 compared to diabetic control group (db/db-Sal).

4.3.3 Cardiac Inflammatory Markers

The inflammatory process has been suggested to be involved in the development of diabetic cardiomyopathy. The expression of cardiac inflammatory markers was examined by real time RT-PCR. *APELIN* gene expression in the heart was not significantly changed among all groups (Fig 4.4A, $P>0.05$). In the heart of db/db diabetic mice, there was an increase in mRNA concentration of *Wnt5a* ($P<0.05$) relative to non-diabetic control mice (Fig 4.4B). The transcript expression of *TLR4* in the heart of diabetic mice was significantly decreased when compared to non-diabetic control heart (by 29.8%, $P<0.05$) as shown in Fig 4.4C.

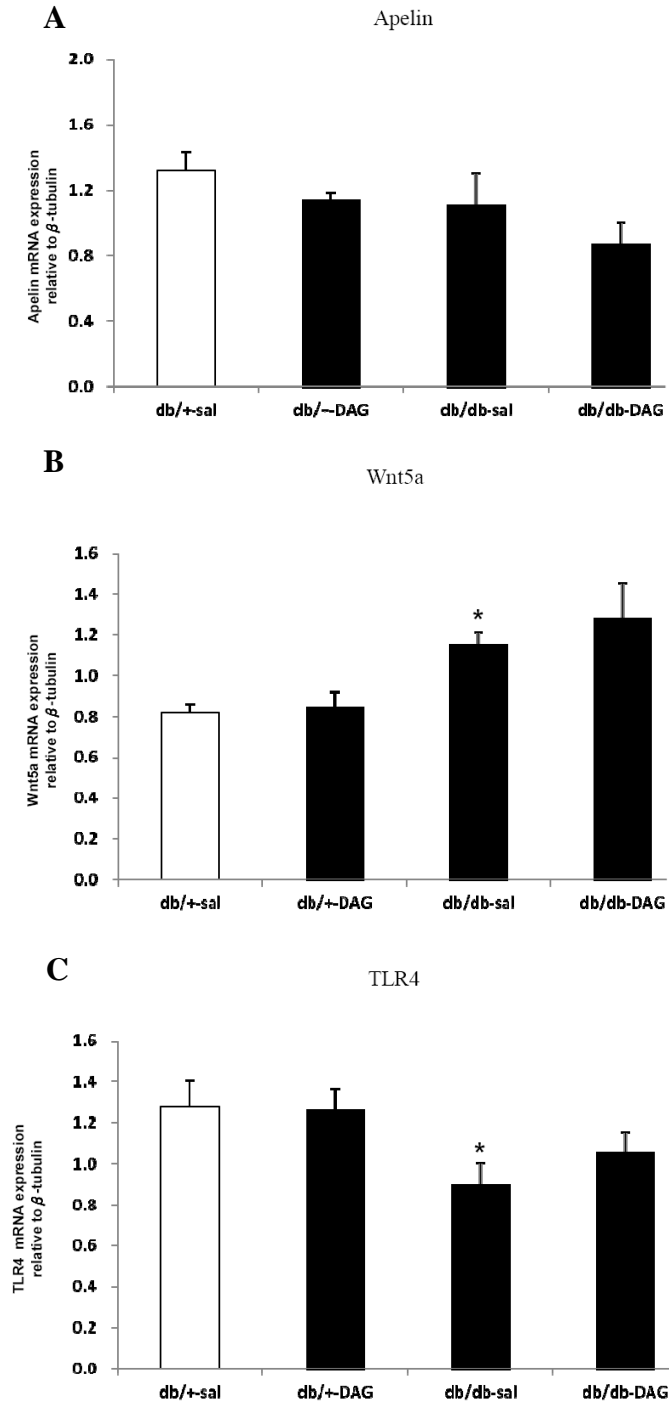


Fig 4.4 The transcript expression of Apelin (A), Wnt5a (B), and TLR4 (C). Data were presented as expression ratio normalized to β -tubulin gene. Data are expressed as mean \pm SEM (n = 6 per group). *P < 0.05 compared to non-diabetic control group (db/+Sal), #P < 0.01 compared to diabetic control group (db/db-Sal).

4.3.4 Cardiac Autophagic Markers: Beclin1 and Atg5-Atg12 Conjugation

The protein content of autophagic markers including Beclin1 and Atg5-Atg12 conjugation were measured in the hearts. The protein expression of Beclin1 was reduced (by 29%, $P < 0.05$) in the heart of db/db diabetic mice but this reduction was observed to be reversed by desacyl ghrelin treatment (Fig 4.5A). No significant change was observed in the level of Atg5-Atg12 Conjugation in the heart of db/db diabetic mice when compared to non-diabetic db/+ control heart. However, desacyl ghrelin treatment was found to enhance the conjugation of Atg5 and Atg12 in the heart of db/db diabetic mice (by 149%, $P < 0.05$) (Fig 4.5B).

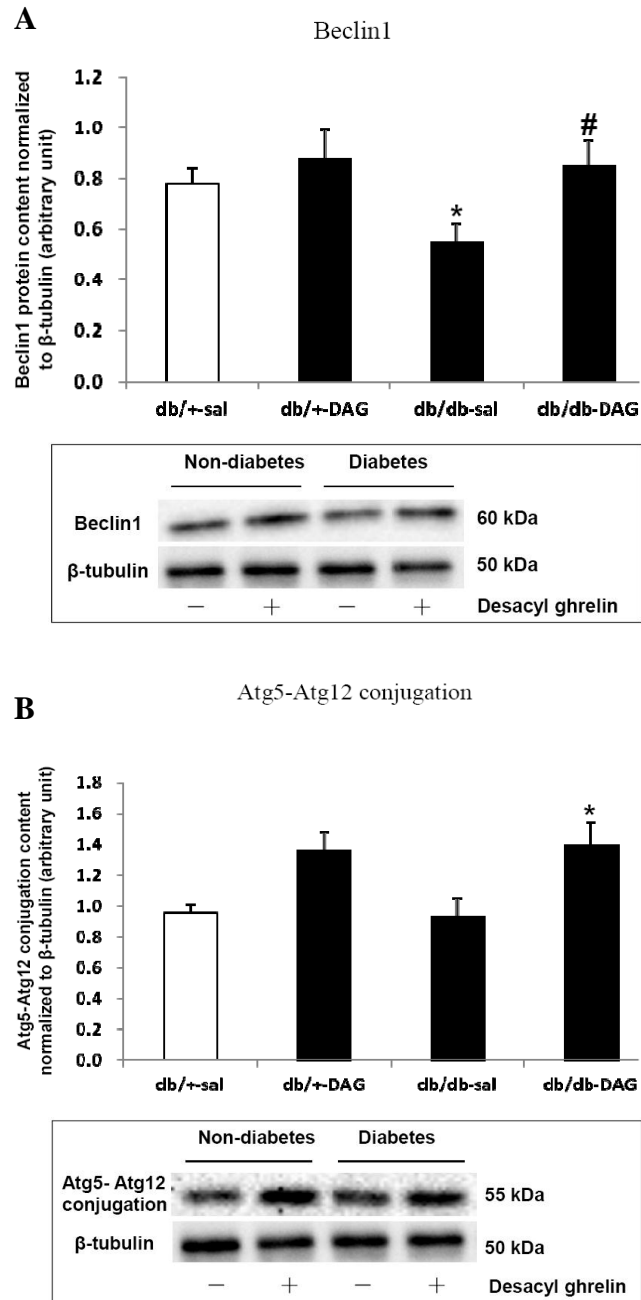


Fig 4.5 The protein abundance of Beclin1 (A) and The conjugation of Atg5 and Atg12 (B).

Desitometric quantification was performed and data were presented as net intensity x resulting band area and expressed in arbitrary units. Results were normalized to corresponding β -tubulin signal. Data are expressed as mean \pm SEM (n = 6 per group). *P < 0.05 compared to non-diabetic control group (db/+Sal), #P < 0.01 compared to diabetic control group (db/db-Sal).

4.3.5 Other Factors: Endothelial Dysfunction (Edn3), Cardiomyocyte Differentiation (p21 and GATA6), and FK506 Binding Protein (FKBP5 and FKBP10)

The cardiac gene expressions of Edn3, GATA6, and FKBP10 were increased in diabetic animals when compared to non-diabetic animals but were not altered by desacyl ghrelin treatment (Fig 4.6A, 4.6B, and 4.6C). The transcript expression of p21 in the heart was reduced in diabetic mice relative to the non-diabetic mice and was not changed by desacyl ghrelin treatment (Fig 4.6D). No significant difference in cardiac FKBP5 mRNA level was found between db/db diabetic mice and non-diabetic control mice (Fig 4.6E).

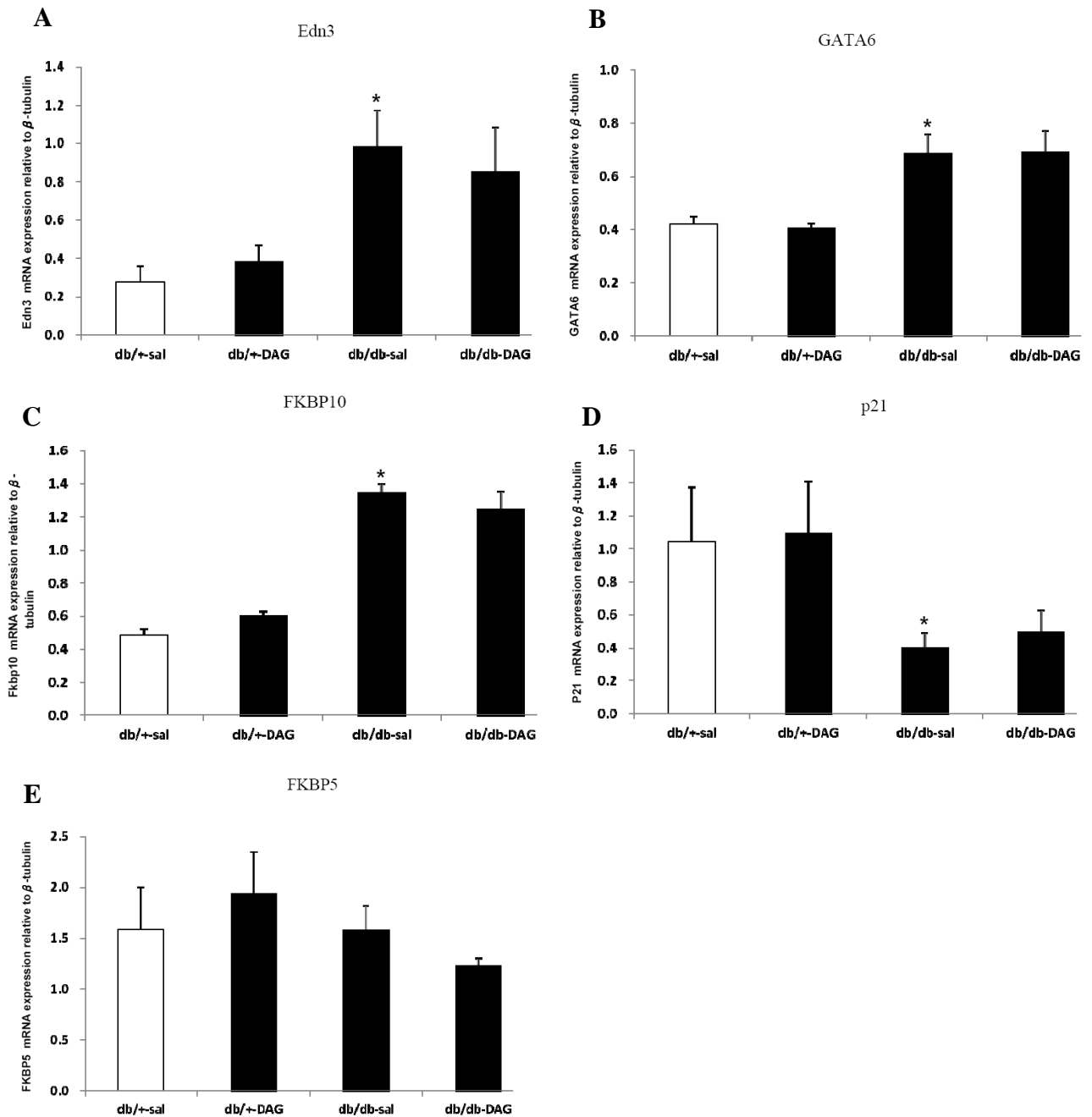


Fig 4.6 The transcript expression of Edn3 (A), GATA6 (B), FKBP10 (C), p21 (D), and FKBP5 (E) in mice heart. Data were presented as expression ratio normalized to β -tubulin gene. Data are expressed as mean \pm SEM (n = 6 per group). *P < 0.05 compared to non-diabetic control group (db/+Sal).

4.3.6 AMPK, Akt, ERK1/2 and GSK3 α / β Signaling

AMPK activity in the heart was determined by measuring the ratio of phospho-AMPK-to-total AMPK. AMPK activity was not found to be significantly inhibited in the heart of db/db diabetic mice when compared to non-diabetic control heart. The administration of desacyl ghrelin enhanced the phosphorylation level of cardiac AMPK in diabetic mice (by 150%) but not in the db/+ non-diabetic mice (Fig 4.7). Pro-survival Akt signaling was significantly suppressed in diabetic heart as indicated by the decreased ratio of phospho-Akt-to-total Akt (by 72%, $P < 0.01$) in db/db diabetic mice relative to db/+ non-diabetic mice. This decrease was not found in the db/db mice treated with desacyl ghrelin (Fig 4.8A). Although significant decrease in the ratio of phospho-ERK1/2-to-total-ERK1/2 was not seen in diabetic heart, desacyl ghrelin was observed to significantly activate ERK1/2 signaling in diabetic heart (by 327%, $P < 0.01$) when compared to the diabetic control (Fig 4.8B). As a target of Akt signaling, a similar changing pattern with Akt phosphorylation was found in GSK3 α / β signaling. The ratio of phospho-GSK3 α / β -to-total GSK3 α / β was significantly reduced (by 40%, $P < 0.05$) in db/db diabetic mice relative to the db/+ non-diabetic mice. Desacyl ghrelin was found to reverse this reduction of the GSK3 α / β phosphorylation in diabetic heart (Fig 4.9).

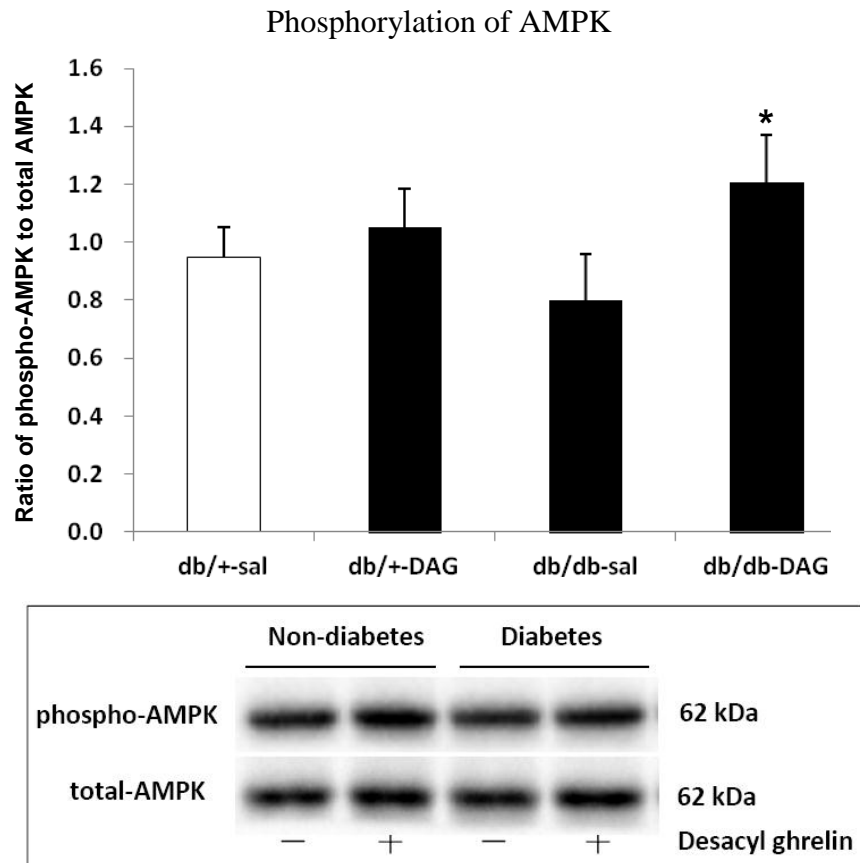


Fig 4.7 AMPK signaling in heart. Protein abundances of phospho-AMPK and total AMPK were examined by Western blot analysis and the ratio of phospho-AMPK-to-total AMPK was presented. Data are expressed as mean \pm SEM (n = 6 per group). *P < 0.05 compared to diabetic control group (db/db-Sal).

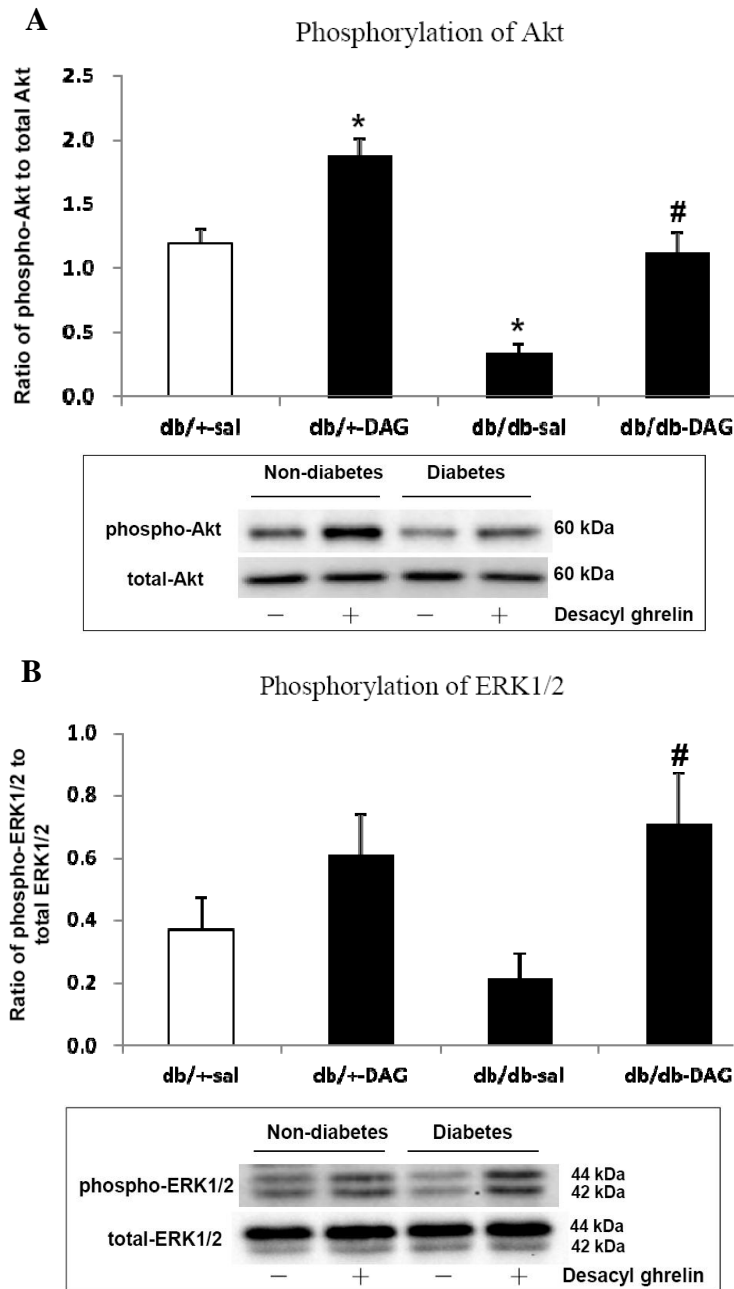


Fig 4.8 Akt (A) and ERK1/2 signaling (B) in heart. Protein abundances of phospho-Akt, total Akt, phospho-ERK1/2 and total ERK1/2 were examined by Western blot analysis and the ratio of phospho-Akt-to-total Akt, phospho-ERK1/2-to-total ERK1/2 were presented. Data are expressed as mean \pm SEM (n = 6 per group). *P < 0.05 compared to non-diabetic control group (db/+Sal), #P < 0.01 compared to diabetic control group (db/db-Sal).

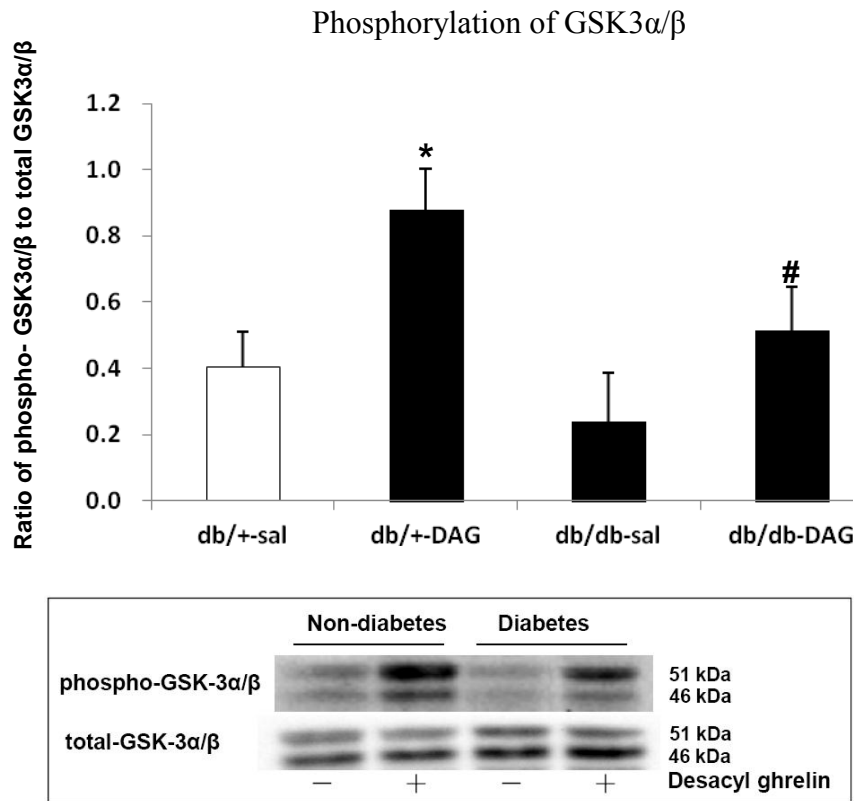


Fig 4.9 GSK3 α/β signaling in heart. Protein abundances of phospho- GSK3 α/β and total GSK3 α/β were examined by Western blot analysis and the ratio of phospho- GSK3 α/β -to-total GSK3 α/β was presented. Data are expressed as mean \pm SEM (n = 6 per group). *P < 0.05 compared to non-diabetic control group (db/+Sal), #P < 0.01 compared to diabetic control group (db/db-Sal).

4.4 Discussion

4.4.1 Desacyl Ghrelin Improves Cardiac Dysfunction in Diabetic Cardiomyopathy

The pathophysiology of type 2 diabetic cardiomyopathy is multifactorial, and factors such as accumulated collagen deposition, altered cardiac autophagy, metabolism, and pro-survival signaling all contribute to the development of diabetic cardiomyopathy. The major findings of the present study are that desacyl ghrelin was shown to have protective effects on diabetic cardiomyopathy by reversing the diabetes-associated inhibition of the pro-survival signaling and thus preventing the progression of the adverse cardiac functional and structural changes.

At the age of 14 weeks, cardiac systolic function (as indicated by ventricular fractional shortening) was observed to be decreased in db/db diabetic mice. This reduction of fractional shortening demonstrated the presence of diabetic cardiomyopathy which is consistent with the previous report showing the development of cardiomyopathy in db/db diabetic mice (Aasum *et al.*, 2003). Existing data showing the beneficial effects of desacyl ghrelin on cardiovascular diseases such as diabetic cardiomyopathy are very limited. The focus of many previously conducted *in vivo* studies has been on the effects of acylated form of ghrelin on cardiovascular disorders. However, in this study we have, for the first time, demonstrated that the administration of desacyl ghrelin was effective to alleviate the cardiac dysfunction induced by diabetic

cardiomyopathy.

4.4.2 Desacyl Ghrelin Alleviates Cardiac Fibrosis in Diabetic Cardiomyopathy

Myocardial fibrosis is a critical structural change contributed to the functional impairment caused by diabetic cardiomyopathy. Cardiac collagen deposition was found to be obviously increased in the untreated db/db diabetic mice, and this finding was consistent with the previous reports showing that six-week-old db/db diabetic mice exhibited diastolic dysfunction and adverse myocardial fibrosis (Huynh *et al.*, 2012). Cardiac dysfunction might be an outcome caused by fibrosis-induced myocardial stiffness, and importantly, treatment of desacyl ghrelin showed promising inhibitory effect on this increase in collagen deposition in diabetic heart.

Cardiac fibrotic regulators including adiponectin, MMP-8, MMP-13, and Wnt5a were investigated in this study. Adiponectin is a multi-functional adipokine secreted by the adipose tissue. It was suggested that adiponectin was involved in the maintenance of insulin sensitivity and energy metabolism. Recent findings have demonstrated the protective role of adiponectin in fibrosis-related diseases. For example, adiponectin was shown to exert an inhibitory role in hepatic stellate cell proliferation and liver fibrosis (Caligiuri *et al.*, 2008; Subramaniam *et al.*, 2012). Moreover, adiponectin has been demonstrated to prevent myocardial hypertrophy and fibrosis (Essick *et al.*,

2011;Shibata *et al.*, 2004). Consistent with these findings, a reduction of adiponectin expression was observed in the heart of our db/db diabetic mice. This might partly explain for the development of cardiac fibrosis in diabetic cardiomyopathy. Although the detailed mechanisms remain to be elucidated, the observed attenuation of cardiac fibrosis by desacyl ghrelin might be resulted from the induction of adiponectin expression in the heart by the treatment of desacyl ghrelin.

Two of the fibrotic factors considered in this study belong to a group of enzymes known as matrix metalloproteinase (MMP) such as MMP-8 and MMP-13 which are mostly involved in collagen cleavage in many connective tissues. The expression and activity of collagenase-2 (MMP-8) are strongly associated with chronic inflammation and fibrosis (Khatwa *et al.*, 2010). MMP-8 mRNA levels was increased by 30-fold in human heart failure patients (Gunja-Smith *et al.*, 1996). MMP-8 has been shown to act as a pro-fibrotic factor that promotes fibrosis via TGF- β -independent pathway (Craig *et al.*, 2013). Wilson and co-workers have reported that the expression of *MMP-8 gene* was up-regulated by type 2 diabetes in the hearts of db/db mice (Wilson *et al.*, 2008). In concurrence with findings of the study conducted by Wilson and colleagues, increased expression of MMP-8 in the heart of the untreated db/db mice was observed in the present study. Increased MMP-8 indicates granulocyte accumulation and/ or stimulation, which reflects the inflammatory processes in the heart (Takatsu *et al.*, 1999). Alternatively, there was a down

regulation of MMP-13 in type 2 diabetic heart. MMP-13 is the primary collagenase found in rodent myocardial samples and cleaves type II collagen more efficiently than types I and III (Spinale, 2007). However, according to our results, changes in the expression of MMP-8 and MMP-13 were not affected by desacyl ghrelin. Our data implicate that significant accumulation of collagen in diabetic heart was partly resulted from the up-regulation of MMP-8 and down regulation of MMP-13 due to the lack of substantial collagenase-mediated cleavage.

4.4.3 Genes Involved in Diabetic Cardiomyopathy But Not Affected by Desacyl Ghrelin

A number of genes were involved in type 2 diabetic cardiomyopathy but some of them were not yet affected by the treatment of desacyl ghrelin. Our data suggested that the induction and development of type 2 diabetic cardiomyopathy might be influenced by the expression of various gene products including Wnt5a, TLR4, Edn3, p21, GATA6, and FKBP10. However, administration of desacyl ghrelin showed no effect on the expression of these genes. These findings preliminarily indicated that the desacyl ghrelin-mediated improvement of cardiac dysfunction in type 2 diabetes might not be associated with cardiac inflammation (Wnt5a), endothelial dysfunction (Edn3), cardiomyocyte differentiation (p21 and GATA6) and FK506 binding proteins (FKBP10).

Cardiac inflammation is an important mechanism underlying the development of type 2 diabetic cardiomyopathy. Therefore, several inflammatory markers including Apelin, Wnt5a, and TLR4 were evaluated to examine the cardiac inflammation. Apelin is a kind of adipocytokine secreted by white adipose tissue. Apelin and its receptor are also expressed in cardiovascular system (El-Shehaby *et al.*, 2010). However, our data indicated that apelin signaling might not be involved in diabetic cardiomyopathy and contributed to the effects desacyl ghrelin.

A significant increase in the expression of Wnt5a was found in diabetic cardiomyopathy. Activation of Wnt5a/ β -catenin-independent signaling has been shown to contribute to the induction of inflammation (Kikuchi *et al.*, 2012). However, a human study reported that plasma Wnt5a levels were decreased in type 2 diabetes (Lu *et al.*, 2013). The role of Wnt5a/ β -catenin-independent signaling in diabetic cardiomyopathy is still not clear. In the present study, we observed that there was a significant increase in the expression of Wnt5a gene in diabetic heart, suggesting that Wnt5a might have contributed to the progression of cardiac inflammation in type 2 diabetic cardiomyopathy.

Toll-like receptors (TLRs) are crucial components of the innate immune system. TLR4 signaling leads to inflammation-induced cardiac injury and it is thought to be a key mediator of the development of inflammation-related cardiovascular diseases (Jenke *et al.*, 2013). TLR-4 deficient mice showed increase in obesity,

but with prevention of insulin resistance induced by high-fat diet (Shi *et al.*, 2006). Our data gave evidence that expression of TLR4 gene in the heart was down regulated in type 2 diabetic condition and this change was not affected by the treatment of desacyl ghrelin. However, the other components of TLR4 signaling such as CD14, MyD88, and its downstream signaling (NF- κ B pathway) were not examined in the present study and they might be worth for further investigation.

4.4.4 Enhanced Cardiac Autophagy by Desacyl Ghrelin in Diabetic Cardiomyopathy

Autophagy is the process of controlling degradation and recycle of proteins and cytoplasmic organelles. Beclin1 (mammalian Atg6) initiates the formation of the autophagosomal membrane whereas Atg5-Atg12 are responsible for the membrane elongation. In the present study, cardiac autophagy was suppressed by type 2 diabetes as indicated by the reduced expression of Beclin1 proteins. The suppression of autophagy in diabetic heart might result in accumulation of abnormal proteins and organelles, which further leads to cardiac dysfunction (Xie *et al.*, 2011b). For the first time we demonstrated that, the up-regulatory effect of desacyl ghrelin on cardiac Beclin1 level and Atg5-Atg12 conjugation in an *in vivo* diabetic setting. The improved cardiac autophagy might contribute to the protective effect of desacyl ghrelin on diabetic cardiomyopathy. The detailed regulatory machinery and signaling involving mTOR pathway might be worth to be further investigated to fully reveal the autophagic effects of

desacyl ghrelin in diabetic heart.

4.4.5 Activation of AMPK, ERK1/2, Akt and GSK3 α / β Signaling by Desacyl Ghrelin in Diabetic Cardiomyopathy

The possible molecular mechanisms and intracellular pathways involved in the protective effects of desacyl ghrelin were investigated. Desacyl ghrelin induced the phosphorylation of AMPK and improved the impaired pro-survival signaling such as Akt, ERK1/2 and GSK3 α / β in the heart of db/db diabetic mice.

AMPK is a key regulator of cellular energy metabolism and it is activated by the increased ratio of AMP-to-ATP. Apart from being the cellular energy sensor, AMPK also regulates cardiac autophagy and it is thought to be important in the heart remodeling. An *in vivo* study conducted earlier using type 1 diabetic OVE26 mouse model has demonstrated that the suppression of AMPK activity might be related to the reduction of cardiac autophagy and dysfunction (Xie *et al.*, 2011a). It is well-known that an anti-diabetes drug, metformin, exerts cardio-protective effect in myocardial complications via the stimulation of the activity of AMPK (El *et al.*, 2013).

Desacyl ghrelin did not show the effect of AMPK stimulation in murine HL-1 adult cardiomyocytes (Lear *et al.*, 2010). However, the present results have extended our understanding by showing the effect of desacyl ghrelin on AMPK activation in diabetic heart. Desacyl ghrelin has been showed to exert cyto-

protective effects on H9c2 cardiomyocytes (Baldanzi *et al.*, 2002), human pancreatic islet microendothelial cells (Favaro *et al.*, 2012) and rat visceral adipocytes (Baragli *et al.*, 2011) through the activation of Akt and ERK1/2 signaling. Additionally, our data confirmed that desacyl ghrelin protected the heart against cardiac dysfunction by improving the suppressed Akt and ERK1/2 signaling in type 2 diabetic cardiomyopathy. Furthermore, the present study showed that desacyl ghrelin inactivated GSK3 α/β by increasing phosphorylation. GSK3 α/β is a down-stream target molecule of several pro-survival protein kinases including Akt and ERK1/2 (Wong *et al.*, 2005). Collectively, our findings suggested that administration of desacyl ghrelin partly alleviated cardiac dysfunction in type 2 diabetic cardiomyopathy via Akt/ERK1/2/ GSK3 α/β signaling pathway.

CHAPTER 5

DOX-induced Cardiotoxicity in Type 2

Diabetic Heart

5.1 Introduction

Diabetes mellitus and cancer are two of the leading causes of death in the world according to the figures reported by World Health Organization. Epidemiological studies have evidently demonstrated that there is a strong connection between certain cancers and type 2 diabetes mellitus (Giovannucci *et al.*, 2010), although the detailed mechanisms explaining this connection are not very clear. Indeed, type 2 diabetes has been shown to increase the risk and mortality of breast, liver, colorectal and pancreatic cancers (Cannata *et al.*, 2010). Thus, it is not uncommon to see the diagnosis of both diabetes and cancer in the same individuals. As the number of people suffered from type 2 diabetes is predicted to be dramatically increased in the coming years, it is expected that the number of diabetic cancer patients will also be largely increased.

Cancer patients with long standing diabetic cardiomyopathy may present a difficult situation of cancer treatment using chemotherapy. This is attributed to the fact that most of the chemotherapeutic agents used to treat cancer have severe side effects on major vital organs such as the cardiotoxicity induced by DOX. DOX is extensively used for treating various cancers including breast, stomach, lung, and bladder cancers (Rahman *et al.*, 2007). However, DOX induces a life-threatening cardiomyopathy and irreversible cardiac damage (Swain *et al.*, 2003). Therefore, it is reasonable to expect that a cancer patient with diabetic cardiomyopathy would be more susceptible to the DOX-induced

cardiac damage due to the already existing cardiac dysfunction in the diabetic heart.

Currently, there is no study that has been conducted to examine the detrimental effects of DOX on the heart of diabetic individuals. The underlying mechanisms of the DOX-induced cardiotoxicity in diabetic heart are also completely unknown. It is also not clear whether the signaling events that mediate the cardiac toxic effects of DOX are different in the hearts between diabetic and non-diabetic individuals. These pieces of information are essential for the development of effective therapeutic strategies to address this complicated clinical situation in the diabetic cancer patients. Therefore, this study aimed to investigate the DOX-induced cardiotoxicity in type 2 diabetic hearts. This study was also designed to distinguish the signaling mechanisms responsible for the DOX-induced cardiotoxic effects between the diabetic and non-diabetic hearts.

5.2 Methods

5.2.1 Animals

Male 14- to 18-week-old db/db mice (leptin receptor deficient transgenic mice which is a well-established animal model of type 2 diabetes mellitus) obtained from the Laboratory Animal Services Centre of The Chinese University of Hong Kong were used in this study. Non diabetic db/+ mice were used as the healthy control because of the similar genetic background with db/db mice.

Mice were housed in a temperature- and humidity-controlled environment and were exposed to a 12:12-hour light: dark cycle in the Centralised Animal Facilities of The Hong Kong Polytechnic University. Mice were allowed to have access to standard animal diet and water ad libitum. Animal ethics approval was obtained from the Animal Ethics Sub-committee of The Hong Kong Polytechnic University.

5.2.2 Experimental Protocol

Two experimental time points (i.e., 5-day and 7-day after the administration of DOX) were investigated in this study. Moreover, the survival of the mice was analyzed by Kaplan-Meier method during an experimental period of 14 days following the administration of DOX. Non-diabetic (db/+) and diabetic (db/db) mice were randomly assigned to the following groups: db/+Saline (n = 8), db/+DOX (DOX, DOX; n = 8), db/db-Saline (n = 8) and db/db-DOX (n = 8). Mice assigned to DOX group were exposed to an intraperitoneal (i.p.) injection of DOX (Pharmacia & Upjohn SpA, Milan, Italy) at a dose of 15 mg/kg to induce cardiomyopathy as shown in a previous study (Suliman *et al.*, 2007). Mice in sham groups (Saline) were i.p. injected with the same volume of saline instead of DOX. Mice were euthanized by overdose of ketamine and xylazine on day 5 or day 7 after the administration of DOX. Heart was immediately removed and washed with cold phosphate buffered saline (PBS). Left ventricle was quickly dissected and frozen in liquid nitrogen and stored at -80°C for later analysis.

5.2.3 Measurement of Cardiac Function by Echocardiography

After the experimental period, cardiac function of mice was detected by echocardiography on day 5 and day 7. The detailed procedure of the measurement of the cardiac function using echocardiography was described in CHAPTER 2.

5.2.4 Protein Fraction Preparation

The protein fraction of cardiac muscle samples was prepared by adopting the protocol described in CHAPTER 2.

5.2.5 Apoptotic Cell Death Enzyme-linked Immunosorbent Assay (ELISA)

The extent of apoptosis was measured by Cell Death ELISA and the procedure was described in CHAPTER 2.

5.2.6 RNA Extraction and Microarray Analysis

The method of total RNA extraction was described in CHAPTER 2. In this study, the technique of microarray analysis was adopted to examine the changes of the whole transcriptional profile in response to the administration of DOX in diabetic heart. RNA samples extracted from the ventricular tissues of mice in db/db-Saline and db/db-DOX at 5-day after the DOX administration were used in the microarray analysis. RNA samples (3 µg) from the hearts of two mice in

each group were pooled to generate four biological replicates in db/db-Saline and db/db-DOX. The RNA quantity and quality were assessed before microarray analysis. RNA quantity was detected by NanoDrop 1000 Spectrophotometer. The purity of RNA was assured by examining the OD260/280 ratio. The RNA integrity was assessed by Agilent 2100 bioanalyzer by following the manufacturer's instruction. It is noted that the RNA sample could be applied for array hybridization only if samples showed intact bands corresponding to 18S and 28S ribosomal RNA and the RNA Integrity Number (RIN) was > 7.

Microarray analysis was performed using the Agilent Service Platform with Agilent two-color mouse 4X44k microarray slides. Samples from the DOX-treated diabetic mice (db/db-DOX) were labelled by Cy5 dye (red channel) whereas samples from diabetic control mice (db/db-Saline) were labelled by Cy3 dye (green channel). Five hundreds ng of Cy3-labelled and Cy5-labelled cRNA were mixed and incubated with the Agilent microarray slide (G2519F) for 17 hours at 65°C in the dark. Slide was washed and scanned using an Agilent DNA microarray scanner. Raw data were obtained using Agilent's Feature Extraction Software. Further analysis of the raw data was performed by comprehensive R- and Bioconductor-based web service for microarray data analysis. Several normalizations were performed for the pre-processing of the raw data including background correction by subtraction method, removal of dye bias by lowess normalization and multiple testing correction by BH

adjusted P-values for the Benjamini & Hochberg step-up FDR controlling procedure (Benjamini and Hochberg 1995). Gene expression values were calculated by log base 2 ratio of red channel intensity (mean) and green channel intensity (mean). Functional classification of highly regulated genes was analyzed by GeneOntology database.

5.2.7 Real Time Quantitative PCR Analysis

The expression of selected genes from microarray analysis (S100A8 and S100A9) was confirmed by real time quantitative PCR. The procedure of PCR was described in CHAPTER 2.

5.2.8 Western Blot Analysis

The protein expression of apoptotic markers (Bcl-2 and Bax) and autophagic factors (Beclin1) in the heart samples was measured by Western Blot. The details were described in CHAPTER 2.

5.2.9 Statistical Analysis

Data were expressed as mean \pm standard error of mean. Statistical analysis was performed by using Statistics Package for Social Science (SPSS) version 11.0. Differences among groups were evaluated by ANOVA followed by Tukey's HSD post hoc test. Statistical significance was set at $P < 0.05$.

5.3 Results

5.3.1 Survival Analysis

The animal survival rates of db/+Sal (Non-diabetic control, n = 20), db/db-Sal (Diabetic control, n = 20), db/+DOX (Non-diabetic with DOX, n = 20) and db/db-DOX (Diabetic with DOX, n = 20) were analyzed by Kaplan-Meier approach (Fig 5.1). Fourteen days after the administration of DOX, the survival rate was significantly reduced in type 2 diabetes mice treated with DOX when compared to non-diabetic mice treated with DOX (60% vs. 10%, $P < 0.001$). The survival rate was also significantly decreased in DOX-treated mice compared with untreated controls in both db/+ non-diabetic mice and db/db diabetic mice (db/+DOX vs. db/+Saline, 60% vs 100%, $P < 0.01$; db/db-Dox vs db/db-Saline, 10% vs 100%, $P < 0.001$) (Fig 5.1).

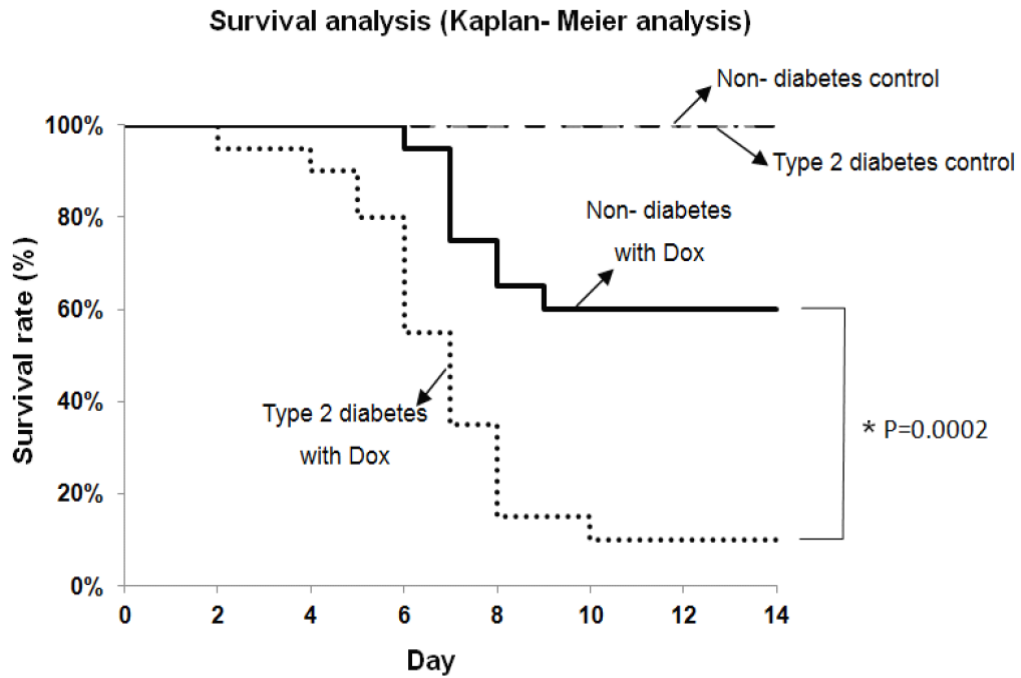


Fig 5.1 Decreased survival rate in db/+DOX (non-diabetic mice treated with DOX, n = 20 per group) and db/db-DOX (diabetic mice treated with DOX, n = 20 per group). *P < 0.001 compared to non-diabetic mice treated with DOX.

5.3.2 Fractional Shortening of Left Ventricle

DOX induced cardiac dysfunction in db/+ non-diabetic mice on day 5 after the administration of DOX as illustrated by a significant reduction from 69.3% to 52.1% in the cardiac fractional shortening ($P < 0.05$, Fig 5.2). The cardiac dysfunction resulted from type 2 diabetes was evident by observing a significant decrease in fractional shortening from 69.5% in db/+ non-diabetic mice to 55% in diabetic db/db mice at the pre-intervention level ($P < 0.05$). However, further decrease in fractional shortening was not observed in diabetic db/db mice on day 5 after the administration of DOX. Nonetheless, DOX was found to significantly induced a further impairment of cardiac contractile function in db/db diabetic mice when compared to db/+ non-diabetic mice on day 7 after the DOX administration as indicated by a decrease in fractional shortening from 53.1% to 39.9% in the db/db diabetic mice treated with DOX ($P < 0.05$, Fig 5.3).

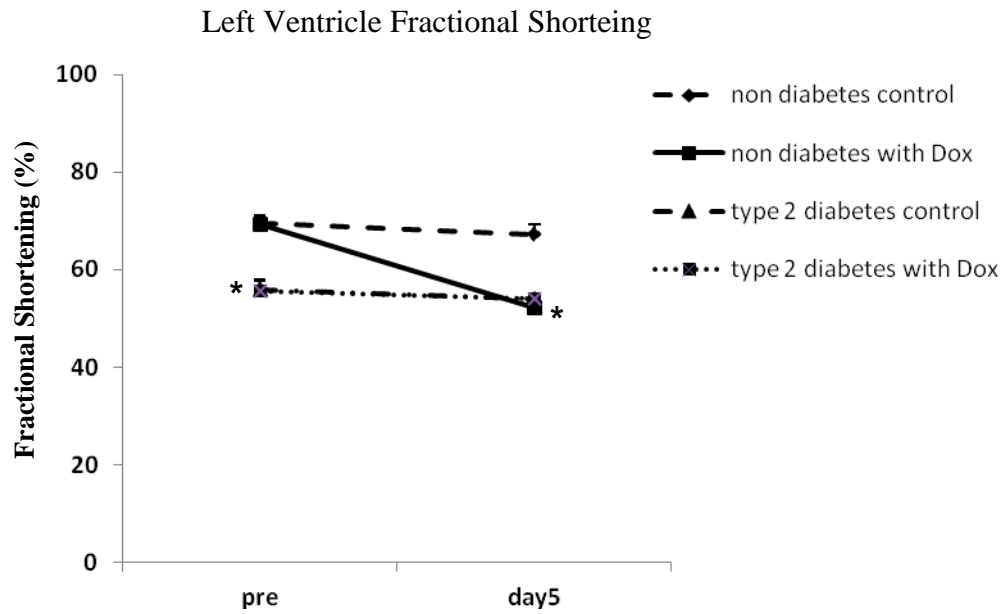


Fig 5.2 Cardiac function in DOX-treated non-diabetic mice and diabetic mice on day 5 after the administration of DOX. Fractional shortening was detected by echocardiography. Data are expressed as mean \pm SEM (n = 8 per group). *P < 0.05 compared to non-diabetic control (db/+Sal).

Left Ventricle Fractional Shortening

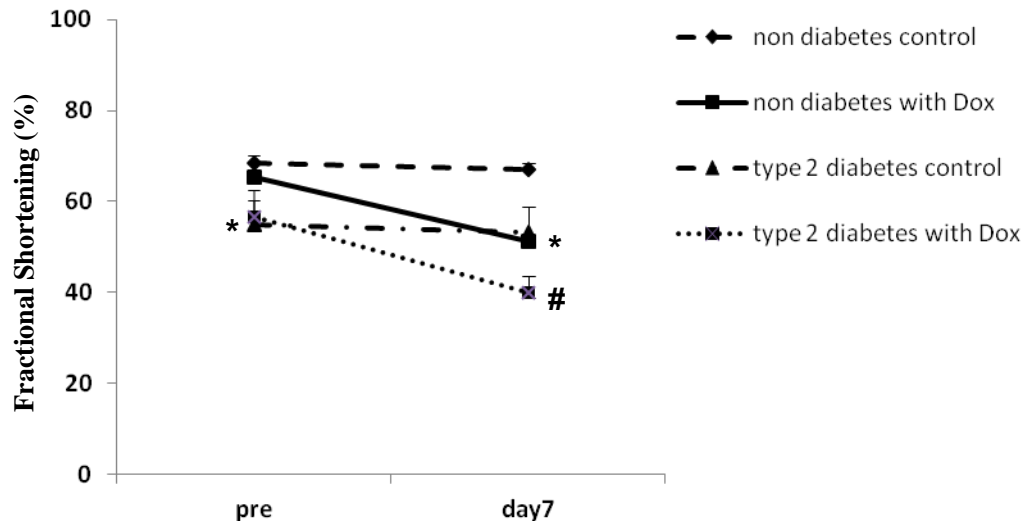


Fig 5.3 Cardiac function in DOX-treated non-diabetic mice and diabetic mice on day 7 after the administration of DOX. Fractional shortening was detected by echocardiography. Data are expressed as mean \pm SEM (n = 8 per group). *P < 0.05 compared to non-diabetic control (db/+Sal). #P < 0.05 compared to diabetic control group (db/db-Sal).

5.3.3 Cardiac Apoptosis and Apoptotic Regulatory Factor

The level of apoptotic DNA fragmentation was increased (by 396%; $P < 0.05$, Fig 5.4) in db/+ non-diabetic mice treated with DOX relative to non-diabetic control mice on day 5 after the DOX administration. However, DOX did not significantly induce the increase in apoptotic fragmentation in db/db diabetic mice. The protein content of anti-apoptotic Bcl-2 in mice heart was not found to be significantly changed among all groups (Fig 5.5A). However, the protein content of pro-apoptotic Bax in the heart was significantly increased by DOX in both the non-diabetic mice (by 163%, $P < 0.05$) and diabetic mice (by 177%, $P < 0.05$) (Fig 5.5B). The protein expression ratio of Bcl-2-to-Bax was not found to be significantly altered by DOX in both non-diabetic and diabetic mice whereas this ratio was significantly increased in db/db diabetic heart when compared to db/+ non-diabetic heart (Fig 5.5C).

Apoptotic DNA fragmentation

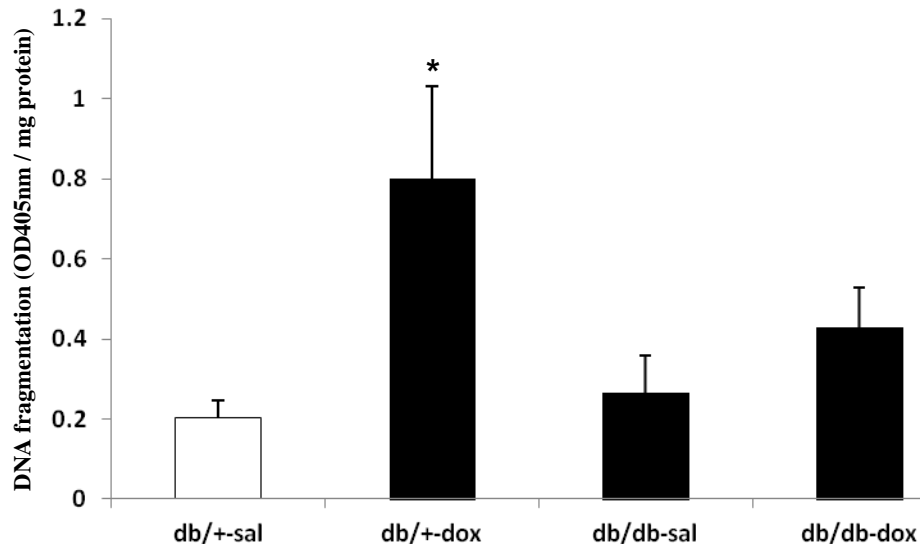


Fig 5.4 Apoptotic DNA fragmentation in heart. The extent of apoptotic DNA fragmentation was estimated by measuring the cytosolic mono- and oligo-nucleosomes. The optical density at 405 nm (OD405) was normalized to the amount of protein used in the assay. Data are expressed as mean \pm SEM (n = 8 per group). *P < 0.01 compared to non-diabetic control (db/+Sal).

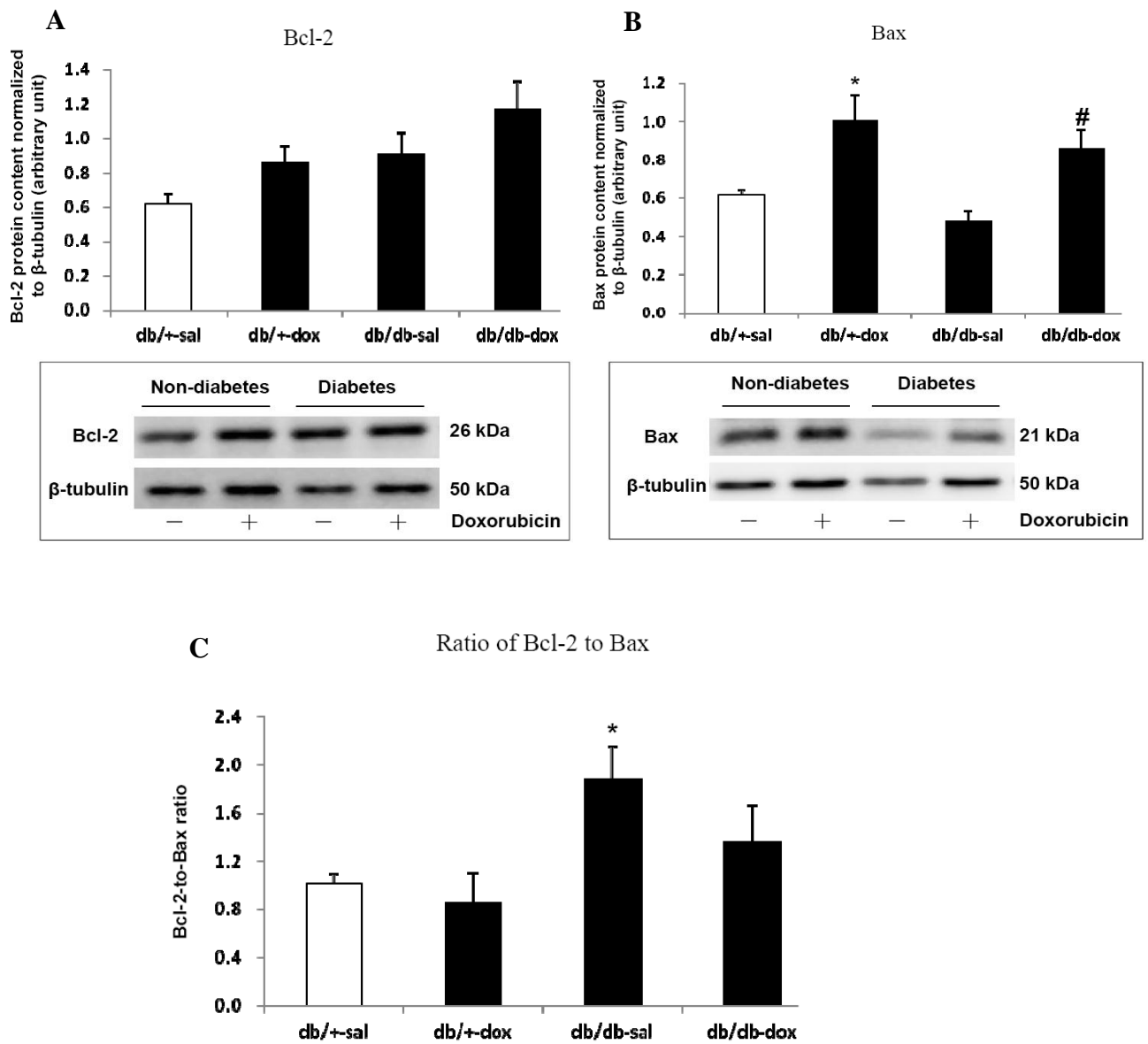


Fig 5.5 The protein abundance of Bcl-2 (A) and Bax (B) in mice heart were determined by Western blot analysis. Desitometric quantification was performed and data were presented as net intensity x resulting band area and expressed in arbitrary units. Results were normalized to corresponding β -tubulin signal. The ratio of the protein level of Bcl-2-to-Bax was shown (C). Data are expressed as mean \pm SEM (n = 8 per group). *P < 0.05 compared to non-diabetic control group (db/+Sal), #P < 0.01 compared to diabetic control group (db/db-Sal).

5.3.4 Cardiac Autophagic Factor: Beclin1

The protein content of autophagic marker Beclin1 in heart was observed to be significantly decreased (by 46%, $P < 0.05$) in db/db diabetic control mice relative to db/+ non-diabetic control mice (Fig 5.6). The protein content of Beclin1 in the heart was not found to be significantly changed by DOX in both non-diabetic and diabetic animals.

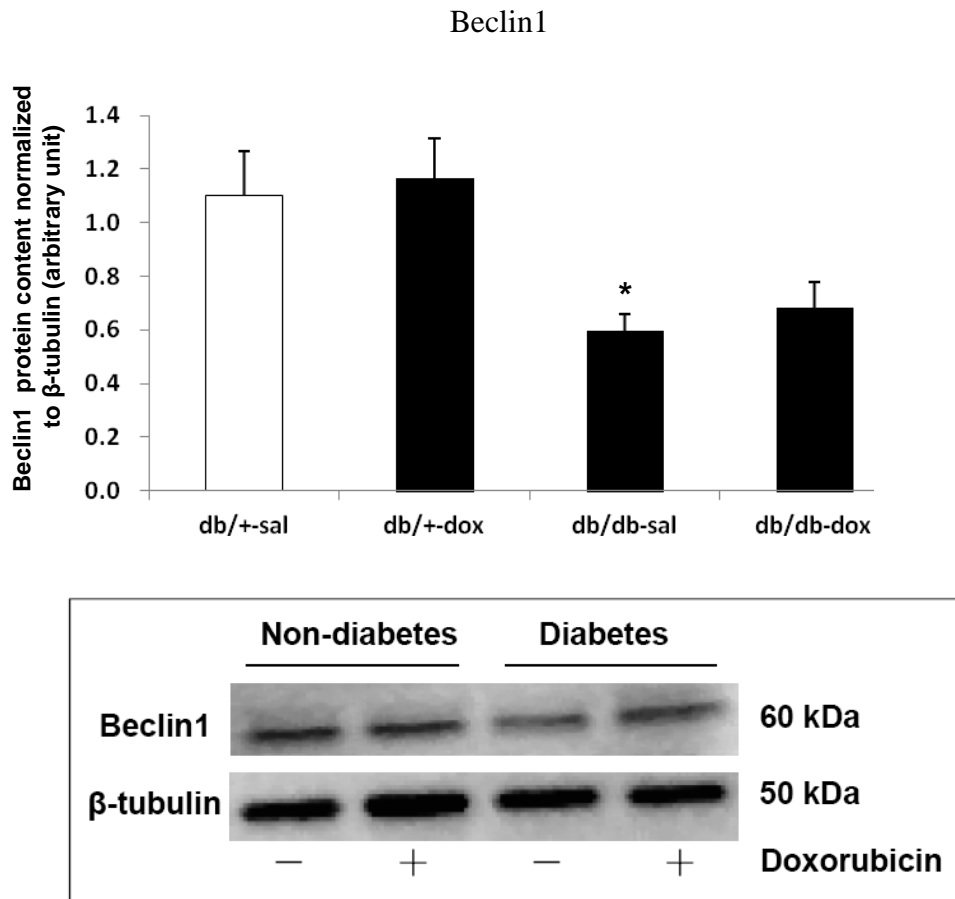


Fig 5.6 The protein abundance of Beclin1 was determined by Western blot analysis. Desitometric quantification was performed and data were presented as net intensity x resulting band area and expressed in arbitrary units. Results were normalized to corresponding β -tubulin signal. Data are expressed as mean \pm SEM (n = 8 per group). *P < 0.05 compared to non-diabetic control group (db/+-sal).

5.3.5 Microarray Analysis of the Effect of DOX on Diabetic Heart

5.3.5.1 Gene Expression Profile by Microarray Analysis

Gene expression profiles in left ventricle of diabetic mice with and without DOX treatment were examined by microarray analysis. In our analysis, only those genes with the transcriptional level changes of 2-fold or higher were identified as significantly regulated. According to our criteria, totally 709 genes were significantly affected by DOX administration in db/db diabetic heart. Of these, 408 genes were up-regulated and 301 genes were down regulated by DOX in db/db diabetic heart. Selected genes expressions with significant alteration induced by DOX in diabetic heart were shown in Table 5.1. Furthermore, our functional enrichment analysis by GeneOntology demonstrated that the sets of highly regulated genes that we observed in the DOX-treated diabetic heart involved in a spectrum of cellular component, biological process and molecular function (Table 5.2, 5.3, and 5.4).

Table 5.1 Significantly regulated genes in response to DOX in diabetic heart

Gene Name	P-value	Fold Change
<i>Cardiac Remodeling and Matrix</i>		
Matrix metalloproteinase 8	0.016	3.21
Collagen, type I, alpha 2	0.002	0.43
Collagen, type III, alpha 1	0.009	0.39
<i>Inflammatory/ Immune response</i>		
S100 calcium binding protein A8 (calgranulin A)	0.017	5.89
S100 calcium binding protein A9 (calgranulin B)	0.028	4.08
Tumor necrosis factor receptor superfamily, member 13c	0.002	2.17
Chemokine (C-C motif) ligand 4	0.01	0.44
Chemokine (C-X-C motif) ligand 9	0.04	0.35
Tumor necrosis factor receptor superfamily, member 9	0.0002	2.07
Interleukin 7	0.004	3.02
Interleukin 2 receptor, gamma chain	0.015	0.45
CD248 antigen	0.013	0.48
<i>Oxidative stress related</i>		
Glutathione S-transferase, alpha 2 (Yc2)	0.0004	3.27
Carbonic anhydrase 3	0.047	0.4
<i>DNA/RNA Synthesis/Stability/Repair</i>		
Histone cluster 2, H4	1.75E-05	2.11
Histone cluster 4, H4	3.82E-05	2.6
<i>Cell division regulators</i>		
Cyclin-dependent kinase inhibitor	0.0004	2.28
Cyclin B2	0.02	0.47
Cyclin-dependent kinase inhibitor 1A (P21)	0.0004	2.28
<i>Signaling molecules</i>		
Guanine nucleotide binding protein (G protein)	0.04	0.48
<i>Akt and ERK signalling</i>		
Protein tyrosine phosphatase	0.03	2.02
<i>Signal transduction/transcription protein</i>		
E2F transcription factor 2	0.041	0.45
Chromodomain helicase DNA binding protein 1	0.011	0.41
G protein-coupled receptor 31, D17Leh66c region	0.015	2.73
Wingless-related MMTV integration site 5A	0.002	0.48
Ubiquitin-conjugating enzyme E2C	0.008	0.48
Small G protein signaling modulator 1	0.0005	0.42
<i>Metabolism</i>		
Glucagon-like peptide 2 receptor	0.03	3.48
Fatty acid binding protein 6	0.03	3.31
Glycogen synthase 2	0.04	2.55
Insulin-like growth factor binding protein 3	0.001	2.06

Table 5.2 Results of GO Mapping, GO Terms, P-values and Count, Cellular Component

Ontology

	GOCCID	Pvalue	OddsRatio	ExpCount	Count	Size	Term
1	GO: 0044421	0.00	2.41	13.81	31	633	Extracellular region part
2	GO: 0042613	0.00	25.86	0.24	4	11	MHC class II protein complex
3	GO: 0005581	0.00	15.08	0.35	4	16	Collagen
4	GO: 0005578	0.00	2.84	5.23	14	242	Proteinaceous extracellular matrix
5	GO: 0044459	0.00	1.64	25.66	40	1176	Plasma membrane part
6	GO: 0005833	0.00	30.03	0.11	2	5	Hemoglobin complex
7	GO: 0000780	0.01	22.52	0.13	2	6	Condensed nuclear chromosome
8	GO: 0044421	0.01	22.52	0.13	2	6	Juxtaparanode region of axon
9	GO: 0000307	0.02	12.87	0.20	2	9	Cyclin- dependent protein kinase holoenzyme complex
10	GO: 0005576	0.02	1.61	17.42	27	834	Extracellular region
11	GO: 0032982	0.02	11.26	0.22	2	10	Myosin filament
12	GO: 0044463	0.02	2.89	2.18	6	100	Cell projection part
13	GO: 0009986	0.03	2.12	4.89	10	224	Cell surface
14	GO: 0005834	0.04	4.36	0.74	3	34	Heterotrimeric G- protein complex
15	GO: 0042383	0.04	4.23	0.76	3	35	Sarcolemma
16	GO: 0030892	0.04	44.94	0.04	1	2	Mitotic cohesin complex

Table 5.3 Results of GO Mapping, GO Terms, P-values and Count, Cellular Component

Ontology

	GOCCID	Pvalue	OddsRatio	ExpCount	Count	Size	Term
1	GO: 0018894	0.00	91.87	0.06	2	3	Dibenzo-p-dioxin metabolic process
2	GO: 0007155	0.00	2.06	11.22	22	524	Cell adhesion
3	GO: 0009404	0.00	45.93	0.09	2	4	Toxin metabolic process
4	GO: 0005578	0.00	2.84	5.23	14	242	Proteinaceous extracellular matrix
5	GO: 0009605	0.00	1.95	11.82	22	552	Response to external stimulus
6	GO: 0007623	0.00	6.83	0.66	4	31	Circadian rhythm
7	GO: 0050665	0.00	30.62	0.11	2	5	Hydrogen peroxide biosynthetic process
8	GO: 0051301	0.00	2.33	6.29	14	294	Cell division

Table 5.4 Results of GO Mapping, GO Terms, P-values and Count, Cellular Component

Ontology

	GOCCID	Pvalue	OddsRatio	ExpCount	Count	Size	Term
1	GO: 0019838	0.00	5.77	1.16	6	54	Growth factor binding
2	GO: 0005201	0.00	9.62	0.50	4	23	Extracellular matrix structural constituent
3	GO: 0050840	0.00	9.62	0.50	4	23	Extracellular matrix binding
4	GO: 0030414	0.00	3.63	2.66	9	123	Peptidase inhibitor activity
5	GO: 0004869	0.00	8.31	0.56	4	26	Cysteine- type endopeptidase inhibitor activity
6	GO: 0015075	0.01	1.83	12.53	22	580	Ion tranmembrane transporter activity
7	GO: 0046943	0.01	4.01	1.34	5	62	Carboxylic acid transmembrane transporter activity
8	GO: 0005267	0.01	3.06	2.42	7	112	Potassium channel activity
9	GO: 0015114	0.01	15.17	0.17	2	8	Phosphate transmembrane transporter activity
10	GO: 0019825	0.02	13.00	0.19	2	9	Oxygen binding
11	GO: 0022838	0.02	2.00	7.28	14	337	Substrate- specific channel activity
12	GO: 0004896	0.02	4.45	0.97	4	45	Cytokine receptor activity

5.3.5.2 Pathway Analysis by Metacore™

The significantly regulated genes (fold change > 2) were selected for further pathway analysis by Metacore (Version 6). The top four scored pathways (the pathway map with the lowest P-value) were identified and these included 1) Cell Adhesion - ECM Remodeling, 2) Transcription - Role of AP-1 in Regulation of Cellular Metabolism, 3) Immune Response - IL 13 Signaling via JAK STAT, and 4) Transcription - Androgen Receptor Nuclear Signaling.

5.3.5.2.1 Cell Adhesion - ECM Remodeling

The top first pathway map “Cell Adhesion - ECM Remodeling” is shown in Fig 5.7. According to our analysis, cell adhesion ECM (extracellular matrix) remodeling was the most significant pathways involved in DOX-induced toxicity in diabetic cardiomyopathy. In particular, gene expressions of Collagen I, Collagen III, and Osteonectin in diabetic heart were down regulated by DOX treatment, and Kallikrein 3 was up-regulated through DOX administration. The pathway map is shown in Fig 5.7.

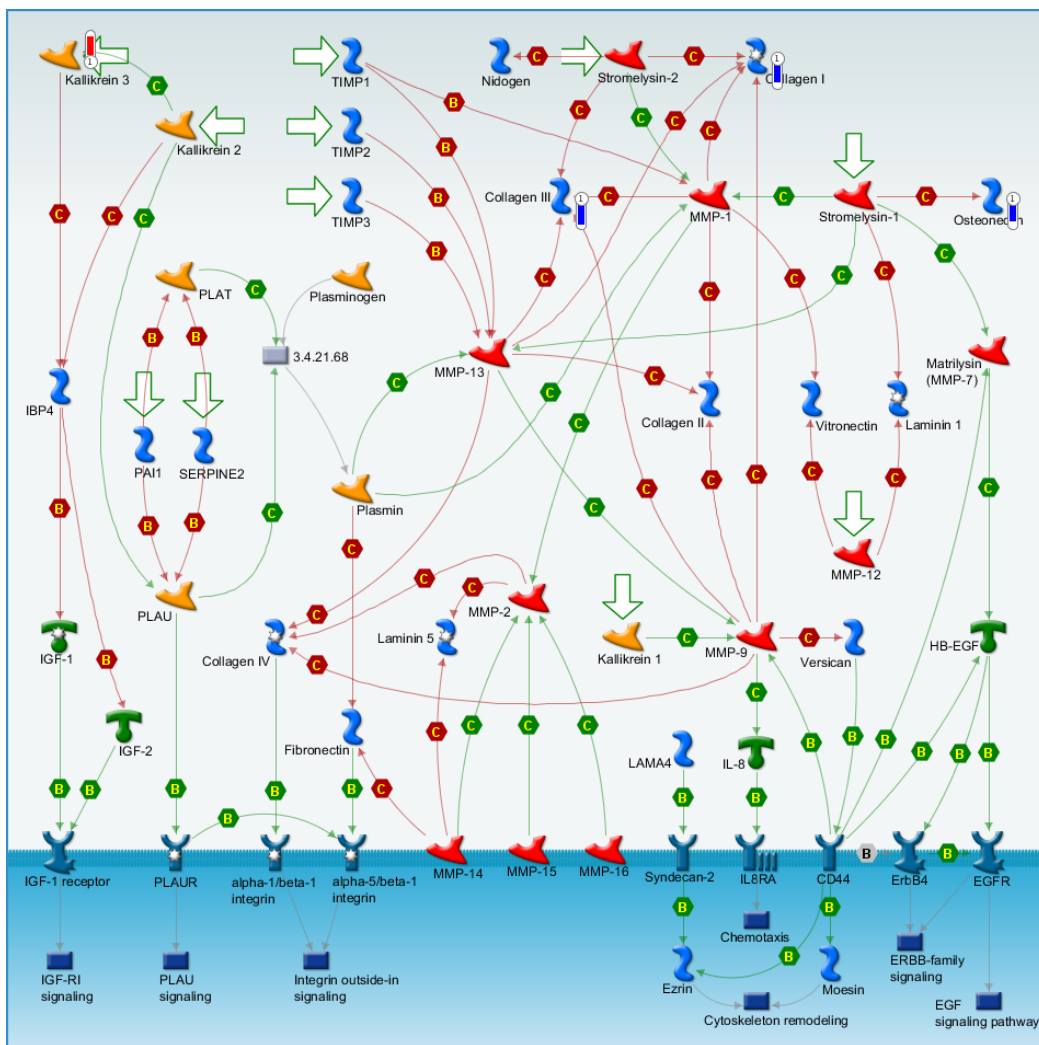


Figure 5.7 Cell Adhesion - ECM Remodeling. The top scored map (map with the lowest P-value) based on the enrichment distribution sorted by 'Statistically significant Maps' set.

Experimental data from all files is linked to and visualized on the maps as thermometer-like figures. Up-ward thermometers have red color and indicate up-regulated signals and down-ward (blue) ones indicate down-regulated expression levels of the genes.

Collagen I gene is responsible for encoding collagen I which is the most abundant form of collagen in human body. However, the transcription of collagen I gene is up-regulated by stromelysin-2, MMP-1, MMP-9 and MMP-13. Collagen I gene activation mediates its activity through integrin outside-in signaling. For instance, MMP-9 and MMP-13 both of which activates collagen I gene also activates collagen IV which leads to down regulation of alpha-1/beta-1 integrin as a result of integrin outside-in signaling up regulation. MMP-9 is responsible for collagen I down regulation and also for the down regulation of IL-8 and IL8RA eventually leading to up-regulation of chemotaxis in cardiomyocytes. Furthermore, MMP-9 up-regulates verscan gene leading to down regulation of CD44 which then down regulates matrilysin (MMP-7) which subsequently down regulates heparin-binding EGF-like growth factor (HB-EGF). HB-EGF then down regulates erythroblastic leukemia viral oncogene homolog (ErbB4) and epidermal growth factor receptor (EGFR) both of which up-regulates the activity of ERBB-family signaling. In addition, EGFR also up-regulates the activity of epidermal growth factor (EGF) signaling pathway.

Collagen III gene is responsible for encoding collagen III protein. Down regulation of collagen III gene is mediated by MMP-1, MMP-13 and stromelysin-2. However, the down regulation of collagen III seems to act through similar mechanism with collagen I, which is centrally controlled by MMP-13 and is up-regulated by tissue inhibitor of metalloproteinase 1 (TIMP1),

TIMP2 and TIMP3 whereas is down regulated by stromelysin-1 and plasmin. However, MMP-2, MMP-9 and MMP-13 are responsible for collagen IV up-regulation which subsequently leads to down regulation of alpha-1/beta-1 integrin eventually leading to up-regulation of integrin outside-in signaling through which it mediates its effects during DOX-induced fibrosis which then results in cardiomyopathy. MMP-13 is responsible for collagen III up-regulation and also for MMP-9 down regulation which then down regulates IL-8 and IL8RA eventually leading to up-regulation of chemotaxis in cardiomyocytes. Furthermore, MMP-9 up-regulates verscan gene leading to down regulation of CD44 which then down regulates HB-EGF. HB-EGF then down regulates ErbB4 and EGFR both of which up-regulates the activity of ERBB-family signaling. In addition, EGFR also up-regulates the activity of EGF signaling pathway.

Osteonectin gene is another gene which is down regulated by Stromelysin-1 as a result of DOX administration. However, osteonectin which is secreted by osteoblasts shows affinity for collagen as well as mediating functions such as collagen binding and cell-matrix interactions. Moreover, osteonectin is also involved in increasing the production and activity of matrix metalloproteinases (MMP), enzymes that play a crucial role in collagen cleavage.

The up-regulation of kallikrein 3 is another effect observed following DOX administration. The up-regulation of kallikrein 3 gene caused by DOX

administration is down regulated by kallikrein 2 and both kallikrein 2 and kallikrein 3 are responsible for up-regulation of insulin-like growth factor binding protein 4 (IBP4). Subsequently, IBP4 leads to the up-regulation of IGF-1 and IGF-2 both of which lead to down regulation of IGF-1 receptor eventually leading to up-regulation of the activity of IGF-1R signaling. These pathways are responsible for the mechanisms through which kallikrein 3 mediates its effects in DOX-induced toxicity in diabetic cardiomyopathy.

5.3.5.2.2 Transcription - Role of AP-1 in Regulation of Cellular Metabolism

The top second pathway map is shown in Fig 5.8. The pathway map of Transcription - Role of activator protein 1 (AP-1) in Regulation of Cellular Metabolism shows a series of processes and pathways that are the potential mechanisms underlying the DOX-induced toxicity in diabetic cardiomyopathy.

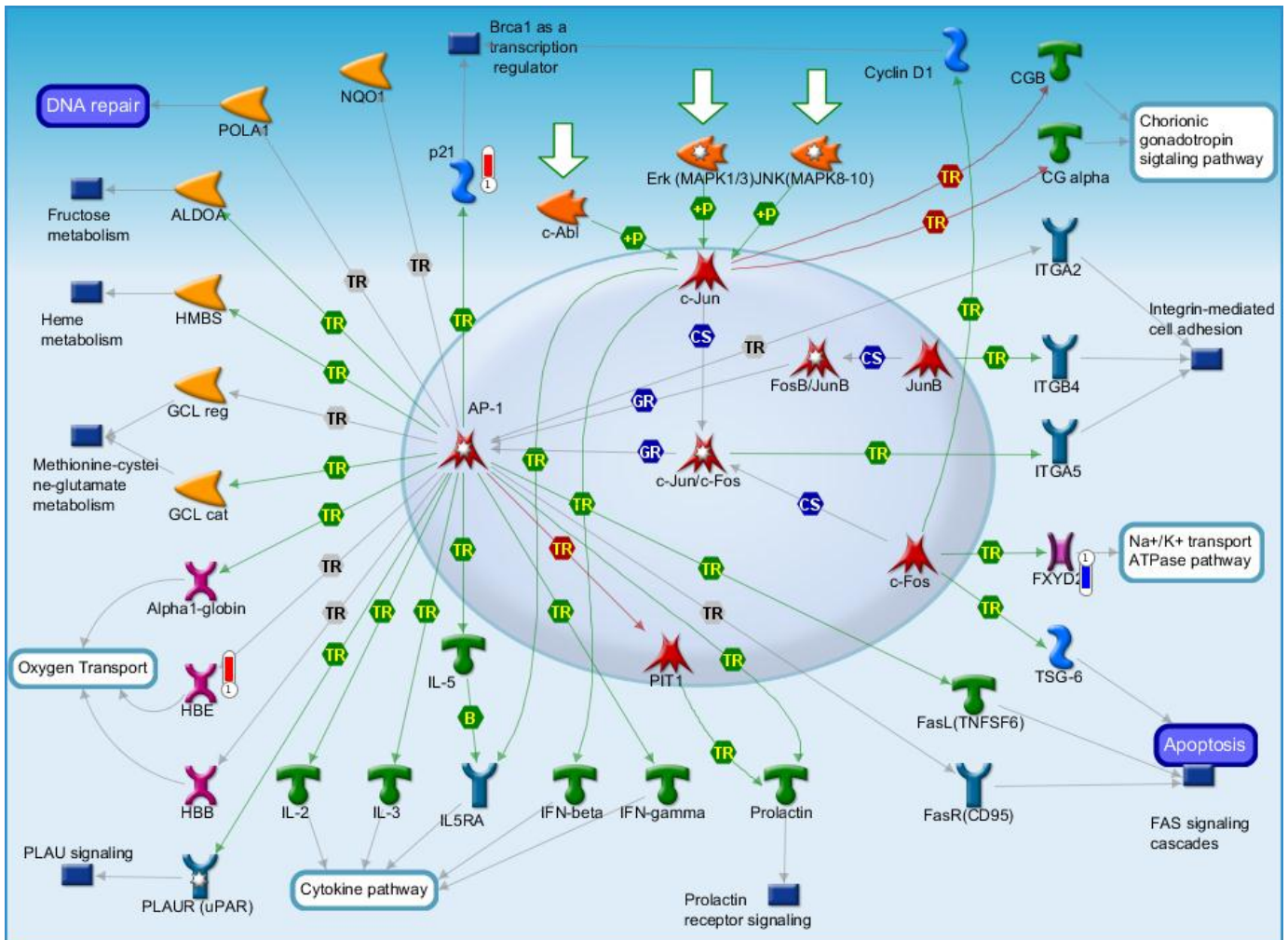


Figure 5.8 Transcription - Role of AP 1 in regulation of cellular metabolism. The second scored map (map with the second lowest P-value) based on the enrichment distribution sorted by 'Statistically significant Maps' set. Experimental data from all files is linked to and visualized on the maps as thermometer-like figures. Up-ward thermometers have red color and indicate up-regulated signals and down-ward (blue) ones indicate down-regulated expression levels of the genes.

Most of the pathways illustrated in this pathway map center around the activity of AP-1, which is especially central in terms of its activation of other elements depicted in this pathway map. The AP-1 is, by itself, involved in one quasi-cyclical and self-reinforcing relationship of mutual influence with integrin alpha 2 (ITGA2, which also influences Integrin-mediated cell adhesion but is otherwise not connected to other elements contained within the pathway map or relevant to the research at hand). AP-1 is further impacted by the activity of FosB/JunB, which in turn is activated by JunB (which also activates ITGB4 and leads to further Integrin-mediated cell adhesion activation). The third and final line of influence leading to the activation of AP-1 comes from c-Fos, which also triggers tumor necrosis factor-stimulated gene 6 (TSG-6, known to trigger Apoptosis and FAS signaling cascades) and FXYD domain containing ion transport regulator 2 (FXYD2), the down regulated gene by DOX treatment in diabetic heart on this pathway map. AP-1 is of further interest and will be described further below, but a description of FXYD2 is now in order to be described.

FXYD2 controls the sodium and potassium transport ATPase pathway, and its down regulation as part of the process depicted in this pathway map is a direct result of the activation of the c-Fos element illustrated (with no triggering event provided on this pathway map). c-Fos also triggers Cyclin D1 which in turn impacts Brca1 as a transcription regulator, as well as triggering the TSG-6 gene as mentioned (which triggers Apoptosis) and triggering the c-Jun/c-Fos cluster,

which triggers the AP-1 (again, AP-1 serves as the most central element of this pathway map and an element of direct importance to this research, as will be described shortly). Down regulation of the FXVD2 sodium and potassium transport ATPase pathway is the most significant direct effect of c-Fos activation from the perspective of the given research questions, and the down regulation observed in the research and depicted in this pathway map has direct implications for further inquiry into the development of concrete responses to these questions.

AP-1 directly influences the expression of hemoglobin E (HBE), up regulating it to a significant degree. HBE impacts oxygen transport, as does Alpha 1-globin and β -globin protein (HBB). Both HBB and Alpha 1-globin are also influenced by AP-1, and as the pathway map shows none of these elements are interconnected nor do they show any other areas or directions of influence – they are each activated by AP-1 and each in turn affects oxygen transport, without influencing expression or activation of any other element. These straight through-lines of influence radiating out from AP-1 make for a much different pathway map than in Pathway Map 1, though the many different influences and impacts of AP-1 activation are ultimately quite complex.

AP-1's activation of HBE, and of Alpha 1-globin and HBB, and the resulting effect on oxygen transport is deemed especially significant due to the strength of the up-regulating effect observed in the results. Significant up-regulation of

HBE by DOX would come with a significant impact on oxygen transport, and this could have serious implications in regards to the exact mechanism by which DOX can be causal of heart failure. Though there are other elements at work to impact the oxygen transport via the same mechanism, the findings in regard to HBE are considered more significant for the degree of up regulation observed and for the relative novelty of the finding in relation to previous research.

AP-1 also strongly up-regulates p21, which is the target gene of DOX in this pathway map deemed to be of special importance and interest to this particular research inquiry. The up-regulation of p21 by AP-1 leads to an increased activation of Brca 1 as a transcription regulator – the same impact noted for Cyclin D, which is connected to the down regulation of the FXVD2 sodium and potassium ATPase pathway through the activation of the c-Fos element (which triggers both the down regulation of the FXVD2 sodium and potassium ATPase pathway and Cyclin D1 as well as indirectly activating AP-1 through the activation of the c-Jun/c-Fos bundle). The c-Fos element thus impacts AP-1 and through this oxygen transport, the FXVD2 sodium and potassium ATPase pathway (and related transport through the channel), and transcription regulation through both Cyclin D1 and the more research-relevant p21.

5.3.5.2.3 Immune Response - IL 13 Signaling via JAK STAT

Cardiac inflammation is one of the most significant mechanisms underlying the development of cardiomyopathy. Several inflammatory markers have been significantly regulated by DOX treatment in diabetic cardiomyopathy. In this pathway map (Fig 5.9), three key genes including MMP-8, RSNB and COL1A are involved in cardiotoxicity induced by DOX potentially leading to congestive heart failure and are discussed as follows.

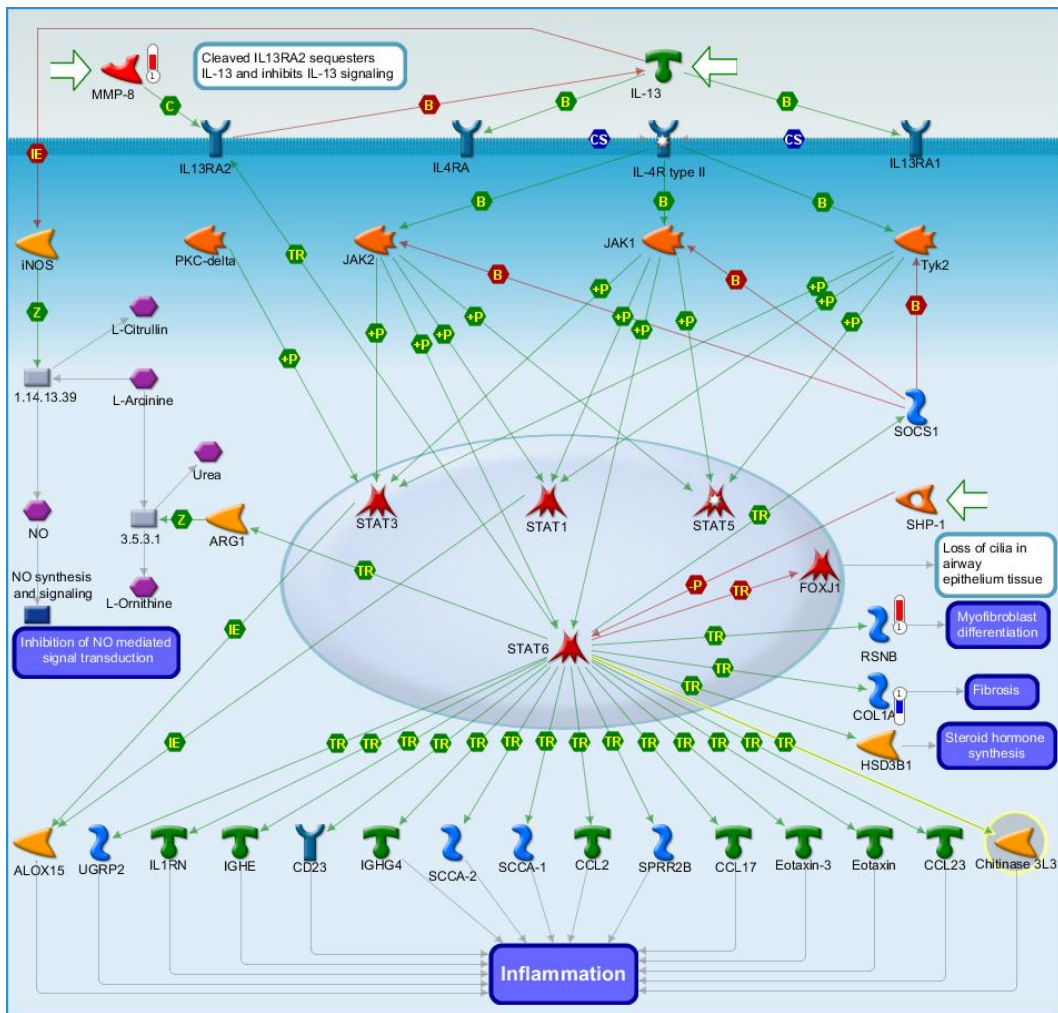


Figure 5.9 Immune response - IL 13 signaling via JAK STAT. The third scored map (map with the third lowest P-value) based on the enrichment distribution sorted by 'Statistically significant Maps' set. Experimental data from all files is linked to and visualized on the maps as thermometer-like figures. Up-ward thermometers have red color and indicate up-regulated signals and down-ward (blue) ones indicate down-regulated expression levels of the genes.

The pathway map “Immune Response - IL 13 Signaling via JAK STAT” indicates that there are three genes that are affected by DOX administration including MMP-8, RSNB and COL1A. MMP-8 gene is responsible for encoding matrix metalloproteinase-8 which is one of the most important genes that mediate the effects of DOX in diabetic cardiomyopathy. However, MMP-8 which also acts as a fibrotic factor belongs to the group of enzymes known as matrix metalloproteinase (MMP) which has a considerable number of isoforms which are mostly involved in collagen cleavage in many connective tissues and they are encoded by MMP genes which are localized at chromosome 11q22.3. Up-regulation of MMP-8 leads to down regulation of IL13RA2. However, IL13RA2 up-regulates IL-13. This occurs through the cleavage of IL13RA2 leading to sequestration of IL-13 and subsequent inhibition of IL-13 signaling. Moreover, the generated IL-13 leads to down regulation of INOS which eventually results in inhibition of NO synthesis and signaling. Subsequently, this leads to inhibition of NO-mediated signal transduction.

DOX mediates the up-regulation of RSNB at the center of STAT 6 gene which leads to eventual up-regulation of RSNB gene whose expression products are responsible for the activation of myofibroblast differentiation. However, STAT 6 is up-regulated by SHP-1 leading to mediation of activation of multiple molecules all of which eventually lead to inflammation activation. COL1A gene which is located on chromosome 2 is responsible for encoding of collagen alpha-1(I) chain, a protein that is found in many connective tissues. However,

administration of DOX leads to down regulation of COL1A in type 2 diabetic heart. The down regulation of COL1A in DOX-induced cardiomyopathy is centrally mediated by STAT 6. However, SHP-1 leads to up-regulation of STAT 6 which is then responsible for the down regulation of COL1A gene leading to the mediation of fibrosis in DOX-induced toxicity in type 2 diabetic cardiomyopathy.

5.3.5.2.4 Transcription - Androgen Receptor Nuclear Signaling

Three significant genes namedly WNT, p21, and Kallikrein 3 were identified in the Pathway Map “Transcription - Androgen Receptor Nuclear Signaling” (Fig 5.10).

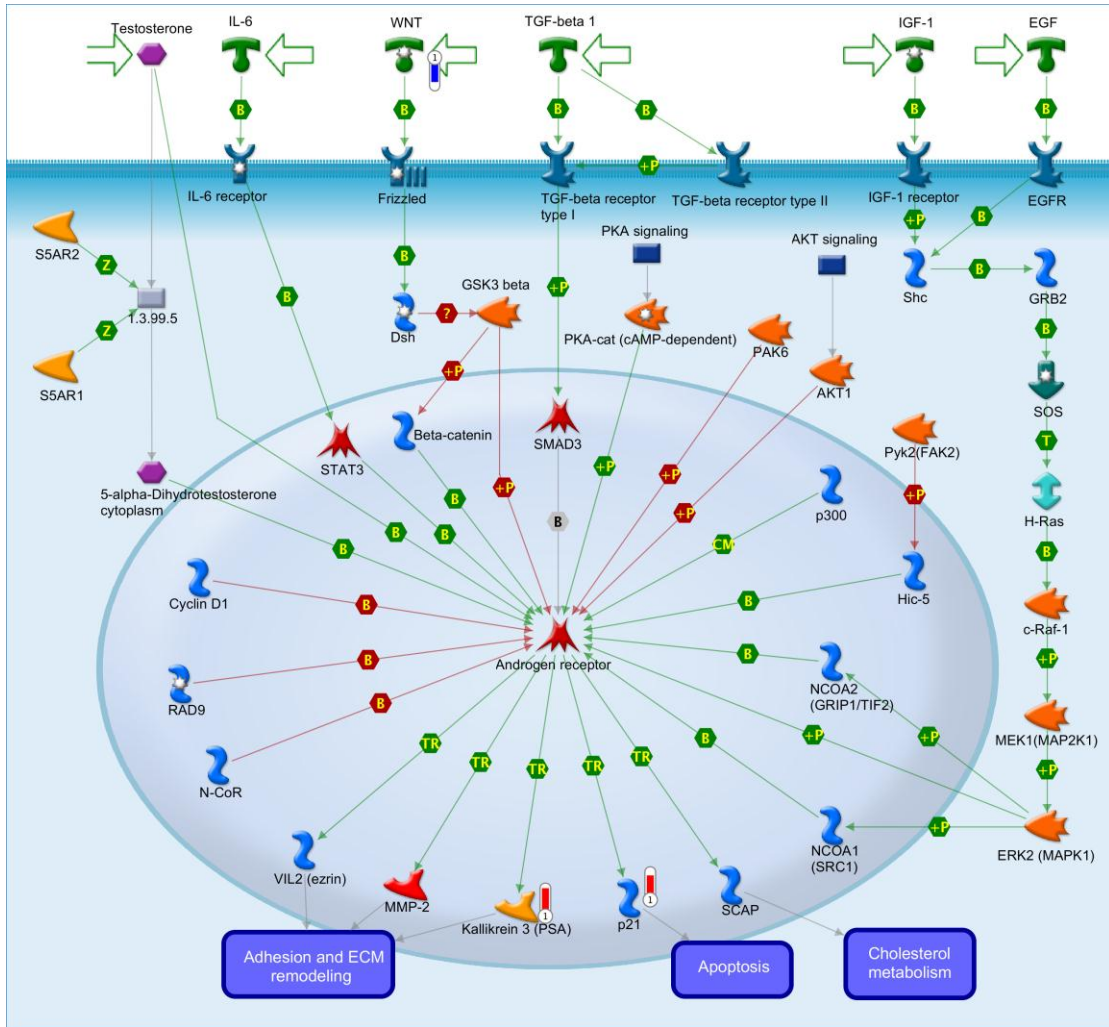


Figure 5.10 Transcription - Androgen Receptor Nuclear Signaling. The fourth scored map (map with the third lowest P-value) based on the enrichment distribution sorted by 'Statistically significant Maps' set. Experimental data from all files is linked to and visualized on the maps as thermometer-like figures. Up-ward thermometers have red color and indicate up-regulated signals and down-ward (blue) ones indicate down-regulated expression levels of the genes.

WNT acts via Dsh to down regulate GSK3 beta, which normally down regulates the Androgen receptor. GSK3 also normally down regulates Beta-catenin, which normally up-regulates the Androgen receptor, and thus GSK3 beta is an important regulatory agent for the Androgen receptor. The down regulation of GSK3 beta by activated Dsh, which occurs through the action of WNT, means that the Androgen receptor is allowed to remain more active, though as the pathway map shows there are many different factors influencing the activity level of the Androgen receptor.

An activated Androgen receptor has many different effects, and two of which stand out for their importance in this research. Kallikrein 3, as illustrated in Pathway Map 1, is up-regulated by an active Androgen receptor; WNT activity thus leads to increased Kallikrein 3 activity and an increase in the cascade of events described in Pathway Map 1. An active Androgen receptor also up-regulates p21, as discussed in Pathway Map 2, which leads to Apoptosis. The findings illustrated in this pathway map are especially useful in helping to fit together certain pieces of early and directly relevant pathway maps, providing greater fodder for a meaningful reflection of these results.

5.3.6 Confirmation of Selected Gene Expressions by Real Time

RT-PCR

The transcriptional expression changes of two target genes namely S100A8 (S100 calcium binding protein A8) and S100A9 (S100 calcium binding protein A9) demonstrated by microarray analysis were further confirmed by real time RT-PCR analysis. The gene expression of S100A8 was found to be only significantly elevated by DOX in diabetic heart on day 5 (by 2.8 fold) and day 7 (by 23 fold) after DOX administration relative to the diabetic control (Fig 5.11). These data suggested that S100A8 might not be involved in DOX-induced cardiotoxicity in non-diabetic mice but was associated with the DOX cardiotoxicity in diabetic hearts. The transcriptional expression of S100A9 in the heart was up-regulated by DOX in db/+ non-diabetic mice on day 5 after DOX administration (by 24.1 fold, $P < 0.001$) and no further change on day 7 after the DOX administration (Fig 5.12). Similarly, the transcriptional expression of S100A9 in heart was increased by DOX in db/db diabetic mice on day 5 (by 6.7 fold, $P < 0.01$), but dramatically elevated by DOX on day 7 following DOX administration (by 46.3 fold, $P < 0.001$). Moreover, the gene expression of S100A9 was up-regulated in db/db diabetic heart (by 20.2 fold, $P < 0.001$) when compared to non-diabetic heart (Fig 5.12).

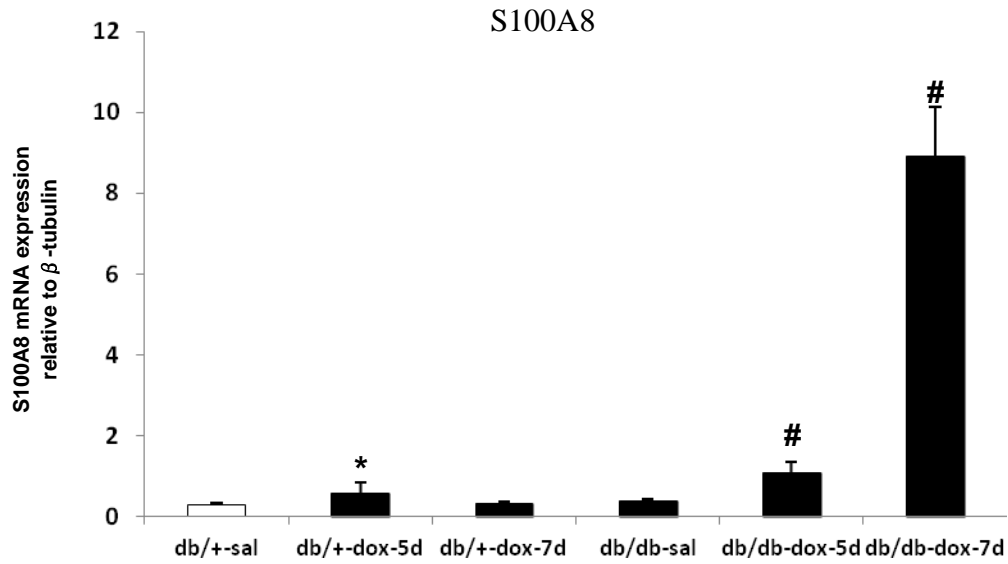


Fig 5.11 The transcriptal expression levels of S100A8. Data were presented as expression ratio normalized to β -tubulin gene. Data are expressed as mean \pm SEM (n = 6 per group).

*P < 0.01 compared to non-diabetic control group (db/+sal), #P < 0.001 compared to diabetic control group (db/db-sal).

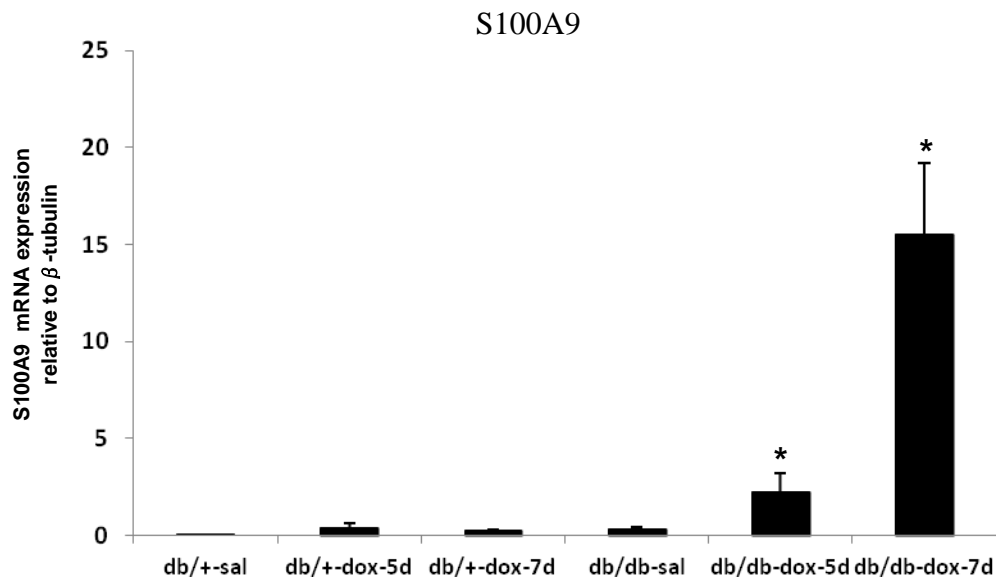


Fig 5.12 The transcript expression levels of S100A9. Data were presented as expression ratio normalized to β -tubulin gene. Data are expressed as mean \pm SEM (n = 6 per group).

*P < 0.001 compared to diabetic control group (db/db-sal).

5.3.7 Pathway Network: Inflammation Amphoterin Signaling

Pathway network of S100A8 (Calgranulin A) and S100A9 (Calgranulin B) was then analyzed by Metacore. The pathway network shown in Fig 5.13 is an outline of inflammation Amphoterin signaling pathway map, in which two main genes Calgranulin A and Calgranulin B are highlighted. It has been observed that Calgranulin B has an effect on NF- κ B while a complex of Calgranulin A and Calgranulin B is believed to act on RAGE leading to activation of p38 MAPK.

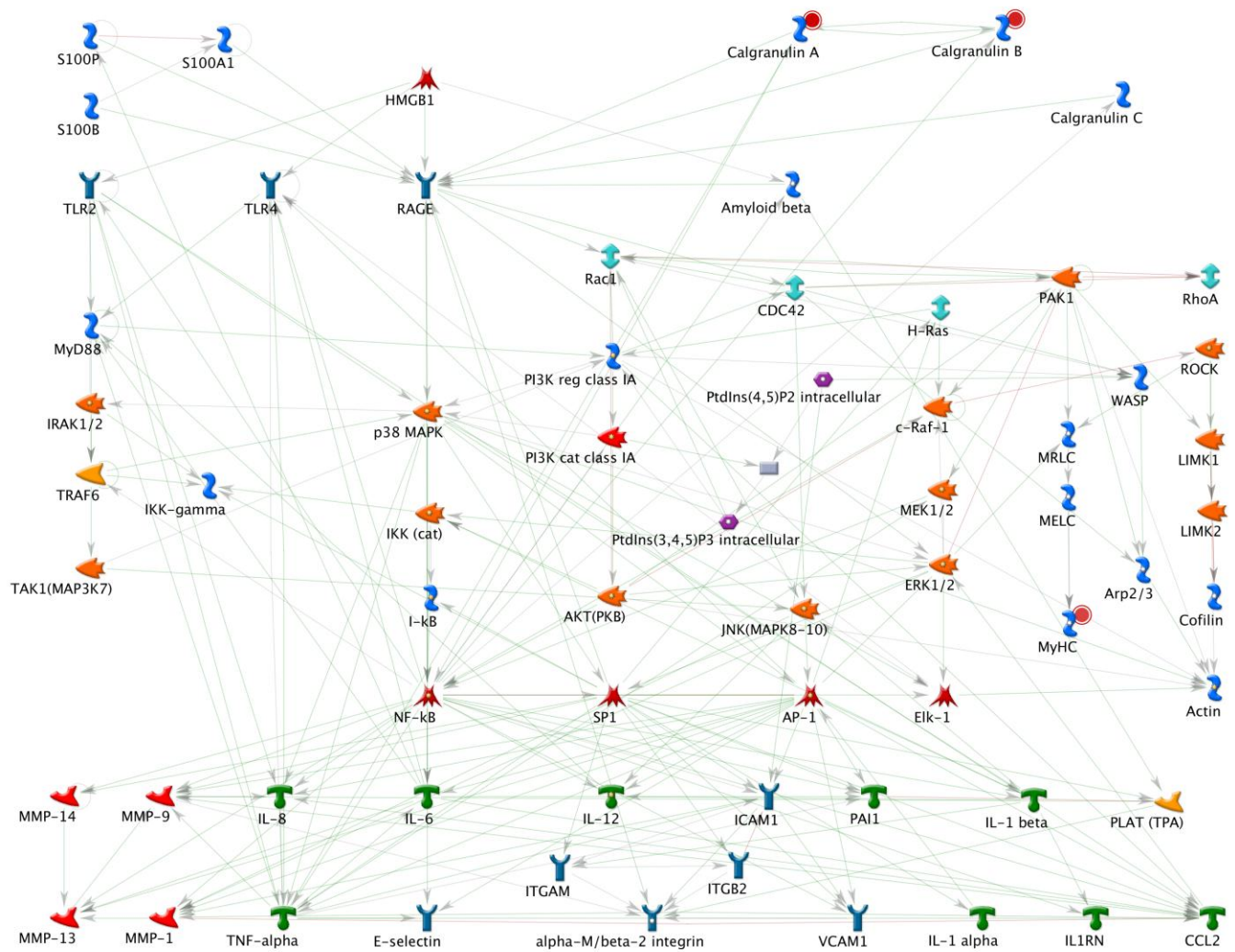


Fig 5.13 Pathway Network: Inflammation Amphoterin Signaling. The pathway network shows an illustration of genes that are significantly regulated by DOX in diabetic heart.

Amphoterin is at the center of the inflammation pathway map which involves cardiotoxicity induced by DOX in type 2 diabetic cardiomyopathy. Amphoterin receptor referred to as receptor for advanced glycation end products (RAGE), is a cell surface molecule which belongs to the family of multi-ligand immunoglobulin and is involved in interacting with distinct molecules that facilitate inflammation. Inflammation Amphoterin signaling pathway map is mediated by the binding of various ligands, particularly the Amphoterin to RAGE which leads to the triggering of the activation of key cellular signaling pathways, such as NF- κ B, MAP kinases, p21ras and cdc42/rac, thereby leading to the reprogramming of cellular properties. It is important to note that in the inflammatory Amphoterin signaling, RAGE acts as the central cell surface receptor for Amphoterin. Indeed, the binding of Amphoterin to RAGE mediates a multitude of biochemical inflammation pathways in cardiomyocytes. Inflammatory Amphoterin signaling during DOX-induced toxic effects in diabetic heart involves mediation of effects on Calgranulin A and Calgranulin B genes. This is attributed to the fact that DOX directly influences these two genes that subsequently lead to a multitude of molecular pathways involving up-regulation and down regulation of many genes. This pathway network should receive more attention in the future research in the cardiotoxicity of DOX.

Calgranulin A is one of the most important molecules that mediate the inflammatory Amphoterin pathway. This molecule is also involved in acting on

many other molecules on which it leads to their up-regulation or down regulation. For instance, Calgranulin A binds to RAGE which also binds to many other molecules. The binding of Calgranulin to RAGE leads to activation of p38 MAPK which then activates IKK followed by activation of I- κ B. Subsequently, I- κ B acts on NF- κ B leading to activation of IL-6 and E-selectin. In addition, p38 MAPK is activated by Calgranulin A and leads to the activation of SP1 which then activates ITGAM and ITGB2. Eventually, both ITGAM and ITGB2 lead to activation of alpha-M/beta-2 integrin. However, RAGE is activated by Calgranulin A and leads to direct activation of alpha-M/beta-2 integrin. Moreover, a complex of both Calgranulin A and Calgranulin B also binds to RAGE leading to activation of p38 MAPK which then activates IKK followed by the activation of I- κ B. Subsequently, I- κ B acts on NF- κ B leading to activation of IL-6 and E-selectin as observed in Calgranulin A alone.

Calgranulin B is another important molecule that mediates the inflammatory Amphoterin pathway. Calgranulin B is also involved in acting on many other molecules on which it leads to their up-regulation or down regulation. However, in the inflammatory Amphoterin pathway, Calgranulin B has an effect on NF- κ B which leads to the activation of several other pathways. NF- κ B activation leads to direct activation of TNF-alpha. NF- κ B also acts on IL-12 which leads to activation of alpha-M/beta-2 integrin. In addition, activation of NF- κ B by Calgranulin B leads to activation of SP1 which then activates ITGAM and ITGB2. Eventually, both ITGAM and ITGB2 lead to activation of alpha-

M/beta-2 integrin.

5.4 Discussion

5.4.1 Further Decrease in Cardiac Contractile Function at 7-day After DOX Administratio in Diabetic Heart

It is well-known that DOX induces acute cardiac toxicity *in vivo* (Childs *et al.*, 2002; Suliman *et al.*, 2007). Our data showed DOX induced cardiac dysfunction in non-diabetic mice at 5-day after the administration of DOX. The presently adopted animal model, db/db leptin receptor deficient mice, developed the phenotype of type 2 diabetes with increased body weight, hyperinsulinemia and hyperglycemia from the age of 12 weeks accompanied with decreased cardiac contractility (Belke *et al.*, 2004). Consistent with these previous findings, our data indicated that the ventricular fractional shortening was suppressed in db/db diabetic mice when compared to db/+ non-diabetic mice at the pre-intervention (i.e., baseline) level.

Up to now, there is no study reporting the effects of DOX on type 2 diabetic heart. In this dissertation, we reasonably hypothesized that the diabetic heart was more susceptible to the DOX-induced cardiac damage when compared to non-diabetic heart. Interestingly, our data clearly indicated that there was a further suppression of cardiac fractional shortening at 7-day after DOX administration, but this cardiac functional suppression was not observed at 5-day after DOX administration in db/db diabetic mice. These results evidently demonstrated that DOX caused more severe cardiac damage in the heart of diabetic mice relative to non-diabetic heart.

5.4.2 Underlying Mechanism of DOX-induced Cardiotoxicity in Diabetic Heart

Extensive evidences propose that cardiac apoptosis contributes to the development of cardiomyopathy induced by DOX (Takemura & Fujiwara, 2007; Childs *et al.*, 2002). Myocardial apoptosis is thought to be an essential determinant of cardiac pathogenesis because it results in a loss of contractile units, conduction disturbances, compensatory hypertrophy of myocardial cells and accumulated fibrosis (Takemura & Fujiwara, 2007). Inhibition of cardiac apoptosis has become a potential therapeutic target in the treatment of cardiomyopathy induced by DOX. In agreement with the findings of the previous studies, our data illustrated that cardiac apoptosis was obviously induced by the administration of DOX in db/+ non-diabetic heart. However, the induction of myocardial apoptosis after the DOX administration was not observed at 5-day after the DOX administration in db/db diabetic mice. This might partly explain why the cardiac dysfunction in diabetic mice was not further suppressed by DOX at 5-day after the DOX administration.

Cardiac autophagy has been proposed to be involved in cardiac physiological and pathological conditions such as myocardial hypertrophy, ischemia reperfusion injury and heart failure (Gottlieb & Mentzer, Jr., 2012; Wang *et al.*, 2012c). Although the changes of autophagy in diabetic heart was not found to be consistent in different experimental conditions, the suppressed autophagy as

shown by the down regulation of Beclin1 expression was observed in diabetic heart in the present study. The inhibition of autophagy might further induce accumulation of abnormal proteins and organelles resulting in cardiac dysfunction. However, this inhibition of cardiac autophagy was not observed to be affected by DOX in diabetic heart at 5-day after the DOX administration. In type 1 diabetic heart, the pharmacokinetics and acute cardiotoxicity of DOX were altered by hyperglycemia (Al-Shabanah *et al.*, 2000). Thus, we hypothesized that the molecular mechanisms underlying diabetic heart in response to DOX at the early stage are distinct from the DOX-induced cardiotoxicity in non-diabetic normal heart. Therefore, we next investigated the whole transcriptional profiling aimed to reveal what the mechanisms were responsible for the DOX-induced effects on type 2 diabetic hearts by using microarray technique.

Our microarray data first revealed the unique genes that were involved in exerting the effects of DOX on the hearts in type 2 diabetic animals. Combined with Gene Ontology analysis, it was found that the genes that are significantly regulated were mainly responsible for several cellular mechanisms including cardiac remodeling and matrix, inflammatory and immune response, DNA/RNA stability and repair, oxidative stress, metabolism and specific signal transduction.

The first pathway map, Cell Adhesion ECM Remodeling, is the Pathway Map

carrying the most significant P-value when examined from the perspective of the particular research questions raised. As this pathway map is the most strongly indicated by the Metacore analysis and therefore we interpreted that this pathway should play a very important role in the DOX-induced toxicity in the heart of type 2 diabetic individuals.

Kallikrein 3 was the first component on Pathway Map 1 “Cell Adhesion ECM Remodeling” that was identified as with specific importance to the research question. Kallikrein 3 cleaves IBP4 (Insulin-like growth factor binding protein 4) and these fragments then lose their capacity to bind to Insulin-like growth factors 1 and 2 (IGF-1 and IGF-2). With IGF-1 and IGF-2 unbound and freely available, IGF-1 receptors receive excess stimulation and this has an impact on the rate of cell growth and proliferation. This supports several of the hypotheses regarding DOX toxicity in cardiac tissue as described above. Although Kallikrein 3 does not provide a complete or conclusive explanation but the direct effect of Kallikrein 3 shown in Pathway Map 1 is still potentially significant in explaining our observations. Other downstream effects of IBP4 cleaving and resulting cascades could potentially be involved in the mechanism creating DOX toxicity in type 2 diabetic cardiac hearts. Nevertheless, this proposition requires to be further confirmed by more thorough and focused investigations.

Collagen I and Collagen III are involved in wound repair, and their down

regulations as illustrated in Pathway Map 1 is achieved primarily through the degrading effects of MMP1, MMP-13, and Stromelysin-2. The MMPs are activated in part by the release of plasmin, which itself is triggered by the PLAU activation that is the end result of the Kallikrein 3/Kallikrein 2 cycle and cascade, thus the activation of Kallikrein 3 as discussed above is also in part responsible for the down regulation of Collagen I and Collagen II proteins during the processes depicted in this pathway map. Stromelysin 2 also activates MMP-1 while working to directly degrade Collagen I and Collagen III, and thus has a reinforcing role in the breakdown and down regulation of these components. Again, specific studies that look into this mechanism would be necessary to determine its role in DOX toxicity in the diabetic hearts, but our findings at least suggest that the breakdown of these proteins is significantly involved in the underlying mechanisms responsible for the detrimental effects of DOX in diabetic heart.

Our pathway analysis suggests that Stromelysin-1 activates MMP-1 (leading to the breakdown of Collagen I and Collagen III) and degrades Osteonectin (secreted protein acidic and rich in cysteine or SPARC). The degradation of this component, which is related to collagen proteins in terms of wound repair, could also be a potential cause of the eventual failure of cardiac tissue as a result from DOX damage. Further research is needed to determine how the degradation of Collagen I, Collagen III, and Osteonectin might impact the cardiac tissue death.

In addition, the early transcriptional response of DOX-treated diabetic hearts showed several novel and potentially critical targets such as S100 calcium binding protein A8 (S100A8), S100 calcium binding protein A9 (S100A9) and MMP-8. S100A8 and S100A9 are the members of the S100 family that contain two calcium binding sites and are involved in the inflammatory process and immune diseases (Otsuka *et al.*, 2009). A recent human study reported that S100A8/S100A9 complex could be an useful biomarker for the prediction of one year mortality in elderly patients with severe heart failure (Ma *et al.*, 2012a). Moreover, an *in vivo* study showed that the activation of S100A8/S100A9 was crucial for the development of post-ischemic heart failure via the activation of the receptor of advanced glycation end products (RAGE) and Toll-like receptors (Volz *et al.*, 2012). Therefore, based on our findings, S100A8/S100A9 might play an important role in the pathophysiology of heart diseases such as DOX-induced cardiomyopathy in diabetic heart. Our microarray and RT-PCR data showed that the gene expression of S100A8 and S100A9 was significantly upregulated by DOX in the heart of type 2 diabetic mice at 5-day after DOX administration. Most importantly, the changes of the expression of S100A8 and S100A9 indeed corresponded to the further suppression of cardiac contractile function at 7-day after the administration of DOX. The transcriptional level of S100A8 and S100A9 was found to be dramatically increased by 23-fold and 46-fold, respectively, when compared to db/db diabetic control. These findings importantly suggested that S100A8 and

S100A9 might be importantly involved in the development of cardiac dysfunction in diabetic heart in response to the administration of DOX. The precise mechanisms that involve S100A8 and S100A9 in the detrimental effects of DOX in diabetic heart are worth to be further investigated. The understanding of the role of S100A8 and S100A9 might contribute significantly to the unraveling of the molecular mechanisms responsible for the distinct response to DOX in diabetic heart.

CHAPTER 6

Overall Discussion and Future Direction

6.1 Main Findings

6.1.1 Aims of the Dissertation

The general aims of this dissertation were 1) to identify the protective effects of desacyl ghrelin on DOX-induced cardiomyopathy in a mouse model, 2) to investigate the beneficial roles of desacyl ghrelin in type 2 diabetic cardiomyopathy using a diabetic mouse model, and 3) to further elucidate the potential mechanisms responsible for the cardiotoxic effects of DOX on type 2 diabetic hearts.

6.1.2 Summary of Main Findings

The results described in CHAPTER 3 clearly demonstrated that desacyl ghrelin protected cardiomyocytes against DOX-induced cardiomyopathy by preventing the activation of cardiac fibrosis and apoptosis and the effects were found to be mediated through GHSR-independent mechanisms. The study reported in CHAPTER 4 provided novel *in vivo* evidence demonstrating that desacyl ghrelin protected the heart against type 2 diabetic cardiomyopathy by improving cardiac fibrosis, autophagic signaling, and cardiac inflammation. The work described in CHAPTER 5 focused on DOX-induced cardiotoxic effects on type 2 diabetic heart. The microarray results illustrated the molecular mechanisms that were importantly involved in the DOX-induced toxicity in diabetic hearts. The main findings of the aforementioned studies in this

dissertation are summarized in Fig 6.1.

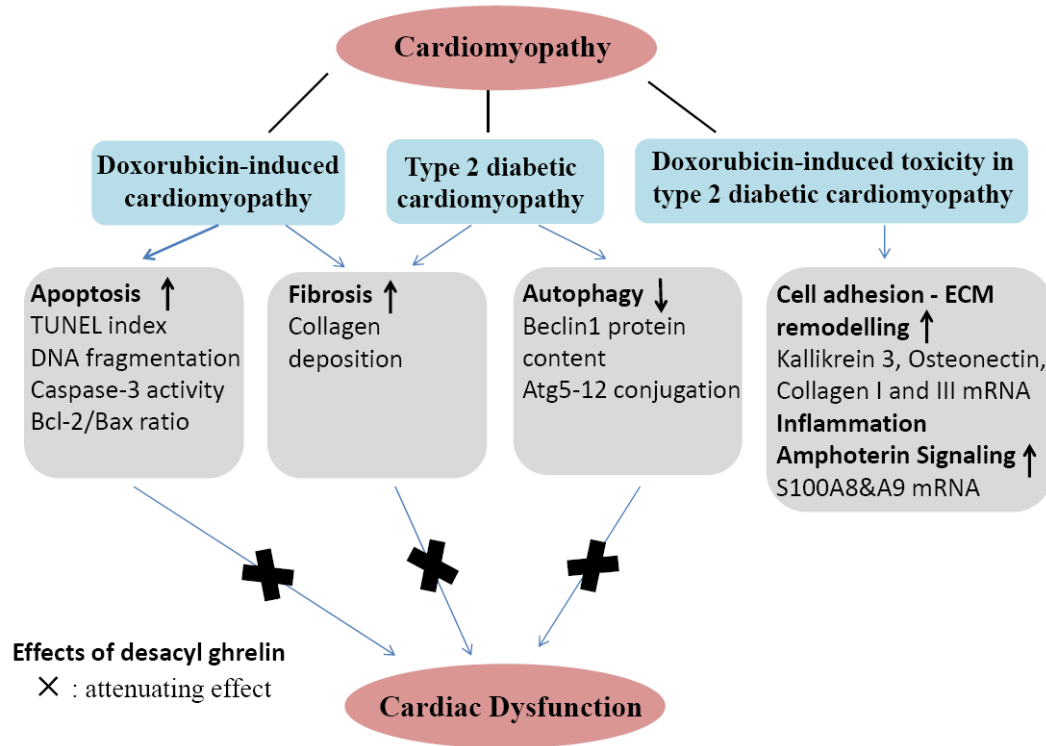


Fig 6.1 The Summary of Main Findings in the Dissertation.

6.2 Cardiac Dysfunction of Cardiomyopathy Induced by Anti-cancer Drug DOX and Type 2 Diabetes Mellitus

During the development of cardiomyopathy, the heart muscle becomes structurally and functionally abnormal and these changes would ultimately result in fatal heart failure. In order to maintain the cardiac systolic and diastolic function, the heart needs to develop adaptive responses to detrimental stimuli (Harvey & Leinwand, 2011). Cardiac morphological and structural changes occur when compensatory mechanisms are activated in the heart to maintain the cardiac physiological contractile and relaxation function. Studies presented in this dissertation focused on the investigation of the potential therapeutic targets and mechanisms in two acquired cardiomyopathies namely DOX-induced cardiomyopathy and diabetic cardiomyopathy. The prevalence of these two types of cardiomyopathy is high as they are associated with cancer chemotherapy and type 2 diabetes, which are both commonly diagnosed in our population.

Studies have demonstrated that DOX leads to acute and chronic dilated cardiomyopathy indicated by the decreased ejection fraction in cancer patients (Poterucha *et al.*, 2012; Schwartz *et al.*, 2013; Dodos *et al.*, 2008). Cancer patients under DOX treatment showed the reduction of cardiac ejection fraction, which might have resulted from a reduction of T-cell leukemia/lymphoma 1A (TCL1A) levels further leading to the increase in the apoptotic sensitivity of cardiomyocytes (McCaffrey *et al.*, 2013). Our data confirmed that DOX results

in acute cardiomyopathy indicated by the decrease in ventricular fractional shortening and ejection fraction in an experimental mouse model with the administration of anti-cancer drug DOX. The dosage of DOX adopted in this dissertation was well-established and has been reported to cause cardiomyopathy in the previous animal studies. The work described in CHAPTER 4 focused on cardiovascular complications of type 2 diabetes – diabetic cardiomyopathy. It has been demonstrated that the systolic functional disorders as indicated by the decrease in ejection fraction, fractional shortening, and cardiac output were present in the patients with type 2 diabetic cardiomyopathy (Chavali *et al.*, 2013;Mytas *et al.*, 2009;Mihm *et al.*, 2001). The cardiac dysfunction was consistently observed in different animal models of type 2 diabetes including db/db mice (An & Rodrigues, 2006) and Zucker diabetic rats (Forcheron *et al.*, 2009). In agreement with the literature, our data also demonstrated the occurrence of cardiac systolic dysfunction as measured by echocardiography in diabetic db/db (leptin receptor deficient) mice at the age of 12 weeks.

There is limited information about DOX-induced cardiac toxicity in the individual with type 2 diabetes mellitus. An *in vivo* study showed that the pharmacokinetics of DOX was affected by hyperglycemia and the cardiac accumulation of DOX was increased in streptozotocin-induced type 1 diabetic rats (Al-Shabanah *et al.*, 2000). Providing the fact that both the DOX and diabetic condition have adverse effects on the heart, we reasonably

hypothesized that DOX would further impair the cardiac function under diabetic condition in type 2 diabetic db/db mice. Nonetheless, our functional data demonstrated that db/db diabetic mice exhibited the same extent of cardiac dysfunction five days after the DOX administration. However, intriguingly a further decrease in cardiac systolic function was noticed at seven days after the DOX treatment in db/db diabetic mice but not in the non-diabetic normal animals. Our further microarray analysis revealed that different molecular mechanisms were responsible for the cardiotoxic effects of DOX between type 2 diabetic hearts and non-diabetic normal hearts. Our findings suggested that additional investigations were warranted to fully determine the precise cellular mechanisms of the detrimental effects of DOX in diabetic hearts. Most importantly, our results illustrated that the molecular targets for exploring the cardioprotective regimens in DOX-induced cardiac damage might be different between the diabetic hearts and normal hearts.

6.3 Potential Mechanisms of Cardiomyopathy Induced by DOX and Type 2 Diabetes

6.3.1 Cardiac Cell Death

Adult heart cells have limited ability to regenerate and repair; therefore they are very sensitive and adaptable to the intrinsic and extrinsic stimuli (Chiong *et al.*, 2011). Two types of cardiac cell deaths, namely apoptosis and autophagy, are the key cellular events in the development of the heart disorders including

cardiomyopathy (Cai *et al.*, 2006;Harvey & Leinwand, 2011), heart failure, myocardial infarction, and ischemia/reperfusion (Whelan *et al.*, 2010).

6.3.1.1 Cardiac Apoptosis

Experimental studies have shown that apoptosis played an important role in the development of the dilated cardiomyopathy (Yamamoto *et al.*, 2003) and hypertensive cardiomyopathy (Gonzalez *et al.*, 2003). Increase in cardiac apoptosis has been demonstrated in cardiomyocyte treated with DOX no matter through acute or chronic DOX administration (Wang *et al.*, 2013;Chicco *et al.*, 2006;An *et al.*, 2013). In this dissertation, a single treatment of DOX was shown to result in the activation of apoptosis indicated by the increased TUNEL index, apoptotic DNA fragmentation and caspase-3 activity. These observations were in agreement with the findings of previous studies that adopted a similar DOX treatment protocol (Kawamura *et al.*, 2004). Apoptosis is regulated by intrinsic and extrinsic pathways, which have both been investigated in cardiomyocytes (Whelan *et al.*, 2010). It has been suggested that mitochondria-mediated intrinsic apoptotic pathway was involved in DOX-induced cardiotoxicity based on the previous *in vivo* and *in vitro* findings (An *et al.*, 2013;Tacar *et al.*, 2013;Wang *et al.*, 2012a;Spallarossa *et al.*, 2004;Heon *et al.*, 2003). Anti-apoptotic Bcl-2 and pro-apoptotic Bax are two crucial regulators in the intrinsic apoptotic pathway. Permeability of mitochondrial membrane was stabilized by the formation of homodimers of Bcl-2 and the Bcl-2 homodimers play against the release of cytochrome c and caspase-3 activation

(Wang *et al.*, 1998). However, this protective effect of Bcl-2 was diminished when the formation of the heterodimers of Bax-Bcl-2 is increased. Moreover, the formation of the homodimers of Bax could promote the activation of caspase-3 independently by creating the pores on the mitochondrial outer membrane to induce the efflux of cytochrome c (Childs *et al.*, 2002). Consistently, our data showed that the activation of apoptosis was induced by DOX and this was associated with the elevation of the ratio of anti-apoptotic Bcl-2 to pro-apoptotic Bax in the hearts examined. Together with the findings of previous studies, our results suggested that mitochondria-mediated apoptosis played an essential role in the DOX-induced cardiac dysfunction.

6.3.1.2 Cardiac Autophagy

Autophagy regulates the abundance and quality of intracellular components through the self-destruction and recycle of intracellular organelles and proteins. Autophagy also provides cells with nutrients and energy under stressful conditions such as starvation. Therefore, autophagy has been suggested to be a survival promoting process in the cells. Aberrantly regulated autophagy has been observed in diabetic cardiomyopathy. Six month-old OVE26 mice (a type 1 diabetic mouse model) have showed the suppressed autophagic activity in the heart characterized by a decrease in expression of lipidated microtubule-associated protein 1 light chain 3 (LC3 II) (Xie *et al.*, 2011b). Moreover, autophagy in cardiomyocytes isolated from db/db mice (a type 2 diabetic mouse model) was shown to be impaired as illustrated by the reduction of Beclin-1 in

the diabetic heart when compared to the non-diabetic cardiomyocytes (Marsh *et al.*, 2013). Consistently, our *in vivo* data substantiated that the db/db diabetic mice exhibited a decrease in the cardiac expression of Beclin 1 in diabetic animals when compared to the db/+ non-diabetic mice. Beclin 1 is crucial for the early stages of autophagosome formation, and its interaction with PI3KC3/Vps34 is essential for the localization of the other important autophagic proteins to the autophagosome. The down regulation of Beclin 1 in the heart of diabetic animals indicated that autophagy was suppressed and thus resulted in the accumulation of abnormal organelles and proteins in the diabetic hearts.

Furthermore, the modification of Beclin1 is also involved in the regulation of autophagy. Beclin1 can be phosphorylated by death-associated protein kinase (DAPK) on Thr 119 at its BH3 domain, which promotes the dissociation of Beclin1 from Bcl-XL and subsequently inducing autophagy (Zalckvar *et al.*, 2009). In addition, ubiquitination of Beclin1 by the tumor necrosis factor receptor-associated factor 6 (TRAF6) initiates the formation of autophagosomes via activation of PI3KC3 (Shi & Kehrl, 2010). Thus, it is necessary for future investigation of the interaction of Beclin1 and Bcl-XL, phosphorylation and ubiquitination of Beclin1 in type 2 diabetes induced cardiac autophagy.

6.3.2 Cardiac Fibrosis

The fibrotic process is shown to be important in the pathogenesis of different cardiovascular diseases. Myocardial fibrosis contributes to ventricular stiffening and impairs the cardiac systolic and diastolic function (Mewton *et al.*, 2011). Indeed, cardiac fibrosis has been detected by T1 magnetic resonance imaging in patients with DOX-induced cardiomyopathy (Jiji *et al.*, 2012) and type 2 diabetic cardiomyopathy (Pitt & Zannad, 2012). Unsurprisingly, excessive collagen deposition was observed in the heart treated with DOX in both the diabetic and non-diabetic mice by Masson's Trichome staining. However, the mechanisms of myocardial fibrosis in the DOX-induced cardiomyopathy and diabetic cardiomyopathy might be different. In the acute DOX-induced cardiomyopathy, myocardial fibrosis occurred as a response to cardiomyocyte loss (Feridooni *et al.*, 2011) whereas cardiac fibrosis is thought to be an adaptive process to the chronic pathophysiological stimuli such as the elevated inflammation in type 2 diabetic heart (Pitt & Zannad, 2012). In addition, the cross-link of collagen with advanced glycation end products (AGEs) in diabetic hearts might be an additional factor to aggravate ventricular stiffness (Asbun & Villarreal, 2006).

TGF- β 1, a potent pro-fibrotic stimulator of extracellular matrix production and deposition, is thought to contribute to the increased fibrosis in heart disease. Inhibition of TGF- β 1 or TGF- β 1 signaling appears to be the potential therapeutic target for hepatic and cardiac fibrosis (Leask, 2010; Liu *et al.*, 2006).

However, the regulation of TGF- β 1 was not involved in the model of DOX-induced cardiotoxicity (Miyata *et al.*, 2010;Li *et al.*, 2007). Correspondingly, there was no significant effect of DOX on the expression of TGF- β 1 gene in the heart shown in the experimental model in this dissertation. In contrast to DOX-induced cardiotoxicity, an increase in the expression of TGF- β 1 protein was demonstrated in the myocardium of rodents with diabetic cardiomyopathy (Ban & Twigg, 2008). TGF- β 1 activity and signaling in diabetic heart are worth to be further investigated in the future.

Another pro-fibrotic cytokine, connective tissue growth factor (CTGF), acts as a downstream and cooperative mediator of TGF- β 1 in the fibrogenic process. We observed that DOX induced the up-regulation of CTGF expression in the heart. This is in agreement with the notion that fibrosis in renal and heart may not be fully regulated by TGF- β , but greatly depended on CTGF (Zhou *et al.*, 2004;Way *et al.*, 2002). DOX also substantially increased the ratio of CTGF-to-brain natriuretic peptide (BNP). The balance between CTGF and BNP in cardiomyocytes was suggested to be a key determinant of cardiac fibrosis (Koitabashi *et al.*, 2007). Our findings suggested that CTGF and its interaction with BNP played an important role in DOX-induced fibrotic injury through a TGF- β -independent mechanism.

Adiponectin is an adipocyte-derived cytokine that plays an anti-diabetic (Konishi *et al.*, 2011) and anti-fibrotic role (Fang *et al.*, 2012). Plasma

adiponectin level has been shown to be suppressed in type 2 diabetic patients (Hotta *et al.*, 2000). In cardiovascular system, adiponectin level in circulation has been demonstrated to be negatively associated with the risk of myocardial infarction (Pischon *et al.*, 2004). Adiponectin has been exhibited to be expressed in cardiac myocytes. Dysregulation of cardiac adiponectin is suggested to have a role in the pathogenesis of dilated cardiomyopathy (Skurk *et al.*, 2008). Indeed, the gene expression of adiponectin has been reported to be significantly decreased in leptin-deficient db/db mice diabetic heart with severe inflammatory injury (Takahashi *et al.*, 2006). Similarly, our current data showed that cardiac adiponectin mRNA level was significantly down regulated in db/db type 2 diabetic mice, implicating the role of myocardial adiponectin in the pathophysiology of diabetic cardiomyopathy. Our data confirmed the microarray findings of a previous study that adiponectin gene expression was decreased in the hearts of db/db diabetic mice by 4.6-fold when compared to that of db/+ non-diabetic mice (Wilson *et al.*, 2008). Moreover, severe cardiac fibrosis was observed in angiotensin II-infused adiponectin-knockout mice via the activation of PPAR α (Fujita *et al.*, 2008). Taken together, myocardial fibrosis in type 2 diabetic mice might be attributed to the reduction of the expression of adiponectin.

6.4 Protective Effects of Desacyl Ghrelin on Cardiomyopathy

In this dissertation, desacyl ghrelin generally exhibited cardioprotective effects on DOX-induced cardiomyopathy and diabetic cardiomyopathy. These

protective effects included the improvement of cardiac contractile performance, myocardial apoptosis, autophagy and fibrosis via the activation of Akt/ERK1/2 cellular pro-survival signaling pathway in the experimental animal models examined.

Desacyl ghrelin is thought to be a degradation product of acylated ghrelin through the removal of the acylation. Desacyl ghrelin is shown to lack of the endocrine activity such as the stimulation of growth hormone release and food intake. However, accumulating evidences demonstrated that desacyl ghrelin might have multiple biological activities (Delhanty *et al.*, 2012). Nonetheless, studies have evidently demonstrated the beneficial effects of desacyl ghrelin on cardiovascular system. For example, desacyl ghrelin has been shown to inhibit myocardial apoptosis induced by DOX in H9c2 cardiomyocytes and endothelial cells (Baldanzi *et al.*, 2002), to protect the heart against isoproterenol-induced myocardial injury in a rat model (Li *et al.*, 2006), and to improve vascular remodeling in the patients with type 2 diabetes mellitus (Togliatto *et al.*, 2010).

The mRNA expression of ghrelin has been observed in HL-1 cardiomyocytes, human atrium and myocardium (Zhang *et al.*, 2010). Our studies successfully reproduced and extended the findings of the previous cell culture studies that desacyl ghrelin exerted the anti-apoptotic effects on DOX-induced cardiomyopathy. Moreover, our work was the first to demonstrate the cardioprotection mediated by desacyl ghrelin in diabetic hearts. Administration

of desacyl ghrelin was shown to effectively up-regulate Beclin 1 expression in type 2 diabetic heart, which sufficiently increased cardiac autophagy (Zhu *et al.*, 2007). Additionally, our data demonstrated that desacyl ghrelin enhanced the conjugation of Atg5-Atg12 in the hearts of db/db diabetic mice, and it was expected to promote the elongation of pre-autophagosomal membrane to initiate the autophagic process.

In this dissertation, cardiac fibrosis was shown to be a common feature involved in the DOX-induced cardiomyopathy and diabetic cardiomyopathy. Previous studies have suggested that acylated ghrelin might have a therapeutic effect on different disorders including cardiac injury (Li *et al.*, 2006), systemic sclerosis (Ota *et al.*, 2013), bleomycin-induced acute lung injury (Imazu *et al.*, 2011), liver injury (Moreno *et al.*, 2010) due to the anti-fibrotic effects of acylated ghrelin. However, there are limited publications relate to the role of desacyl ghrelin in fibrosis and the mediating effect of desacyl ghrelin in the heart is largely unknown. Li and co-workers have documented that desacyl ghrelin exerted the anti-fibrotic effects on isoproterenol-induced myocardial injury via growth hormone-independent pathway (Li *et al.*, 2006). Consistently, in this dissertation, desacyl ghrelin was shown to reduce the collagen accumulation in the heart of mice treated with DOX and of diabetes. Interestingly, the observed anti-fibrotic effect of desacyl ghrelin was not found to be diminished by the application of GHSR antagonist [D-Lys3]-GHRP-6 in DOX-induced cardiomyopathy. Although the exact mechanisms of the effect of

desacyl ghrelin on fibrosis in diabetic hearts still need to be fully elucidated, our data suggested that the cardioprotection mediated by desacyl ghrelin was, at least partly, explained by the anti-fibrotic mechanism.

Desacyl ghrelin seems to exert multiple biological functions through the activation of Akt and ERK1/2 signaling. It has been demonstrated that desacyl ghrelin stimulated the proliferation of small intestinal IEC-6 cells (Yu *et al.*, 2013), inhibition of DOX-induced apoptosis in H9c2 cardiomyocytes (Baldanzi *et al.*, 2002), and suppression of glucose-induced apoptosis in human pancreatic islet microendothelial cells (Favaro *et al.*, 2012). In our present work, the treatment of desacyl ghrelin was consistently shown to increase the phosphorylation of Akt and ERK1/2 in the heart. These changes might be important in mediating the cellular survival signaling by normalizing the suppression of Akt and ERK1/2 signaling as induced by DOX and diabetic condition. Furthermore, our results indicated that the activation of Akt signaling in DOX-induced cardiomyopathy caused by desacyl ghrelin was not affected by GHSR antagonist [D-Lys3]-GHRP-6. This further suggested that the administration of exogenous desacyl ghrelin activated Akt signaling through a GHSR-independent pathway.

6.5 Limitations and Future Direction

Acylated ghrelin plays its central and peripheral biological roles via its binding to GHSR-1a. Although the binding receptors of desacyl ghrelin have been

explored, the specific receptor for desacyl ghrelin is not yet identified. A limitation of this dissertation is the missing piece of information about the exact direct receptor-mediated mechanisms responsible for the protective effects of desacyl ghrelin on cardiomyopathy. In addition, our data indicated that the treatment of desacyl ghrelin enhanced the transcriptional expression of adiponectin in type 2 diabetic heart. It might be worth to further explore the protein expression, post-translational modification and the protein-protein interactions of adiponectin in response to desacyl ghrelin intervention in our experimental settings.

According to our microarray analysis, two gene products namely S100A8 and S100A9 were identified as the crucial genes responsible for the DOX-induced cardiotoxicity in type 2 diabetic heart. Additional investigation will be required to further reveal the pathological role of these two gene products in the the DOX-induced cardiomyopathy in the diabetic heart. Probably, these two gene products might serve to be the potential therapeutic targets for combating the DOX-induced cardiotoxicity under the diabetic condition. The detailed investigation of the precise S100A8- and S100A9-associated molecular mechanisms and signaling network in the diabetic DOX cardiotoxicity would be very valuable.

6.6 Clinical Applications

Desacyl ghrelin accounts for majority (i.e., 80-90%) of ghrelin in the

circulation (10-20% are acylated ghrelin). Desacyl ghrelin is devoid of endocrine activity such as stimulation of growth hormone release as it lacks the post-translational modification of acylation. However, given a variety of the beneficial effects of desacyl ghrelin on cardiovascular system as well as glucose and lipid metabolism, there are many potential clinical applications for desacyl ghrelin. This dissertation demonstrated that desacyl ghrelin improved cardiac contractility, apoptosis, and fibrosis in mice treated with DOX. These findings suggested that desacyl ghrelin is worth to be further explored as a potential treatment modality for the DOX-induced cardiomyopathy. For the development of ghrelin as an adjuvant regimen to protect the heart during cancer chemotherapy, it is worth to note that desacyl ghrelin might be a better choice compared to acylated ghrelin because of the cell proliferating side effects of growth hormone induced by the acylated ghrelin. By using desacyl ghrelin as the cardioprotective agent, the enhancement of the growth hormone-induced cancer cell growth could be avoided in cancer patients undergoing chemotherapy. This is the rationale why the focus of this dissertation was on desacyl ghrelin instead of acylated ghrelin.

Furthermore, in contrast to acylated ghrelin, desacyl ghrelin exerts beneficial effects on metabolism of both glucose and lipid. Desacyl ghrelin has been shown to promote glucose and free fatty acid uptake by cardiomyocytes (Lear *et al.*, 2010). Most importantly, the use of desacyl ghrelin is favorable to individuals with diabetes as desacyl ghrelin has been demonstrated to alleviate

hyperglycemia in diabetic animal induced by streptozotocin (Granata *et al.*, 2010). Decrease in insulin level, improvement of high-fat diet-induced insulin sensitivity and prevention of accumulation of fat mass have all been exhibited by the treatment of desacyl ghrelin (Delhanty *et al.*, 2013). Furthermore, desacyl ghrelin analogs have been shown to prevent the development of diabetes in streptozotocin-treated rats (Granata *et al.*, 2012) and the high-fat diet-induced metabolic syndrome in mice (Delhanty *et al.*, 2013). In clinical settings, administration of desacyl ghrelin has been shown to reverse the hyperglycemic effect of acylated ghrelin in healthy people (Broglia *et al.*, 2004). Taken together with the anti-diabetic effects of desacyl ghrelin, the findings of this dissertation reasonably propose that desacyl ghrelin to be a potential candidate that could be used for the treatment of diabetic cardiomyopathy.

Reference List

- Aasum E, Hafstad AD, Severson DL, & Larsen TS (2003). Age-dependent changes in metabolism, contractile function, and ischemic sensitivity in hearts from db/db mice. *Diabetes* **52**, 434-441.
- Al-Shabanah OA, El-Kashef HA, Badary OA, Al-Bekairi AM, & Elmazar MM (2000). Effect of streptozotocin-induced hyperglycaemia on intravenous pharmacokinetics and acute cardiotoxicity of doxorubicin in rats. *Pharmacol Res* **41**, 31-37.
- An D & Rodrigues B (2006). Role of changes in cardiac metabolism in development of diabetic cardiomyopathy. *Am J Physiol Heart Circ Physiol* **291**, H1489-H1506.
- An T, Zhang Y, Huang Y, Zhang R, Yin S, Guo X, Wang Y, Zou C, Wei B, Lv R, Zhou Q, & Zhang J (2013). Neuregulin-1 protects against doxorubicin-induced apoptosis in cardiomyocytes through an Akt-dependent pathway. *Physiol Res*.
- Aneja A, Tang WH, Bansilal S, Garcia MJ, & Farkouh ME (2008). Diabetic cardiomyopathy: insights into pathogenesis, diagnostic challenges, and therapeutic options. *Am J Med* **121**, 748-757.
- Aoki H, Nakata M, Dezaki K, Lu M, Gantulga D, Yamamoto K, Shimada K, Kario K, & Yada T (2013). Ghrelin counteracts salt-induced hypertension via promoting diuresis and renal nitric oxide production in Dahl rats. *Endocr J*.
- Arai M, Tomaru K, Takizawa T, Sekiguchi K, Yokoyama T, Suzuki T, & Nagai R (1998). Sarcoplasmic reticulum genes are selectively down-regulated in cardiomyopathy produced by doxorubicin in rabbits. *J Mol Cell Cardiol* **30**, 243-254.
- Arcamone F, Cassinelli G, Fantini G, Grein A, Orezzi P, Pol C, & Spalla C (1969). Adriamycin, 14-hydroxydaunomycin, a new antitumor antibiotic from *S. peucetius* var. *caesius*. *Biotechnol Bioeng* **11**, 1101-1110.

- Aronson D (2003). Cross-linking of glycated collagen in the pathogenesis of arterial and myocardial stiffening of aging and diabetes. *J Hypertens* **21**, 3-12.
- Arvat E, Maccario M, Di VL, Broglio F, Benso A, Gottero C, Papotti M, Muccioli G, Dieguez C, Casanueva FF, Deghenghi R, Camanni F, & Ghigo E (2001). Endocrine activities of ghrelin, a natural growth hormone secretagogue (GHS), in humans: comparison and interactions with hexarelin, a nonnatural peptidyl GHS, and GH-releasing hormone. *J Clin Endocrinol Metab* **86**, 1169-1174.
- Asbun J & Villarreal FJ (2006). The pathogenesis of myocardial fibrosis in the setting of diabetic cardiomyopathy. *J Am Coll Cardiol* **47**, 693-700.
- Avogaro A, Nosadini R, Doria A, Fioretto P, Velussi M, Vigorito C, Sacca L, Toffolo G, Cobelli C, Trevisan R, & . (1990). Myocardial metabolism in insulin-deficient diabetic humans without coronary artery disease. *Am J Physiol* **258**, E606-E618.
- Baldanzi G, Filigheddu N, Cutrupi S, Catapano F, Bonisconi S, Fubini A, Malan D, Baj G, Granata R, Broglio F, Papotti M, Surico N, Bussolino F, Isgaard J, Deghenghi R, Sinigaglia F, Prat M, Muccioli G, Ghigo E, & Graziani A (2002). Ghrelin and des-acyl ghrelin inhibit cell death in cardiomyocytes and endothelial cells through ERK1/2 and PI 3-kinase/AKT. *J Cell Biol* **159**, 1029-1037.
- Ban CR & Twigg SM (2008). Fibrosis in diabetes complications: pathogenic mechanisms and circulating and urinary markers. *Vasc Health Risk Manag* **4**, 575-596.
- Baragli A, Ghe C, Arnoletti E, Granata R, Ghigo E, & Muccioli G (2011). Acylated and unacylated ghrelin attenuate isoproterenol-induced lipolysis in isolated rat visceral adipocytes through activation of phosphoinositide 3-kinase gamma and phosphodiesterase 3B. *Biochim Biophys Acta* **1811**, 386-396.
- Barazzoni R, Bosutti A, Stebel M, Cattin MR, Roder E, Visintin L, Cattin L, Biolo G, Zanetti M, & Guarnieri G (2005a). Ghrelin regulates mitochondrial-lipid metabolism gene expression and tissue fat distribution in liver and skeletal muscle. *Am J Physiol Endocrinol Metab* **288**, E228-E235.
- Barazzoni R, Zanetti M, Ferreira C, Vinci P, Pirulli A, Mucci M, Dore F, Fonda M, Ciochi B, Cattin L, & Guarnieri G (2007). Relationships between

desacylated and acylated ghrelin and insulin sensitivity in the metabolic syndrome. *J Clin Endocrinol Metab* **92**, 3935-3940.

Barouch LA, Gao D, Chen L, Miller KL, Xu W, Phan AC, Kittleson MM, Minhas KM, Berkowitz DE, Wei C, & Hare JM (2006). Cardiac myocyte apoptosis is associated with increased DNA damage and decreased survival in murine models of obesity. *Circ Res* **98**, 119-124.

Bastard JP, Maachi M, Lagathu C, Kim MJ, Caron M, Vidal H, Capeau J, & Feve B (2006). Recent advances in the relationship between obesity, inflammation, and insulin resistance. *Eur Cytokine Netw* **17**, 4-12.

Bednarek MA, Feighner SD, Pong SS, McKee KK, Hreniuk DL, Silva MV, Warren VA, Howard AD, Van Der Ploeg LH, & Heck JV (2000). Structure-function studies on the new growth hormone-releasing peptide, ghrelin: minimal sequence of ghrelin necessary for activation of growth hormone secretagogue receptor 1a. *J Med Chem* **43**, 4370-4376.

Belke DD, Larsen TS, Gibbs EM, & Severson DL (2000a). Altered metabolism causes cardiac dysfunction in perfused hearts from diabetic (db/db) mice. *Am J Physiol Endocrinol Metab* **279**, E1104-E1113.

Belke DD, Swanson EA, & Dillmann WH (2004). Decreased sarcoplasmic reticulum activity and contractility in diabetic db/db mouse heart. *Diabetes* **53**, 3201-3208.

Ben Q, Xu M, Ning X, Liu J, Hong S, Huang W, Zhang H, & Li Z (2011). Diabetes mellitus and risk of pancreatic cancer: A meta-analysis of cohort studies. *Eur J Cancer* **47**, 1928-1937.

Berdichevski A, Meiry G, Milman F, Reiter I, Sedan O, Eliyahu S, Duffy HS, Youdim MB, & Binah O (2010). TVP1022 protects neonatal rat ventricular myocytes against doxorubicin-induced functional derangements. *J Pharmacol Exp Ther* **332**, 413-420.

Berg AH & Scherer PE (2005). Adipose tissue, inflammation, and cardiovascular disease. *Circ Res* **96**, 939-949.

Bers DM (2002). Cardiac excitation-contraction coupling. *Nature* **415**, 198-205.

Bertoni AG, Tsai A, Kasper EK, & Brancati FL (2003). Diabetes and idiopathic cardiomyopathy: a nationwide case-control study. *Diabetes Care* **26**, 2791-2795.

Bonen A, Campbell SE, Benton CR, Chabowski A, Coort SL, Han XX, Koonen DP, Glatz JF, & Luiken JJ (2004). Regulation of fatty acid transport by fatty acid translocase/CD36. *Proc Nutr Soc* **63**, 245-249.

Bordoni A, Biagi P, & Hrelia S (1999). The impairment of essential fatty acid metabolism as a key factor in doxorubicin-induced damage in cultured rat cardiomyocytes. *Biochim Biophys Acta* **1440**, 100-106.

Borges GR, de OM, Salgado HC, & Fazan R, Jr. (2006). Myocardial performance in conscious streptozotocin diabetic rats. *Cardiovasc Diabetol* **5**, 26.

Boudina S, Sena S, Theobald H, Sheng X, Wright JJ, Hu XX, Aziz S, Johnson JI, Bugger H, Zaha VG, & Abel ED (2007). Mitochondrial energetics in the heart in obesity-related diabetes: direct evidence for increased uncoupled respiration and activation of uncoupling proteins. *Diabetes* **56**, 2457-2466.

Broglio F, Arvat E, Benso A, Gottero C, Muccioli G, Papotti M, van der Lely AJ, Deghenghi R, & Ghigo E (2001). Ghrelin, a natural GH secretagogue produced by the stomach, induces hyperglycemia and reduces insulin secretion in humans. *J Clin Endocrinol Metab* **86**, 5083-5086.

Broglio F, Gottero C, Benso A, Prodam F, Destefanis S, Gauna C, Maccario M, Deghenghi R, van der Lely AJ, & Ghigo E (2003). Effects of ghrelin on the insulin and glycemic responses to glucose, arginine, or free fatty acids load in humans. *J Clin Endocrinol Metab* **88**, 4268-4272.

Broglio F, Gottero C, Prodam F, Gauna C, Muccioli G, Papotti M, Abribat T, Van Der Lely AJ, & Ghigo E (2004). Non-acylated ghrelin counteracts the metabolic but not the neuroendocrine response to acylated ghrelin in humans. *J Clin Endocrinol Metab* **89**, 3062-3065.

Bruchim I, Attias Z, & Werner H (2009). Targeting the IGF1 axis in cancer proliferation. *Expert Opin Ther Targets* **13**, 1179-1192.

Cai L & Kang YJ (2003). Cell death and diabetic cardiomyopathy. *Cardiovasc Toxicol* **3**, 219-228.

Cai L, Li W, Wang G, Guo L, Jiang Y, & Kang YJ (2002). Hyperglycemia-induced apoptosis in mouse myocardium: mitochondrial cytochrome C-mediated caspase-3 activation pathway. *Diabetes* **51**, 1938-1948.

Cai L, Wang Y, Zhou G, Chen T, Song Y, Li X, & Kang YJ (2006). Attenuation by metallothionein of early cardiac cell death via suppression of mitochondrial oxidative stress results in a prevention of diabetic cardiomyopathy. *J Am Coll Cardiol* **48**, 1688-1697.

Caligiuri A, Bertolani C, Guerra CT, Aleffi S, Galastri S, Trappoliere M, Vizzutti F, Gelmini S, Laffi G, Pinzani M, & Marra F (2008). Adenosine monophosphate-activated protein kinase modulates the activated phenotype of hepatic stellate cells. *Hepatology* **47**, 668-676.

Camina JP (2006). Cell biology of the ghrelin receptor. *J Neuroendocrinol* **18**, 65-76.

Cannata D, Fierz Y, Vijayakumar A, & LeRoith D (2010). Type 2 diabetes and cancer: what is the connection? *Mt Sinai J Med* **77**, 197-213.

Carley AN & Severson DL (2005). Fatty acid metabolism is enhanced in type 2 diabetic hearts. *Biochim Biophys Acta* **1734**, 112-126.

Carvalho RA, Sousa RP, Cadete VJ, Lopaschuk GD, Palmeira CM, Bjork JA, & Wallace KB (2010). Metabolic remodeling associated with subchronic doxorubicin cardiomyopathy. *Toxicology* **270**, 92-98.

Chang L, Ren Y, Liu X, Li WG, Yang J, Geng B, Weintraub NL, & Tang C (2004). Protective effects of ghrelin on ischemia/reperfusion injury in the isolated rat heart. *J Cardiovasc Pharmacol* **43**, 165-170.

Chappell J, Leitner JW, Solomon S, Golovchenko I, Goalstone ML, & Draznin B (2001). Effect of insulin on cell cycle progression in MCF-7 breast cancer cells. Direct and potentiating influence. *J Biol Chem* **276**, 38023-38028.

Chavali V, Tyagi SC, & Mishra PK (2013). Predictors and prevention of diabetic cardiomyopathy. *Diabetes Metab Syndr Obes* **6**, 151-160.

Chen MM, Lam A, Abraham JA, Schreiner GF, & Joly AH (2000a). CTGF expression is induced by TGF- β in cardiac fibroblasts and cardiac myocytes: a potential role in heart fibrosis. *J Mol Cell Cardiol* **32**, 1805-1819.

Chen S, Evans T, Mukherjee K, Karmazyn M, & Chakrabarti S (2000b). Diabetes-induced myocardial structural changes: role of endothelin-1 and its receptors. *J Mol Cell Cardiol* **32**, 1621-1629.

Chen X, Chen Y, Bi Y, Fu N, Shan C, Wang S, Aslam S, Wang PW, & Xu J (2007). Preventive cardioprotection of erythropoietin against doxorubicin-induced cardiomyopathy. *Cardiovasc Drugs Ther* **21**, 367-374.

Chicco AJ, Hydock DS, Schneider CM, & Hayward R (2006). Low-intensity exercise training during doxorubicin treatment protects against cardiotoxicity. *J Appl Physiol* **100**, 519-527.

Childs AC, Phaneuf SL, Dirks AJ, Phillips T, & Leeuwenburgh C (2002). Doxorubicin treatment in vivo causes cytochrome C release and cardiomyocyte apoptosis, as well as increased mitochondrial efficiency, superoxide dismutase activity, and Bcl-2:Bax ratio. *Cancer Res* **62**, 4592-4598.

Chiong M, Wang ZV, Pedrozo Z, Cao DJ, Troncoso R, Ibacache M, Criollo A, Nemchenko A, Hill JA, & Lavandero S (2011). Cardiomyocyte death: mechanisms and translational implications. *Cell Death Dis* **2**, e244.

Chiu HC, Kovacs A, Blanton RM, Han X, Courtois M, Weinheimer CJ, Yamada KA, Brunet S, Xu H, Nerbonne JM, Welch MJ, Fettig NM, Sharp TL, Sambandam N, Olson KM, Ory DS, & Schaffer JE (2005). Transgenic expression of fatty acid transport protein 1 in the heart causes lipotoxic cardiomyopathy. *Circ Res* **96**, 225-233.

Chiu HC, Kovacs A, Ford DA, Hsu FF, Garcia R, Herrero P, Saffitz JE, & Schaffer JE (2001). A novel mouse model of lipotoxic cardiomyopathy. *J Clin Invest* **107**, 813-822.

Choi EH, Lee N, Kim HJ, Kim MK, Chi SG, Kwon DY, & Chun HS (2008). Schisandra fructus extract ameliorates doxorubicin-induced cytotoxicity in

cardiomyocytes: altered gene expression for detoxification enzymes. *Genes Nutr* **2**, 337-345.

Chung H, Kim E, Lee DH, Seo S, Ju S, Lee D, Kim H, & Park S (2007). Ghrelin inhibits apoptosis in hypothalamic neuronal cells during oxygen-glucose deprivation. *Endocrinology* **148**, 148-159.

Coughlin SS, Calle EE, Teras LR, Petrelli J, & Thun MJ (2004). Diabetes mellitus as a predictor of cancer mortality in a large cohort of US adults. *Am J Epidemiol* **159**, 1160-1167.

Cowley MA, Smith RG, Diano S, Tschop M, Pronchuk N, Grove KL, Strasburger CJ, Bidlingmaier M, Esterman M, Heiman ML, Garcia-Segura LM, Nillni EA, Mendez P, Low MJ, Sotonyi P, Friedman JM, Liu H, Pinto S, Colmers WF, Cone RD, & Horvath TL (2003). The distribution and mechanism of action of ghrelin in the CNS demonstrates a novel hypothalamic circuit regulating energy homeostasis. *Neuron* **37**, 649-661.

Craig VJ, Quintero PA, Fyfe SE, Patel AS, Knolle MD, Kobzik L, & Owen CA (2013). Profibrotic activities for matrix metalloproteinase-8 during bleomycin-mediated lung injury. *J Immunol* **190**, 4283-4296.

Craven PA, Davidson CM, & DeRubertis FR (1990). Increase in diacylglycerol mass in isolated glomeruli by glucose from de novo synthesis of glycerolipids. *Diabetes* **39**, 667-674.

Date Y, Murakami N, Kojima M, Kuroiwa T, Matsukura S, Kangawa K, & Nakazato M (2000). Central effects of a novel acylated peptide, ghrelin, on growth hormone release in rats. *Biochem Biophys Res Commun* **275**, 477-480.

de Bakker JM, van Capelle FJ, Janse MJ, Tasseron S, Vermeulen JT, de JN, & Lahpor JR (1996). Fractionated electrograms in dilated cardiomyopathy: origin and relation to abnormal conduction. *J Am Coll Cardiol* **27**, 1071-1078.

De VC & Delporte C (2008). Ghrelin: a new peptide regulating growth hormone release and food intake. *Int J Biochem Cell Biol* **40**, 1420-1424.

Delhanty PJ, Huisman M, Baldeon-Rojas LY, van dB, I, Grefhorst A, Aribat T, Leenen PJ, Themmen AP, & van der Lely AJ (2013). Des-acyl ghrelin analogs

prevent high-fat-diet-induced dysregulation of glucose homeostasis. *FASEB J* **27**, 1690-1700.

Delhanty PJ, Neggers SJ, & van der Lely AJ (2012). Mechanisms in endocrinology: Ghrelin: the differences between acyl- and des-acyl ghrelin. *Eur J Endocrinol* **167**, 601-608.

Delhanty PJ, Sun Y, Visser JA, van KA, Huisman M, van Ijcken WF, Swagemakers S, Smith RG, Themmen AP, & van der Lely AJ (2010). Unacylated ghrelin rapidly modulates lipogenic and insulin signaling pathway gene expression in metabolically active tissues of GHSR deleted mice. *PLoS One* **5**, e11749.

Dittoe N, Stultz D, Schwartz BP, & Hahn HS (2007). Quantitative left ventricular systolic function: from chamber to myocardium. *Crit Care Med* **35**, S330-S339.

Diwan A, Wansapura J, Syed FM, Matkovich SJ, Lorenz JN, & Dorn GW (2008). Nix-mediated apoptosis links myocardial fibrosis, cardiac remodeling, and hypertrophy decompensation. *Circulation* **117**, 396-404.

Dodos F, Halbsguth T, Erdmann E, & Hoppe UC (2008). Usefulness of myocardial performance index and biochemical markers for early detection of anthracycline-induced cardiotoxicity in adults. *Clin Res Cardiol* **97**, 318-326.

Dyntar D, Eppenberger-Eberhardt M, Maedler K, Pruschy M, Eppenberger HM, Spinass GA, & Donath MY (2001). Glucose and palmitic acid induce degeneration of myofibrils and modulate apoptosis in rat adult cardiomyocytes. *Diabetes* **50**, 2105-2113.

Eckel J & Reinauer H (1990). Insulin action on glucose transport in isolated cardiac myocytes: signalling pathways and diabetes-induced alterations. *Biochem Soc Trans* **18**, 1125-1127.

Egido EM, Rodriguez-Gallardo J, Silvestre RA, & Marco J (2002). Inhibitory effect of ghrelin on insulin and pancreatic somatostatin secretion. *Eur J Endocrinol* **146**, 241-244.

El MS, Rongen GA, & Riksen NP (2013). Metformin therapy in diabetes: the role of cardioprotection. *Curr Atheroscler Rep* **15**, 314.

El-Shehaby AM, El-Khatib MM, Battah AA, & Roshdy AR (2010). Apelin: a potential link between inflammation and cardiovascular disease in end stage renal disease patients. *Scand J Clin Lab Invest* **70**, 421-427.

Essick EE, Ouchi N, Wilson RM, Ohashi K, Ghobrial J, Shibata R, Pimentel DR, & Sam F (2011). Adiponectin mediates cardioprotection in oxidative stress-induced cardiac myocyte remodeling. *Am J Physiol Heart Circ Physiol* **301**, H984-H993.

Fang F, Liu L, Yang Y, Tamaki Z, Wei J, Marangoni RG, Bhattacharyya S, Summer RS, Ye B, & Varga J (2012). The adipokine adiponectin has potent anti-fibrotic effects mediated via adenosine monophosphate-activated protein kinase: novel target for fibrosis therapy. *Arthritis Res Ther* **14**, R229.

Favaro E, Granata R, Miceli I, Baragli A, Settanni F, Cavallo PP, Ghigo E, Camussi G, & Zanone MM (2012). The ghrelin gene products and exendin-4 promote survival of human pancreatic islet endothelial cells in hyperglycaemic conditions, through phosphoinositide 3-kinase/Akt, extracellular signal-related kinase (ERK)1/2 and cAMP/protein kinase A (PKA) signalling pathways. *Diabetologia* **55**, 1058-1070.

Feridooni T, Hotchkiss A, Remley-Carr S, Saga Y, & Pasumarthi KB (2011). Cardiomyocyte specific ablation of p53 is not sufficient to block doxorubicin induced cardiac fibrosis and associated cytoskeletal changes. *PLoS One* **6**, e22801.

Finck BN, Lehman JJ, Leone TC, Welch MJ, Bennett MJ, Kovacs A, Han X, Gross RW, Kozak R, Lopaschuk GD, & Kelly DP (2002). The cardiac phenotype induced by PPARalpha overexpression mimics that caused by diabetes mellitus. *J Clin Invest* **109**, 121-130.

Fiordaliso F, Li B, Latini R, Sonnenblick EH, Anversa P, Leri A, & Kajstura J (2000). Myocyte death in streptozotocin-induced diabetes in rats in angiotensin II- dependent. *Lab Invest* **80**, 513-527.

Floyd JD, Nguyen DT, Lobins RL, Bashir Q, Doll DC, & Perry MC (2005). Cardiotoxicity of cancer therapy. *J Clin Oncol* **23**, 7685-7696.

Forcheron F, Basset A, Abdallah P, Del CP, Gadot N, & Beylot M (2009). Diabetic cardiomyopathy: effects of fenofibrate and metformin in an experimental model--the Zucker diabetic rat. *Cardiovasc Diabetol* **8**, 16.

Frascarelli S, Ghelardoni S, Ronca-Testoni S, & Zucchi R (2003). Effect of ghrelin and synthetic growth hormone secretagogues in normal and ischemic rat heart. *Basic Res Cardiol* **98**, 401-405.

Frustaci A, Kajstura J, Chimenti C, Jakoniuk I, Leri A, Maseri A, Nadal-Ginard B, & Anversa P (2000). Myocardial cell death in human diabetes. *Circ Res* **87**, 1123-1132.

Fujita K, Maeda N, Sonoda M, Ohashi K, Hibuse T, Nishizawa H, Nishida M, Hiuge A, Kurata A, Kihara S, Shimomura I, & Funahashi T (2008). Adiponectin protects against angiotensin II-induced cardiac fibrosis through activation of PPAR-alpha. *Arterioscler Thromb Vasc Biol* **28**, 863-870.

Gambliel HA, Burke BE, Cusack BJ, Walsh GM, Zhang YL, Mushlin PS, & Olson RD (2002). Doxorubicin and C-13 deoxydoxorubicin effects on ryanodine receptor gene expression. *Biochem Biophys Res Commun* **291**, 433-438.

Garcia EA & Korbonits M (2006). Ghrelin and cardiovascular health. *Curr Opin Pharmacol* **6**, 142-147.

Gauna C, Delhanty PJ, Hofland LJ, Janssen JA, Broglio F, Ross RJ, Ghigo E, & van der Lely AJ (2005). Ghrelin stimulates, whereas des-octanoyl ghrelin inhibits, glucose output by primary hepatocytes. *J Clin Endocrinol Metab* **90**, 1055-1060.

Gauna C, Kiewiet RM, Janssen JA, van de ZB, Delhanty PJ, Ghigo E, Hofland LJ, Themmen AP, & van der Lely AJ (2007). Unacylated ghrelin acts as a potent insulin secretagogue in glucose-stimulated conditions. *Am J Physiol Endocrinol Metab* **293**, E697-E704.

Gauna C, Meyler FM, Janssen JA, Delhanty PJ, Abribat T, van KP, Hofland LJ, Broglio F, Ghigo E, & van der Lely AJ (2004). Administration of acylated ghrelin reduces insulin sensitivity, whereas the combination of acylated plus unacylated ghrelin strongly improves insulin sensitivity. *J Clin Endocrinol Metab* **89**, 5035-5042.

Geraldes P & King GL (2010). Activation of protein kinase C isoforms and its impact on diabetic complications. *Circ Res* **106**, 1319-1331.

Giovannucci E (1995). Insulin and colon cancer. *Cancer Causes Control* **6**, 164-179.

Giovannucci E, Harlan DM, Archer MC, Bergenstal RM, Gapstur SM, Habel LA, Pollak M, Regensteiner JG, & Yee D (2010). Diabetes and cancer: a consensus report. *Diabetes Care* **33**, 1674-1685.

Glatz JF, Luiken JJ, & Bonen A (2010). Membrane fatty acid transporters as regulators of lipid metabolism: implications for metabolic disease. *Physiol Rev* **90**, 367-417.

Glenn DJ, Wang F, Nishimoto M, Cruz MC, Uchida Y, Holleran WM, Zhang Y, Yeghiazarians Y, & Gardner DG (2011). A murine model of isolated cardiac steatosis leads to cardiomyopathy. *Hypertension* **57**, 216-222.

Gnanapavan S, Kola B, Bustin SA, Morris DG, McGee P, Fairclough P, Bhattacharya S, Carpenter R, Grossman AB, & Korbonits M (2002). The tissue distribution of the mRNA of ghrelin and subtypes of its receptor, GHS-R, in humans. *J Clin Endocrinol Metab* **87**, 2988.

Gonzalez A, Fortuno MA, Querejeta R, Ravassa S, Lopez B, Lopez N, & Diez J (2003). Cardiomyocyte apoptosis in hypertensive cardiomyopathy. *Cardiovasc Res* **59**, 549-562.

Gottlieb RA & Mentzer RM, Jr. (2012). Autophagy: an affair of the heart. *Heart Fail Rev*.

Granado M, Chowen JA, Garcia-Caceres C, gado-Rubin A, Barrios V, Castellero E, Argente J, & Frago LM (2009). Ghrelin treatment protects lactotrophs from apoptosis in the pituitary of diabetic rats. *Mol Cell Endocrinol* **309**, 67-75.

Granata R, Settanni F, Julien M, Nano R, Togliatto G, Trombetta A, Gallo D, Piemonti L, Brizzi MF, Abribat T, van Der Lely AJ, & Ghigo E (2012). Des-acyl ghrelin fragments and analogues promote survival of pancreatic beta-cells and human pancreatic islets and prevent diabetes in streptozotocin-treated rats. *J Med Chem* **55**, 2585-2596.

Granata R, Volante M, Settanni F, Gauna C, Ghe C, Annunziata M, Deidda B, Gesmundo I, Abribat T, van der Lely AJ, Muccioli G, Ghigo E, & Papotti M

(2010). Unacylated ghrelin and obestatin increase islet cell mass and prevent diabetes in streptozotocin-treated newborn rats. *J Mol Endocrinol* **45**, 9-17.

Gunja-Smith Z, Morales AR, Romanelli R, & Woessner JF, Jr. (1996). Remodeling of human myocardial collagen in idiopathic dilated cardiomyopathy. Role of metalloproteinases and pyridinoline cross-links. *Am J Pathol* **148**, 1639-1648.

Hardefeldt PJ, Edirimanne S, & Eslick GD (2012). Diabetes increases the risk of breast cancer: a meta-analysis. *Endocr Relat Cancer* **19**, 793-803.

Harvey PA & Leinwand LA (2011). The cell biology of disease: cellular mechanisms of cardiomyopathy. *J Cell Biol* **194**, 355-365.

Hataya Y, Akamizu T, Takaya K, Kanamoto N, Ariyasu H, Saijo M, Moriyama K, Shimatsu A, Kojima M, Kangawa K, & Nakao K (2001). A low dose of ghrelin stimulates growth hormone (GH) release synergistically with GH-releasing hormone in humans. *J Clin Endocrinol Metab* **86**, 4552.

Heon S, Bernier M, Servant N, Dostanic S, Wang C, Kirby GM, Alpert L, & Chalifour LE (2003). Dexrazoxane does not protect against doxorubicin-induced damage in young rats. *Am J Physiol Heart Circ Physiol* **285**, H499-H506.

Holmes A, Abraham DJ, Sa S, Shiwen X, Black CM, & Leask A (2001). CTGF and SMADs, maintenance of scleroderma phenotype is independent of SMAD signaling. *J Biol Chem* **276**, 10594-10601.

Hong YM, Kim HS, & Yoon HR (2002). Serum lipid and fatty acid profiles in adriamycin-treated rats after administration of L-carnitine. *Pediatr Res* **51**, 249-255.

Hosoda H, Kojima M, Mizushima T, Shimizu S, & Kangawa K (2003). Structural divergence of human ghrelin. Identification of multiple ghrelin-derived molecules produced by post-translational processing. *J Biol Chem* **278**, 64-70.

Hotta K, Funahashi T, Arita Y, Takahashi M, Matsuda M, Okamoto Y, Iwahashi H, Kuriyama H, Ouchi N, Maeda K, Nishida M, Kihara S, Sakai N, Nakajima T, Hasegawa K, Muraguchi M, Ohmoto Y, Nakamura T, Yamashita

- S, Hanafusa T, & Matsuzawa Y (2000). Plasma concentrations of a novel, adipose-specific protein, adiponectin, in type 2 diabetic patients. *Arterioscler Thromb Vasc Biol* **20**, 1595-1599.
- Hu FB, Manson JE, Liu S, Hunter D, Colditz GA, Michels KB, Speizer FE, & Giovannucci E (1999). Prospective study of adult onset diabetes mellitus (type 2) and risk of colorectal cancer in women. *J Natl Cancer Inst* **91**, 542-547.
- Huang CX, Yuan MJ, Huang H, Wu G, Liu Y, Yu SB, Li HT, & Wang T (2009). Ghrelin inhibits post-infarct myocardial remodeling and improves cardiac function through anti-inflammation effect. *Peptides* **30**, 2286-2291.
- Huang XM, Zhu WH, & Kang ML (2003). Study on the effect of doxorubicin on expressions of genes encoding myocardial sarcoplasmic reticulum Ca²⁺-transport proteins and the effect of taurine on myocardial protection in rabbits. *J Zhejiang Univ Sci* **4**, 114-120.
- Huxley R, nsary-Moghaddam A, Berrington de GA, Barzi F, & Woodward M (2005). Type-II diabetes and pancreatic cancer: a meta-analysis of 36 studies. *Br J Cancer* **92**, 2076-2083.
- Huynh K, Kiriazis H, Du XJ, Love JE, Jandeleit-Dahm KA, Forbes JM, McMullen JR, & Ritchie RH (2012). Coenzyme Q10 attenuates diastolic dysfunction, cardiomyocyte hypertrophy and cardiac fibrosis in the db/db mouse model of type 2 diabetes. *Diabetologia* **55**, 1544-1553.
- Hwang JM, Wu CH, Kuo WW, Jong GP, Lai CH, Tsai CH, Tsai FJ, Chang MH, Wu JP, & Huang CY (2012). Pro-inflammation and pro-fibrosis factors were highly induction in heart tissues of carotid arteries balloon-injured animal model. *Cell Biochem Funct*.
- Iglesias MJ, Pineiro R, Blanco M, Gallego R, Dieguez C, Gualillo O, Gonzalez-Juanatey JR, & Lago F (2004). Growth hormone releasing peptide (ghrelin) is synthesized and secreted by cardiomyocytes. *Cardiovasc Res* **62**, 481-488.
- Imazu Y, Yanagi S, Miyoshi K, Tsubouchi H, Yamashita S, Matsumoto N, Ashitani J, Kangawa K, & Nakazato M (2011). Ghrelin ameliorates bleomycin-induced acute lung injury by protecting alveolar epithelial cells and suppressing lung inflammation. *Eur J Pharmacol* **672**, 153-158.

Inoguchi T, Battan R, Handler E, Sportsman JR, Heath W, & King GL (1992). Preferential elevation of protein kinase C isoform beta II and diacylglycerol levels in the aorta and heart of diabetic rats: differential reversibility to glycemic control by islet cell transplantation. *Proc Natl Acad Sci U S A* **89**, 11059-11063.

Iseri SO, Sener G, Saglam B, Ercan F, Gedik N, & Yegen BC (2008). Ghrelin alleviates biliary obstruction-induced chronic hepatic injury in rats. *Regul Pept* **146**, 73-79.

Isgaard J & Johansson I (2005). Ghrelin and GHS on cardiovascular applications/functions. *J Endocrinol Invest* **28**, 838-842.

Jenke A, Wilk S, Poller W, Eriksson U, Valaperti A, Rauch BH, Stroux A, Liu P, Schultheiss HP, Scheibenbogen C, & Skurk C (2013). Adiponectin protects against Toll-like receptor 4 mediated cardiac inflammation and injury. *Cardiovasc Res*.

Jiji RS, Kramer CM, & Salerno M (2012). Non-invasive imaging and monitoring cardiotoxicity of cancer therapeutic drugs. *J Nucl Cardiol* **19**, 377-388.

Kalivendi SV, Kotamraju S, Zhao H, Joseph J, & Kalyanaraman B (2001). Doxorubicin-induced apoptosis is associated with increased transcription of endothelial nitric-oxide synthase. Effect of antiapoptotic antioxidants and calcium. *J Biol Chem* **276**, 47266-47276.

Kalyanaraman B, Joseph J, Kalivendi S, Wang S, Konorev E, & Kotamraju S (2002). Doxorubicin-induced apoptosis: implications in cardiotoxicity. *Mol Cell Biochem* **234-235**, 119-124.

Kamegai J, Tamura H, Shimizu T, Ishii S, Sugihara H, & Wakabayashi I (2001). Chronic central infusion of ghrelin increases hypothalamic neuropeptide Y and Agouti-related protein mRNA levels and body weight in rats. *Diabetes* **50**, 2438-2443.

Kanamoto N, Akamizu T, Tagami T, Hataya Y, Moriyama K, Takaya K, Hosoda H, Kojima M, Kangawa K, & Nakao K (2004). Genomic structure and characterization of the 5'-flanking region of the human ghrelin gene. *Endocrinology* **145**, 4144-4153.

Kankaanpää M, Lehto HR, Parkka JP, Komu M, Viljanen A, Ferrannini E, Knuuti J, Nuutila P, Parkkola R, & Iozzo P (2006). Myocardial triglyceride content and epicardial fat mass in human obesity: relationship to left ventricular function and serum free fatty acid levels. *J Clin Endocrinol Metab* **91**, 4689-4695.

Kannel WB & McGee DL (1979). Diabetes and cardiovascular disease. The Framingham study. *JAMA* **241**, 2035-2038.

Kawamura T, Hasegawa K, Morimoto T, Iwai-Kanai E, Miyamoto S, Kawase Y, Ono K, Wada H, Akao M, & Kita T (2004). Expression of p300 protects cardiac myocytes from apoptosis in vivo. *Biochem Biophys Res Commun* **315**, 733-738.

Khan R & Sheppard R (2006). Fibrosis in heart disease: understanding the role of transforming growth factor-beta in cardiomyopathy, valvular disease and arrhythmia. *Immunology* **118**, 10-24.

Khatwa UA, Kleibrink BE, Shapiro SD, & Subramaniam M (2010). MMP-8 promotes polymorphonuclear cell migration through collagen barriers in obliterative bronchiolitis. *J Leukoc Biol* **87**, 69-77.

Kiencke S, Handschin R, von DR, Muser J, Brunner-Larocca HP, Schumann J, Felix B, Berneis K, & Rickenbacher P (2010). Pre-clinical diabetic cardiomyopathy: prevalence, screening, and outcome. *Eur J Heart Fail* **12**, 951-957.

Kikuchi A, Yamamoto H, Sato A, & Matsumoto S (2012). Wnt5a: its signalling, functions and implication in diseases. *Acta Physiol (Oxf)* **204**, 17-33.

Kim SW, Her SJ, Park SJ, Kim D, Park KS, Lee HK, Han BH, Kim MS, Shin CS, & Kim SY (2005). Ghrelin stimulates proliferation and differentiation and inhibits apoptosis in osteoblastic MC3T3-E1 cells. *Bone* **37**, 359-369.

Klein MJ, Maguire JJ, Skepper JN, & Davenport AP (2006). Functional and immunocytochemical evidence for a role of ghrelin and des-octanoyl ghrelin in the regulation of vascular tone in man. *Cardiovasc Res* **69**, 227-235.

Kobashi M, Yanagihara M, Fujita M, Mitoh Y, & Matsuo R (2009). Fourth ventricular administration of ghrelin induces relaxation of the proximal stomach in the rat. *Am J Physiol Regul Integr Comp Physiol* **296**, R217-R223.

Koitabashi N, Arai M, Kogure S, Niwano K, Watanabe A, Aoki Y, Maeno T, Nishida T, Kubota S, Takigawa M, & Kurabayashi M (2007). Increased connective tissue growth factor relative to brain natriuretic peptide as a determinant of myocardial fibrosis. *Hypertension* **49**, 1120-1127.

Kojima M, Hosoda H, Date Y, Nakazato M, Matsuo H, & Kangawa K (1999). Ghrelin is a growth-hormone-releasing acylated peptide from stomach. *Nature* **402**, 656-660.

Kojima M & Kangawa K (2005). Ghrelin: structure and function. *Physiol Rev* **85**, 495-522.

Konishi M, Haraguchi G, Ohigashi H, Ishihara T, Saito K, Nakano Y, & Isobe M (2011). Adiponectin protects against doxorubicin-induced cardiomyopathy by anti-apoptotic effects through AMPK up-regulation. *Cardiovasc Res* **89**, 309-319.

Kui L, Weiwei Z, Ling L, Daikun H, Guoming Z, Linuo Z, & Renming H (2009). Ghrelin inhibits apoptosis induced by high glucose and sodium palmitate in adult rat cardiomyocytes through the PI3K-Akt signaling pathway. *Regul Pept* **155**, 62-69.

Kuramoto H, Hongo A, Liu YX, Ojima Y, Nakamura K, Seki N, Kodama J, & Hiramatsu Y (2008). Immunohistochemical evaluation of insulin-like growth factor I receptor status in cervical cancer specimens. *Acta Med Okayama* **62**, 251-259.

Lang RM, Bierig M, Devereux RB, Flachskampf FA, Foster E, Pellikka PA, Picard MH, Roman MJ, Seward J, Shanewise J, Solomon S, Spencer KT, St John SM, & Stewart W (2006). Recommendations for chamber quantification. *Eur J Echocardiogr* **7**, 79-108.

Larsson SC, Mantzoros CS, & Wolk A (2007). Diabetes mellitus and risk of breast cancer: a meta-analysis. *Int J Cancer* **121**, 856-862.

Lear PV, Iglesias MJ, Feijoo-Bandin S, Rodriguez-Penas D, Mosquera-Leal A, Garcia-Rua V, Gualillo O, Ghe C, Arnoletti E, Muccioli G, Dieguez C, Gonzalez-Juanatey JR, & Lago F (2010). Des-acyl ghrelin has specific binding sites and different metabolic effects from ghrelin in cardiomyocytes. *Endocrinology* **151**, 3286-3298.

Leask A (2010). Potential therapeutic targets for cardiac fibrosis: TGFbeta, angiotensin, endothelin, CCN2, and PDGF, partners in fibroblast activation. *Circ Res* **106**, 1675-1680.

Lee JY, Oh TH, & Yune TY (2011). Ghrelin inhibits hydrogen peroxide-induced apoptotic cell death of oligodendrocytes via ERK and p38MAPK signaling. *Endocrinology* **152**, 2377-2386.

Lee Y, Hong Y, Lee SR, Chang KT, & Hong Y (2012). Autophagy contributes to retardation of cardiac growth in diabetic rats. *Lab Anim Res* **28**, 99-107.

Lefrak EA, Pitha J, Rosenheim S, & Gottlieb JA (1973b). A clinicopathologic analysis of adriamycin cardiotoxicity. *Cancer* **32**, 302-314.

Leite-Moreira AF & Soares JB (2007). Physiological, pathological and potential therapeutic roles of ghrelin. *Drug Discov Today* **12**, 276-288.

Lewin TM, de JH, Schwerbrock NJ, Hammond LE, Watkins SM, Combs TP, & Coleman RA (2008). Mice deficient in mitochondrial glycerol-3-phosphate acyltransferase-1 have diminished myocardial triacylglycerol accumulation during lipogenic diet and altered phospholipid fatty acid composition. *Biochim Biophys Acta* **1781**, 352-358.

Li D, Tang H, Hassan MM, Holly EA, Bracci PM, & Silverman DT (2011). Diabetes and risk of pancreatic cancer: a pooled analysis of three large case-control studies. *Cancer Causes Control* **22**, 189-197.

Li L, Takemura G, Li Y, Miyata S, Esaki M, Okada H, Kanamori H, Ogino A, Maruyama R, Nakagawa M, Minatoguchi S, Fujiwara T, & Fujiwara H (2007). Granulocyte colony-stimulating factor improves left ventricular function of doxorubicin-induced cardiomyopathy. *Lab Invest* **87**, 440-455.

Li L, Zhang LK, Pang YZ, Pan CS, Qi YF, Chen L, Wang X, Tang CS, & Zhang J (2006). Cardioprotective effects of ghrelin and des-octanoyl ghrelin on

myocardial injury induced by isoproterenol in rats. *Acta Pharmacol Sin* **27**, 527-535.

Liu TJ, Yeh YC, Ting CT, Lee WL, Wang LC, Lee HW, Wang KY, Lai HC, & Lai HC (2008). Ginkgo biloba extract 761 reduces doxorubicin-induced apoptotic damage in rat hearts and neonatal cardiomyocytes. *Cardiovasc Res* **80**, 227-235.

Liu X, Hu H, & Yin JQ (2006). Therapeutic strategies against TGF-beta signaling pathway in hepatic fibrosis. *Liver Int* **26**, 8-22.

Loegering DJ & Lennartz MR (2011). Protein kinase C and toll-like receptor signaling. *Enzyme Res* **2011**, 537821.

Lu YC, Wang CP, Hsu CC, Chiu CA, Yu TH, Hung WC, Lu LF, Chung FM, Tsai IT, Lin HC, & Lee YJ (2013). Circulating secreted frizzled-related protein 5 and wingless-type MMTV integration site family member 5a levels in patients with type 2 diabetes mellitus. *Diabetes Metab Res Rev*.

Luo W, Cao Y, Liao C, & Gao F (2012). Diabetes mellitus and the incidence and mortality of colorectal cancer: a meta-analysis of 24 cohort studies. *Colorectal Dis* **14**, 1307-1312.

Ma LP, Haugen E, Ikemoto M, Fujita M, Terasaki F, & Fu M (2012a). S100A8/A9 complex as a new biomarker in prediction of mortality in elderly patients with severe heart failure. *Int J Cardiol* **155**, 26-32.

Ma Y, Zhang L, Edwards JN, Launikonis BS, & Chen C (2012b). Growth hormone secretagogues protect mouse cardiomyocytes from in vitro ischemia/reperfusion injury through regulation of intracellular calcium. *PLoS One* **7**, e35265.

Mao Y, Tokudome T, Otani K, Kishimoto I, Nakanishi M, Hosoda H, Miyazato M, & Kangawa K (2012). Ghrelin prevents incidence of malignant arrhythmia after acute myocardial infarction through vagal afferent nerves. *Endocrinology* **153**, 3426-3434.

Marsh SA, Powell PC, Dell'italia LJ, & Chatham JC (2013). Cardiac O-GlcNAcylation blunts autophagic signaling in the diabetic heart. *Life Sci* **92**, 648-656.

Matsudo Y, Takamori Y, Fujimura L, Nishio S, Sasagawa K, Komuro I, Tokuhisa T, & Hatano M (2006). Overexpression of Nd1, a novel Kelch family protein, in the heart of transgenic mice protects against doxorubicin-induced cardiomyopathy. *Transgenic Res* **15**, 573-581.

Maya L & Villarreal FJ (2010). Diagnostic approaches for diabetic cardiomyopathy and myocardial fibrosis. *J Mol Cell Cardiol* **48**, 524-529.

McCaffrey TA, Tziros C, Lewis J, Katz R, Siegel R, Weglicki W, Kramer J, Mak IT, Toma I, Chen L, Benas E, Lowitt A, Rao S, Witkin L, Lian Y, Lai Y, Yang Z, & Fu SW (2013). Genomic Profiling Reveals the Potential Role of TCL1A and MDR1 Deficiency in Chemotherapy-Induced Cardiotoxicity. *Int J Biol Sci* **9**, 350-360.

Mellor KM, Bell JR, Young MJ, Ritchie RH, & Delbridge LM (2011). Myocardial autophagy activation and suppressed survival signaling is associated with insulin resistance in fructose-fed mice. *J Mol Cell Cardiol* **50**, 1035-1043.

Mewton N, Liu CY, Croisille P, Bluemke D, & Lima JA (2011). Assessment of myocardial fibrosis with cardiovascular magnetic resonance. *J Am Coll Cardiol* **57**, 891-903.

Mihm MJ, Seifert JL, Coyle CM, & Bauer JA (2001). Diabetes related cardiomyopathy time dependent echocardiographic evaluation in an experimental rat model. *Life Sci* **69**, 527-542.

Mitra MS, Donthamsetty S, White B, & Mehendale HM (2008). High fat diet-fed obese rats are highly sensitive to doxorubicin-induced cardiotoxicity. *Toxicol Appl Pharmacol* **231**, 413-422.

Miyagawa K, Emoto N, Widyantoro B, Nakayama K, Yagi K, Rikitake Y, Suzuki T, & Hirata K (2010). Attenuation of Doxorubicin-induced cardiomyopathy by endothelin-converting enzyme-1 ablation through prevention of mitochondrial biogenesis impairment. *Hypertension* **55**, 738-746.

Miyata S, Takemura G, Kosai K, Takahashi T, Esaki M, Li L, Kanamori H, Maruyama R, Goto K, Tsujimoto A, Takeyama T, Kawaguchi T, Ohno T, Nishigaki K, Fujiwara T, Fujiwara H, & Minatoguchi S (2010). Anti-Fas gene therapy prevents doxorubicin-induced acute cardiotoxicity through mechanisms independent of apoptosis. *Am J Pathol* **176**, 687-698.

- Mizushige K, Yao L, Noma T, Kiyomoto H, Yu Y, Hosomi N, Ohmori K, & Matsuo H (2000). Alteration in left ventricular diastolic filling and accumulation of myocardial collagen at insulin-resistant prediabetic stage of a type II diabetic rat model. *Circulation* **101**, 899-907.
- Moreno M, Chaves JF, Sancho-Bru P, Ramalho F, Ramalho LN, Mansego ML, Ivorra C, Dominguez M, Conde L, Millan C, Mari M, Colmenero J, Lozano JJ, Jares P, Vidal J, Forns X, Arroyo V, Caballeria J, Gines P, & Bataller R (2010a). Ghrelin attenuates hepatocellular injury and liver fibrogenesis in rodents and influences fibrosis progression in humans. *Hepatology* **51**, 974-985.
- Muccioli G, Pons N, Ghe C, Catapano F, Granata R, & Ghigo E (2004). Ghrelin and des-acyl ghrelin both inhibit isoproterenol-induced lipolysis in rat adipocytes via a non-type 1a growth hormone secretagogue receptor. *Eur J Pharmacol* **498**, 27-35.
- Mytas DZ, Stougiannos PN, Zairis MN, Foussas SG, Pyrgakis VN, & Kyriazis IA (2009). Diabetic myocardial disease: pathophysiology, early diagnosis and therapeutic options. *J Diabetes Complications* **23**, 273-282.
- Nagaya N, Uematsu M, Kojima M, Ikeda Y, Yoshihara F, Shimizu W, Hosoda H, Hirota Y, Ishida H, Mori H, & Kangawa K (2001). Chronic administration of ghrelin improves left ventricular dysfunction and attenuates development of cardiac cachexia in rats with heart failure. *Circulation* **104**, 1430-1435.
- Nakamura T, Ueda Y, Juan Y, Katsuda S, Takahashi H, & Koh E (2000). Fas-mediated apoptosis in adriamycin-induced cardiomyopathy in rats: In vivo study. *Circulation* **102**, 572-578.
- Newton AC (2003). Regulation of the ABC kinases by phosphorylation: protein kinase C as a paradigm. *Biochem J* **370**, 361-371.
- Nickerson JG, Alkhateeb H, Benton CR, Lally J, Nickerson J, Han XX, Wilson MH, Jain SS, Snook LA, Glatz JF, Chabowski A, Luiken JJ, & Bonen A (2009). Greater transport efficiencies of the membrane fatty acid transporters FAT/CD36 and FATP4 compared with FABPpm and FATP1 and differential effects on fatty acid esterification and oxidation in rat skeletal muscle. *J Biol Chem* **284**, 16522-16530.
- Nickerson JG, Momken I, Benton CR, Lally J, Holloway GP, Han XX, Glatz JF, Chabowski A, Luiken JJ, & Bonen A (2007). Protein-mediated fatty acid

uptake: regulation by contraction, AMP-activated protein kinase, and endocrine signals. *Appl Physiol Nutr Metab* **32**, 865-873.

Ogunleye AA, Ogston SA, Morris AD, & Evans JM (2009). A cohort study of the risk of cancer associated with type 2 diabetes. *Br J Cancer* **101**, 1199-1201.

Ohnishi H, Oka T, Kusachi S, Nakanishi T, Takeda K, Nakahama M, Doi M, Murakami T, Ninomiya Y, Takigawa M, & Tsuji T (1998). Increased expression of connective tissue growth factor in the infarct zone of experimentally induced myocardial infarction in rats. *J Mol Cell Cardiol* **30**, 2411-2422.

Olson EN (2004). A decade of discoveries in cardiac biology. *Nat Med* **10**, 467-474.

Olson RD, Gambliel HA, Vestal RE, Shadle SE, Charlier HA, Jr., & Cusack BJ (2005). Doxorubicin cardiac dysfunction: effects on calcium regulatory proteins, sarcoplasmic reticulum, and triiodothyronine. *Cardiovasc Toxicol* **5**, 269-283.

Ota Y, Kawaguchi Y, Takagi K, Ichida H, Gono T, Hanaoka M, Higuchi T, & Yamanaka H (2013). Ghrelin attenuates collagen production in lesional fibroblasts from patients with systemic sclerosis. *Clin Immunol* **147**, 71-78.

Otsuka K, Terasaki F, Ikemoto M, Fujita S, Tsukada B, Katashima T, Kanzaki Y, Sohmiya K, Kono T, Toko H, Fujita M, & Kitaura Y (2009). Suppression of inflammation in rat autoimmune myocarditis by S100A8/A9 through modulation of the proinflammatory cytokine network. *Eur J Heart Fail* **11**, 229-237.

Pacifico L, Poggiogalle E, Costantino F, Anania C, Ferraro F, Chiarelli F, & Chiesa C (2009). Acylated and nonacylated ghrelin levels and their associations with insulin resistance in obese and normal weight children with metabolic syndrome. *Eur J Endocrinol* **161**, 861-870.

Pannala R, Leirness JB, Bamlet WR, Basu A, Petersen GM, & Chari ST (2008). Prevalence and clinical profile of pancreatic cancer-associated diabetes mellitus. *Gastroenterology* **134**, 981-987.

Park JM, Kakimoto T, Kuroki T, Shiraishi R, Fujise T, Iwakiri R, & Fujimoto K (2008). Suppression of intestinal mucosal apoptosis by ghrelin in fasting rats. *Exp Biol Med (Maywood)* **233**, 48-56.

Patel AD, Stanley SA, Murphy KG, Frost GS, Gardiner JV, Kent AS, White NE, Ghatei MA, & Bloom SR (2006). Ghrelin stimulates insulin-induced glucose uptake in adipocytes. *Regul Pept* **134**, 17-22.

Pischon T, Girman CJ, Hotamisligil GS, Rifai N, Hu FB, & Rimm EB (2004). Plasma adiponectin levels and risk of myocardial infarction in men. *JAMA* **291**, 1730-1737.

Pitt B & Zannad F (2012). The detection of myocardial fibrosis: an opportunity to reduce cardiovascular risk in patients with diabetes mellitus? *Circ Cardiovasc Imaging* **5**, 9-11.

Poole AW, Pula G, Hers I, Crosby D, & Jones ML (2004). PKC-interacting proteins: from function to pharmacology. *Trends Pharmacol Sci* **25**, 528-535.

Popovic V, Miljic D, Micic D, Damjanovic S, Arvat E, Ghigo E, Dieguez C, & Casanueva FF (2003). Ghrelin main action on the regulation of growth hormone release is exerted at hypothalamic level. *J Clin Endocrinol Metab* **88**, 3450-3453.

Poterucha JT, Kutty S, Lindquist RK, Li L, & Eidem BW (2012). Changes in left ventricular longitudinal strain with anthracycline chemotherapy in adolescents precede subsequent decreased left ventricular ejection fraction. *J Am Soc Echocardiogr* **25**, 733-740.

Rahman AM, Yusuf SW, & Ewer MS (2007). Anthracycline-induced cardiotoxicity and the cardiac-sparing effect of liposomal formulation. *Int J Nanomedicine* **2**, 567-583.

Rajesh M, Mukhopadhyay P, Batkai S, Mukhopadhyay B, Patel V, Hasko G, Szabo C, Mabley JG, Liaudet L, & Pacher P (2009). Xanthine oxidase inhibitor allopurinol attenuates the development of diabetic cardiomyopathy. *J Cell Mol Med* **13**, 2330-2341.

Rajesh M, Mukhopadhyay P, Batkai S, Patel V, Saito K, Matsumoto S, Kashiwaya Y, Horvath B, Mukhopadhyay B, Becker L, Hasko G, Liaudet L,

Wink DA, Veves A, Mechoulam R, & Pacher P (2010). Cannabidiol attenuates cardiac dysfunction, oxidative stress, fibrosis, and inflammatory and cell death signaling pathways in diabetic cardiomyopathy. *J Am Coll Cardiol* **56**, 2115-2125.

Richardson P, McKenna W, Bristow M, Maisch B, Mautner B, O'Connell J, Olsen E, Thiene G, Goodwin J, Gyarfás I, Martin I, & Nordet P (1996). Report of the 1995 World Health Organization/International Society and Federation of Cardiology Task Force on the Definition and Classification of cardiomyopathies. *Circulation* **93**, 841-842.

Rijzewijk LJ, van der Meer RW, Lamb HJ, de Jong HW, Lubberink M, Romijn JA, Bax JJ, de RA, Twisk JW, Heine RJ, Lammertsma AA, Smit JW, & Diamant M (2009). Altered myocardial substrate metabolism and decreased diastolic function in nonischemic human diabetic cardiomyopathy: studies with cardiac positron emission tomography and magnetic resonance imaging. *J Am Coll Cardiol* **54**, 1524-1532.

Rodriguez A, Gomez-Ambrosi J, Catalan V, Gil MJ, Becerril S, Sainz N, Silva C, Salvador J, Colina I, & Fruhbeck G (2009). Acylated and desacyl ghrelin stimulate lipid accumulation in human visceral adipocytes. *Int J Obes (Lond)* **33**, 541-552.

Roglic G & Unwin N (2010). Mortality attributable to diabetes: estimates for the year 2010. *Diabetes Res Clin Pract* **87**, 15-19.

Rubler S, Dlugash J, Yuceoglu YZ, Kumral T, Branwood AW, & Grishman A (1972). New type of cardiomyopathy associated with diabetic glomerulosclerosis. *Am J Cardiol* **30**, 595-602.

Russo SB, Baicu CF, Van LA, Geng T, Kasiganesan H, Zile MR, & Cowart LA (2012). Ceramide synthase 5 mediates lipid-induced autophagy and hypertrophy in cardiomyocytes. *J Clin Invest* **122**, 3919-3930.

Sato T, Nakamura Y, Shiimura Y, Ohgusu H, Kangawa K, & Kojima M (2012). Structure, regulation and function of ghrelin. *J Biochem* **151**, 119-128.

Sawaya H, Sebag IA, Plana JC, Januzzi JL, Ky B, Cohen V, Gosavi S, Carver JR, Wiegers SE, Martin RP, Picard MH, Gerszten RE, Halpern EF, Passeri J, Kuter I, & Scherrer-Crosbie M (2011). Early detection and prediction of cardiotoxicity in chemotherapy-treated patients. *Am J Cardiol* **107**, 1375-1380.

Sayed-Ahmed MM, Shaarawy S, Shouman SA, & Osman AM (1999). Reversal of doxorubicin-induced cardiac metabolic damage by L-carnitine. *Pharmacol Res* **39**, 289-295.

Schwartz RG, Jain D, & Storzynsky E (2013). Traditional and novel methods to assess and prevent chemotherapy-related cardiac dysfunction noninvasively. *J Nucl Cardiol*.

Shafie SM & Hilf R (1981). Insulin receptor levels and magnitude of insulin-induced responses in 7,12-dimethylbenz(a)anthracene-induced mammary tumors in rats. *Cancer Res* **41**, 826-829.

Shan YX, Liu TJ, Su HF, Samsamshariat A, Mestrlil R, & Wang PH (2003). Hsp10 and Hsp60 modulate Bcl-2 family and mitochondria apoptosis signaling induced by doxorubicin in cardiac muscle cells. *J Mol Cell Cardiol* **35**, 1135-1143.

Sharma H, Pathan RA, Kumar V, Javed S, & Bhandari U (2010). Anti-apoptotic potential of rosuvastatin pretreatment in murine model of cardiomyopathy. *Int J Cardiol*.

Sharma S, Adroque JV, Golfman L, Uray I, Lemm J, Youker K, Noon GP, Frazier OH, & Taegtmeier H (2004). Intramyocardial lipid accumulation in the failing human heart resembles the lipotoxic rat heart. *FASEB J* **18**, 1692-1700.

Shen X, Ye G, Metreveli NS, & Epstein PN (2005). Cardiomyocyte defects in diabetic models and protection with cardiac-targeted transgenes. *Methods Mol Med* **112**, 379-388.

Shi CS & Kehrl JH (2010). TRAF6 and A20 regulate lysine 63-linked ubiquitination of Beclin-1 to control TLR4-induced autophagy. *Sci Signal* **3**, ra42.

Shi H, Kokoeva MV, Inouye K, Tzameli I, Yin H, & Flier JS (2006). TLR4 links innate immunity and fatty acid-induced insulin resistance. *J Clin Invest* **116**, 3015-3025.

Shibata R, Ouchi N, Ito M, Kihara S, Shiojima I, Pimentel DR, Kumada M, Sato K, Schiekofer S, Ohashi K, Funahashi T, Colucci WS, & Walsh K (2004).

Adiponectin-mediated modulation of hypertrophic signals in the heart. *Nat Med* **10**, 1384-1389.

Shizukuda Y, Reyland ME, & Buttrick PM (2002). Protein kinase C-delta modulates apoptosis induced by hyperglycemia in adult ventricular myocytes. *Am J Physiol Heart Circ Physiol* **282**, H1625-H1634.

Simunek T, Klimtova I, Kaplanova J, Mazurova Y, Adamcova M, Sterba M, Hrdina R, & Gersl V (2004). Rabbit model for in vivo study of anthracycline-induced heart failure and for the evaluation of protective agents. *Eur J Heart Fail* **6**, 377-387.

Sirotkin AV, Meszarosova M, Grossmann R, Benco A, & Valenzuela F (2011). Effect of inhibitor and activator of ghrelin receptor (GHS-R1a) on porcine ovarian granulosa cell functions. *Gen Comp Endocrinol* **173**, 105-110.

Siu PM, Bae S, Bodyak N, Rigor DL, & Kang PM (2007). Response of caspase-independent apoptotic factors to high salt diet-induced heart failure. *J Mol Cell Cardiol* **42**, 678-686.

Siu PM, Bryner RW, Martyn JK, & Alway SE (2004). Apoptotic adaptations from exercise training in skeletal and cardiac muscles. *FASEB J* **18**, 1150-1152.

Siu PM, Bryner RW, Murlasits Z, & Alway SE (2005). Response of XIAP, ARC, and FLIP apoptotic suppressors to 8 wk of treadmill running in rat heart and skeletal muscle. *J Appl Physiol* **99**, 204-209.

Skurk C, Wittchen F, Suckau L, Witt H, Noutsias M, Fechner H, Schultheiss HP, & Poller W (2008). Description of a local cardiac adiponectin system and its deregulation in dilated cardiomyopathy. *Eur Heart J* **29**, 1168-1180.

Smith RG, Van der Ploeg LH, Howard AD, Feighner SD, Cheng K, Hickey GJ, Wyvratt MJ, Jr., Fisher MH, Nargund RP, & Patchett AA (1997). Peptidomimetic regulation of growth hormone secretion. *Endocr Rev* **18**, 621-645.

Soeki T, Kishimoto I, Schwenke DO, Tokudome T, Horio T, Yoshida M, Hosoda H, & Kangawa K (2008). Ghrelin suppresses cardiac sympathetic activity and prevents early left ventricular remodeling in rats with myocardial infarction. *Am J Physiol Heart Circ Physiol* **294**, H426-H432.

Spallarossa P, Garibaldi S, Altieri P, Fabbi P, Manca V, Nasti S, Rossettin P, Ghigliotti G, Ballestrero A, Patrone F, Barsotti A, & Brunelli C (2004). Carvedilol prevents doxorubicin-induced free radical release and apoptosis in cardiomyocytes in vitro. *J Mol Cell Cardiol* **37**, 837-846.

Spinale FG (2007). Myocardial matrix remodeling and the matrix metalloproteinases: influence on cardiac form and function. *Physiol Rev* **87**, 1285-1342.

Stanley WC, Lopaschuk GD, & McCormack JG (1997). Regulation of energy substrate metabolism in the diabetic heart. *Cardiovasc Res* **34**, 25-33.

Stein AB, Tiwari S, Thomas P, Hunt G, Levent C, Stoddard MF, Tang XL, Bolli R, & Dawn B (2007). Effects of anesthesia on echocardiographic assessment of left ventricular structure and function in rats. *Basic Res Cardiol* **102**, 28-41.

Su D, Li HY, Yan HR, Liu PF, Zhang L, & Cheng JH (2009). Astragalus Improved Cardiac Function of Adriamycin-Injured Rat Hearts by Upregulation of SERCA2a Expression. *Am J Chin Med* **37**, 519-529.

Subramaniam N, Sherman MH, Rao R, Wilson C, Coulter S, Atkins AR, Evans RM, Liddle C, & Downes M (2012). Metformin-mediated Bambi expression in hepatic stellate cells induces prosurvival Wnt/beta-catenin signaling. *Cancer Prev Res (Phila)* **5**, 553-561.

Suliman HB, Carraway MS, Ali AS, Reynolds CM, Welty-Wolf KE, & Piantadosi CA (2007). The CO/HO system reverses inhibition of mitochondrial biogenesis and prevents murine doxorubicin cardiomyopathy. *J Clin Invest* **117**, 3730-3741.

Swain SM, Whaley FS, & Ewer MS (2003). Congestive heart failure in patients treated with doxorubicin: a retrospective analysis of three trials. *Cancer* **97**, 2869-2879.

Tacar O, Sriamornsak P, & Dass CR (2013). Doxorubicin: an update on anticancer molecular action, toxicity and novel drug delivery systems. *J Pharm Pharmacol* **65**, 157-170.

Takahashi T, Yu F, Saegusa S, Sumino H, Nakahashi T, Iwai K, Morimoto S, Kurabayashi M, & Kanda T (2006). Impaired expression of cardiac adiponectin in leptin-deficient mice with viral myocarditis. *Int Heart J* **47**, 107-123.

Takatsu H, Duncker CM, Arai M, & Becker LC (1999). Granulocyte accumulation in ischemic/reperfused myocardium: assessment with a technetium-99m-labeled antigranulocyte monoclonal antibody in the dog. *J Nucl Cardiol* **6**, 641-650.

Takaya K, Ariyasu H, Kanamoto N, Iwakura H, Yoshimoto A, Harada M, Mori K, Komatsu Y, Usui T, Shimatsu A, Ogawa Y, Hosoda K, Akamizu T, Kojima M, Kangawa K, & Nakao K (2000). Ghrelin strongly stimulates growth hormone release in humans. *J Clin Endocrinol Metab* **85**, 4908-4911.

Takemura G & Fujiwara H (2007). Doxorubicin-induced cardiomyopathy from the cardiotoxic mechanisms to management. *Prog Cardiovasc Dis* **49**, 330-352.

Tamura N, Ogawa Y, Chusho H, Nakamura K, Nakao K, Suda M, Kasahara M, Hashimoto R, Katsuura G, Mukoyama M, Itoh H, Saito Y, Tanaka I, Otani H, & Katsuki M (2000). Cardiac fibrosis in mice lacking brain natriuretic peptide. *Proc Natl Acad Sci U S A* **97**, 4239-4244.

Tanaka M, Hayashida Y, Iguchi T, Nakao N, Nakai N, & Nakashima K (2001). Organization of the mouse ghrelin gene and promoter: occurrence of a short noncoding first exon. *Endocrinology* **142**, 3697-3700.

Taylor MS, Hwang Y, Hsiao PY, Boeke JD, & Cole PA (2012). Ghrelin O-acyltransferase assays and inhibition. *Methods Enzymol* **514**, 205-228.

Tesauro M, Schinzari F, Caramanti M, Lauro R, & Cardillo C (2010). Metabolic and cardiovascular effects of ghrelin. *Int J Pept* **2010**.

Tian R, Halow JM, Meyer M, Dillmann WH, Figueredo VM, Ingwall JS, & Camacho SA (1998). Thermodynamic limitation for Ca²⁺ handling contributes to decreased contractile reserve in rat hearts. *Am J Physiol* **275**, H2064-H2071.

Togliatto G, Trombetta A, Dentelli P, Baragli A, Rosso A, Granata R, Ghigo D, Pegoraro L, Ghigo E, & Brizzi MF (2010). Unacylated ghrelin rescues endothelial progenitor cell function in individuals with type 2 diabetes. *Diabetes* **59**, 1016-1025.

Tokarska-Schlattner M, Zaugg M, Zuppinger C, Wallimann T, & Schlattner U (2006). New insights into doxorubicin-induced cardiotoxicity: the critical role of cellular energetics. *J Mol Cell Cardiol* **41**, 389-405.

Tong J, Ganguly PK, & Singal PK (1991). Myocardial adrenergic changes at two stages of heart failure due to adriamycin treatment in rats. *Am J Physiol* **260**, H909-H916.

Tsubota Y, Owada-Makabe K, Yukawa K, & Maeda M (2005). Hypotensive effect of des-acyl ghrelin at nucleus tractus solitarii of rat. *Neuroreport* **16**, 163-166.

van Acker SA, Kramer K, Voest EE, Grimbergen JA, Zhang J, van d, V, & Bast A (1996). Doxorubicin-induced cardiotoxicity monitored by ECG in freely moving mice. A new model to test potential protectors. *Cancer Chemother Pharmacol* **38**, 95-101.

van de WT, Schrauwen-Hinderling VB, & Schrauwen P (2011a). Lipotoxicity in type 2 diabetic cardiomyopathy. *Cardiovasc Res* **92**, 10-18.

van der Lely AJ, Tschop M, Heiman ML, & Ghigo E (2004). Biological, physiological, pathophysiological, and pharmacological aspects of ghrelin. *Endocr Rev* **25**, 426-457.

van Herpen NA & Schrauwen-Hinderling VB (2008). Lipid accumulation in non-adipose tissue and lipotoxicity. *Physiol Behav* **94**, 231-241.

Vasquez-Vivar J, Martasek P, Hogg N, Masters BS, Pritchard KA, Jr., & Kalyanaraman B (1997). Endothelial nitric oxide synthase-dependent superoxide generation from adriamycin. *Biochemistry* **36**, 11293-11297.

Ventura-Clapier R, Garnier A, & Veksler V (2004). Energy metabolism in heart failure. *J Physiol* **555**, 1-13.

Volz HC, Laohachewin D, Seidel C, Lasitschka F, Keilbach K, Wienbrandt AR, Andrassy J, Bierhaus A, Kaya Z, Katus HA, & Andrassy M (2012). S100A8/A9 aggravates post-ischemic heart failure through activation of RAGE-dependent NF-kappaB signaling. *Basic Res Cardiol* **107**, 250.

Von Hoff DD, Layard MW, Basa P, Davis HL, Jr., Von Hoff AL, Rozenzweig M, & Muggia FM (1979). Risk factors for doxorubicin-induced congestive heart failure. *Ann Intern Med* **91**, 710-717.

Von Hoff DD, Rozenzweig M, Layard M, Slavik M, & Muggia FM (1977). Daunomycin-induced cardiotoxicity in children and adults. A review of 110 cases. *Am J Med* **62**, 200-208.

Voulgari C, Papadogiannis D, & Tentolouris N (2010). Diabetic cardiomyopathy: from the pathophysiology of the cardiac myocytes to current diagnosis and management strategies. *Vasc Health Risk Manag* **6**, 883-903.

Wakasugi S, Fischman AJ, Babich JW, Callahan RJ, Elmaleh DR, Wilkinson R, & Strauss HW (1993). Myocardial substrate utilization and left ventricular function in adriamycin cardiomyopathy. *J Nucl Med* **34**, 1529-1535.

Wang L, Ma W, Markovich R, Chen JW, & Wang PH (1998). Regulation of cardiomyocyte apoptotic signaling by insulin-like growth factor I. *Circ Res* **83**, 516-522.

Wang L, Saint-Pierre DH, & Tache Y (2002). Peripheral ghrelin selectively increases Fos expression in neuropeptide Y - synthesizing neurons in mouse hypothalamic arcuate nucleus. *Neurosci Lett* **325**, 47-51.

Wang Q, Usinger W, Nichols B, Gray J, Xu L, Seeley TW, Brenner M, Guo G, Zhang W, Oliver N, Lin A, & Yeowell D (2011). Cooperative interaction of CTGF and TGF-beta in animal models of fibrotic disease. *Fibrogenesis Tissue Repair* **4**, 4.

Wang WC, Uen YH, Chang ML, Cheah KP, Li JS, Yu WY, Lee KC, Choy CS, & Hu CM (2012a). Protective effect of guggulsterone against cardiomyocyte injury induced by doxorubicin in vitro. *BMC Complement Altern Med* **12**, 138.

Wang Y, Zheng D, Wei M, Ma J, Yu Y, Chen R, Lacefield JC, Xu H, & Peng T (2013). Over-expression of calpastatin aggravates cardiotoxicity induced by doxorubicin. *Cardiovasc Res*.

Wang ZV, Ferdous A, & Hill JA (2012b). Cardiomyocyte autophagy: metabolic profit and loss. *Heart Fail Rev*.

Wang ZV, Ferdous A, & Hill JA (2012c). Cardiomyocyte autophagy: metabolic profit and loss. *Heart Fail Rev*.

Way KJ, Isshiki K, Suzuma K, Yokota T, Zvagelsky D, Schoen FJ, Sandusky GE, Pechous PA, Vlahos CJ, Wakasaki H, & King GL (2002). Expression of connective tissue growth factor is increased in injured myocardium associated with protein kinase C beta2 activation and diabetes. *Diabetes* **51**, 2709-2718.

Whelan RS, Kaplinskiy V, & Kitsis RN (2010). Cell death in the pathogenesis of heart disease: mechanisms and significance. *Annu Rev Physiol* **72**, 19-44.

Whiting DR, Guariguata L, Weil C, & Shaw J (2011). IDF diabetes atlas: global estimates of the prevalence of diabetes for 2011 and 2030. *Diabetes Res Clin Pract* **94**, 311-321.

Will JC, Galuska DA, Vinicor F, & Calle EE (1998). Colorectal cancer: another complication of diabetes mellitus? *Am J Epidemiol* **147**, 816-825.

Williams DL, Grill HJ, Cummings DE, & Kaplan JM (2003). Vagotomy dissociates short- and long-term controls of circulating ghrelin. *Endocrinology* **144**, 5184-5187.

Wilson KD, Li Z, Wagner R, Yue P, Tsao P, Nestorova G, Huang M, Hirschberg DL, Yock PG, Quertermous T, & Wu JC (2008). Transcriptome alteration in the diabetic heart by rosiglitazone: implications for cardiovascular mortality. *PLoS One* **3**, e2609.

Wong WR, Chen YY, Yang SM, Chen YL, & Horng JT (2005). Phosphorylation of PI3K/Akt and MAPK/ERK in an early entry step of enterovirus 71. *Life Sci* **78**, 82-90.

Wren AM, Seal LJ, Cohen MA, Brynes AE, Frost GS, Murphy KG, Dhillon WS, Ghatei MA, & Bloom SR (2001). Ghrelin enhances appetite and increases food intake in humans. *J Clin Endocrinol Metab* **86**, 5992.

Wu W, Lee WL, Wu YY, Chen D, Liu TJ, Jang A, Sharma PM, & Wang PH (2000). Expression of constitutively active phosphatidylinositol 3-kinase inhibits activation of caspase 3 and apoptosis of cardiac muscle cells. *J Biol Chem* **275**, 40113-40119.

Xie Z, He C, & Zou MH (2011a). AMP-activated protein kinase modulates cardiac autophagy in diabetic cardiomyopathy. *Autophagy* **7**, 1254-1255.

Xie Z, Lau K, Eby B, Lozano P, He C, Pennington B, Li H, Rathi S, Dong Y, Tian R, Kem D, & Zou MH (2011b). Improvement of cardiac functions by chronic metformin treatment is associated with enhanced cardiac autophagy in diabetic OVE26 mice. *Diabetes* **60**, 1770-1778.

Xu Z, Lin S, Wu W, Tan H, Wang Z, Cheng C, Lu L, & Zhang X (2008). Ghrelin prevents doxorubicin-induced cardiotoxicity through TNF-alpha/NF-kappaB pathways and mitochondrial protective mechanisms. *Toxicology* **247**, 133-138.

Xu Z, Wu W, Zhang X, & Liu G (2007). Endogenous ghrelin increases in adriamycin-induced heart failure rats. *J Endocrinol Invest* **30**, 117-125.

Yamamoto S, Yang G, Zablocki D, Liu J, Hong C, Kim SJ, Soler S, Odashima M, Thaisz J, Yehia G, Molina CA, Yatani A, Vatner DE, Vatner SF, & Sadoshima J (2003). Activation of Mst1 causes dilated cardiomyopathy by stimulating apoptosis without compensatory ventricular myocyte hypertrophy. *J Clin Invest* **111**, 1463-1474.

Yang C, Wang Y, Liu H, Li N, Sun Y, Liu Z, & Yang P (2012). Ghrelin protects H9c2 cardiomyocytes from angiotensin II-induced apoptosis through the endoplasmic reticulum stress pathway. *J Cardiovasc Pharmacol* **59**, 465-471.

Yang J, Brown MS, Liang G, Grishin NV, & Goldstein JL (2008). Identification of the acyltransferase that octanoylates ghrelin, an appetite-stimulating peptide hormone. *Cell* **132**, 387-396.

Yang M, Hu S, Wu B, Miao Y, Pan H, & Zhu S (2007). Ghrelin inhibits apoptosis signal-regulating kinase 1 activity via upregulating heat-shock protein 70. *Biochem Biophys Res Commun* **359**, 373-378.

Yoon HR, Hong YM, Boriack RL, & Bennett MJ (2003). Effect of L-carnitine supplementation on cardiac carnitine palmitoyltransferase activities and plasma carnitine concentrations in adriamycin-treated rats. *Pediatr Res* **53**, 788-792.

- Younce CW, Wang K, & Kolattukudy PE (2010a). Hyperglycaemia-induced cardiomyocyte death is mediated via MCP-1 production and induction of a novel zinc-finger protein MCP1P. *Cardiovasc Res* **87**, 665-674.
- Young ME, Guthrie PH, Razeghi P, Leighton B, Abbasi S, Patil S, Youker KA, & Taegtmeier H (2002). Impaired long-chain fatty acid oxidation and contractile dysfunction in the obese Zucker rat heart. *Diabetes* **51**, 2587-2595.
- Yu H, Xu G, & Fan X (2013). The effect of ghrelin on cell proliferation in small intestinal IEC-6 cells. *Biomed Pharmacother* **67**, 235-239.
- Zalckvar E, Berissi H, Mizrachy L, Idelchuk Y, Koren I, Eisenstein M, Sabanay H, Pinkas-Kramarski R, & Kimchi A (2009). DAP-kinase-mediated phosphorylation on the BH3 domain of beclin 1 promotes dissociation of beclin 1 from Bcl-XL and induction of autophagy. *EMBO Rep* **10**, 285-292.
- Zhang G, Yin X, Qi Y, Pendyala L, Chen J, Hou D, & Tang C (2010). Ghrelin and cardiovascular diseases. *Curr Cardiol Rev* **6**, 62-70.
- Zhang GG, Teng X, Liu Y, Cai Y, Zhou YB, Duan XH, Song JQ, Shi Y, Tang CS, Yin XH, & Qi YF (2009). Inhibition of endoplasm reticulum stress by ghrelin protects against ischemia/reperfusion injury in rat heart. *Peptides* **30**, 1109-1116.
- Zhang W, Chai B, Li JY, Wang H, & Mulholland MW (2008). Effect of des-acyl ghrelin on adiposity and glucose metabolism. *Endocrinology* **149**, 4710-4716.
- Zhang W, Lin TR, Hu Y, Fan Y, Zhao L, Stuenkel EL, & Mulholland MW (2004). Ghrelin stimulates neurogenesis in the dorsal motor nucleus of the vagus. *J Physiol* **559**, 729-737.
- Zhao H, Liu G, Wang Q, Ding L, Cai H, Jiang H, & Xin Z (2007). Effect of ghrelin on human endothelial cells apoptosis induced by high glucose. *Biochem Biophys Res Commun* **362**, 677-681.
- Zhou G, Li C, & Cai L (2004a). Advanced glycation end-products induce connective tissue growth factor-mediated renal fibrosis predominantly through transforming growth factor beta-independent pathway. *Am J Pathol* **165**, 2033-2043.

Zhou YT, Grayburn P, Karim A, Shimabukuro M, Higa M, Baetens D, Orci L, & Unger RH (2000). Lipotoxic heart disease in obese rats: implications for human obesity. *Proc Natl Acad Sci U S A* **97**, 1784-1789.

Zhu H, Tannous P, Johnstone JL, Kong Y, Shelton JM, Richardson JA, Le V, Levine B, Rothermel BA, & Hill JA (2007). Cardiac autophagy is a maladaptive response to hemodynamic stress. *J Clin Invest* **117**, 1782-1793.

Zhu W, Shou W, Payne RM, Caldwell R, & Field LJ (2008). A mouse model for juvenile doxorubicin-induced cardiac dysfunction. *Pediatr Res* **64**, 488-494.

Zou MH & Xie Z (2013). Regulation of interplay between autophagy and apoptosis in the diabetic heart: New role of AMPK. *Autophagy* **9**.